



University of Kentucky  
**UKnowledge**

---

University of Kentucky Doctoral Dissertations

Graduate School

---

2006

# MULTIFUNCTIONAL POTENTIAL THERAPEUTICS TOWARDS OXIDATIVE STRESS MEDIATED NEURODEGENERATIVE DISORDERS AND MODELS THEREOF

Gururaj Joshi

*University of Kentucky*, [gururaj75@gmail.com](mailto:gururaj75@gmail.com)

[Right click to open a feedback form in a new tab to let us know how this document benefits you.](#)

---

## Recommended Citation

Joshi, Gururaj, "MULTIFUNCTIONAL POTENTIAL THERAPEUTICS TOWARDS OXIDATIVE STRESS MEDIATED NEURODEGENERATIVE DISORDERS AND MODELS THEREOF" (2006). *University of Kentucky Doctoral Dissertations*. 298.

[https://uknowledge.uky.edu/gradschool\\_diss/298](https://uknowledge.uky.edu/gradschool_diss/298)

This Dissertation is brought to you for free and open access by the Graduate School at UKnowledge. It has been accepted for inclusion in University of Kentucky Doctoral Dissertations by an authorized administrator of UKnowledge. For more information, please contact [UKnowledge@lsv.uky.edu](mailto:UKnowledge@lsv.uky.edu).

ABSTRACT OF DISSERTATION

Gururaj joshi

The Graduate School

University of Kentucky

2006

MULTIFUNCTIONAL POTENTIAL THERAPEUTICS TOWARDS OXIDATIVE  
STRESS MEDIATED NEURODEGENERATIVE DISORDERS AND MODELS  
THEREOF

---

ABSTRACT OF DISSERTATION

---

A dissertation submitted in partial fulfillment of the  
requirements for the degree of Doctor of Philosophy in the  
College of Arts and Sciences  
at the University of Kentucky

By

Gururaj Joshi

Lexington, Kentucky

Director: Dr. D. Allan Butterfield, Professor of Chemistry

Lexington, Kentucky

2006

Copyright © Gururaj Joshi 2006

## ABSTRACT OF DISSERTATION

### MULTIFUNCTIONAL POTENTIAL THERAPEUTICS TOWARDS OXIDATIVE STRESS MEDIATED NEURODEGENERATIVE DISORDERS AND MODELS THEREOF

The studies described in this dissertation were performed with the goal of understanding the function of antioxidant compounds delivered *in vivo* to rodents and the implication of the results towards oxidative stress (OS)-related neurodegenerative disorders with particular emphasis on Alzheimer's disease (AD). OS has been implicated in AD and is characterized by extensive oxidative damage to protein, lipids and DNA. A major thrust of this dissertation work was to gain insight into antioxidant properties of compounds used in the following studies and their efficacy as potential therapeutics for treatment of OS-related disorders.

D609, a glutathione (GSH) mimetic is known to trap OH<sup>•</sup> Radicals, scavenge H<sub>2</sub>O<sub>2</sub> and reduce the A $\beta$  (1-42)-induced OS and cytotoxicity in neurons. The present dissertation study showed *in vivo* protective effect of D609 in synaptosomes and mitochondria isolated from gerbils against OS mediated by Fe<sup>2+</sup>/H<sub>2</sub>O<sub>2</sub>, AAPH, and A $\beta$  (1-42). Upon intraperitoneal (i.p.) injection of gerbils, D609 showed protection of subsequently isolated brain moieties against OS. *In vivo* administration of D609 also modulates brain GSH levels and increases the activity of key GSH-related enzymes, thereby likely provides a protection against OS.

Adriamycin (ADR), a quinone-containing chemotherapeutic, is known to produce ROS in heart. Patients under treatment with ADR often show persistent changes in cognitive function (effect called as chemobrain by patients). Upon i.p. injection, ADR causes OS, increases expression of multidrug resistant protein-1 (MRP-1) in brain and alters GSH levels and its related enzyme activities.  $\gamma$ -Glutamyl cysteinyl ethyl ester (GCEE) is known to increase GSH levels in brain, *in vivo*. Research reported in this dissertation shows that *in vivo* GCEE reverses the ADR-mediated OS in mice brain.

N-acetylcysteine (NAC), a GSH precursor provides the limiting substrate cysteine in GSH synthesis. Previously, our laboratory showed increased GSH levels post i.p. injection of NAC and reduces OS in synaptosomes treated with acrolein. The present study showed that NAC given in drinking water to APP/PS-1 mice, a model of AD can significantly reduce OS.

These results provide a potential therapeutic intervention by antioxidants that can modulate GSH in OS-mediated neurodegenerative disorders.

KEYWORDS: Oxidative stress, Free radicals, Glutathione, Antioxidants, Alzheimer's disease.

---

Gururaj Joshi

---

11/02/2006

---

MULTIFUNCTIONAL POTENTIAL THERAPEUTICS TOWARDS OXIDATIVE  
STRESS MEDIATED NEURODEGENERATIVE DISORDERS AND MODELS  
THEREOF

By

Gururaj Joshi

Professor Allan Butterfield

---

Director of Dissertation

Dr. Robert Grossman

---

Director of Graduate Studies

11/02/2006

---

Date

## **RULES FOR THE USE OF DISSERTATIONS**

Unpublished dissertations submitted for the Doctor's degree and deposited in the University of Kentucky Libraries are as a rule open for inspection, but are to be used only with due regard to the rights of the authors. Bibliographical references may be noted, but quotations or summaries of part may be published only with the permission of the author, and with the usual scholarly acknowledgements.

Extensive copying or publication of the dissertation in whole or in part also requires the consent of the Dean of Graduate School of the University of Kentucky.

A library that borrows this dissertation for use by its patrons is expected to secure the signature of each user.

Name

Date

---

---

---

---

---

---

---

---

---

---

---

---

---

---

---

DISSERTATION

Gururaj Joshi

The Graduate School  
University of Kentucky

2006

MULTIFUNCTIONAL POTENTIAL THERAPEUTICS TOWARDS OXIDATIVE  
STRESS MEDIATED NEURODEGENERATIVE DISORDERS AND MODELS  
THEREOF

---

DISSERTATION

---

A dissertation submitted in partial fulfillment of the  
requirements for the degree of Doctor of Philosophy in the  
College of Arts and Sciences  
at the University of Kentucky

By

Gururaj Joshi

Lexington, Kentucky

Director: Dr. D. Allan Butterfield, Professor of Chemistry

Lexington, Kentucky

2006

Copyright © Gururaj Joshi 2006



To My Parents

## ACKNOWLEDGEMENTS

I would like to extend my greatest thanks and appreciation to my advisor, Professor D. Allan Butterfield. Your unwavering support, mentorship and guidance for me during my time at the University of Kentucky will never be forgotten. His NIH grants [AG-10836; AG-05119] helped conduct this research. I would like to thank my committee members (Drs., Leonidas Bachas, Mark Lovell and George Smith) for providing professional support and direction. I am very grateful to the postdocs in our lab, Drs., Rukhsana Sultana (who has helped me in all my projects), Mubeen Ansari and Hafiz Mohammed Abdul for their knowledgeable scientific views. This work is not completed without thanking my collaborators. Dr. Daret K St. Clair was very instrumental in providing inputs for the entire ADR project and also provided us with APP/PS-1 transgenic mice for NAC project. I would like to thank Marsha Paulette Cole and Jitbanjong (Noi) Tangpong for collaborating in ADR project. Dr. St Clair's grant [CA-80152; CA-94853] helped support this research. Dr. William Markesbery provided support and direction in the NAC project. I would like to thank Drs., Marzia Perluigi and Vittorio Calabrese for helping me with the D609 and FAEE studies.

I cannot forget the love and affection given to me by Ms. Marsha Butterfield, my colleagues, lab mates, and departmental staff. A special Thanks to Ms. Mollie Fraim in getting this dissertation thesis in proper shape. I would like to thank Drs. Fai poon and Wycliff Opii in whom I found great friends. Dr. Jennifer Drake was very helpful in teaching me most of the laboratory skills. I would like to thank my close friends, Navneeth, Sarang, Dr. Ram Chander (RC), Satya and Bipin for all the good times. I can't thank my parents and sister (Vani) enough for their patience, perseverance and belief in me that made this dissertation work possible. Last and most important person I want to

thank is my wife Ranjani Joshi, for all the love, support and sacrifice. I want to thank her for standing by my side during the most difficult times in our lives.

## TABLE OF CONTENTS

ACKNOWLEDGEMENTS .....	iii
LIST OF TABLES .....	xvii
LIST OF FIGURES .....	xviii
Chapter 1: Introduction .....	1
Chapter 2: Background .....	8
2.1. Oxidative Stress and Neurodegeneration .....	8
2.1.1. Overview of oxidative stress .....	8
2.1.2. Free radical theory in neurodegeneration .....	9
2.1.3. Targets of Oxidation .....	11
2.1.3.1. Proteins .....	11
2.1.3.2. Lipids .....	14
2.2. Alzheimer's Disease .....	17
2.2.1. Overview .....	17
2.2.2. A $\beta$ (1-42)-mediated oxidative stress in AD .....	17
2.2.3. APP/PS-1 human double mutant knock-in mice as an AD model..	19
2.3. Synaptosomes .....	20
2.4. Mitochondria .....	21
2.5. Glutathione .....	23
2.5.1. GSH metabolism and biosynthesis .....	23
2.5.2. GSH and Oxidative stress .....	26
2.5.3. Glutathione Peroxidase .....	28
2.5.4. Glutathione Reductase .....	28
2.5.5. Glutathione-S-Transferase .....	29

2.6. Superoxide Dismutase .....	30
2.7. Proteomics.....	30
Chapter 3: Experimental Procedure .....	33
3.1. Synaptosome Isolation .....	33
3.2. Mitochondria Isolation.....	34
3.3. Protein Concentration .....	35
3.4. DCF Fluorescence.....	35
3.5. Protein oxidation (Slot blot).....	38
3.5.1. Protein carbonyl.....	38
3.5.2. 3-Nitrotyrosine.....	40
3.6. Lipid peroxidation (Slot blot) .....	41
3.7. GSH and GSSG assays .....	44
3.8. Enzyme Activities.....	46
3.8.1. Glutathione peroxidase .....	46
3.8.2. Glutathione reductase.....	47
3.8.3. Glutathione-S-transferase .....	47
3.8.4. Total superoxide dimutase .....	47
3.9. Western blot.....	48
3.10. Proteomics.....	48
3.10.1. Iso-electric focusing (First dimension) .....	49
3.10.2. SDS-PAGE (Second dimension) .....	49
3.10.3. 2D Western blots.....	51
3.10.4. PD-Quest analysis.....	52
3.10.5. In-gel digestion .....	52

3.10.6. Mass spectrometry .....	53
3.10.7. Ion source.....	53
3.10.8. Time-of-flight (TOF) analyzer.....	54
3.10.9. Database searching.....	55
Chapter 4: Free radical mediated oxidative stress and toxic side effects in brain induced by the anti cancer drug Adriamycin: Insight into chemo brain .....	57
4.1. Overview of the Study .....	57
4.2. Introduction.....	58
4.3. Purpose of the study.....	59
4.4. Experimentals .....	59
4.4.1 Animals .....	59
4.4.2 Material and Method.....	60
4.4.2.1 Chemicals.....	60
4.4.2.2 Preparation of brain homogenate .....	60
4.4.2.3. Protein Carbonyls.....	61
4.4.2.4. 3NT .....	62
4.4.2.5. Protein-bound HNE .....	62
4.4.2.6. Western Blot .....	63
4.4.2.7. Statistical analysis.....	64
4.5. Results.....	64
4.5.1. Protein carbonyls .....	64
4.5.2. 3NT .....	65
4.5.3. HNE .....	66
4.5.4. MRP-1 expression.....	69

4.6. Discussion .....	71
Chapter 5: Alteration in glutathione level and glutathione-related enzyme expression and activity in brain induced by the anti-cancer drug Adriamycin: Implications for oxidative stress-mediated CNS toxicity.....	76
5.1. Overview of study .....	76
5.2. Introduction.....	77
5.3. Experimentals .....	80
5.3.1. Animals .....	80
5.3.2. Chemicals.....	80
5.3.3 Preparation of brain homogenate .....	80
5.3.4. GSH assay .....	81
5.3.5. Western blots .....	81
5.3.6. Enzyme activity assays .....	82
5.3.6.1. Estimation of glutathione-S-transferase activity.....	82
5.3.6.2. Estimation of glutathione peroxidase activity.....	82
5.3.6.3. Estimation of glutathione reductase activity.....	82
5.3.6.4. Estimation of total SOD activity.....	83
5.4. Statistical analysis.....	83
5.5. Results.....	83
5.5.1. GSH assay .....	83
5.5.2. Western blot analysis .....	84
5.5.3. Enzyme activities .....	87
5.6. Discussion .....	88

Chapter 6: Proteomic identification of differentially expressed proteins and redox proteomic identification of specifically oxidized proteins in brain isolated from adriamycin-injected mice: Potential targets for therapeutics.....	92
6.1. Overview of study.....	92
6.2. Introduction.....	93
6.3. Purpose of the study.....	95
6.4. Experimentals .....	96
6.4.1. Chemicals.....	96
6.4.2. Animals.....	96
6.4.3. Preperation of brain homogenate .....	97
6.4.4. 2-dimentional gel electrophoresis .....	97
6.4.5. Western blotting.....	97
6.4.6. Image analysis.....	98
6.4.7. Trypsin digestion .....	98
6.4.8. Mass spectrometry .....	98
6.5. Statistics .....	99
6.6. Results.....	99
6.6.1. Expression proteomics .....	100
6.6.2. Redox proteomics .....	103
6.7. Disscussion .....	106
6.7.1. Transport/mobility and cytoskeleton .....	107
6.7.2. Energy Metabolism.....	108
6.7.3. Antioxidant proteins.....	111
6.7.4. Regulation/Homeostasis .....	112



Chapter 7: Glutathione elevation by $\gamma$ -glutamyl cysteine ethyl ester as a potential therapeutic strategy towards preventing oxidative stress in brain mediated by in vivo administration of adriamycin: Implication for chemobrain. ....	116
7.1. Overview of the study .....	116
7.2. Introduction.....	117
7.3. Purpose of the study .....	120
7.4. Experimentals .....	122
7.4.1. Animals .....	122
7.4.2. Chemicals.....	122
7.4.3. Treatments.....	122
7.4.4. Preparation of brain homogenate .....	123
7.4.5. GSH assay .....	123
7.4.6. Protein Carbonyls.....	124
7.4.7. 4-Hydroxynonenal (HNE) .....	124
7.4.8. 3-Nitrotyrosine (3-NT).....	125
7.4.9. Enzyme activity assays .....	125
7.5. Statistical analysis.....	125
7.6. Results.....	126
7.6.1. GSH assay .....	126
7.6.2. Protein carbonyl, 3 nitrotyrosine and 4-hydroxynonenal .....	127
7.6.3. GST activity .....	131
7.7. Discussion .....	133

Chapter 8: In Vivo Protection of Synaptosomes from Oxidative Stress Mediated by Fe <sup>2+</sup> /H <sub>2</sub> O <sub>2</sub> or 2,2-Azobis (2-amidino-propane) dihydrochloride (AAPH) by the Glutathione Mimetic Tricyclodecan-9-yl-xanthogenate (D609) .....	137
8.1. Overview of the study .....	137
8.2. Introduction.....	138
8.3. Purpose of the study .....	140
8.4. Experimentals .....	140
8.4.1. Animals .....	140
8.4.2. Chemicals.....	140
8.4.3. Preparation of Synaptosomes.....	141
8.4.4. DCF fluorescence.....	142
8.4.5. Protein carbonyls .....	142
8.4.6. 4-Hydroxynonenal (HNE) .....	143
8.4.7. 3-Nitrotyrosine (3NT).....	144
8.4.8. Western blot for Protein oxidation.....	144
8.5. Statistical analysis.....	145
8.6. Results.....	145
8.6.1. DCF fluorescence.....	145
8.6.2. Protein carbonyl.....	149
8.6.3. HNE .....	152
8.6.4. 3NT .....	152
8.7. Discussion .....	155
Chapter 9: In vivo protection by the xanthate D609 against amyloid $\beta$ -peptide (1-42)-induced oxidative stress: Implications for Alzheimer's disease .....	161

9.1. Overview of the study .....	161
9.2. Introduction.....	162
9.3. Purpose of the study .....	164
9.4. Experimentals .....	165
9.4.1. Chemicals.....	165
9.4.2. Animals .....	165
9.4.3. Synaptosomal preparation.....	166
9.4.4. Reactive oxygen species (ROS) measurements .....	166
9.4.5. Protein carbonyl measurement.....	167
9.4.6. 3NT .....	168
9.4.7. HNE .....	168
9.4.8. GSH assay .....	169
9.4.9. iNOS expression levels .....	169
9.5. Statistical analysis.....	170
9.6. Results.....	170
9.6.1. D609 prevents in vivo ROS accumulation.....	170
9.6.2. D609 in vivo protects against A $\beta$ (1-42)-induced protein oxidation and lipid peroxidation .....	172
9.6.3. D609 modulates A $\beta$ (1-42)-induced iNOS expression levels.....	178
9.7. Discussion .....	180
Chapter 10: In vivo administration of D609 leads to protection of subsequently isolated gerbil brain mitochondria subjected to in vitro oxidative stress inducers: Relavance to Alzheimer's disease and other oxidative stress related neurodegenerative disorders ....	186
10.1. Overview of the study .....	186

10.2. Introduction.....	187
10.3. Purpose of the study .....	190
10.4. Experimentals .....	191
10.4.1. Animals.....	191
10.4.2. Chemicals.....	191
10.4.3. Preparation of mitochondria .....	191
10.4.4. Protein estimation and treatment .....	192
10.4.5. Protein carbonyls .....	193
10.4.6. 3NT .....	193
10.4.7. HNE .....	194
10.4.8. Estimation of cytochrome-c release.....	195
10.4.9. Estimation of reduced glutathione (GSH).....	195
10.4.11. Estimation of oxidized glutathione (GSSG) .....	195
10.4.12. Enzyme activities .....	196
10.4.12.1. Estimation of glutathione-S-transferase activity .....	196
10.4.12.2.....	196
10.4.12.3. Estimation of glutathione reductase activity.....	196
10.5. Statistical analysis.....	197
10.6. Results.....	197
10.6.1. Protein Oxidation and Lipid Peroxidation .....	197
10.6.2. Reduced glutathione (GSH).....	201
10.6.3. Oxidized Glutathione (GSSG) .....	201
10.6.4. The Ratio of Reduced and Oxidized Glutathione (GSH/GSSG) .....	201
10.6.5. Cytochrome-c Release .....	205

10.6.6. The Activity of GSH-relevant Enzymes .....	207
10.7. Discussion .....	208
Chapter 11: N-Acetyl cysteine-mediated protection against oxidative stress in APP/PS-1 mouse: A pilot study towards therapeutic modulation of mild cognitive impairment (MCI) .....	
	214
11.1. Overview of the Study .....	214
11.2. Introduction.....	215
11.3. Purpose of the study.....	219
11.4. Experimentals .....	219
11.4.1. Chemicals.....	219
11.4.2. Animals .....	220
11.4.3. Treatments.....	220
11.4.4. Preparation of brain homogenate .....	221
11.4.5. Protein Carbonyls.....	221
11.4.6. HNE .....	222
11.4.7. 3NT .....	222
11.4.8. Western blots .....	223
11.4.9. Enzyme activity assay.....	223
11.4.9.1. Estimation of glutathione peroxidase activity.....	223
11.5. Statistical analysis.....	224
11.6. Results.....	224
11.6.1. NAC protects APP/PS-1 mice brains against protein oxidation and lipid peroxidation .....	224

11.6.2. NAC increased GPx expression and activity in APP/PS-1 mice	
brain .....	228
11.7. Discussion .....	231
Chapter 12: Conclusion and future studies .....	236
12.1 Conclusions .....	236
12.2 Future studies .....	238
Appendix I: In Vivo Protection of Synaptosomes from Oxidative Stress Mediated by 2,2-Azobis (2-amidino-propane) Dihydrochloride (AAPH) or Fe <sup>2+</sup> /H <sub>2</sub> O <sub>2</sub> by Ferulic Acid Ethyl Ester (FAEE): Insight into Mechanisms of Neuroprotection and Relevance to Oxidative Stress Related neurodegenerative Disorders .....	240
A.1. Overview of the study .....	240
A.2. Introduction .....	241
A.3. Purpose of the study .....	244
A.4. Experimentals .....	244
A.4.1. Animals .....	244
A.4.2. Chemicals .....	245
A.4.3. Preparation of Synaptosomes .....	245
A.4.4. DCF fluorescence .....	246
A.4.5. Protein carbonyls .....	247
A.4.6. HNE .....	248
A.4.7. 3NT .....	248
A.4.8. Specificity of HNE and 3-NT antibodies .....	248
A.4.9. Western blots .....	249
A.5. Statistical analysis .....	249

A.6. Results.....	249
A.6.1. FAEE reduces ROS generation in synaptosomes .....	249
A.6.2. FAEE <i>in vivo</i> inhibits protein oxidation .....	252
A.6.3. FAEE <i>in vivo</i> prevents nitration of tyrosine residues .....	253
A.6.4. FAEE <i>in vivo</i> inhibits HNE formation.....	253
A.6.5. FAEE <i>in vivo</i> induces HO-1 and HSP-70 expression.....	258
A.6.6. FAEE <i>in vivo</i> suppresses iNOS expression.....	258
A.7. Discussion .....	261
A.8. Acknowledgements.....	269
Appendix II: Supporting DATA .....	270
Reference .....	280
Vita.....	332

## LIST OF TABLES

<b>Table 5.1</b>	GSH-related enzymes and SOD activity in brain homogenate obtained from mice, 72 h post i.p. injection of saline (control) or ADR .....	87
<b>Table 6.1</b>	Proteins showing decreased levels in brain isolated from ADR-injected mice when compared to saline-injected control, as determined by PDQuest analysis on gels obtained from 2DE .....	104
<b>Table 6.2</b>	Proteins showing increased oxidation levels in brain isolated from ADR-injected mice when compared to saline-injected control, as determined by PDQuest analysis on the blots obtained from 2DE followed by Western Blot.....	105
<b>Table 9.1</b>	D609 does not influence total brain GSH levels. Results presented are the mean $\pm$ S.E.M, n=6. Total GSH levels, following i.p D609 injection, were measured by a GSH assay kit as described in the Chapter 3.....	184
<b>Table 10.1</b>	Activities of some GSH-related enzymes in post mitochondrial supernatant obtained from gerbil brain mitochondria that were previously injected i.p. with saline (control) or D609.....	207



## LIST OF FIGURES

<b>Figure 2.1</b>	Reaction leading to formation of ROS/RNS.....	9
<b>Figure 2.2</b>	Adriamycin.....	10
<b>Figure 2.3</b>	Glycerophospholipids. Adapted from (Garrett and Grisham, 1995) with slight modification.....	15
<b>Figure 2.4</b>	Reaction of reactive alkenals with histidine, cysteine and lysine to form Michael adducts. P1 refers to another protein. Figure also shows formation of cross-linked derivatives between proteins. Adapted from (Stadtman and Berlett, 1997).....	16
<b>Figure 2.5</b>	A $\beta$ (1-42) generation by APP processing. Adapted from (Butterfield and Boyd-Kimball, 2005).....	19
<b>Figure 2.6</b>	Diagram of human mitochondrion (Adapted from wikipedia).....	22
<b>Figure 2.7</b>	GSH synthesis.....	25
<b>Figure 2.8</b>	The reaction catalyzed by GR and GPx in conjugation with GSH and GSSG.....	27
<b>Figure 2.9</b>	Detoxification process involving GST and MRP-1 to remove GS-conjugates out of the cell.....	29
<b>Figure 3.1</b>	Sucrose density gradient for isolation of purified synaptosomes.....	34
<b>Figure 3.2</b>	DCF assay.....	37
<b>Figure 3.3</b>	Derivatization of protein by DNPH.....	39
<b>Figure 3.4</b>	Slot blot apparatus assembly.....	40
<b>Figure 3.5</b>	Reaction of HNE with cysteine.....	43
<b>Figure 3.6</b>	GSH assay.....	45
<b>Figure 3.7</b>	2-Dimensional Gel Electrophoresis.....	51
<b>Figure 3.8</b>	Diagram showing sequence of events involved in redox proteomics	56
<b>Figure 4.1</b>	Increased <i>in vivo</i> protein oxidation in brain isolated from mice previously treated with adriamycin (20mg/kg body weight) 72 hours post i.p injection compared to brain isolated from saline injected mice. *P< 0. 001, n=5. (434.5 arbitrary unit was taken as 100% for control).....	65
<b>Figure 4.2</b>	Increased <i>in vivo</i> 3-Nitrotyrosine levels in brain isolated from mice previously treated with adriamycin (20mg/kg body weight) 72 hours post i.p. injection, compared to brain isolated from saline injected mice. *P< 0. 001, n=5. (151.67 arbitrary unit was taken as 100% for control).....	67
<b>Figure 4.3</b>	Increased <i>in vivo</i> protein bound HNE in brain isolated from mice previously treated with adriamycin (20mg/kg body weight) 72 hours post i.p. injection, compared to brain isolated from saline injected mice. * P<0.001, n=5. (526 arbitrary unit was taken as 100% for control).....	68
<b>Figure 4.4</b>	Plot showing significant increase in MRP1 levels in brain isolated from mice injected i.p with adriamycin compared to saline injected control mice. *P< 0.05, n=3. (272 arbitrary unit was taken as 100% for control). Also shown in the figure is a representative western blot showing increased MRP1 expression in brain isolated from mice injected with ADR.....	70
<b>Figure 5.1</b>	Brain total GSH level in saline-injected and ADR-injected mice,	

	72 h post i.p. injections. A significant reduction in GSH level is seen in brain isolated from ADR-injected mice when compared to control. * $p < 0.05$ , $n = 5$ . The data are presented as mean $\pm$ SEM expressed as percentage of control.....	84
<b>Figure 5.2</b>	Representative Western blots of brain GPx, GST and GR 72 h post i.p. injection of saline or ADR in mice. GAPDH is used as a loading control.....	85
<b>Figure 5.3</b>	Representative plot of GST, GPx and GR levels in saline-injected and ADR-injected mice brain, 72 h post i.p. injections. A significant increase in GST, GPx and GR level is seen in ADR-injected mice brain when compared to control. * $p < 0.05$ , $n = 5$ . The data are presented as mean $\pm$ SEM expressed as percentage of control.....	86
<b>Figure 6.1 a &amp; b</b>	Representative 2DE gels of brain proteins from saline-injected and ADR-injected mice, respectively. The labeled proteins on respective gels showed significantly lower expression in brain isolated from ADR-injected mice when compared to saline-injected control. ( $p < 0.05$ , $n = 5$ ).....	101
<b>Figure 6.2 a &amp; b</b>	Representative Western blot obtained from 2DE gels of brain proteins from saline-injected and ADR-injected mice, respectively. The labeled proteins on respective blots showed significantly increased oxidation in brain isolated from ADR-injected mice when compared to saline-injected control. ( $p < 0.05$ , $n = 5$ ).....	102
<b>Figure 7.1</b>	Levels of GSH in all the treatment groups. There is a significant decrease in GSH level in brain isolated from ADR-injected mice when compared to control (* $p < 0.05$ , $n = 5$ ). I.p injection of GCEE increases GSH level significantly in brain. The brain isolated from GCEE-injected mice followed by ADR injection shows a significant increase in GSH levels when compared to the levels in brain isolated from ADR injected mice that were previously injected with saline (* $p < 0.05$ , $n = 5$ ). The data are presented as mean $\pm$ SEM expressed as percentage of control.....	127
<b>Figure 7.2</b>	Levels of protein carbonyl in all the treatment groups. There is a significant increase in protein carbonyl level in brain isolated from ADR-injected mice when compared to control (* $p < 0.05$ , $n = 5$ ). I.p injection of GCEE decreases protein carbonyl level significantly in brain. The brain isolated from GCEE-injected mice followed by ADR injection shows a significant decrease in protein carbonyl levels when compared to the levels in brain isolated from ADR injected mice that were previously injected with saline (* $p < 0.05$ , $n = 5$ ). The data are presented as mean $\pm$ SEM expressed as percentage of control.....	128
<b>Figure 7.3</b>	Levels of 3NT in all the treatment groups. There is a significant increase in 3NT level in brain isolated from ADR-injected mice when compared to control (* $p < 0.05$ , $n = 5$ ). I.p injection of GCEE decreases 3NT level significantly in brain. The brain isolated from GCEE-injected mice followed by ADR injection shows a significant decrease in 3NT levels when compared to the	

	levels in brain isolated from ADR injected mice that were previously injected with saline (* p < 0.05, n = 5). The data are presented as mean ± SEM expressed as percentage of control.....	129
<b>Figure 7.4</b>	Levels of HNE in all the treatment groups. There is a significant increase in HNE level in brain isolated from ADR-injected mice when compared to control (* p < 0.05, n = 5). I.p injection of GCEE decreases HNE level significantly in brain. The brain isolated from GCEE-injected mice followed by ADR injection shows a significant decrease in HNE levels when compared to the levels in brain isolated from ADR injected mice that were previously injected with saline (* p < 0.05, n = 5). The data are presented as mean ± SEM expressed as percentage of control.....	130
<b>Figure 7.5</b>	Plot of activity of GST in all the treatment groups. There is a significant decrease in GST activity in brain isolated from ADR-injected mice when compared to control (* p < 0.05, n = 5). I.p injection of GCEE increases GST activity significantly in brain. The brain isolated from GCEE-injected mice followed by ADR injection shows a significant increase in GST activity when compared to the activity in brain isolated from ADR injected mice that were previously injected with saline (** p < 0.01, n = 5). The data are presented as mean ± SEM expressed as percentage of control.....	132
<b>Figure 8.1</b>	Tricyclodecan-9-yl-xanthogenate (D609).....	140
<b>Figure 8.2</b>	Significant increase in ROS in synaptosomes isolated from saline injected gerbils and subsequently treated with Fe <sup>2+</sup> /H <sub>2</sub> O <sub>2</sub> or AAPH compared to ROS in synaptosomes isolated from saline-injected gerbils, * p < 0.005. Decreased ROS in synaptosomes isolated from gerbils injected i.p. with D609 subsequently treated with Fe <sup>2+</sup> /H <sub>2</sub> O <sub>2</sub> or AAPH relative to ROS in synaptosomes isolated from gerbils injected with saline and subsequently treated with Fe <sup>2+</sup> /H <sub>2</sub> O <sub>2</sub> or AAPH, ** p < 0. 005; the data are the mean ± SEM expressed as percentage of control values, (n = 6).....	147
<b>Figure 8.3</b>	Measurement of ROS generation using the oxidation-insensitive probe C369. The oxidation-insensitive fluorescence probe C369 was used as control to show esterase activity and drug efflux changes of DCFH-DA.....	148
<b>Figure 8.4</b>	Significant increase in protein carbonyl levels in synaptosomes isolated from saline injected gerbils and subsequently treated with Fe <sup>2+</sup> /H <sub>2</sub> O <sub>2</sub> or AAPH compared to protein carbonyls in synaptosomes isolated from saline injected gerbils, * p < 0.005. Decreased protein carbonyl level in synaptosomes isolated from gerbils injected i.p. with D609 subsequently treated with Fe <sup>2+</sup> /H <sub>2</sub> O <sub>2</sub> or AAPH relative to protein carbonyl level in synaptosomes isolated from gerbils injected with saline and subsequently treated with Fe <sup>2+</sup> /H <sub>2</sub> O <sub>2</sub> or AAPH, ** p < 0. 005; the data are the mean ± SEM expressed as percentage of control values, (n = 6).....	150
<b>Figure 8.5</b>	Representative western blot showing protein carbonyl levels from various treatments.....	151

<b>Figure 8.6</b>	Significant increase in protein bound HNE levels in synaptosomes isolated from saline injected gerbils and subsequently treated with $\text{Fe}^{2+}/\text{H}_2\text{O}_2$ or AAPH compared to protein carbonyls in synaptosomes isolated from saline injected gerbils, * $p < 0.005$ . Decreased protein bound HNE level in synaptosomes isolated from gerbils injected i.p. with D609 subsequently treated with $\text{Fe}^{2+}/\text{H}_2\text{O}_2$ or AAPH relative to protein carbonyl level in synaptosomes isolated from gerbils injected with saline and subsequently treated with $\text{Fe}^{2+}/\text{H}_2\text{O}_2$ or AAPH, ** $p < 0.005$ ; the data are the mean $\pm$ SEM expressed as percentage of control values, (n = 6).....	153
<b>Figure 8.7</b>	Significant increase in 3NT levels in synaptosomes isolated from saline-injected gerbils and subsequently treated with $\text{Fe}^{2+}/\text{H}_2\text{O}_2$ or AAPH compared to 3-NT levels in synaptosomes isolated from saline-injected gerbils, * $p < 0.005$ . Decreased 3NT levels in synaptosomes isolated from gerbils injected i.p. with D609 subsequently treated with $\text{Fe}^{2+}/\text{H}_2\text{O}_2$ or AAPH relative to protein carbonyl level in synaptosomes isolated from gerbils injected with saline and subsequently treated with $\text{Fe}^{2+}/\text{H}_2\text{O}_2$ or AAPH, ** $p < 0.005$ ; the data are the mean $\pm$ SEM expressed as percentage of control values, (n = 6).....	154
<b>Figure 9.1</b>	D609 prevents $\text{A}\beta(1-42)$ -induced ROS production. ROS levels were determined by the DCF fluorescence assay. Ctr = synaptosomes isolated from saline injected gerbils with no further treatment (n=6, six separate sets of experiments); D609 = synaptosomes isolated from D609 injected gerbils with no further treatment (n=6); $\text{A}\beta(1-42)$ = synaptosomes isolated from saline injected gerbils and treated with 10 $\mu\text{M}$ $\text{A}\beta(1-42)$ for 6 hrs (n=6); $\text{A}\beta(1-42)$ + D609 = synaptosomes isolated from D609 injected gerbils and treated with 10 $\mu\text{M}$ $\text{A}\beta(1-42)$ for 6hrs (n=6). The data are the mean $\pm$ S.E.M of six independent experiments, expressed as percentage of control values. Statistical comparison was made using ANOVA test (n=6 for each group). (*) $p < 0.005$ , $\text{A}\beta(1-42)$ vs Control; (**) $p < 0.002$ , $\text{A}\beta(1-42)$ vs $\text{A}\beta(1-42)$ + D609.....	171
<b>Figure 9.2a</b>	Protective effects of D609 on $\text{A}\beta$ -induced protein oxidation. Synaptosomes isolated from saline injected gerbils and treated with 10 $\mu\text{M}$ $\text{A}\beta(1-42)$ demonstrate a higher level of protein carbonyls than that of untreated controls (Ctr and D609). (*) $p < 0.001$ , $\text{A}\beta(1-42)$ vs Control. Synaptosomes isolated from D609 injected gerbils were completely protected from $\text{A}\beta$ -induced oxidative modifications [ $\text{A}\beta(1-42)$ + D609]. (**) $p < 0.004$ , $\text{A}\beta(1-42)$ vs $\text{A}\beta(1-42)$ + D609. (Data collected in collaboration with Dr. Marzia Perluigi).....	173
<b>Figure 9.2b</b>	Protective effects of D609 on $\text{A}\beta$ -induced protein oxidation. Synaptosomes isolated from saline injected gerbils and treated with 10 $\mu\text{M}$ $\text{A}\beta(1-42)$ and 10 $\mu\text{M}$ $\text{A}\beta(1-40)$ demonstrate a higher level of protein carbonyls than that of untreated controls, whereas 10 $\mu\text{M}$ $\text{A}\beta(42-1)$ did not show any significant increase in protein	

	carbonyls. Synaptosomes isolated from D609 injected gerbils were completely protected from A $\beta$ (1-42) and A $\beta$ (1-40) induced oxidative modifications. (*) p < 0.05, n = 5.....	174
<b>Figure 9.3</b>	Protective effect of D609 on A $\beta$ -induced 3-NT formation. 3-NT levels were determined as described in the “Material and Methods” section. Ctr = synaptosomes isolated from saline or D609 injected gerbils with no further treatment; D609 = synaptosomes isolated from D609 injected gerbils with no further treatment; A $\beta$ (1-42) = synaptosomes isolated from saline injected gerbils and treated with 10 $\mu$ M A $\beta$ (1-42) for 6 hrs; A $\beta$ (1-42) + D609 = synaptosomes isolated from D609 injected gerbils and treated with 10 $\mu$ M A $\beta$ (1-42) for 6 hrs. The data are the mean $\pm$ S.E.M expressed as percentage of control values (n=6). (*) p < 0.005, A $\beta$ (1-42) vs Control; (**) p < 0.05, A $\beta$ (1-42) vs A $\beta$ (1-42) + D609. (Data collected in collaboration with Dr. Marzia Perluigi).....	175
<b>Figure 9.4</b>	Protective effect of D609 on A $\beta$ -induced lipid peroxidation (HNE levels). HNE levels were determined as described in the “Material and Methods” section. Ctr = synaptosomes isolated from saline/D609 injected gerbils; D609 = synaptosomes isolated from D609 injected gerbils with no further treatment; A $\beta$ (1-42) = synaptosomes isolated from saline injected gerbils and treated with 10 $\mu$ M A $\beta$ (1-42) for 6 hrs; A $\beta$ (1-42) + D609 = synaptosomes isolated from D609 injected gerbils and treated with 10 $\mu$ M A $\beta$ (1-42) for 6 hrs. The data are the mean $\pm$ SEM expressed as percentage of control values (n=6). (*) p < 0.005, A $\beta$ (1-42) vs Control; (**) p < 0.05, A $\beta$ (1-42) vs A $\beta$ (1-42) + D609. (Data collected in collaboration with Dr. Marzia Perluigi).....	177
<b>Figure 9.5</b>	Western blot analysis of synaptosomes for iNOS protein expression levels. Samples containing 50 $\mu$ g of protein were loaded onto 10% SDS-PAGE gels, and the blots were probed with the polyclonal anti-iNOS antibody (1:1000) for 2 h. Immunoblots were scanned by densitometry and all values were normalized to $\beta$ -actin. A representative immunoblot (A) and densitometric values (B) are shown. Densitometric values represent the mean $\pm$ S.E.M. obtained from three independent experiments. Significant differences were assessed by ANOVA. * p < 0.01, control vs A $\beta$ (1-42); ** p < 0.05, A $\beta$ (1-42) + D609. (Data collected in collaboration with Dr. Marzia Perluigi).....	179
<b>Figure 10.1</b>	Shows the increment in protein carbonyl formation in brain mitochondria isolated from saline-injected gerbils and treated with various oxidants compared to control. The protective effects of D609 against protein carbonyl formation in brain mitochondria isolated from gerbils injected i.p. 1h before sacrifice with D609 and treated with AAPH, Fe <sup>2+</sup> /H <sub>2</sub> O <sub>2</sub> and A $\beta$ (1-42) also are shown. *p<0.01 and **p<0.001 compared to control and # p<0.01 compared to oxidant treatment. The data are presented as mean $\pm$ SEM expressed as percentage of control (n=6). (Data collected in	

	collaboration with Dr MubeenAnsari).....	198
<b>Figure 10.2</b>	Shows the increment in 3-NT levels in brain mitochondria isolated from saline-injected gerbils and subsequently treated with AAPH, $\text{Fe}^{2+}/\text{H}_2\text{O}_2$ or $\text{A}\beta$ (1-42) compared to 3NT levels in brain mitochondria isolated from saline-injected gerbil that received no treatment of any oxidant, * $p<0.01$ and ** $p<0.001$ . This figure also shows decreased 3NT levels shows in brain mitochondria isolated from gerbils previously injected i.p. with D609 1 h before sacrifice and treated with AAPH, $\text{Fe}^{2+}/\text{H}_2\text{O}_2$ or $\text{A}\beta$ (1-42) compared to the oxidant treatment but no prior injection of D609, # $p<0.01$ . The data are presented as mean $\pm$ SEM expressed as percentage of control (n=6). (Data collected in collaboration with Dr Mubeen Ansari).....	199
<b>Figure 10.3</b>	Shows the significantly elevated protein-bound HNE content in brain mitochondria isolated from saline-injected gerbils and treated with different oxidants [AAPH, $\text{Fe}^{2+}/\text{H}_2\text{O}_2$ or $\text{A}\beta$ (1-42)]. The protective effects of D609 against HNE formation of protein-bound HNE in brain mitochondria isolated from gerbil injected i.p. with D609 1 h before sacrifice and treated with AAPH, $\text{Fe}^{2+}/\text{H}_2\text{O}_2$ or $\text{A}\beta$ (1-42) also are shown. * $p<0.01$ and ** $p<0.001$ compared to control, # $p<0.01$ and ## $p<0.001$ compared to oxidant treatment. The data are presented as mean $\pm$ SEM expressed as percentage of control (n=6). (Data collected in collaboration with Dr Mubeen Ansari).....	200
<b>Figure 10.4a</b>	Shows a significant decrement in GSH levels in brain mitochondria isolated from saline-injected gerbils and subsequently treated with AAPH, $\text{Fe}^{2+}/\text{H}_2\text{O}_2$ or $\text{A}\beta$ (1-42) compared to GSH levels in brain mitochondria isolated from saline-injected gerbils not subjected to treatment of any oxidant. Also shown is the protection of GSH levels in brain mitochondria isolated from gerbils previously injected i.p. with D609 1 h before sacrifice and treated with AAPH, $\text{Fe}^{2+}/\text{H}_2\text{O}_2$ or $\text{A}\beta$ (1-42) compared to GSH levels in brain mitochondria isolated from saline-treated gerbils and then treated with oxidants. * $p<0.01$ and ** $p<0.001$ compared to control, # $p<0.01$ and ## $p<0.01$ compared to oxidant treatment. The data are presented as mean $\pm$ SEM expressed as percentage of control (n=6).....	202
<b>Figure 10.4b</b>	Shows the increased level of GSSG in brain mitochondria isolated from saline-injected gerbils and subsequently treated with AAPH, $\text{Fe}^{2+}/\text{H}_2\text{O}_2$ or $\text{A}\beta$ (1-42) as compared to GSSG levels in brain mitochondria isolated from saline-injected gerbils but not subjected to treatment of any oxidant. The reduction in GSSG level shows in brain mitochondria isolated from gerbils previously injected i.p. with D609 1 h before sacrifice and treated with AAPH, $\text{Fe}^{2+}/\text{H}_2\text{O}_2$ or $\text{A}\beta$ (1-42) compared to GSSG levels in brain mitochondria isolated from saline-treated gerbil and then treated with oxidants. * $p<0.01$ and ** $p<0.001$ compared to control, # $p<0.01$ and ##	

	p<0.01 compared to oxidant treatment. The data are presented as mean $\pm$ SEM expressed as percentage of control (n=6).....	203
<b>Figure 10.4c</b>	Shows the ratio of GSH/GSSG, decreased in brain mitochondria isolated from saline-injected gerbils and subsequently treated with AAPH, Fe <sup>2+</sup> /H <sub>2</sub> O <sub>2</sub> or A $\beta$ (1-42), compared to the GSH/GSSG ratio in brain mitochondria isolated from saline-injected gerbils but not subjected to treatment of any oxidant. The increment in the ratio of GSH/GSSG in brain mitochondria isolated from gerbils previously injected i.p. with D609 1 h before sacrifice and then treated with AAPH, Fe <sup>2+</sup> /H <sub>2</sub> O <sub>2</sub> or A $\beta$ (1-42) compared to this ratio determined in brain from mice treated with oxidant but no pre-injection of gerbils with D609 is also shown. *p<0.01 and **p<0.001 compared to control, # p<0.01 and ## p<0.01 compared to oxidant treatment. The data are presented as mean $\pm$ SEM expressed as percentage of control (n=6).....	204
<b>Figure 10.5</b>	Shows the increased level of cytochrome-c released from brain mitochondria isolated from saline-injected gerbils and treated with various oxidants (AAPH, Fe <sup>2+</sup> /H <sub>2</sub> O <sub>2</sub> or A $\beta$ (1-42) as compared to cytochrome-c released from brain mitochondria isolated from saline-injected gerbils but not subjected to treatment of any oxidant. Also shown is the decrement of cytochrome-c release from brain mitochondria isolated from gerbils previously injected i.p. with D609 1 h before sacrifice and treated with AAPH, Fe <sup>2+</sup> /H <sub>2</sub> O <sub>2</sub> or A $\beta$ (1-42) compared to that released from brain mitochondria isolated from gerbils subjected to oxidant treatment. The D609 only treatment shows significantly less cytochrome-c release compared control. *p<0.01 as compared to control, # p<0.01 compared to oxidant treatment. The data are presented as mean $\pm$ SEM expressed as percentage of control (n=5). (Data collected in collaboration with Dr Mubeen Ansari).....	206
<b>Figure 11.1</b>	Levels of protein carbonyl in all the treatment groups. There is a significant increase in protein carbonyl level in brain isolated from APP/PS-1 mice that were given normal drinking water when compared to WT groups (* p < 0.05, n = 6). Administration of NAC in drinking water to APP/PS-1 mice decreases protein carbonyl level significantly in brain. The brain isolated from APP/PS-1 mice treated with NAC in water shows a significant decrease in protein carbonyl levels when compared to the levels in brain isolated from APP/PS-1 mice that were given normal drinking water (* p < 0.05, n = 6). The data are presented as mean $\pm$ SEM expressed as percentage of control.....	225
<b>Figure 11.2</b>	Levels of 3NT in all the treatment groups. There is a significant increase in 3NT level in brain isolated from APP/PS-1 mice that were given normal drinking water when compared to WT groups (* p < 0.05, n = 6). Administration of NAC in drinking water to APP/PS-1 mice decreases 3NT level significantly in brain. The brain isolated from APP/PS-1 mice treated with NAC in water shows a significant decrease in 3NT levels when compared to the	

	levels in brain isolated from APP/PS-1 mice that were given normal drinking water (* p < 0.05, n = 6). The data are presented as mean ± SEM expressed as percentage of control.....	226
<b>Figure 11.3</b>	Levels of protein-bound HNE in all the treatment groups. There is a significant increase in protein-bound HNE level in brain isolated from APP/PS-1 mice that were given normal drinking water when compared to WT groups (* p < 0.05, n = 6). Administration of NAC in drinking water to APP/PS-1 mice decreases protein-bound HNE level significantly in brain. The brain isolated from APP/PS-1 mice treated with NAC in water shows a significant decrease in protein-bound HNE levels when compared to the levels in brain isolated from APP/PS-1 mice that were given normal drinking water (* p < 0.05, n = 6). The data are presented as mean ± SEM expressed as percentage of control.....	227
<b>Figure 11.4a</b>	Levels of GPx in all the treatment groups. There is a significant decrease in GPx level in brain isolated from APP/PS-1 mice that were given normal drinking water when compared to WT groups (* p < 0.05, n = 6). Administration of NAC in drinking water to APP/PS-1 mice increased GPx level significantly in brain. The brain isolated from APP/PS-1 mice treated with NAC in water shows a significant increase in GPx levels when compared to the levels in brain isolated from APP/PS-1 mice that were given normal drinking water (* p < 0.05, n = 6). The data are presented as mean ± SEM expressed as percentage of control.....	229
<b>Figure 11.4b</b>	A representative western blot showing levels of GPx in various treatment groups. GAPDH was used as loading control.....	230
<b>Figure 11.5</b>	Activity of GPx in all the treatment groups. There is a significant decrease in GPx activity in brain isolated from APP/PS-1 mice that were given normal drinking water when compared to WT groups (* p < 0.05, n = 6). Administration of NAC in drinking water to APP/PS-1 mice increased GPx activity significantly in brain. The brain isolated from APP/PS-1 mice treated with NAC in water shows a significant increase in GPx activity when compared to the activity in brain isolated from APP/PS-1 mice that were given normal drinking water (* p < 0.05, n = 6). The data are presented as mean ± SEM expressed as percentage of control.....	231



## **Chapter 1**

### **Introduction**

The studies presented in this dissertation were completed with the goal of understanding the role of oxidative stress in various neurodegenerative condition, specifically focusing on Alzheimer's disease (AD) and finding efficient therapeutic towards reducing oxidative stress in these neurodegenerative conditions. Oxidative stress plays a key role in cause or consequence of various neurodegenerative disorders including AD (Hensley, Hall et al., 1995; Markesbery and Lovell, 1998; Butterfield, Drake et al., 2001; Butterfield and Lauderback, 2002), which affects more than 4 million American and is one of the leading causes of death in United States. There is no efficient therapy towards treatment of this dreaded disease as of now. Pathologically, AD is characterized by presence of senile plaques comprising aggregated amyloid  $\beta$ -peptide ( $A\beta$ ), neurofibrillary tangles consisting of hyperphosphorylated tau, and synapse loss (Katzman and Saitoh, 1991; Bosetti, Brizzi et al., 2002). Etiologically, the free radical-mediated oxidative stress hypothesis in AD has gained considerable importance in recent times (Butterfield, Drake et al., 2001). In AD brain, oxidative stress leads to significant protein oxidation (Butterfield and Lauderback, 2002), DNA and RNA oxidation (Mecocci, MacGarvey et al., 1993; Lovell, Gabbita et al., 1999; Nunomura, Perry et al., 1999; Wang, Xiong et al., 2005), lipid peroxidation (Markesbery and Lovell, 1998), and neuronal dysfunction or death. Increased production of ROS and RNS along with depletion in antioxidant capacity is observed in AD and other neurodegenerative disorders [reviewed in (Beckman and Ames, 1998)], and, consistent with this observation,  $\alpha$ -tocopherol (vitamin E) administration in AD patients delayed its

progression when compared to placebo treated control (Sano, Ernesto et al., 1997), suggesting that oxidative stress-mediated AD pathogenesis can be altered by antioxidant therapy. In contrast, recent studies with mild cognitive impairment (MCI), arguably the earliest form of AD, do not support this view (Petersen, Thomas et al., 2005).

Mitochondrial electron transport is a potential source of ROS production (Ide, Tsutsui et al., 1999). It is now well known that ROS such as superoxide radical anion ( $O_2^{\cdot-}$ ), hydroxyl radical ( $OH^{\cdot}$ ), hydrogen peroxide ( $H_2O_2$ ), and peroxynitrite ( $ONOO^{\cdot}$ ) contribute to neurodegeneration (Zhang, Dawson et al., 1994; Cadenas and Davies, 2000; Rego and Oliveira, 2003; Ansari, Ahmad et al., 2004; Tangpong, Cole et al., 2006a; Tangpong, Cole et al., 2006b). Mitochondrial membrane potential depolarization induces cytochrome-c release into the cytoplasm and elevates the activity of caspase-3, suggesting a role for mtDNA-derived mitochondrial dysfunction in AD degeneration (Bosetti, Brizzi et al., 2002).

Protein oxidation either by ROS or lipid peroxidation products such as 4-hydroxy 2- nonenal results in altered protein structure or loss of protein function, which may lead to neuronal degeneration (Stadtman and Berlett, 1997). Protein oxidation markers such as introduction of carbonyl functionality or nitration of tyrosine residues on proteins often lead to conformation changes in proteins (Subramaniam, Roediger et al., 1997) that often leads to protein dysfunction (Butterfield and Stadtman, 1997). As a part of this dissertation, we have used four different oxidants,  $Fe^{2+}/H_2O_2$  (hydroxyl radical producer) or 2,2- Azobis (2-amidino-propane) dihydrochloride (AAPH) (alkoxyl and peroxy radical producers), A $\beta$  (1-42) and adriamycin (ADR). All these oxidants are known to cause protein oxidation and lipid peroxidation.

Major pathological hallmarks of AD include loss of synapses and the presence of senile plaques and neurofibrillary tangles (Katzman and Saitoh, 1991). The major protein component of the core of senile plaques is A $\beta$ . The mechanisms involved in the A $\beta$ -mediated neurotoxicity are unknown, but there is evidence suggesting that oxidative stress plays a key role (Butterfield, Drake et al., 2001; Butterfield and Lauderback, 2002; Canevari, Abramov et al., 2004; Butterfield and Boyd-Kimball, 2005). Increased production of reactive oxygen and nitrogen species such as superoxide and nitric oxide together with imbalance of antioxidant defenses was observed in neuronal systems after A $\beta$ (1-42) treatment (Keller, Pang et al., 1997; Yatin, Varadarajan et al., 1999; Varadarajan, Yatin et al., 2000; Butterfield, 2002). Previous studies from our laboratory and others reported that A $\beta$ (1-42) induces reactive oxygen species (ROS) production, *in vitro* and *in vivo* protein oxidation, DNA and RNA oxidation and lipid peroxidation (Keller, Lauderback et al., 2000; Butterfield, 2002; Boyd-Kimball, Castegna et al., 2005).

ADR, a cancer chemotherapeutic drug used to treat solid tumors, is known to cause side effects in heart and brain (Steinherz, Steinherz et al., 1991; Joshi, Sultana et al., 2005b; Tangpong, Cole et al., 2006a; Tangpong, Cole et al., 2006b). Cardiomyocytes treated with ADR have elevated levels of protein oxidation and lipid peroxidation (DeAtley, Aksenov et al., 1998). Free radical scavengers are known to protect cardiomyocytes from this effect (DeAtley, Aksenov et al., 1999). Brain isolated from mice treated peripherally with ADR shows evidence of oxidative damage and mitochondrial dysfunction (Joshi, Sultana et al., 2005b; Tangpong, Cole et al., 2006a; Tangpong, Cole et al., 2006b). Patients under long-term treatment with ADR for breast and lung cancer have shown symptoms of cognitive dysfunction such as lack of

concentration, forgetfulness inability to multi-task, short term memory impairment and dizziness, often lasting years after cessation of therapy (Meyers, 2000; Schagen, Hamburger et al., 2001; Freeman and Broshek, 2002). The side effects in heart limit the use of ADR in chemotherapy, while the side effects in brain limit the quality of life of patients undergoing chemotherapy.

Recently, proteomics along with advances in bioinformatics tools have lead to the identification, characterization and sequencing of proteins in various organisms, including humans. Using redox proteomics (Dalle-Donne, Scaloni et al., 2006) our laboratory has shown many key proteins that are oxidized or differentially expressed in various neurodegenerative conditions or models thereof, such as Alzheimer's disease (AD) (Butterfield and Boyd-Kimball, 2004), ageing (Poon, Calabrese et al., 2006), amyotrophic lateral sclerosis (ALS) (Perluigi, Fai Poon et al., 2005; Poon, Hensley et al., 2005), Parkinson's disease (PD) (Poon, Frasier et al., 2005), mild cognitive impairment (MCI) (Butterfield, Poon et al., 2006) and Huntington's disease (Perluigi, Poon et al., 2005). Although it is clear from the dissertation research described below that *in vivo* ADR increases protein oxidation in brain, it is not clear which specific brain proteins show increased oxidative damage. We used 2-dimensional gel electrophoresis (2DE) coupled with mass spectrometric analysis (expression proteomics) to identify proteins that are differentially expressed and 2DE followed by Western blot coupled with mass spectrometric analysis (redox proteomics) to identify proteins that are oxidized in brain isolated from mice injected i.p. with ADR as a part of this dissertation.

Glutathione (GSH) is the most abundant endogenous nonenzymatic antioxidant present in brain and is found in millimolar concentrations. GSH is an oxyradical

scavenger, thereby protecting against oxidative damage by free radicals and inhibits lipid peroxidation and DNA damage (Meister, 1995; Darley-USmar and Halliwell, 1996; Sies, 1999; Schulz, Lindenau et al., 2000; Hansen, Go et al., 2006). GSH has been implicated in a wide range of metabolic processes, including cell division, DNA repair, regulation of enzyme activity, activation of transcription factors, cellular homeostasis and protection against oxidative damage (Meister and Anderson, 1983). The nervous system is particularly susceptible to oxidative insults, and dependent on its glutathione defense.

Due to the involvement of oxidative stress-mediated toxicity in neurodegenerative events and neuronal cell death (Good, Werner et al., 1996; Moreira, Smith et al., 2005), various experimental approaches for effective protection by antioxidants have emerged. In addition, antioxidant therapy is being discussed for Parkinson's disease (Ebadi, Srinivasan et al., 1996; Prasad, Cole et al., 1999), ischemia (Marczin, El-Habashi et al., 2003) as well as for AD (Grundman and Delaney, 2002; Gilgun-Sherki, Melamed et al., 2003) and other age-related disorders (Ames, 2004). Numerous potential free-radical scavengers have been tested in different experimental paradigms of oxidative stress-induced cell death, such as Vitamin E (Behl, Davis et al., 1992), Vitamin C, melatonin (Pappolla, Sos et al., 1997), ginkgo biloba (Smith and Luo, 2003), steroid hormones (Goodman, Bruce et al., 1996; Behl, Skutella et al., 1997), N-acetylcysteine (Adair, Knoefel et al., 2001), etc. However, many clinical trials are still unsuccessful because most of the antioxidants tested are poorly active in crossing the blood brain barrier (BBB).

Depletion of GSH is known to be involved in several neurodegenerative disorders (Benzi and Moretti, 1995b; Markesbery, 1997; Butterfield, Castegna et al., 2002a). Many

attempts have been made to develop antioxidant compounds that can act as precursor of GSH or mimic GSH as scavenger of reactive oxygen species (ROS) and to maintain the intracellular redox state. Increase in endogenous GSH levels by dietary or pharmacological intake of GSH precursor or GSH mimetic protects brain against oxidative stress (Anderson and Luo, 1998; Butterfield, Drake et al., 2001; Halliwell, 2001). Considering the importance of developing new antioxidant compounds and the relevance of their application in the treatment of neurodegenerative diseases, in this dissertation research we focused our attention on glutathione mimetic, tricyclodecan-9-yl-xanthogenate (D609), the glutathione precursor, N-acetylcysteine (NAC), and  $\gamma$ -glutamyl cysteine ethyl ester (GCEE).

In summary, this dissertation research has used synaptosomes, mitochondria and brain homogenates to address the following hypothesis:

1. Adriamycin-mediated oxidative stress leads to significant protein oxidation, lipid peroxidation and alteration in glutathione levels and GSH related enzyme activities.
2.  $\gamma$ -Glutamyl cysteine ethyl ester (GCEE), *in vivo*, increases the GSH level and reduces the protein oxidation and lipid peroxidation in brain isolated from mice that were previously injected with GCEE followed by ADR injection when compared to brain isolated from mice that are previously injected with saline followed by ADR injection.
3. D609 prevents oxidative stress-mediated by  $\text{Fe}^{2+}/\text{H}_2\text{O}_2$ , AAPH and  $\text{A}\beta(1-42)$  in synaptosomes and mitochondria isolated from brain of gerbils previously injected with D609.

4. NAC, delivered via drinking water, decreases oxidative stress, *in vivo*, mediated by A $\beta$ (1-42) in the APP/PS-1 mouse, a model of AD.

## **Chapter 2**

### **Background**

#### **2.1. Oxidative Stress and Neurodegeneration**

##### **2.1.1. Overview of oxidative stress**

Free radical-mediated oxidative stress has been implicated in numerous disorders, particularly in neurodegenerative disorders. However, the term “oxidative stress” is often misinterpreted since the processes involved are poorly understood. A free radical is a species that contains one or more unpaired electrons. Generally, free radicals are highly reactive and are known to react vigorously with other less reactive non-radical species to produce new free radicals in a chain reaction. It is these chain reactions that can lead to formation of ROS (e.g., superoxide radical  $O_2^{\cdot -}$  or hydrogen peroxide  $H_2O_2$ ) and RNS (e.g. nitric Oxide radical  $NO^{\cdot}$  or dinitrogen tetroxide  $N_2O_4$ ) that can further damage biomolecules such as proteins and lipids (Halliwell, 2001). Reactive species are found both intracellularly and extracellularly. The source of free radicals could be exogenous environmental factors such as ionizing radiation, photochemical reactions, among others or endogenous biochemical and enzymatic processes. Figure 2.1 shows some of the reactions that lead to the formation of ROS/RNS.

Various antioxidant systems are operational in the human body that inhibits the activity of ROS/RNS. Some of the examples of antioxidant systems are antioxidant enzymes (e.g., superoxide dismutase and glutathione peroxidase), antioxidant proteins (e.g., thioredoxin) and antioxidant molecules (e.g., lipoic acid, GSH, vitamin E), among others. During disease conditions, either the level of ROS/RNS goes up or antioxidant



capacity is decreased or both occur at the same time (Halliwell, 2001). This condition is often described as oxidative stress.

### 2.1.2. Free radical theory in neurodegeneration

Free radicals in biological systems are produced by metal catalyzed reactions called Fenton reaction (Hensley, Carney et al., 1994) as shown in Figure 2.1. The hydroxyl radicals are particularly damaging to proteins, lipids and nearby DNA, reacting at diffusion-limited rates.  $O_2$  is the terminal acceptor of electrons in the electron transport chain of oxidative phosphorylation processes in mitochondria and forms superoxide radicals ( $O_2^{\cdot-}$ ).  $O_2^{\cdot-}$  is relatively stable and being a free radical itself leads to formation of other ROS.  $O_2$  undergoes a four electron reduction process in its conversion to water (Fridovich, 1978a). Approximately 2% of  $O_2$  is leaked out of mitochondria as toxic intermediates before its conversion to water [reviewed in (Beckman and Ames, 1998)]. Trace amount of iron present in cell reacts with the  $O_2$  to form highly toxic hydroxyl radicals.

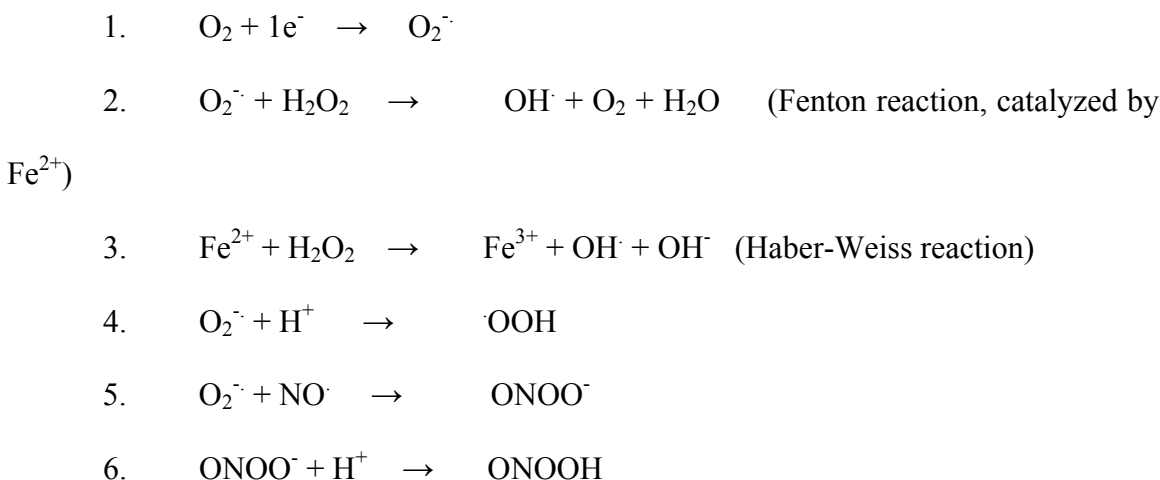


**Figure 2.1:** Reaction leading to formation of ROS/RNS

ADR is a quinone-containing anthracyclin drug (Figure 2.2) used in treating breast cancer and various solid tumors. ADR is known to generate superoxide radical ( $O_2^{\cdot -}$ ) (Deres, Halmosi et al., 2005). A free radical-mediated mechanism of toxicity of ADR is widely accepted. The quinone in ADR undergoes one electron reduction to generate semiquinone, which is a free radical, and in the presence of oxygen converts back to quinone producing  $O_2^{\cdot -}$ , a process known as redox cycling. ADR dependent redox cycling is likely activated by nitric oxide synthase and cytochrome P 450 (Gutierrez, 2000; Deres, Halmosi et al., 2005). Toxicity mediated by ADR is known to target mitochondria, and NADH dehydrogenase, a mitochondrial enzyme, stimulates ADR to form semiquinone radical and  $O_2^{\cdot -}$  (Doroshov and Davies, 1986).  $O_2^{\cdot -}$  radicals are converted to hydrogen peroxide ( $H_2O_2$ ) enzymatically by superoxide dismutase (Fridovich, 1978b). Superoxide radical can react with  $H_2O_2$  and other reactive species to generate various other ROS/RNS (Halliwell and Gutteridge, 1999). All these reactive species target nearby protein, lipids and other biomolecules leading to neurodegeneration.

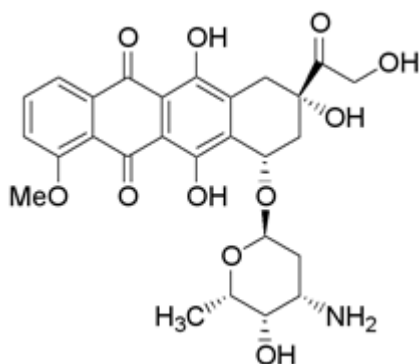


**Figure 2.2:** Adriamycin

The free radical theory of aging proposed by Denham Harman in 1956 (Harman, 1956) states that oxyradicals or ROS, produced during aerobic respiration results in cumulative damage leading to aging and eventual death. The brain is particularly

vulnerable to free radical damage and oxidative stress because of following reasons: the brain has high amount of polyunsaturated fatty acids (PUFA) that are easily oxidizable by ROS; there is a significant amount of trace metal ions such as iron (II) and copper (I) that can catalyze various redox reactions to produce ROS; the brain consumes relatively more oxygen when compared to the other organs; the brain has relatively low antioxidant levels; the terminally differentiated mature neurons in brain are incapable of dividing and hence, once damaged are lost leading to neurodegeneration.

### **2.1.3. Targets of Oxidation**

#### **2.1.3.1. Proteins**

Proteins are one of the most important classes of biomolecules that are involved in almost all physiological and biochemical functions. The genetic message from DNA is expressed in the form of proteins. Twenty different amino acids form the building block of proteins, which are composed of amino acids linked to each other by a peptide bond. An amino acid sequence in the polypeptide chain provides the information of its primary structure. The tertiary or quaternary structure of proteins can provide important clues about their respective function. Among others, the important function of some proteins is biocatalysis as enzymes, cellular functions, such as cell signaling and ligand transport and as structural proteins. Being one of the most important biomolecules, it is important to study protein oxidation, its cause and consequences and any modification or degradation following oxidation.

Proteins are highly sensitive to ROS/RNS-mediated oxidative modifications. Proteins can also be modified by reactive alkenals produced during ROS-mediated oxidation of lipids (Esterbauer, Schaur et al., 1991) and glycated proteins (Nagaraj and

Monnier, 1995). The site of oxidation in proteins is basically amino acid residue side chains that can lead to fragmentation of the polypeptide chain, and the formation of protein-protein cross-linked aggregates that often changes the conformation, including protein unfolding of functional protein and thereby render a protein inactive [Reviewed in (Butterfield and Stadtman, 1997; Stadtman and Berlett, 1997)]. Possible consequences of such changes usually increase the exposure of hydrophobic residues of proteins and thus modify the intrinsic capacity of protein function, such as binding to receptor or ligands, and interaction with membrane lipid bilayer. Among other consequences, protein oxidation also leads to trigger the synthesis of certain “stress proteins”, such as heat shock proteins (HSPs) (Welch, 1992) and/or increases in susceptibility towards proteolytic degradation that is often preceded by their post translational modification, such as ubiquitinylation (Davies, Lin et al., 1987).

The two most important oxidative modifications of proteins are formation of protein carbonyls and nitration of tyrosine residues on protein to form 3-nitrotyrosine (3NT). The carbonyl functionality can be introduced in proteins by mechanisms, such as  $\beta$ -scission and peptide bond cleavage following reaction of  $\text{OH}^\cdot$  radical, formed by metal catalyzed cleavage of  $\text{H}_2\text{O}_2$ , with any amino acid residue on a protein [reviewed in (Stadtman and Berlett, 1997)].

The metal ion-catalyzed oxidation of some amino acid residues on proteins leads to the formation of protein carbonyl derivatives (Levine, Williams et al., 1994). Some of the examples of protein carbonyl derivatives are formation of glutamic semialdehyde derivatives of the protein following metal-catalyzed oxidation of proline and arginine residues of proteins, formation of adipic semialdehyde derivatives following oxidation of

lysine residues (Amici, Levine et al., 1989; Daneshvar, Frandsen et al., 1997; Requena, Chao et al., 2001), oxohystidine, etc. Since the formation of protein carbonyl groups is highly pronounced when compared to other oxidative modifications, determining the level of protein carbonyl groups become the most important marker of protein oxidation during various neurodegenerative disorder conditions including Alzheimer's disease (AD) (Stadtman and Berlett, 1997).

Nitric oxide ( $\text{NO}^\cdot$ ), produced in the metabolism of arginine, reacts rapidly with  $\text{O}_2^\cdot$  to form the highly reactive peroxynitrite ( $\text{ONOO}^\cdot$ ) (Ischiropoulos, Zhu et al., 1992). A key oxidative stress marker of peroxynitrite ( $\text{ONOO}^\cdot$ )-mediated nitration of tyrosine residues on proteins is 3NT.  $\text{CO}_2$  is known to stimulate the ( $\text{ONOO}^\cdot$ )-dependent nitration of tyrosine residues (Denicola, Freeman et al., 1996). Nitration of tyrosine may prevent phosphorylation of tyrosine thereby preventing various signaling pathway that can have profound consequences in rendering protein inactive (Ischiropoulos, Zhu et al., 1992). Elevated levels of 3NT have been found in various neurodegenerative disorders, such as AD when compared to normal subjects (Hensley, Maidt et al., 1998; Castegna, Thongboonkerd et al., 2003; Sultana, Poon et al., 2006a). It has also been shown that several key proteins in AD brain are nitrated when compared to age-matched controls (Castegna, Thongboonkerd et al., 2003). Nitrated tyrosine residues are also found in degenerating motor neurons of amyotrophic lateral sclerosis (ALS) subjects (Abe, Pan et al., 1995) and vulnerable neurons of Parkinson's disease (PD) (Good, Hsu et al., 1998). Hence, detection of 3NT may illustrate an important role in pathogenesis of various neurodegenerative disorders.

### **2.1.3.2. Lipids**

Unlike proteins, lipids are non-polymeric biomolecules, which are relatively small when compared to proteins. Lipids consist of a hydrophilic polar “head” and a hydrophobic “tail” consisting of acyl chains of variable length. As amphipathic molecules, lipids tend to aggregate with their hydrophilic head exposed at the lipid-water interface and their hydrophobic tails sequestered from the aqueous medium. Lipids are the major component of cell membranes and arranged in a bilayer. The formation of lipid bilayers is spontaneous and the increased entropy of the aqueous medium serves as the driving force for this kind of arrangement. This kind of arrangement results in formation of a hydrophobic domain that limits the permeability of polar species.

Glycerophospholipids are major the class of lipids that make the important part of cell membrane. These glycerophospholipids consist of glycerol backbone that is derivatized at the three alcohol functionalities (Figure 2.3). A1 and A2 are acyl chains derived from fatty acids. Fatty acids can be saturated (palmitic and stearic acid) or unsaturated (oleic acid, for example). An acyl chain with more than one unsaturation is known as a polyunsaturated fatty acid (PUFA). Lipids are more susceptible to oxidation if they have more unsaturation in there fatty acid  $\beta$ -chain and high solubility of nonpolar, paramagnetic oxygen in bilayer (Esterbauer and Ramos, 1996). High content of PUFA makes brain more vulnerable to oxidative damage.

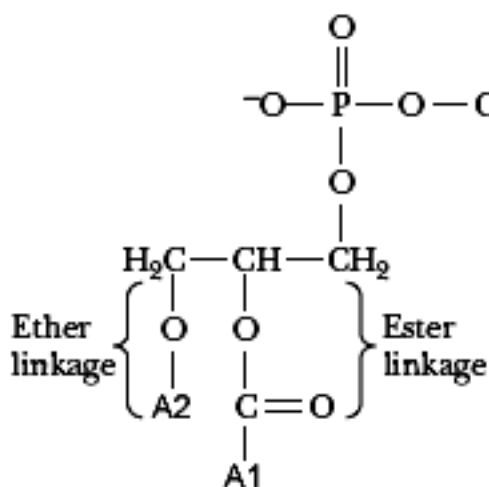
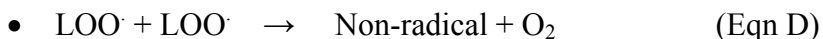


**Figure 2.3:** Glycerophospholipids. Adapted from (Garrett and Grisham, 1995) with slight modification.

Lipids undergo peroxidation upon attack by a free radical. The cascades of events that follow are shown below (Eqn A to D). From the unsaturated sites of lipids, hydrogen is abstracted that results in formation of carbon-centered lipid radical ( $\text{L}^\cdot$ ).  $\text{L}^\cdot$  reacts with readily available paramagnetic  $\text{O}_2$  to form a lipid peroxy radical ( $\text{LOO}^\cdot$ ). These peroxy radicals propagate the chain reaction by reacting with nearby lipids to form lipid hydroperoxide ( $\text{LOOH}$ ) and another carbon-centered lipid radical. The chain reaction is terminated by reaction between two peroxy radical to form a non radical species and  $\text{O}_2$ .



Adapted from (Esterbauer and Ramos, 1996)

Lipid peroxidation often leads to formation of toxic reactive alkenal species, such as 4-hydroxy 2- nonenal (HNE), acrolein (2-propane 1-al) and malenaldehyde. These alkenals binds to the protein by Michael addition to form covalent adducts with cysteine, lysine or histidine residues (Figure 2.4) and render them inactive (Butterfield and Stadtman, 1997). Antioxidant defense systems involving glutathione and its dependent enzyme glutathione-S-transferase help in clearing these lipids peroxidation products with the help of a detoxification protein, the multi drug resistance protein-1 (MRP1) (Sultana and Butterfield, 2004). Growing number of evidences suggest increased lipid peroxidation in various neurodegenerative disorders, including AD. HNE and acrolein are known to be increased in AD brain (Markesbery and Lovell, 1998; Lovell, Xie et al., 2001). Likewise, isoprostanes and neuroprostanes (markers of lipid peroxidation) levels are increased in AD brain (Montine, Neely et al., 2002). Lipid oxidation can also be reduced by lipid soluble antioxidants, such as  $\alpha$ -tocopherol (Esterbauer and Ramos, 1996).

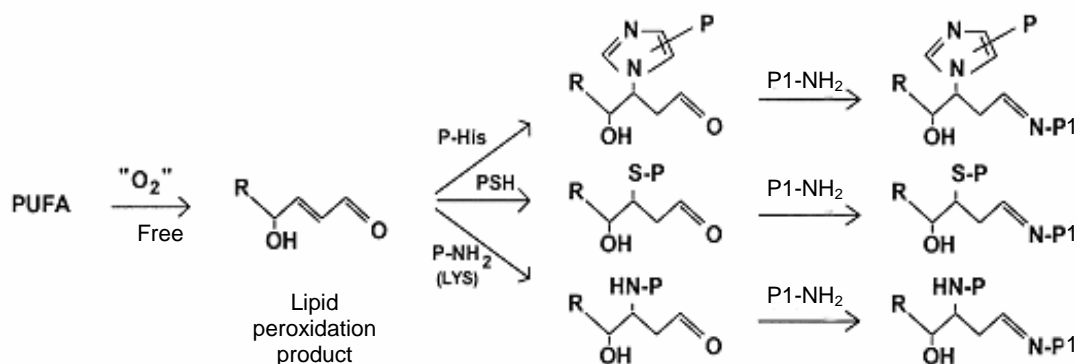


**Figure 2.4:** Reaction of reactive alkenals with histidine, cysteine and lysine to form Michael adducts. P1 refers to another protein. Figure also shows formation of cross-linked derivatives between proteins. Adapted from (Stadtman and Berlett, 1997).



## **2.2. Alzheimer's Disease**

### **2.2.1. Overview**

AD is an age-associated progressive neurodegenerative disorder characterized by memory loss, cognitive dysfunction and is the most common form of dementia in elderly population. More than 4 million Americans are affected by this disease out of which 7-10 % fall in the age group of 65-74 and more 80% are over 85 years of age (Price, Sisodia et al., 1998). Pathological hallmarks of AD includes brain atrophy due to neuronal and synapse loss, senile plaques predominantly consisting of fibrillar amyloid  $\beta$ -peptide and neurofibrillary tangles (NFT) made up of hyperphosphorylated tau, a cytoskeletal protein (Van Uden, Sagara et al., 2000). Some of the major risk factors for AD are unhealthy aging in sporadic AD cases, the presence of ApoE-4 alleles in both sporadic and familial AD (FAD) (Namba, Tomonaga et al., 1991) and genetic factors, such as mutation in amyloid precursor protein (APP) and presenilin-1 in FAD (Lee, Borchelt et al., 1997) among others. Growing evidence shows that AD brain is under tremendous oxidative stress. There is increased protein oxidation [reviewed in (Markesbery, 1997; Butterfield, Drake et al., 2001)] and lipid peroxidation (Markesbery and Lovell, 1998; Lauderback, Hackett et al., 2001; Lovell, Xie et al., 2001) in AD brain when compared to aged matched control, and antioxidant therapy, known to slow progress of AD (Sano, Ernesto et al., 1997), may reduce this effect.

### **2.2.2. $A\beta(1-42)$ -mediated oxidative stress in AD**

The major protein component of senile plaques is amyloid  $\beta$ -peptide ( $A\beta$ ).  $A\beta$  is formed upon proteolytic processing (Figure 2.5) by  $\beta$ - and  $\gamma$ -secretases (Haass and De Strooper, 1999) of the 695 amino acid APP, a ubiquitously expressed transmembrane

glycoprotein (Glennner and Wong, 1984; Glennner, Eanes et al., 1988). The 40 or 42 amino acid A $\beta$  peptide is the major component of senile plaques and are toxic to neuronal cells in culture (Yankner, Duffy et al., 1990). Another secretase involved in APP processing is  $\alpha$ -secretase, the product of which is a large soluble fragment (sAPP $\alpha$ ), which is possibly involved in preventing excitotoxicity by regulating intracellular calcium levels (Mattson, Cheng et al., 1993). The amyloid  $\beta$ -cascade hypothesis, suitably updated, postulates that A $\beta$  is likely central to the pathogenesis of AD (Hardy and Allsop, 1991; Smith, Chen et al., 1999; Selkoe, 2001). The mechanisms involved in the A $\beta$ -mediated neurotoxicity are unknown, but there is evidence suggesting that oxidative stress plays a key role (Butterfield, Drake et al., 2001; Butterfield and Lauderback, 2002; Canevari, Abramov et al., 2004). Growing attention has been focused to investigate the oxidative mechanism of A $\beta$  toxicity and as well in the search for novel neuroprotective agents. Previous studies from our laboratory and others reported that A $\beta$  peptide induces *in vitro* reactive oxygen species production, protein oxidation, DNA and RNA oxidation and lipid peroxidation (Butterfield, 2002). A $\beta$  disrupts Ca<sup>2+</sup> homeostasis in neurons (Mattson, Barger et al., 1993), and increased intracellular Ca<sup>2+</sup> level can increase sphingomyelinase activity to produce ceramide (Di Paola, Zaccagnino et al., 2004). Activation of the apoptogenic sphingomyelin-dependent signaling pathway is mediated by ceramide (Di Paola, Zaccagnino et al., 2004) during oxidative stress to play role in the pathogenesis of neuronal disease (Michel, Lambeng et al., 1999). Increased production of ROS/RNS, such as superoxide and nitric oxide together with imbalance of antioxidant defenses was observed in neuronal systems after A $\beta$ (1-42) treatment (Keller, Pang et al., 1997; Yatin, Varadarajan et al., 1999; Varadarajan, Yatin et al., 2000; Butterfield, 2002). Recently, our

laboratory showed the critical role of methionine at the 35<sup>th</sup> position in Alzheimer's A $\beta$ (1-42)-mediated oxidative stress and toxicity [reviewed in (Butterfield and Boyd-Kimball, 2005)]. In addition, A $\beta$ (1-42) leads to oxidative stress *in vivo* (Yatin, Varadarajan et al., 1999; Drake, Link et al., 2003; Mohammad Abdul, Sultana et al., 2006).

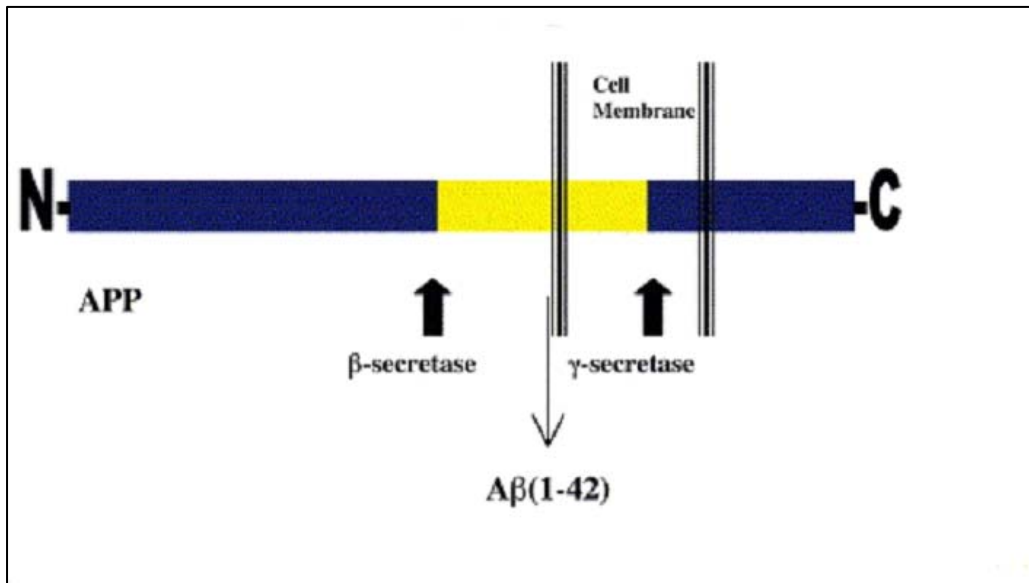


**Figure 2.5:** A $\beta$ (1-42) generation by APP processing. Adapted from (Butterfield and Boyd-Kimball, 2005)

### 2.2.3. APP/PS-1 human double mutant knock-in mice as an AD model

Among the genetic risk factors for AD are included mutations in the presenilin 1 (PS1) gene on chromosome 14 (Sherrington, Rogaev et al., 1995), the presenilin 2 (PS2) gene on chromosome 1 (Rogaev, Sherrington et al., 1995), or the APP gene on chromosome 21 (Chartier-Harlin, Crawford et al., 1991). Around 30% FAD cases have

mutations in PS1 (Schellenberg, 1995). PS1 is part of the  $\gamma$ -secretase complex that cleaves APP to release A $\beta$ (1-42). Mutations in PS1 has been shown to alter APP processing to enhance the generation of A $\beta$ (1-42) peptides (Jarrett, Berger et al., 1993). Synaptosomal proteins from PS-1 mutant mice showed increased oxidative stress and alteration in synaptosomal protein structure when compared to wild type (LaFontaine, Mattson et al., 2002).

Several lines of evidence show that A $\beta$ (1-42) plays a central role in AD pathogenesis and is well documented. Hence, a mouse model was developed by Borchelt et al., which had FAD mutant human PS1-A246E and a chimeric mouse/human (Mo/Hu) APP695 harboring a Hu A $\beta$  domain and mutations (K595N, M596L) linked to Swedish FAD (APP swe) co-expressed (APP/PS-1 human knock-in mouse) (Borchelt, Ratovitski et al., 1997). The APP/PS-1 mice showed increased A $\beta$  production and accelerated amyloid deposition in the brain (Borchelt, Ratovitski et al., 1997). Previous studies from our laboratory have shown that neurons from APP/PS1 have increased basal protein oxidation and lipid peroxidation, and are more vulnerable to oxidation by various exogenous oxidants when compared to wild type (Mohammad Abdul, Sultana et al., 2006). All these studies suggest that APP/PS1 mice can be used as a model of FAD, which is characterized A $\beta$ (1-42)-mediated oxidative stress. Indeed, recently completed initial redox proteomics studies demonstrated elevated oxidized protein in FAD brain (Butterfield, Perluigi et al., 2006).

### **2.3. Synaptosomes**

Synaptosomes are membrane bound sac-like structures that contain synaptic vesicles and mitochondria and nerve terminals isolated from the synapse of neurons.

During brain tissue homogenization, the synaptosomes break away from axon terminal under controlled conditions. Synaptosomes were first isolated by Hebb and Whittaker in 1957. The process of isolation of synaptosomes from detached synapses involves ultracentrifugation and use of a discontinuous sucrose gradient. Synaptosomes are often used for studies involving synaptic transmission because they have machinery similar to a functional synapse. They have functional pumps and channels, synaptic protein and receptors, respond to depolarization, can translocate metabolite and ions and can respire due to the presence of mitochondria (Whittaker, 1993).

In AD, synaptic membranes are known to show increased oxidative stress (Hensley, Carney et al., 1994; Hensley, Hall et al., 1995). Synaptosomes were selected for some of the studies discussed in this dissertation for the following reasons. Synaptic membranes have receptors for glutamate, which mediate increased intracellular  $\text{Ca}^{2+}$  and excitotoxicity and cause production of ROS/RNS that lead to subsequent protein oxidation and lipid peroxidation (Hensley, Carney et al., 1994; Mattson, 1996). Elevation in  $\text{Ca}^{2+}$  levels also causes changes in mitochondrial potential and lead to production of superoxide ion radicals. Due to more energy usage in the synaptic region of neuron, mitochondria are concentrated in these areas of cell. Hence, the synaptic region of neurons becomes more vulnerable to oxidative stress. Synaptosomes virtually “mimic” a functional neuron and are easy to isolate.

#### **2.4. Mitochondria**

Mitochondria, often described as the “cellular power plant” and one of the most important intracellular organelles, occupies up to 25% of the cellular cytoplasm. The main function of mitochondria is to convert organic material into energy in the form of

ATP by a process called oxidative phosphorylation. Mitochondria are bound by an inner and an outer membrane with distinct functions. The mitochondrial matrix, which is the space enclosed by the inner membrane, has various metabolic enzymes involved in electron transport and energy metabolism, mitochondrial DNA (mtDNA) among others (Fig 2.6). The mtDNA is non chromosomal and encodes 13 mitochondrial peptides. Unlike nuclear DNA, mtDNA lacks histones, hence mtDNA becomes more vulnerable to ROS-mediated oxidative damage (Cadenas and Davies, 2000).

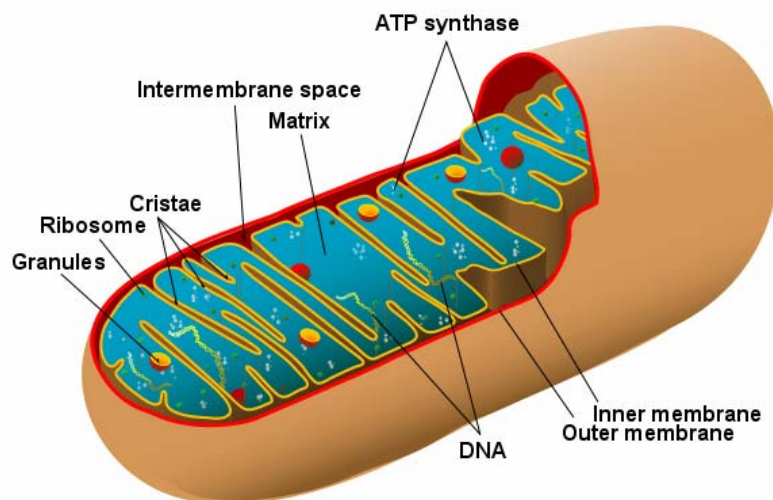


**Figure 2.6:** Diagram of human mitochondrion (Adapted from wikipedia)

Although it is reported that heart mitochondria contain catalase (Radi, Turrens et al., 1991), an enzyme that converts toxic  $H_2O_2$  to water, brain mitochondria lacks catalase. Also, mitochondria lack the enzyme to synthesize GSH; hence, mitochondrial GSH depends on dicarboxylate and 2-oxoglutarate carriers, which aid in uptake of GSH (Chen and Lash, 1998). Mitochondria not only generate energy but are also a source of

free radicals and ROS/RNS. This, combined with factors described above, makes mitochondrial protein and lipids more prone to oxidative insult.

Apart from ATP production, the mitochondrion is also involved in variety of functions, such as regulation of cellular redox state, glutamate-mediated excitotoxicity and apoptosis. Cytochrome C release from an opened mitochondrial permeability transition pore upon oxidative insult or compromise in cellular redox state may initiate apoptosis or programmed cell death. Cytochrome C released into the cytosol forms a complex with caspase-9 and APAF-1 called an apoptosome, which activates caspase-3. Caspase-3 activation leads to apoptosis (Michel, Lambeng et al., 1999; Adrain and Martin, 2001). In this dissertation research, mitochondria were used to study the *in vivo* protective effect of GSH mimetic, D609, from various oxidants.

## **2.5. Glutathione**

### **2.5.1. GSH metabolism and biosynthesis**

GSH is a tripeptide,  $\gamma$ -glutamyl-cysteinyl-glycine (IUPAC name: 2-amino-5-[2-[(carboxymethyl) amino]- 1-(mercaptomethyl)-2-oxoethyl]amino-5-oxopentanoic acid), is the most abundant low molecular weight thiol expressed ubiquitously. Glutathione is widely recognized as an endogenous nonenzymatic antioxidant, an oxyradical scavenger, thereby useful in protecting cells against oxidative damage by free radicals and inhibiting lipid peroxidation and DNA damage (Meister, 1995; Darley-Usmar and Halliwell, 1996; Sies, 1999; Schulz, Lindenau et al., 2000; Hansen, Go et al., 2006). Glutathione has been implicated in a wide range of metabolic processes, including cell division, DNA repair, regulation of enzyme activity, activation of transcription factors, modulation of anion and

cation homeostasis and protection against oxidative damage (Meister and Anderson, 1983).

The synthesis of GSH from glutamate, cysteine, and glycine is catalyzed by two cytosolic enzymes,  $\gamma$ -glutamylcysteine ligase (GCL) and GSH synthetase (GS). It is a two step process and both the steps need ATP as cofactor. The first step involves ligation of  $\gamma$ -glutamate to cysteine to form  $\gamma$ -glutamylcysteine and the reaction is catalyzed by GCL. This step is the rate-limiting step. Cysteine generally is present in micromolar concentration in brain, while glutamate and glycine are present at millimolar levels (Cooper, 1997). GCL is feedback inhibited by GSH itself. GS catalyzes the addition of glycine to the limiting substrate  $\gamma$ -glutamylcysteine (Figure 2.7).



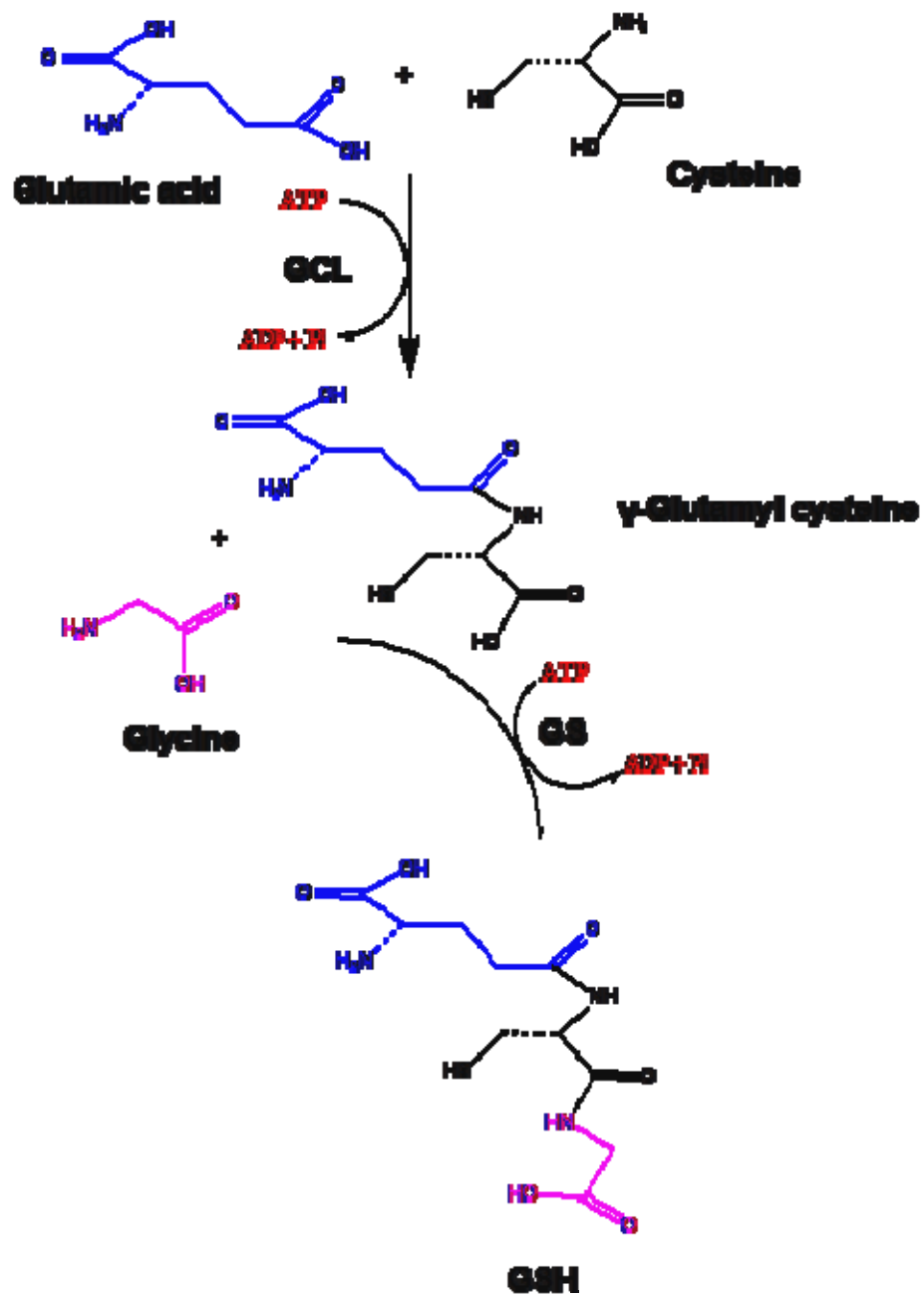
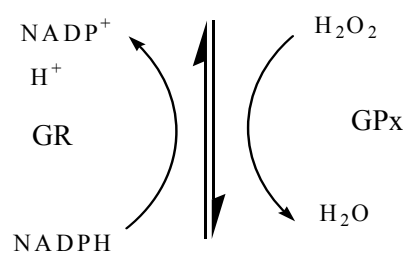


Figure 2.7: GSH synthesis

### **2.5.2. GSH and Oxidative stress**

GSH is present in 1-3mM concentration throughout the brain (Cooper, 1997), acting as a high capacity detoxification agent. GSH maintains the cellular redox balance depending upon the pH of the cellular compartment and is involved in various biosynthetic processes as well (Schulz, Lindenau et al., 2000). The level of GSH is reduced in specific regions of the central nervous system in various neurodegenerative disorders and concomitant increase in oxidized glutathione (GSSG) levels contributes to the oxidative stress-mediated neuronal cell dysfunction and/or loss in these disorders (Benzi and Moretti, 1995a; Cooper, 1997). GSH, in conjugation with glutathione reductase (GR), glutathione peroxidase (GPx), glutathione-S-transferase (GST) and NADPH provide protection against various toxic electrophiles and hydrogen peroxide (Watson, Chen et al., 2003) (fig 2.8).



GSSG

Usually the ratio of GSH to GSSG is maintained towards more reducing state. The GSH/GSSG ratio toward the oxidizing state activates several signaling pathways including protein kinase B, calcineurin, nuclear factor  $\kappa$ B, and mitogen- activated protein kinase (Wu, Fang et al., 2004). Hence, the GSH/GSSG ratio is the important indicator of cellular redox state. Apart from its function as ROS scavenger, GSH reacts with various electrophiles, physiological metabolites and xenobiotics and helps clear the toxic substances. GSH conjugates with NO to form an *S*-nitrosoglutathione adduct, which is cleaved by the thioredoxin system to release GSH and NO.

### **2.5.3. Glutathione Peroxidase**

GPx (EC 1.11.1.9) is the enzyme that helps in detoxification by catalyzing the conversion of  $\text{H}_2\text{O}_2$  to  $\text{H}_2\text{O}$  and  $\text{O}_2$  (Figure 2.8). Different GPx isoforms also detoxify lipid peroxides and alkyl peroxides. The reducing electron comes from GSH. There are various isoforms of GPx and is present in both cytosol and mitochondria. Since mitochondria lacks catalase, GPx becomes particularly important in  $\text{H}_2\text{O}_2$  clearance.  $\text{H}_2\text{O}_2$ , if not cleared, can produce hydroxyl radicals in the presence of  $\text{Fe}^{2+}$  or  $\text{Cu}^+$ .

### **2.5.4. Glutathione Reductase**

GR (EC 1.6.4.2) is the enzyme that keeps the GSSG concentration low compared to GSH and hence helps maintain the redox balance of the cell. GR catalyzes the conversion of GSSG to GSH with the aid of NADPH as cofactor (Figure 2.8). NADPH comes from the pentose phosphate pathway. GR is localized in both brain cytosol and mitochondrial matrix.

### 2.5.5. Glutathione-S-Transferase

GST (EC 2.5.1.18) is the key detoxification enzyme that catalyzes the conjugation of various electrophiles, reactive alkenals, such as 4-hydroxynonenal (HNE) and acrolein, and xenobiotics to GSH. These GSH-S-conjugates are removed from cells by the multidrug resistant protein-1 (MRP-1) (Figure 2.9), an ATP binding cassette (ABC) family protein (Renes, de Vries et al., 2000; Sultana and Butterfield, 2004). MRP-1 is an integral plasma membrane protein that exports glutathione-S conjugates out of the cell in an ATP-dependent manner (Nies, Jedlitschky et al., 2004; Conseil, Deeley et al., 2005). Studies have shown reduced GST activity in brain and ventricular fluids in AD (Lovell, Xie et al., 1998). Increased expression of GST leads to increased resistance towards oxidative stress in neuroblastoma cells and provides protection against HNE mediated toxicity in neuronal cell culture (Lovell, Xie et al., 1998).

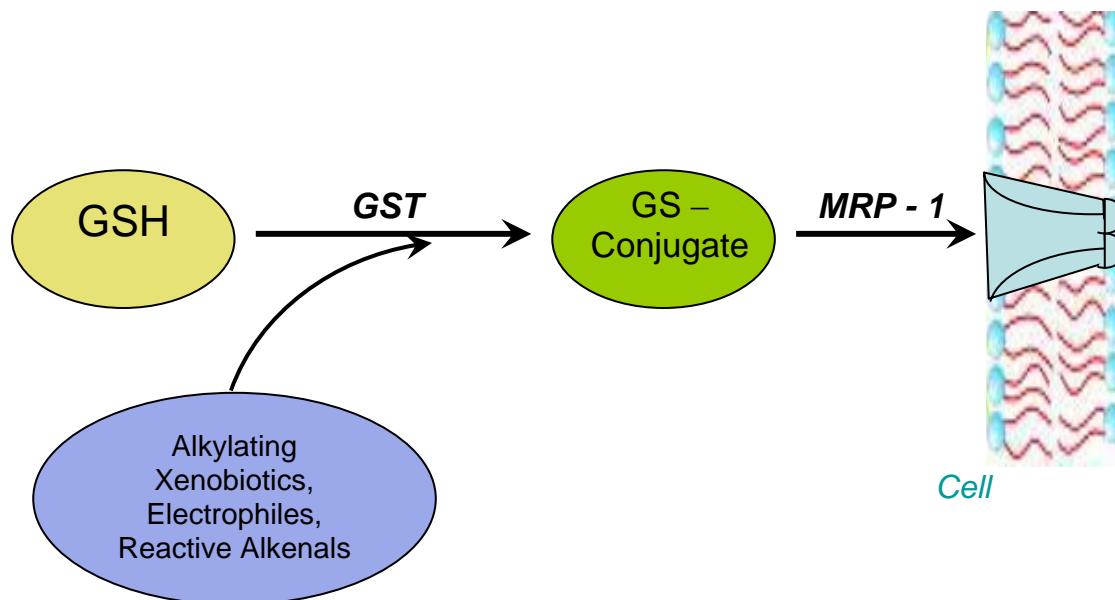
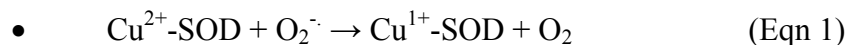
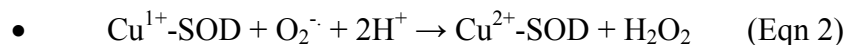


**Figure 2.9:** Detoxification process involving GST and MRP-1 to remove GS-conjugates out of the cell.

## 2.6 Superoxide Dismutase

SOD (EC 1.15.1.1) converts superoxide radicals to hydrogen peroxide and oxygen, the former subsequently is converted to water and oxygen by action of GPx and/or catalase. SOD has various isoforms depending upon their reaction center, but in eukaryotes, two isoforms are predominantly found, Cu/ZnSOD in cytosol and MnSOD in mitochondria. SOD has one of the fastest turn-over numbers among any known enzymes. Mutation in SOD 1 has been linked with familial ALS. Increased expression of certain SODs has shown to be protective against oxidative stress in many disease models (Yen, Oberley et al., 1999). A typical reaction of CuSOD looks like those shown in equations 1 and 2 below:



## 2.7. Proteomics

Proteomics can be broadly defined as the large-scale study of structure, function and localization of proteins. This term was coined to make an analogy with genomics, which is study of genome by gene sequencing. While the genome is static, the proteome is dynamic and more complex, differing from cell to cell and through biochemical interaction constantly keeps changing. The proteome can be defined as an entire protein complement of a biological system at any given time. Protein expression of any organism or cell differs in different parts of body, at different stages of the life cycle and in different environmental conditions. With the completion of the human genome, many researchers are trying to solve the problem related to biological information that cannot be

obtained from genome alone and now examine gene and protein interaction to form other proteins.

We now know that there are far fewer protein coding genes in the human genome (Approximately 20 – 30 K genes) than the actual number of protein in human proteome (> 400 K proteins). Due to this discrepancy, gene expression analysis alone cannot be used to characterize its protein complement. A major diversity in proteins is due to post-translational modification. Proteomics plays an important role in characterizing a particular protein in tissue or organism. Collection of such information offers opportunity to study mechanisms of disease, is instrumental in discovery of biomarker, such as markers that indicate a particular disease and often help in elucidating the pathological events involved in a particular disease condition for therapeutic intervention.

With the technological advances in separation of complex mixture of protein and identification by using soft ionization techniques such as matrix assisted laser desorption and ionization (MALDI) and electrospray ionization (ESI) coupled mass spectrometry, and advances in bioinformatic tools, it has become possible today to meet proteomic demand. Protein expression is dynamically regulated in response to internal and external disturbance under various physiological, pathological, developmental and pharmacological conditions, thereby resulting in the formation of various post-translational modifications. ROS/RNS-mediated oxidative stress leads to the most common post-translational modification, carbonylation. The branch of proteomics that deals with identification of specifically oxidized protein under a given oxidative stress or diseased condition is called “Redox Proteomics”. Oxidative stress has been implicated in many neurodegenerative disorders, including AD. Our laboratory has successfully used

redox proteomics approaches towards identifying specifically oxidized, nitrated and HNE bound proteins in various neurodegenerative disorder condition [reviewed in (Butterfield and Castegna, 2003; Butterfield, 2004; Butterfield, Perluigi et al., 2006; Butterfield, Poon et al., 2006)]. In this dissertation research, the redox proteomics expertise of our laboratory was used to identify specifically oxidized and differentially expressed proteins in brains isolated from mice injected i.p. with ADR.



## Chapter 3

### Experimental Procedure

#### 3.1. Synaptosome Isolation

As previously described in Chapter 2, a series of ultracentrifugation on a discontinuous sucrose gradient was used for synaptosome isolation. For all the studies with synaptosomes, male Mongolian gerbils (2-3 months of age), approximately 60-70 g in size, housed in the University of Kentucky Central Animal Facility in 12-h light/dark conditions and fed standard Purina rodent laboratory chow *ad libitum*, were used. The animal protocols were approved by the University of Kentucky Animal Care and Use Committee.

Gerbils were decapitated during the light phase and the cortex was isolated on ice. The synaptosomal isolation procedure has been described elsewhere (Whittaker, 1993). The isolated cortex was placed in ice-cold 0.32M sucrose isolation buffer containing 4 $\mu$ g/ml leupeptin, 4 $\mu$ g/ml pepstatin, 5  $\mu$ g/ml aprotinin, 2mM ethylenediaminetetraacetic acid (EDTA), 2mM ethylene glycol-bis(tetraacetic acid) (EGTA) and 20mM 4-(2-hydroxyethyl)-1-piperazine-ethanesulfonic acid (HEPES), 20 $\mu$ g/ml trypsin inhibitor and 0.2mM phenylmethanesulfonyl fluoride (PMSF), pH 7.4. The cortex was homogenized by 20 passes with a Wheaton tissue homogenizer. The homogenate was centrifuged at 1500 g for 10 min. The pellet was discarded and the supernatant was retained and centrifuged at 20000 g for 10 min. The resulting pellet was resuspended in approximately 1ml of 0.32M sucrose isolation buffer and layered over discontinuous sucrose gradient (0.85M pH 8.0, 1.0M pH8.0, 1.18M pH8.5 sucrose solutions each containing 2mM EDTA, 2mM EGTA and 10mM HEPES) and spun at 82500g for 1h at 4° C. The purified

synaptosomes were collected from the sucrose gradient interface at the 1.0/1.18M (Fig 3.1) and washed with phosphate buffered saline containing 0.01% (w/v) sodium azide and 0.2% (v/v) Tween 20 (PBS), twice and centrifuged at 32000 g.

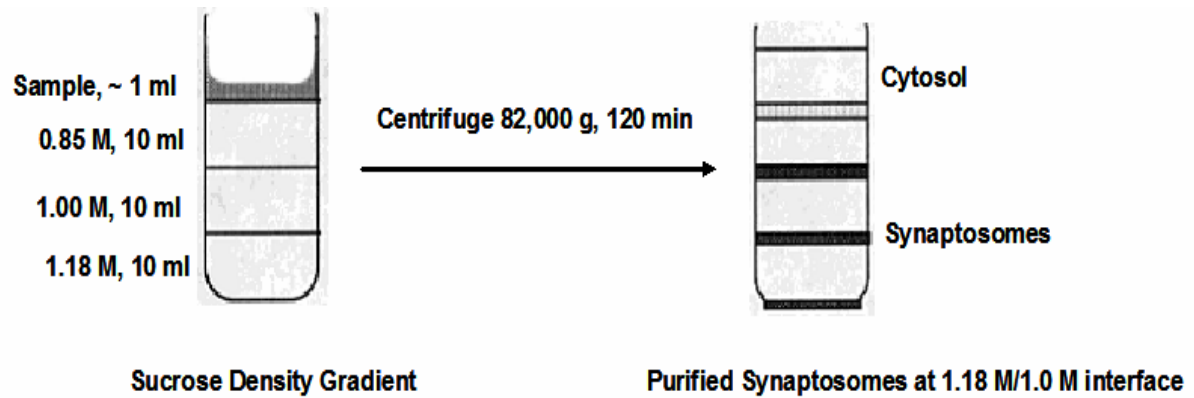


**Figure 3.1:** Sucrose density gradient for isolation of purified synaptosome

### 3.2. Mitochondria Isolation

As discussed in Chapter 2, mitochondria are major source of ROS. The brain mitochondria were isolated according to the procedure of Sims et al. (Sims, 1990) with minor modifications. Gerbils were decapitated in light phase and the whole brain was isolated on ice. Whole brain was homogenized in ice-cold isolation buffer (250 mM sucrose, 10 mM HEPES, and 1 mM potassium EDTA, pH 7.2, 4 µg/ml leupeptin, 4 µg/ml pepstatin, 5 µg/ml aprotinin 20 µg/ml trypsin inhibitor) with 6 passes of a Wheaton tissue homogenizer. The homogenate was centrifuged for 3 min at 1,330× g at 4°C, and the resulting pellet was resuspended in isolation buffer and centrifuged at 1,330× g for 3 min. The supernatants from both spins were combined and spun at 21,200x g for 10 min at 4°C. The pellet was resuspended in 15% Percoll solution (v/v in isolation buffer) and layered onto discontinuous Percoll gradients of 23 and 40% Percoll (v/v in isolation

buffer). Gradients were centrifuged at  $30,700\times g$  for 5 min at  $4^{\circ}\text{C}$ . At the 23-40% Percoll interface, mitochondria were isolated and resuspended in respiration buffer (250 mM sucrose, 2 mM magnesium chloride, 20 mM HEPES, and 2.5 mM phosphate buffer, pH 7.2) and centrifuged at  $16,700\times g$  for 10 min at  $4^{\circ}\text{C}$ . The pellet was resuspended in respiration buffer, centrifuged at  $6,900\times g$  for 10 min at  $4^{\circ}\text{C}$ , and the resulting pellet was washed in PBS at  $6,900\times g$  for 10 min at  $4^{\circ}\text{C}$ .

### **3.3. Protein Concentration**

The subsequently isolated synaptosomes and mitochondria were assayed for protein concentration by Pierce BCA method (Bradford, 1976). The principle behind this assay is to measure the absorbance of  $\text{Cu}^{1+}$  complex with bicinchoninic acid (BCA) at 562 nm in a spectrophotometer. The protein-mediated reduction of  $\text{Cu}^{2+}$  to  $\text{Cu}^{1+}$  in alkaline solution complexes with BCA to give bluish purple color that has strong absorbance at 562 nm. Bovine serum albumin (BSA) was used as standard for all the protein concentration determination studies as a part of this dissertation. Beers law was used to calculate the concentration of unknown samples.

### **3.4. DCF Fluorescence**

Oxidative stress and its implication in neurodegenerative disorders can be understood by studying the levels of intracellular ROS generation. The dichlorofluorescein (DCF) assay is useful in understanding the intracellular ROS generation by various oxidants and can be used to test the efficacy of an antioxidant compound as ROS scavenger. As a part of this dissertation research, DCF assay was used to study the antioxidant properties of D609 and FAEE as ROS scavenger.

DCF is sensitive to many oxidative stress-inducing compounds including hydroxyl radical, ONOO-, AAPH and A $\beta$  (Wang and Joseph, 1999; Keller, Lauderback et al., 2000; Lauderback, Kanski et al., 2002). Dichlorofluorescein diacetate (DCFH-DA) is a membrane permeable non-fluorescent compound that crosses the membrane and is acted upon by the intracellular esterases to form dichlorofluorescein (DCFH). DCFH then reacts with intracellular ROS to form a fluorescent DCF which is measured by spectrofluorometer (Fig 3.2). To ensure that ester cleavage or efflux of the DCFH, prior to the reaction with ROS, was not contributing to changes in fluorescence, the oxidation-insensitive dye (C369) was used in similar studies and was used as control.

In this assay, 10  $\mu$ M DCFH-DA was incubated with synaptosomes (1mg/ml) for 30 minutes at 37° C. Intracellular esterases convert DCFH-DA into anionic DCFH, which because of its negative charge is trapped in the synaptosomes. Upon oxidation with ROS, DCFH is converted to DCF, a fluorescent compound. Synaptosomes were spun at 3000 g in a tabletop Eppendorf centrifuge for 5 minutes at 4° C. Synaptosomes were resuspended in 500  $\mu$ l of PBS and loaded in triplicate (100  $\mu$ l per well) in a black microtiter plate and fluorescence was measured in a Spectramax microtiter plate reader ( $\lambda_{\text{ex}}$  = 495nm,  $\lambda_{\text{em}}$  = 530nm) and quantified using softPro max software. To verify that ester cleavage and efflux of the dye were not contributing to changes in fluorescence, similar studies were done with an oxidation-insensitive dye carboxy-DCFH-DA (C369).

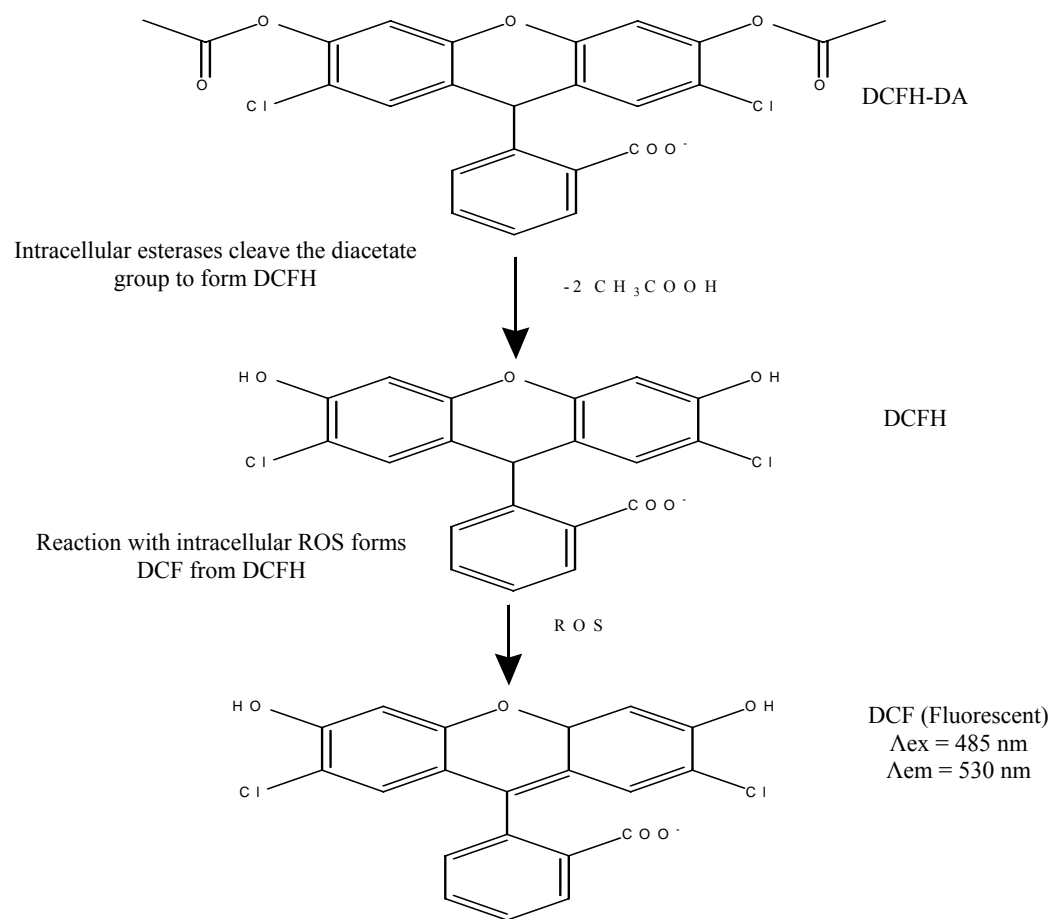


**Figure 3.2:** DCF assay

### **3.5. Protein oxidation (Slot blot)**

As discussed in Chapter 2, free radical mediated oxidative stress causes protein oxidation. Also discussed were the consequences of protein oxidation. The two markers of protein oxidation are formation of protein carbonyl and nitration of tyrosine residues on protein by  $\text{ONOO}^-$ .

#### **3.5.1. Protein carbonyl**

Levels of protein carbonyl can be estimated by immunochemical method. 2, 4-dinitrophenylhydrazine reacts with the carbonyl groups on protein to form a hydrazone adduct (Schiff base) (Fig 3.3). By using a specific antibody for hydrazone, the carbonyl level can be estimated. Briefly, sample (5  $\mu\text{l}$ ) (normalized to 4mg/ml), 5 $\mu\text{l}$  of 12% sodium dodecyl sulfate (SDS) and 10 $\mu\text{l}$  of 10 times diluted 2,4-dinitrophenylhydrazine (DNPH) from 200mM stock were incubated at room temperature for 20 min. Samples were neutralized with 7.5 $\mu\text{l}$  neutralization solution (2M Tris in 30% glycerol). The resulting solution was loaded in each well on nitrocellulose membrane under vacuum using a slot blot apparatus.

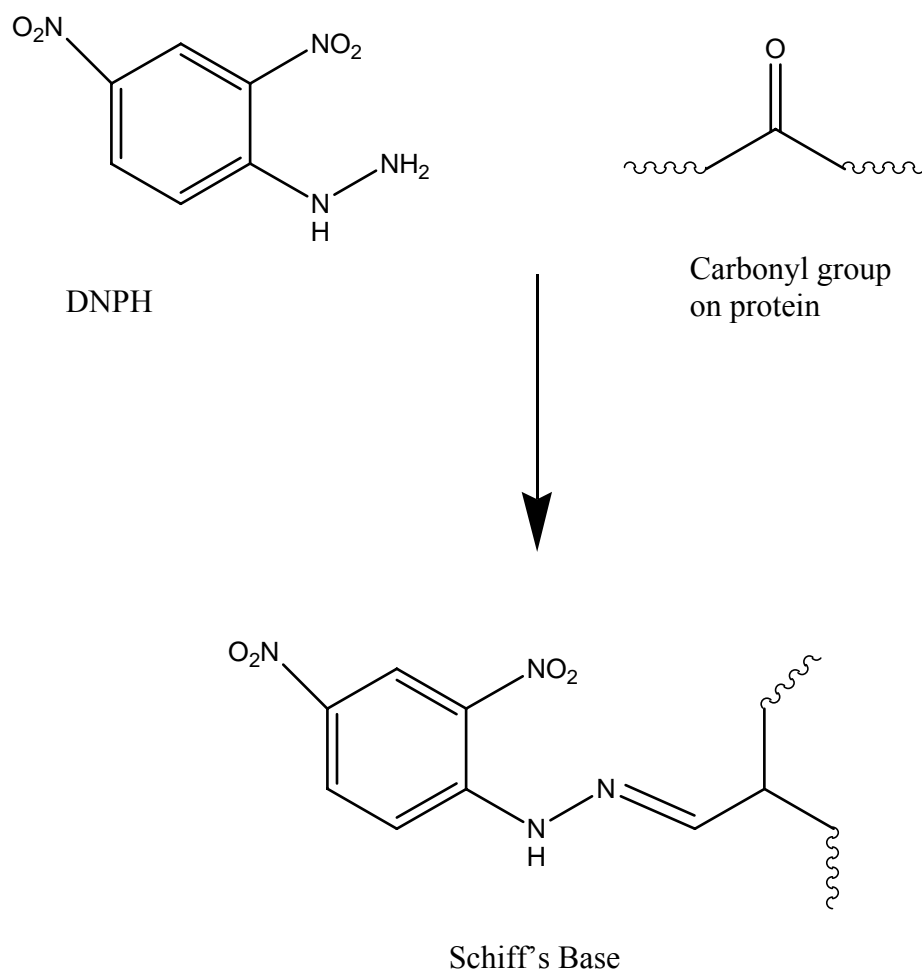


**Figure 3.3:** Derivatization of protein by DNPH

The assembly of the slot blot apparatus is shown below (fig 3.4). The membrane was blocked in blocking buffer (3% bovine serum albumin) in phosphate buffered saline containing 0.01% (w/v) sodium azide and 0.2% (v/v) Tween 20 (PBS) for 1 h and incubated with a 1:100 dilution of anti DNP polyclonal antibody in phosphate buffered saline containing 0.01% (w/v) sodium azide and 0.2% (v/v) Tween 20 (PBS) for 1h. The

membrane was washed three times in PBS and was incubated for 1 h with an anti-rabbit IgG alkaline phosphatase secondary antibody diluted in PBS in a 1:8000 ratio. The membrane was washed for three times in PBS for 5 min and developed in Sigma fast tablets (BCIP/NBT substrate). Blots were dried, scanned with Adobe Photoshop, and quantified with Scion Image (PC version of Macintosh compatible NIH image).

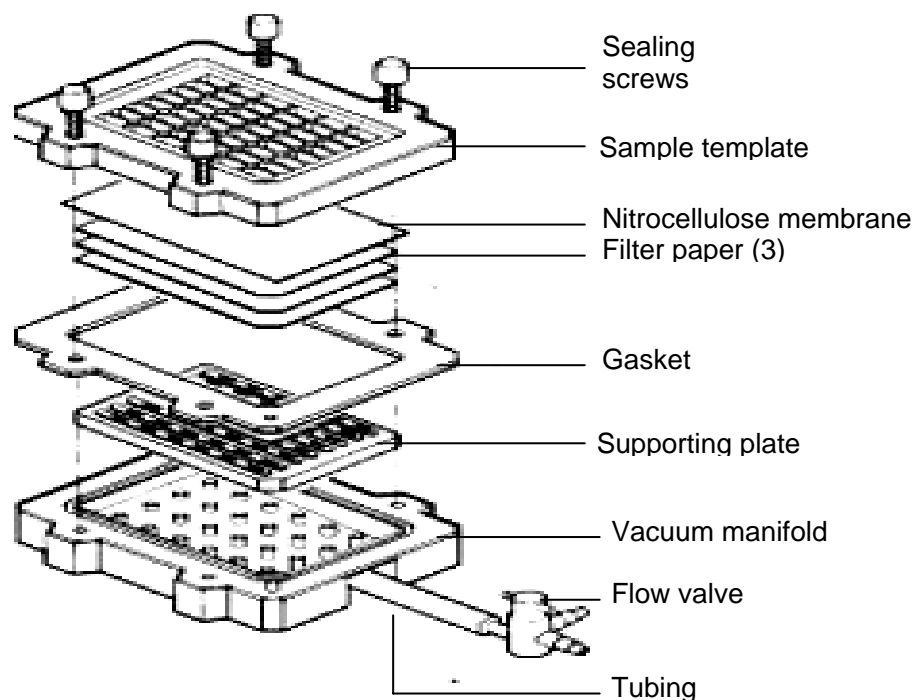


**Figure 3.4:** Slot blot apparatus assembly.

### 3.5.2. 3-Nitrotyrosine

As described in chapter 2, 3NT is a hallmark of  $\text{ONOO}^-$  - mediated protein damage. The 3NT levels were measured in both synaptosomal and mitochondrial suspension. A slot blot technique similar to protein carbonyl was employed to immunochemically detect the levels of 3NT.



The suspended synaptosomes or mitochondria samples (5  $\mu$ l) (normalized to 4mg/ml), 5 $\mu$ l of 12% sodium dodecyl sulfate (SDS) and 5 $\mu$ l of modified Laemmli buffer containing 0.125 M tris base pH 6.8, 4% (v/v) SDS, and 20% (v/v) glycerol were incubated for 20 minutes at room temperature. Sample (250 ng) was loaded in each well on nitrocellulose membrane in slot blot apparatus under vacuum. The membrane was blocked in blocking buffer (3% bovine serum albumin) in phosphate buffered saline containing 0.01% (w/v) sodium azide and 0.2% (v/v) Tween 20 (PBS) for 1 hr and incubated with a 1: 2000 dilution of anti-3-nitrotyrosine (3NT) polyclonal antibody in PBS for 1 h 30 min. The membrane was washed in PBS for 5 min three times after incubation. The membrane was incubated for 1 h, following washing, with an anti-rabbit IgG alkaline phosphatase secondary antibody diluted in PBS in 1:8000 ratio. The membrane was washed for three times in PBS for 5 minutes and developed in Sigma fast tablets. Blots were dried, scanned with Adobe Photoshop, and quantified with Scion Image as above.

### **3.6. Lipid peroxidation (Slot blot)**

As discussed in chapter 2 that lipid peroxidation often leads to formation of byproduct, such as HNE and acrolein. These reactive alkenals bind to the protein by Michael addition and inactivates them. A reaction of HNE with cysteine residues on protein to form a Michael adduct is shown in figure 3.5. Hence, estimating the levels of protein bound lipid peroxidation product can gives the extent of lipid peroxidation. As a part of this dissertation research, protein-bound HNE levels were measured to quantify the extent of lipid peroxidation. The protein-bound HNE levels were measured in both

synaptosomal and mitochondrial suspension. A slot blot technique similar to protein carbonyl was employed to immunochemically detect the levels of protein bound HNE.

Sample (5  $\mu$ l) (normalized to 4mg/ml), 5 $\mu$ l of 12% sodium dodecyl sulfate (SDS) and 5 $\mu$ l of modified Laemmli buffer containing 0.125 M tris base pH 6.8, 4% (v/v) SDS, and 20% (v/v) glycerol were incubated for 20 minutes at room temperature. Sample (250 ng) was loaded in each well on nitrocellulose membrane in slot blot apparatus under vacuum. The membrane was blocked in blocking buffer (3% bovine serum albumin) in phosphate buffered saline containing 0.01% (w/v) sodium azide and 0.2% (v/v) Tween 20 (PBS) for 1 hr and incubated with a 1: 5000 dilution of anti-HNE polyclonal antibody in PBS for 1 h 30 min. The membrane was washed in PBS for 5 min three times after incubation. The membrane was incubated for 1 h, following washing, with an anti-rabbit IgG alkaline phosphatase secondary antibody diluted in PBS in 1:8000 ratio. The membrane was washed three times in PBS for 5 min and developed in Sigma fast tablets (BCIP/NBT substrate). Blots were dried, scanned with Adobe Photoshop, and quantified with Scion Image as above.

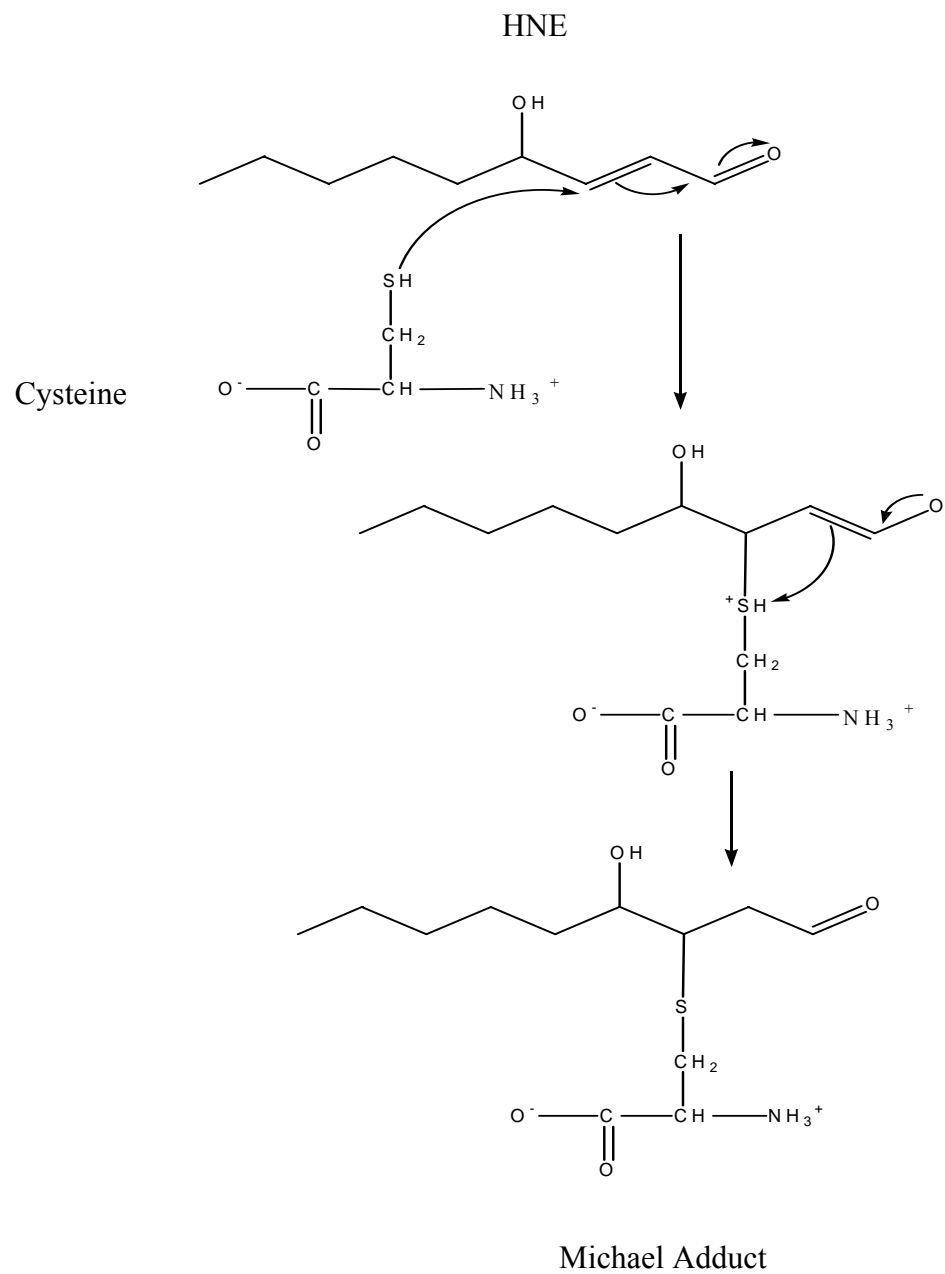


**Figure 3.5:** Reaction of HNE with cysteine

### **3.7. GSH and GSSG assays**

As described in Chapter 2, GSH is the most abundant antioxidant present in millimolar concentration in brain that helps protecting cells against oxidative stress. Hence, it becomes important to study the levels of GSH during neurodegenerative disorder conditions involving oxidative stress. As a part of this dissertation research the GSH and GSSG levels were measured to look for the effect of D609 or GCEE as modulator of GSH, either by mimicking its property or by increasing its levels.

GSH levels were measured by procedure described by Griffith et al., 1980 (Griffith, 1980). 5, 5'-Dithiobis (2-nitrobenzoic acid) (DTNB) is used for detecting sulfhydryl groups. The principle behind this assay is enzymatic recycling method, using GR, for quantification of GSH. GSH reacts with DTNB to form a mixed disulfide and produces a yellow colored 5-thio-2-nitrobenzoic acid (TNB) that has absorbance at 414 nm in spectrophotometer. The GSTNB complex is reduced by GR to form more TNB (Fig 3.6). The rate of formation of TNB is directly proportional to concentration of GSH in the sample. A kit working on this principle was used as a part of some of the dissertation research. Briefly, the cytosolic fraction isolated from brain homogenates was precipitated with 10% (w/v) metaphosphoric acid and then centrifuged for 5 min at 5,000g. The supernatants were neutralized with 4M triethanolamine and then analyzed according to manufacturer instructions. GSH concentration in the samples was calculated using the kinetic method by measuring the absorbance at 405 nm with a Bio-Tek Powerwave X Microtiter Plate Reader (Bio, Inc.). A plot of the corrected absorbance vs the concentration of GSH standards ( $\mu\text{M}$ ) was utilized to calculate the average concentration of GSH present in the samples.

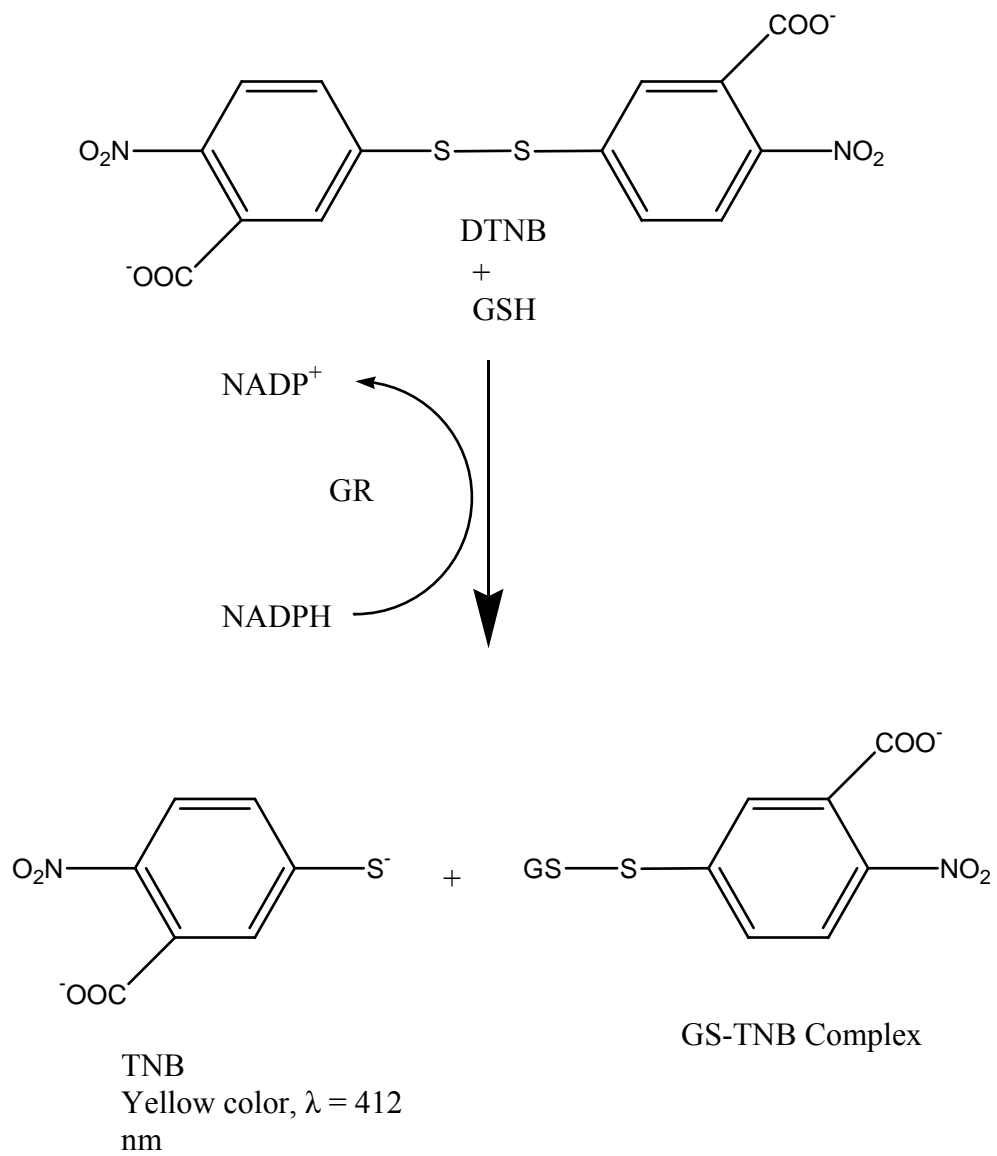


**Figure 3.6:** GSH assay

A fluorescence method was also used to measure the level of GSH in one of the part of this dissertation research. This method is dependent on measuring the florescence of GSH complex with O—phthaldehyde (OPT). Determination of GSH was performed by the method of Hissin and Hilf (Hissin and Hilf, 1976). The reaction mixture containing 0.1 M sodium phosphate buffer (pH-8.0), 5.0 mM EDTA, 10  $\mu$ l OPT (1.0 mg/ml) and 10  $\mu$ l of sample. After incubation for 15 min at room temperature, fluorescence at emission 420 nm was recorded by excitation at 350nm. For assaying levels of GSSG, same method was used. Briefly, the samples were incubated first with 0.04 M N-ethyleimide (NEM) for 30 min to interact with GSH present in sample. The reaction mixture containing 0.1 N NaOH, 5.0 mM EDTA, 10  $\mu$ l *O*-phthaldehyde (1.0 mg/ml) and 10  $\mu$ l of sample. After incubation for 15 min at room temperature, fluorescence at emission 420 nm was recorded by excitation at 350nm.

### **3.8. Enzyme Activities**

#### **3.8.1. Glutathione peroxidase**

As described in Chapter 2, GPx is the enzyme that converts  $\text{H}_2\text{O}_2$  to  $\text{H}_2\text{O}$  and  $\text{O}_2$ . It gets the reducing electrons from the GSH which is converted to GSSG. GPx (EC 1.11.1.9) activity was measured in a 96-well plate reader at 37 °C by a coupled assay system (Wheeler, Salzman et al., 1990). The reaction mixture consisted of 0.2 mM  $\text{H}_2\text{O}_2$ , 1.0 mM GSH, 0.14 U of GR, 1.5 mM NADPH, 1.0 mM sodium azide and 0.1M phosphate buffer (pH 7.4) and 10  $\mu$ l PMS in a total volume of 200  $\mu$ l. The enzyme activity was calculated as nmol NADPH oxidized  $\text{min}^{-1} \text{mg}^{-1}$  protein.

### **3.8.2. Glutathione reductase**

GR is the enzyme that catalyzes conversion of GSSG to GSH as described in Chapter 2. The cofactor for this enzymatic reaction is NADPH. The assay system to estimate GR (EC 1.6.4.2) activity consisted of 0.1 M phosphate buffer (pH 7.6), 0.5 mM EDTA, 1.0 mM oxidized glutathione, 0.1 mM NADPH and 10  $\mu$ l PMS in a total volume of 200  $\mu$ l (Carlberg and Mannervik, 1985). The enzyme activity was assayed in a 96-well plate reader by measuring the disappearance of NADPH at 340 nm and was calculated as nmol NADPH oxidized  $\text{min}^{-1} \text{mg}^{-1}$  protein.

### **3.8.3. Glutathione-S-transferase**

GST catalyzes the conjugation of GSH to various reactive alkenals, electrophiles, and xenobiotics to remove them out of cell. In other word, GST is a detoxification enzyme and functions as described earlier in Chapter 2. GST (EC 2.5.1.18) activity was measured in a 96-well plate reader, with the reaction mixture consisting of 0.1 M phosphate buffer (pH 6.5), 1.0 mM reduced glutathione, 1.0 mM CDNB and 0.1  $\mu$ l of PMS in a total volume of 200  $\mu$ l (Habig, Pabst et al., 1974). The changes in absorbance were recorded at 340 nm, and the enzymatic activity was calculated as nmol CDNB conjugate formed  $\text{min}^{-1} \text{mg}^{-1}$  protein.

### **3.8.4. Total superoxide dismutase**

SOD (EC 1.15.1.1) activity assay reaction consisted of 50 mmol/l glycine buffer, pH 10.4, and 1mg/ml supernatant protein. The reaction was initiated by the addition of 20 mg/ml solution of (–)-epinephrine and absorbance was measured at 480 nm (Stevens, Obrosova et al., 2000). SOD activity was expressed as nmol of (–)-epinephrine protected from oxidation  $\text{min}^{-1} \text{mg}^{-1}$  protein.

### **3.9. Western blot**

This method was used as a part of dissertation research to investigate the expression levels of various proteins involved in oxidative stress-mediated neurodegenerative disorders. In particular, the GSH and its related enzyme expression levels were looked at in brain isolated from ADR injected mice. The principle behind this method is to separate a mixture of protein based on their molecular weight at a specific voltage on a sodium dodecyl sulfate-polyacrylamide gel (SDS-PAGE). Briefly, Samples (100 µg) were incubated with sample loading buffer, and protein samples were denatured and electrophoresed on a 12.5% SDS-PAGE. Proteins were transferred to a nitrocellulose membrane at 90 mA/gel for 2 h. The blots were blocked for 1h in fresh wash buffer (10 mM Tris-HCl, pH7.5), 150 mM NaCl, 0.05% Tween 20, pH 7.4, containing 3% bovine serum albumin) and incubated with a 1:1000 dilution of the respective monoclonal antibody in phosphate buffered saline containing 0.01% (w/v) sodium azide and 0.2% (v/v) Tween 20 (PBS) for 1h. The membrane was washed three times in PBS and was incubated for 1 h with an anti-rabbit IgG alkaline phosphatase secondary antibody diluted in PBS in 1:8000 ratio. The membrane was washed for three times in PBS for 5 min and developed in Sigma fast tablets (BCIP/NBT substrate).

In all cases non-specific background labeling by secondary antibody was negligible.

### **3.10. Proteomics**

2D-PAGE followed by 2D Western blot, coupled with mass spectrometry analysis of the biological sample in single detectable protein spots, has been widely used to identify complex protein mixtures. Recent advances in proteomics have improved result



in identification techniques (Dalle-Donne, Scaloni et al., 2006). As a part of this dissertation research, this method was used to identify specifically expressed protein and differentially oxidized protein in brain samples obtained from ADR-injected mice.

#### **3.10.1. Iso-electric focusing (First dimension)**

The first dimensional separation of proteins is based on their isoelectric point (IP). IP is the pH at which the net charge on a protein is zero. The protein samples are loaded on an immobilized pH gradient (IPG) strip and a potential is supplied. The protein starts moving on the strip and pH gradient allows the migration of protein to a point until the net negative charge is balanced by the same amount of positive charge. At this point the protein becomes neutral and is focused at a particular pH. Due to the neutral charge proteins do not respond to the applied potential. This process is called isoelectric focusing. In IEF, protein solubilization in the sample is a very important step because the higher gel friction coefficient might cause protein precipitation if not solubilized. The sample buffer for IEF consists of urea, which is an effective chaotropic agent, dithiothreitol (DTT) that is a reducing agent along with non-ionic detergents, such as Triton X and CHAPS. The voltage applied depends on nature of sample, solubility of protein and number of IPG strips. Following IEF, the strips are equilibrated with DTT that reduces disulfide bonds and iodoacetamide that derivatizes the cysteine residues.

#### **3.10.2. SDS-PAGE (Second dimension)**

Gel electrophoresis on polyacrylamide matrix is an analytical technique that provides separation of proteins according to the size under applied potential difference. The technique had been described earlier in this chapter. The only difference being that instead of protein sample, the IPG strips on which proteins that are previously separated

based on IP is mounted on top of the gel following equilibration. The separation occurs in presence of detergent, SDS, that solubilizes and denatures the proteins. Due to presence of SDS the protein lose their three-dimensional structure and assume a net negative charge. Hence, unlike IEF the separation is purely based on the molecular migration rate of a denatured protein on a polyacrylamide gel, which is based on size of a protein. Once the proteins are separated into single spot on two different dimensions, the gels are stained with sypro ruby. The result of 2D map provides various information, important one being comparison between different sample to identify difference in protein expression (Tilleman, Stevens et al., 2002). The 2D-PAGE can resolve thousand of protein at once and provide clues even on posttranslational modification. The schematic representation of 2D-PAGE is shown in Figure 3.7.

The overall process of 2D-PAGE follows the method as described. Samples of the proteins from brain homogenate were prepared as previously described (Poon, Castegna et al., 2004). Briefly, for isoelectric focusing, 200µg of protein were applied to a pH 3–10 ReadyStrip™ IPG strip (Bio-Rad), and Linear Gradient (8– 16%) Precast criterion Tris-HCl gels (Bio-Rad) were used to separate proteins according to their molecular migration rate (MrW). Sypro ruby stain was used to stain the gel for ~ 1 h, after which the gels were placed overnight in deionized water for destaining.

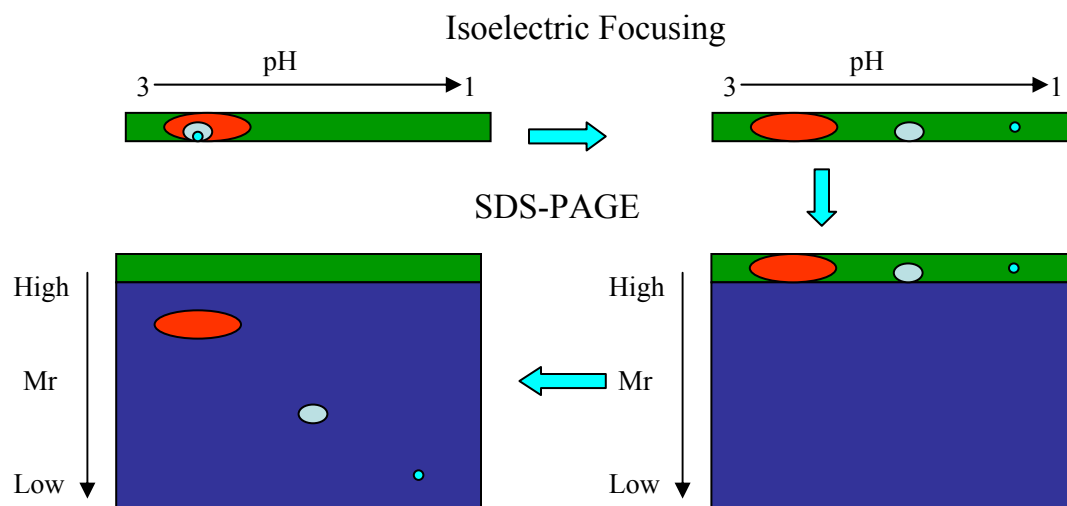


**Figure 3.7:** 2-Dimensional Gel Electrophoresis

### 3.10.3. 2D Western blots

Redox proteomics is the branch of proteomics that is used to identify specifically oxidized protein in a sample mixture. Our laboratory has used the redox proteomics method to identify specifically carbonated, nitrated and HNE-bound protein in various neurodegenerative disorders, including AD [reviewed in (Butterfield, Poon et al., 2006; Sultana, Perluigi et al., 2006)]. As described in Chapter 2, ROS/RNS-mediated oxidative stress leads to the most common post-translational modification, carbonylation. As a part of this dissertation research, redox proteomics approach was used to identify differentially carbonylated protein that index protein oxidation in brain protein samples isolated from ADR-injected mice and were compared with respective control to identify specifically oxidized protein. Briefly, the proteins are derivatized with DNPH and are separated on 2D-PAGE as described in earlier section. The proteins separated on 2D gels

are then transferred on a nitrocellulose membrane (western blotting) and developed immunochemically. Western blotting for 2D-PAGE was performed as previously described (Poon, Castegna et al., 2004). Briefly, 200µg of the brain protein were incubated with 10 mM DNPH solution in 2 N HCl at room temperature (37°C) for 20 min. The gels were prepared in the same manner as for 2DE. The proteins from gels following the second dimension electrophoresis were transferred onto nitrocellulose paper (Bio-Rad) using a Transblot-Blot® SD semi-dry Transfer Cell (Bio-Rad) at 15V for 2 h. The derivatized carbonyl adduct of the brain proteins were detected immunochemically (Butterfield, 2004).

#### **3.10.4. PD-Quest analysis**

Image analysis to identify the protein on gels and blots is done by using PD-Quest software. The sypro ruby stained gels are scanned and saved in TIF format using a Storm 860 Scanner (Molecular Dynamics, Sunnyvale, CA) and the Western blots developed using a specific antibody for DNPH derivatized proteins are scanned and saved in TIF format using Scanjet 3300C (Hewlett Packard, Palo Alto, CA). PD-Quest (Bio-Rad) software was used for matching and analyzing visualized protein spots among multiple gels and oxyblots. After matching all the spots, the normalized intensity of each protein spot from individual gels (or oxyblots) is compared between groups and a protein map is obtained using statistical analysis.

#### **3.10.5. In-gel digestion**

Individual spots that show statistically significant difference between control and treated sample are excised from the gels and are placed in a protease buffer that favors peptide extraction and gets absorbed in the gel surface to cleave the protein into several

peptides in a sequence specific manner. The in-gel digestion was carried out as described previously (Poon, Castegna et al., 2004). Briefly, the excised protein spots were washed with ammonium bicarbonate ( $\text{NH}_4\text{HCO}_3$ ) followed by acetonitrile at room temperature. The gel pieces were digested with 20ng/ $\mu\text{l}$  modified trypsin and incubated at 37°C overnight in a shaking incubator.

#### **3.10.6. Mass spectrometry**

Mass spectrometry is the analytical technique that provides generation, separation and detection of ions formed by fragmentation of a molecule of interest. The ions formed are then separated according to their mass-charge ratio ( $m/z$ ) and are detected by a detector. The  $m/z$  of each ion is collected in the form a mass spectrum that provides structural information of an analyte. A mass spectrometer usually consist of an ion source, an analyzer that separates ions based on  $m/z$ , a detector that quantifies the amount of ions with same  $m/z$  and a computer processor that collects mass spectrum and process the data generated.

#### **3.10.7. Ion source**

As described in Chapter 2, the two types of ion sources used in proteomics study are ESI and MALDI. As a part of this dissertation study, MALDI was used as ionization technique. MALDI produces ions by irradiation of the sample embedded in a matrix of suitable organic compound that mixes with the sample. Sample mixture deposited on a special metal plate is defined as “solid solution” once the solvent is evaporated from the matrix. Upon laser irradiation, the matrix sublimates and the gaseous molecule act as carrier of the analyte into the gas phase. In this way even labile molecules can be ionize without decomposition. The sample preparation and matrix selection is most important

part in MALDI. For our sample, 1  $\mu$ l of  $\alpha$ -cyano-4-hydroxy trans-cinnamic acid (10 mg/ml in 0.1% TFA: ACN, 1:1, v/v) was mixed with tryptic digests (1  $\mu$ l). The mixture (1  $\mu$ l) was deposited onto the surface of a fast evaporation nitrocellulose matrix.

### 3.10.8. Time-of-flight (TOF) analyzer

Each single detectable ion is separated according to  $m/z$  following ionization by MALDI method. This value is measured through a scanner device, which collects the ions coming from ionization source and transmitted on to a time scale. There are several kinds of analyzer based on different principles. In brief they can be divided into two groups: analyzer with flight tube and quadrupole analyzer. MALDI is usually coupled with a time-of-flight (TOF) analyzer. The ions separation in a TOF analyzer depends on the fact that the ions with higher mass will reach the detector slower than the smaller mass ions. Each ion with specific mass will have a specific “time of flight” before reaching the detector. The relationship between mass of ion and time taken to reach the detector can be derived as follows. An ion of mass  $m$  and charge  $q = ze$  accelerated at an applied voltage  $V$ , flying through a distance  $d$  with a velocity  $v$ , will reach the detector after time  $t$

$$T = d/v \text{ (Eqn 1)}$$

The kinetic energy  $K$  of ion

$$K = mv^2/2 = zeV \text{ (Eqn 2)}$$

Combining the two equations we get,

$$t = \sqrt{(m/z) [d^2/2ev]} \text{ (Eqn 3)}$$

It is clear from equation 3 that time to reach detector is directly proportional to mass of ion i.e., higher mass ions take longer time to reach the detector. As a part of this

dissertation study, our samples were analyzed in reflectron mode with a ToFSpec 2E (Micromass, UK) matrix-assisted laser desorption ionization-time of flight (MALDI-TOF) mass spectrometer. The mass axis was adjusted with trypsin autohydrolysis peaks ( $m/z$  2239.14, 2211.10, or 842.51) as lock masses.

### **3.10.9. Database searching**

The peptide mass fingerprints obtained from MS are characteristic of a particular protein. The information retrieved by the mass spectrometry, i.e., a list of peptide masses, is searched against an online database. The Swissprot database is the widest protein sequence database (Hoogland, Sanchez et al., 1999) to which it is possible to submit a protein identification request using special “informatics” tools that are freely accessible through the internet. As a part of this dissertation research, the MALDI spectra used for protein identification from tryptic fragments were searched against the Swissprot protein databases using the MASCOT search engine. Peptide mass fingerprinting used the assumption that peptides are oxidized at methionine residues, are monoisotopic and cysteine residues in peptide are carbamidomethylated (Butterfield and Castegna, 2003; Tangpong, Cole et al., 2006a). Up to 1 missed trypsin cleavage was allowed. Window of error allowed for matching the peptide mass values was set at mass tolerance of 150 ppm. We used the probability-based Mowse score, which indicates the probability that the match between the database and a spectrum is a random event to assign a level of confidence to the identification of specific proteins from the mass spectra. This probability equals  $10^{(-\text{Mowse score}/10)}$ . Mowse scores greater than 53 were considered significant.

The complete flow chart for proteomics is shown in Figure 3.8 below.

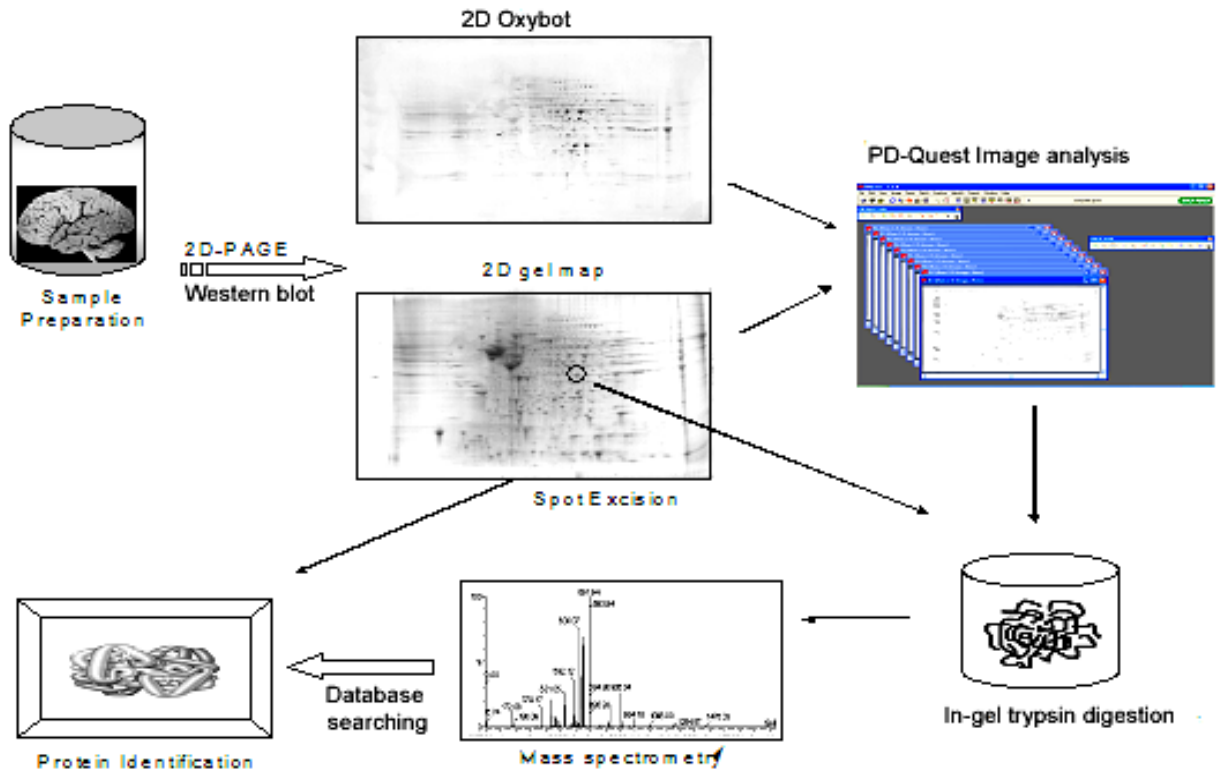


**Figure 3.8:** Diagram showing sequence of events involved in redox proteomics.



## Chapter 4

### **Free radical mediated oxidative stress and toxic side effects in brain induced by the anti cancer drug Adriamycin: Insight into chemobrain**

#### **4.1. Overview of the Study**

Adriamycin (ADR) is a chemotherapeutic agent useful in treating various cancers. Application of this drug can have serious side effects in various tissues, including brain, apart from the known effects such as cardiotoxicity. These effects limit the successful use of this drug in treatment of cancer. ADR is quinone-containing anthracycline chemotherapeutic and is known to produce reactive oxygen species (ROS) in heart. Neurons treated with ADR demonstrate significant protein oxidation and lipid peroxidation. Patients under treatment with this drug often complain of forgetfulness, lack of concentration, dizziness (collectively called somnolence or sometimes called chemobrain). In this study, we tested the hypothesis that ADR induces oxidative stress in brain. Accordingly, we examined the *in vivo* levels of brain protein oxidation and lipid peroxidation induced by i.p. injection of ADR. We also measured levels of the multidrug resistance-associated protein (MRP1) in brain isolated from ADR-injected mice. MRP1 mediates ATP-dependent export of cytotoxic organic anions, glutathione S-conjugates and sulphates. The results showed a significant increase in levels of protein oxidation and lipid peroxidation and increased expression of MRP1 in brain isolated from mice, 72 hrs post i.p injection of ADR. These results are discussed with reference to potential use of this redox cycling chemotherapeutic agent in the treatment of cancer and its side effects in brain.

## 4.2. Introduction

Free radical mediated oxidative stress has been implicated in many neurodegenerative disorders (Butterfield and Kanski, 2001). Reactive oxygen species (ROS) lead to protein oxidation (Hensley, Hall et al., 1995; Stadtman and Berlett, 1997), lipid peroxidation (Markesbery and Lovell, 1998; Butterfield and Lauderback, 2002), DNA and RNA oxidation in brain (Butterfield, Drake et al., 2001) and neuronal dysfunction and death. Oxidation of proteins leads to loss of activity of enzymes critical for cell functioning, and recently our lab identified some of the critical proteins that are oxidized in Alzheimer's disease (AD), by using proteomics (Castegna, Aksenov et al., 2002a; Castegna, Aksenov et al., 2002b; Lauderback, Drake et al., 2003). ROS generation hence becomes imperative in understanding oxidative stress and oxidative stress related disorders.

Adriamycin (ADR) is a cancer chemotherapeutic useful in treating various cancers with especially good potency in the treatment of patients with solid tumors (Weiss, Sarosy et al., 1986; Eisenhauer and Vermorken, 1998). ADR is suggested to act as an antitumor agent by inhibiting DNA replication and DNA synthesis (Cummings, Anderson et al., 1991) by intercalating into grooves of DNA. Another important mechanisms of action of ADR involve its interaction with topoisomerase II, which forms a DNA-cleavable complex (Chuang and Chuang, 1979; Cheng, Cahill et al., 1992). One of the most accepted mechanisms of action of ADR on tumor cells is generation of free radicals by enzymatic electron reduction of ADR by variety of oxidase, reductase and dehydrogenase (Kappus, 1987; Gutierrez, 2000). However, ADR can have serious side effects in various non-involved tissues, including brain, apart from its known cardiotoxic

effects (Steinherz, Steinherz et al., 1991). These latter effects limit the successful use of ADR in cancer treatment. A free radical-mediated mechanism has been proposed to be responsible for ADR-induced toxicity in heart (DeAtley, Aksenov et al., 1998). Cardiomyocytes treated with ADR lead to significant protein oxidation and lipid peroxidation (DeAtley, Aksenov et al., 1998). Free radical scavengers are known to reduce this effect (DeAtley, Aksenov et al., 1999). ADR also disrupts the mitochondrial electron transport system in heart tissues (Davies, Doroshov et al., 1983; Doroshov, 1983; Yen, Oberley et al., 1999). Increased expression of manganese superoxide dismutase (MnSOD) protects complex I against ADR-induced cardiomyopathy (Yen, Oberley et al., 1999). ADR contains a quinone in its structure ( Chapter 2, fig 2.2), and as is well known, quinones undergo one-electron reduction to form semiquinones, which are free radicals (Handa and Sato, 1975; Gutteridge, 1984).

#### **4.3. Purpose of the study**

Although there are numerous reports of dizziness, confusion and dementia of cognitive function (somnolence) in patients treated with ADR (Schagen, Hamburger et al., 2001), little has been reported on oxidative stress in brain due to this drug. Therefore, in this study oxidative stress parameters were studied in brain. Protein carbonyl and 3-nitrotyrosine levels (indices of protein oxidation) and 4-hydroxynonenal levels (index of lipid peroxidation) were determined in brain from mice treated with ADR.

#### **4.4. Experimentals**

##### **4.4.1 Animals**

For the studies, male mice (2-3 months of age), approximately 30 g in size, housed in the University of Kentucky Central Animal Facility in 12-h light/dark

conditions and fed standard Purina rodent laboratory chow *ad libitum*, were used. The animal protocols were approved by the University of Kentucky Animal Care and Use Committee.

#### **4.4.2 Material and Method**

##### **4.4.2.1 Chemicals**

Doxorubicin HCl (ADR) was purchased from Bedford Laboratories. All other chemicals were purchased from Sigma-Aldrich (St. Louis, MO), unless stated otherwise. The protein oxidation detection kit was purchased from Interger (Purchase, NY) and primary antibody for HNE, 3NT and the multidrug resistance-associated protein (MRP1) was purchased from Chemicon International (Temecula, CA).

##### **4.4.2.2 Preparation of brain homogenate**

Brains were isolated and dissected following sacrifice by decapitation from mice treated i.p. with ADR (20mg/kg body weight), 72 h after injection or from saline treated control mice, and placed in lysing buffer containing 4µg/ml leupeptin, 4µg/ml pepstatin, 5 µg/ml aprotinin, 2mM ethylenediaminetetraacetic acid (EDTA), 2mM ethylene glycol-bistetraacetic acid (EGTA) and 10mM 4-(2-hydroxyethyl)-1-piperazine-ethanesulfonic acid (HEPES), pH 7.4. The dosage and time were chosen based on prior studies (Yen, Oberley et al., 1999). The brain was homogenized by 20 passes of a Wheaton tissue homogenizer, and the resulting homogenate was centrifuged at 1500g for 10 minutes. The pellet (nuclear fraction) was suspended in 1ml PBS. The supernatant was retained and centrifuged at 20000g for 10 minutes. The pellet (membrane fraction) was suspended in 1ml phosphate buffered saline (PBS) containing 0.01% (w/v) sodium azide and 0.2%

(v/v) Tween 20 (PBS) and the supernatant (cytosolic fraction) was retained for fluorescence studies. All the fractions suspended in PBS were washed twice with PBS at 32000g for 10 min. The resulting fractions were assayed for protein concentration by the Pierce BCA method (Bradford, 1976).

#### **4.4.2.3. Protein Carbonyls**

As described earlier in chapter 3, protein carbonyls are markers of protein oxidation. The method described in section 3.5.1 was used to measure the levels of protein carbonyl. Briefly, Samples (5 $\mu$ l) of brain homogenate (membrane fraction), 12% sodium dodecyl sulfate (SDS) (5 $\mu$ l), and 10 $\mu$ l of 10 times diluted 2,4-dinitrophenylhydrazine (DNPH) from 200mM stock were incubated at room temperature for 20 min, followed by neutralization with 7.5 $\mu$ l neutralization solution (2M Tris in 30% glycerol). This neutralized solution (250ng) was loaded in each well on a nitrocellulose membrane under vacuum using a slot blot apparatus. The membrane was blocked in blocking buffer (3% bovine serum albumin) in PBS 0.01% (w/v) sodium azide and 0.2% (v/v) Tween 20 for 1h and incubated with a 1:100 dilution of anti-DNP polyclonal antibody in PBS containing 0.01% (w/v) sodium azide and 0.2% (v/v) Tween 20 for 1h. The membrane was washed in PBS following primary antibody incubation three times at intervals of 5 min each. The membrane was incubated following washing with an anti-rabbit IgG alkaline phosphatase secondary antibody diluted in PBS in a 1:8000 ratio for 1h. The membrane was washed for three times in PBS for 5 min and developed in Sigmafast tablets, [5-bromo-4-chloro-3-indolyl phosphate/Nitro blue tetrazolium substrate (BCIP/NBT substrate)]. Blots were dried, scanned with Adobe Photoshop, and quantified with Scion Image (PC version of Macintosh compatible NIH image).

#### **4.4.2.4. 3NT**

As described in chapter 2, 3NT are maker of peroxynitrite-mediated tyrosine nitration. The method described in chapter 3 section 3.5.2 was used. Briefly, Samples (5µl) of brain homogenate (membrane fraction), 12% SDS (5µl), and 5µl of modified Laemmli buffer containing 0.125 M Tris base pH 6.8, 4% (v/v) SDS, and 20% (v/v) glycerol were incubated for 20 min at room temperature and were loaded (250ng) in each well on a nitrocellulose membrane in slot blot apparatus under vacuum. The membrane was blocked in blocking buffer (3% bovine serum albumin) in PBS containing 0.01% (w/v) sodium azide and 0.2% (v/v) Tween 20 for 1h and incubated with a 1: 2000 dilution of anti-3-nitrotyrosine (3NT) polyclonal antibody in PBS for 1h 30min. The membrane was washed in PBS for 5 min three times after incubation. The membrane was incubated, following washing with an anti-rabbit IgG alkaline phosphatase secondary antibody diluted in PBS in 1:8000 ratios for 1h. The membrane was washed for three times in PBS for 5 min and developed in Sigmafast tablets. Blots were dried, scanned with Adobe Photoshop, and quantified with Scion Image.

#### **4.4.2.5. Protein-bound HNE**

As described in chapter 2, HNE are lipid peroxidation products that bind to protein by Michael addition and deactivate the protein. Method described in chapter 3 section 3.6 was used to measure the levels of protein-bound HNE. Briefly, Sample (5µl) of brain homogenate (membrane fraction), 12% SDS (5µl), and 5µl of modified Laemmli buffer containing 0.125 M Tris base pH 6.8, 4% (v/v) SDS, and 20% (v/v) glycerol were incubated for 20 min at room temperature and were loaded (250ng) in each well on a nitrocellulose membrane in a slot blot apparatus under vacuum. The membrane was

blocked in blocking buffer (3% bovine serum albumin) in PBS containing 0.01% (w/v) sodium azide and 0.2% (v/v) Tween 20 for 1h and incubated with a 1: 5000 dilution of anti-HNE polyclonal antibody in PBS for 1h 30min. The membrane was washed in PBS for 5min, three times after incubation. The membrane was incubated, following washing with an anti-rabbit IgG alkaline phosphatase secondary antibody diluted in PBS in 1:8000 ratios for 1h. The membrane was washed for three times in PBS for 5 min and developed in Sigmafast tablets. Blots were dried, scanned with Adobe Photoshop, and quantified with Scion Image.

The specificity was checked for both 3NT and HNE primary antibodies as described elsewhere (Sultana, Newman et al., 2004). The sample were treated with primary antibody reacted with free HNE and free 3NT. HNE blot showed very faint, non-specific binding, which was accounted for background. 3NT blot showed no staining on blot suggesting that there was no protein bound 3NT (data not shown) signifying the specificity of primary antibody.

#### **4.4.2.6. Western Blot**

As described in chapter 3, section 3.9, western blot is the technique used to separate protein based on their molecular weight and identification of expression of protein of interest by immunochemical methods. Briefly, samples (100 µg) were incubated with sample loading buffer, and protein samples were denatured and electrophoresed on a 10% SDS-polyacrylamide gel. Proteins were transferred to a nitrocellulose membrane at 90 mA/gel for 2 h. The blots were blocked for 1h in fresh wash buffer (10 mM Tris-HCl, pH7.5), 150 mM NaCl, 0.05% Tween 20, pH 7.4, containing 3% bovine serum albumin) and incubated with a 1:1000 dilution of anti MRP1

monoclonal antibody in phosphate buffered saline containing 0.01% (w/v) sodium azide and 0.2% (v/v) Tween 20 (PBS) for 1h. The membrane was washed three times in PBS and was incubated for 1 h with an anti-rabbit IgG alkaline phosphatase secondary antibody diluted in PBS in a 1:8000 ratio. The membrane was washed for three times in PBS for 5 min and developed in Sigma fast tablets (BCIP/NBT substrate).

In all cases non-specific background labeling by secondary antibody was negligible.

#### **4.4.2.7. Statistical analysis**

A two-tailed Student's t-test was used to assess statistical significance. P values <0.05 were considered significant for comparison between control and experimental data sets.

### **4.5. Results**

#### **4.5.1. Protein carbonyls**

Protein carbonyls are the most often employed index of protein oxidation (Stadtman and Berlett, 1997). Treatment of mice with ADR (i.p.) revealed an increase in protein carbonyls in brain. Figure 4.1 shows the protein carbonyl levels in brain homogenate extracted from saline-injected mice (control) and brain homogenate extracted from mice injected with ADR. There was a significant increase in protein carbonyl levels in brain homogenates from ADR-injected mice when compared to control ( $p < 0.001$ ,  $n=5$ ).



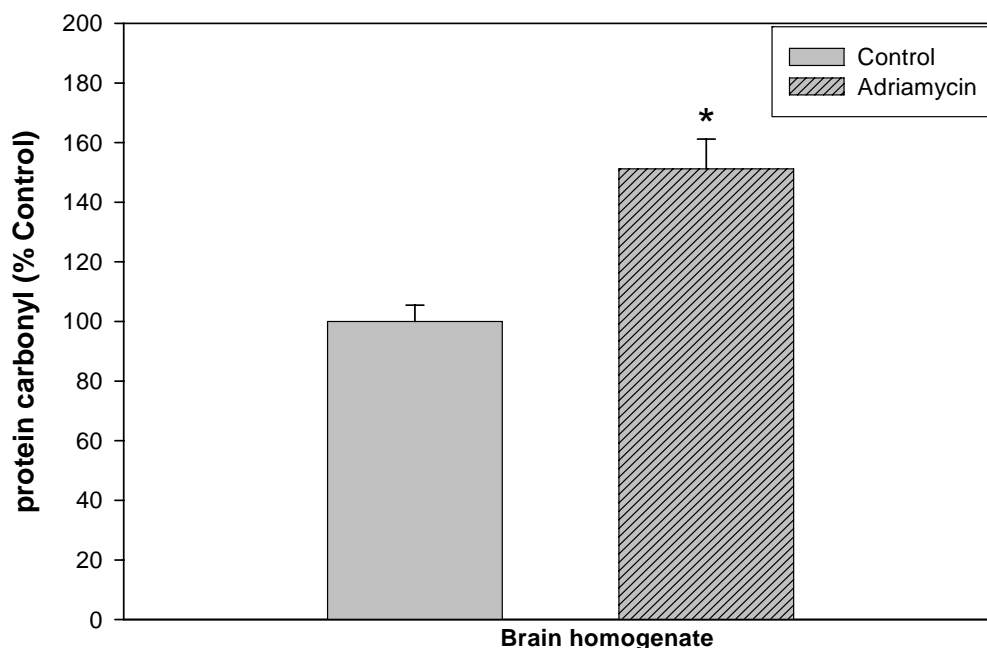


**Figure 4.1:** Increased *in vivo* protein oxidation in brain isolated from mice previously treated with adriamycin (20mg/kg body weight) 72 hours post i.p injection compared to brain isolated from saline injected mice. \*P< 0. 001, n=5. (434.5 arbitrary unit was taken as 100% for control)

#### 4.5.2. 3NT

Nitration of tyrosine residue is the marker of attack by RNS, such as peroxynitrites that may have been formed by free radical mediated oxidative stress (van der Vliet, Eiserich et al., 1996; Castegna, Aksenov et al., 2002a; Castegna, Aksenov et al., 2002b). Figure 4.2 shows 3-NT levels in brain homogenate from saline-injected mice (control) and brain homogenate extracted from mice injected with ADR. There was a

significant increase in 3-NT levels in brain homogenate from ADR-injected mice when compared to control ( $p < 0.001$ ,  $n=5$ ).

#### **4.5.3. HNE**

Arachidonic acid from phospholipids, on attack of free radicals, produces reactive alkenals such as HNE (Lauderback, Hackett et al., 2001). HNE binds to protein and inactivates them by changing their conformation (Subramaniam, Roediger et al., 1997; Markesbery and Lovell, 1998; Lauderback, Hackett et al., 2001). Figure 4.3 shows the protein bound HNE levels in brain homogenate extracted from saline injected mice (control) and brain homogenate extracted from mice injected with ADR. There was a significant increase in protein bound HNE levels in brain homogenate from ADR-injected mice when compared to control ( $p < 0.001$ ,  $n=5$ ).

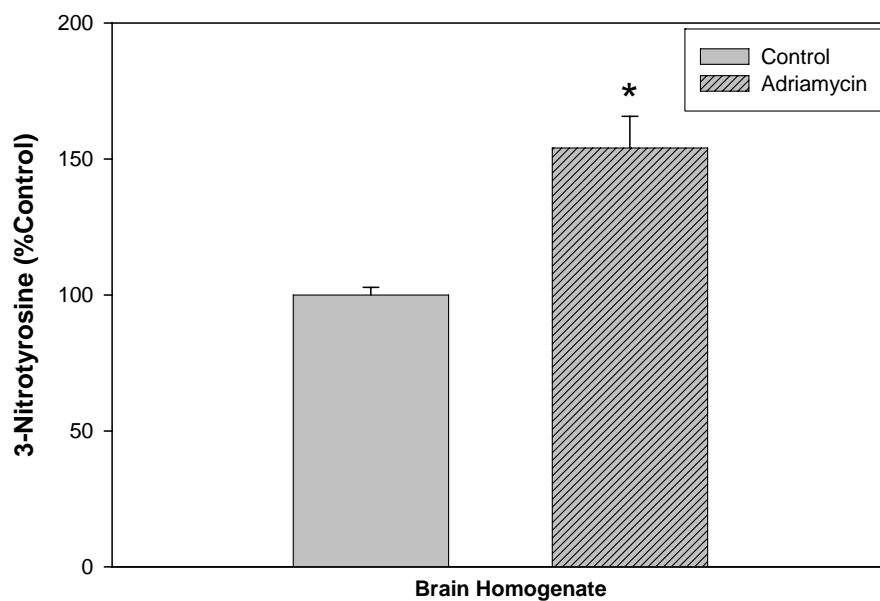


**Figure 4.2:** Increased *in vivo* 3-Nitrotyrosine levels in brain isolated from mice previously treated with adriamycin (20mg/kg body weight) 72 hours post i.p. injection, compared to brain isolated from saline injected mice. \*P< 0. 001, n=5. (151.67 arbitrary unit was taken as 100% for control)

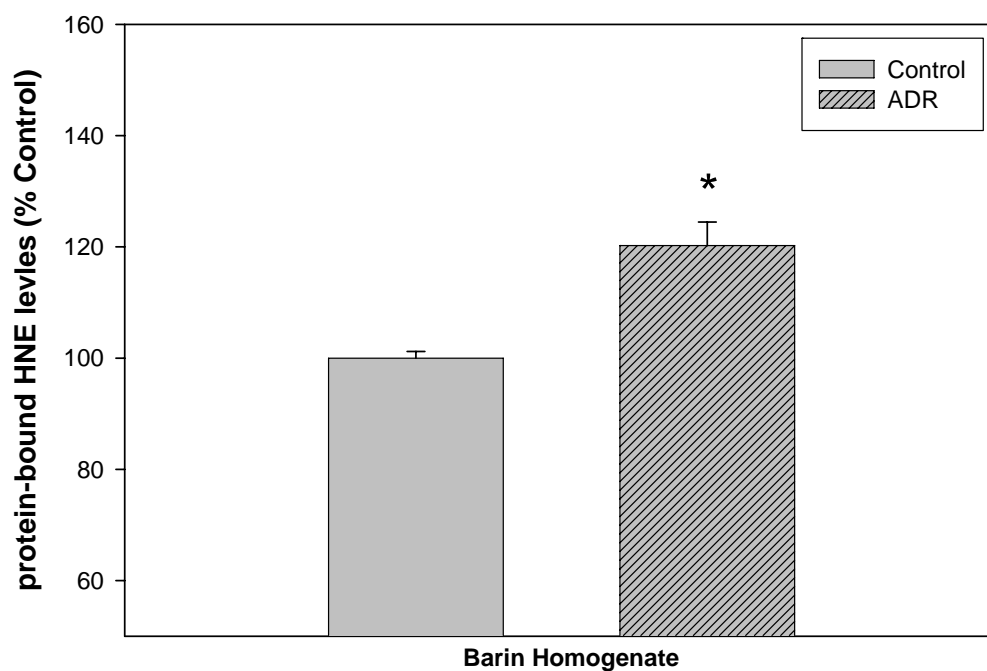


**Figure 4.3:** Increased *in vivo* protein bound HNE in brain isolated from mice previously treated with adriamycin (20mg/kg body weight) 72 hours post i.p. injection, compared to brain isolated from saline injected mice. \*  $P < 0.001$ ,  $n = 5$ . (526 arbitrary unit was taken as 100% for control)

#### **4.5.4. MRP-1 expression**

Glutathione conjugates of ADR are exported from cells via the multi drug resistance-associated protein-1 (MRP-1) (Höpfner, Deeley et al., 1999). Oxidative modification of MRP-1 would likely lead to accumulation of HNE (Sultana and Butterfield, 2004), and in AD brain that is under oxidative stress (Butterfield, Drake et al., 2001; Butterfield and Kanski, 2001; Butterfield and Lauderback, 2002), increased expression of MRP-1 was observed. Consistent with results in AD brain (Sultana and Butterfield, 2004), Figure 4.4 shows that MRP-1 expression is significantly elevated in brain from ADR-injected mice ( $p < 0.05$ ,  $n=3$ ).

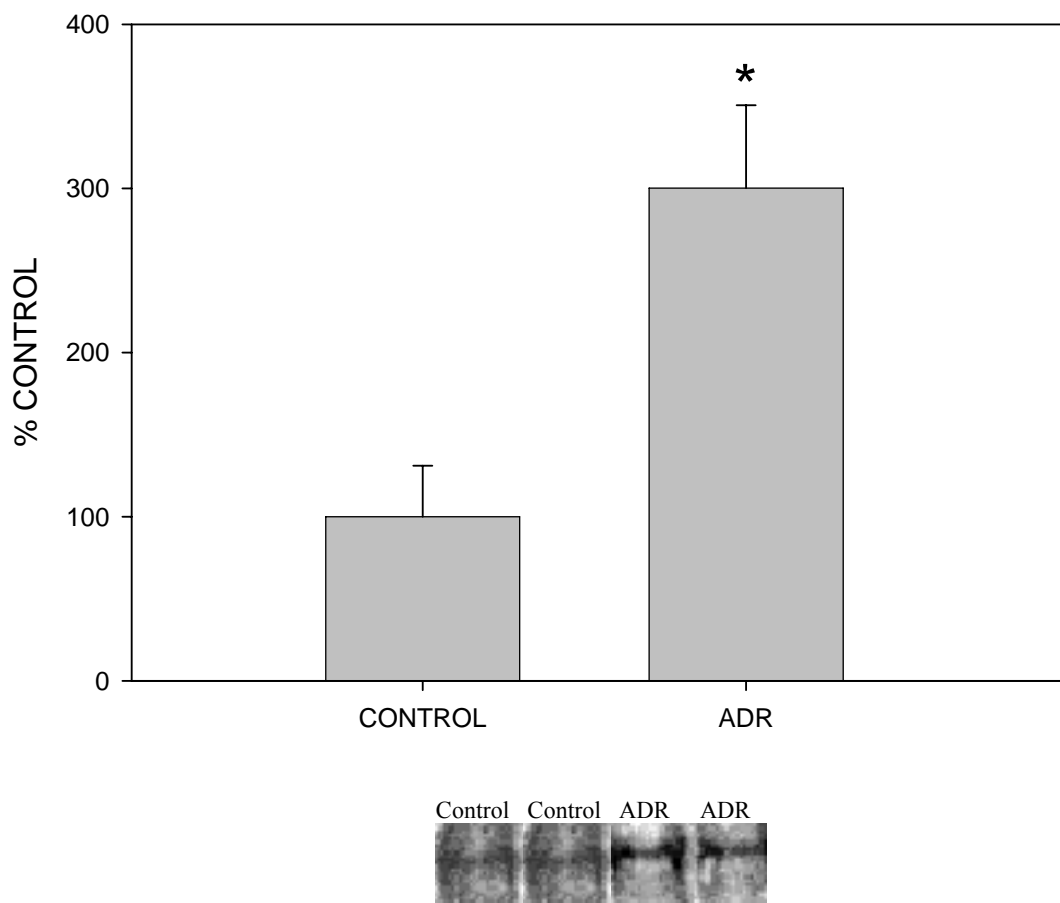


**Figure 4.4:** Plot showing significant increase in MRP1 levels in brain isolated from mice injected i.p. with adriamycin compared to saline injected control mice. \* $P < 0.05$ ,  $n=3$ . (272 arbitrary unit was taken as 100% for control). Also shown in the figure is a representative western blot showing increased MRP1 expression in brain isolated from mice injected with adriamycin. (Data Collected in collaboration with Dr. Rukhsana Sultana)

#### 4.6. Discussion

ADR is a commonly used cancer chemotherapeutic agent for various solid tumors. This agent is known to cause serious side effects in heart. However, ADR also shows side effects in other organs including brain, which has not been studied extensively. ADR causes cardiomyopathy or congestive heart failure. Due to the presence of quinone in its structure, a free radical hypothesis for ADR-mediated oxidative stress and cytotoxicity is widely accepted. In the presence of  $\text{Fe}^{2+}$  free radical production increases (DeAtley, Aksenov et al., 1998).  $\text{Fe}^{2+}$  acts as a catalyst for oxidative stress in neurodegenerative disorders (Stadtman and Berlett, 1997; Kienzl, Jellinger et al., 1999). An elevated level of iron is seen in several neurodegenerative disorders, including Alzheimer's disease (AD). Others showed that there is accumulation of iron in ADR-treated myocardial and neoplastic cells, which leads to increase in oxidative stress (Kwok and Richardson, 2003). In the presence of an iron chelator the ADR induced oxidative stress is reduced in cardiomyocytes (Kalyanaraman, Morehouse et al., 1991; Dorr, 1996).

Nitric oxide synthase and cytochrome P450 reductase are some of the flavoprotein reductases that reportedly activate ADR-dependent redox cycling (Vasquez-Vivar, Martasek et al., 1997). Since mitochondria are target organelles for ADR-induced cytotoxicity in cardiomyocytes (Sarvazyan, 1996; Konorev, Kennedy et al., 1999; Yen, Oberley et al., 1999), NADH dehydrogenase, a mitochondrial enzyme, stimulates ADR to form semiquinone radical and superoxide anion (Davies and Doroshov, 1986).

ADR was shown to induce depletion of glutathione (GSH) in heart tissue (Abd El-Gawad and El-Sawalhi, 2004). GSH is an endogenous antioxidant that is widely present in various tissues (Kotamraju, Konorev et al., 2000). The level of glutathione

peroxidase was also known to be reduced by ADR, and ebselen, a glutathione peroxidase mimetic, significantly inhibits ADR-induced oxidative stress and apoptosis (Kotamraju, Konorev et al., 2000). All these studies provide evidence for a free radical mechanism involved in ADR induced cytotoxicity.

Brain is particularly vulnerable to oxidative stress due to the presence of high levels of polyunsaturated fatty acids, relatively low antioxidant capacity, the presence of redox metal ions, and high oxygen utilization (Stadtman and Berlett, 1997). The free radicals generated in the brain cause damage to proteins, lipids and DNA and subsequently lead to cellular dysfunction or cell death (Yu, 1994; Butterfield, Drake et al., 2001; Butterfield and Lauderback, 2002; Castegna, Aksenov et al., 2002a; Castegna, Aksenov et al., 2002b). Oxidative stress induced by ADR in brain could lead to damage to proteins critical for cell functioning and may also lead to cell death. Involvement of the central nervous system in patients treated with ADR was previously shown (Abali and Celik, 2002). These authors found that patients under treatment with ADR often complain of forgetfulness, lack of concentration and dizziness (collectively called somnolence). We demonstrated that ADR increases oxidative stress and causes cell death in neuronal cell culture (*Vide infra*). The data presented in this paper shows that ADR *in vivo* causes oxidative damage to brain tissue.

Previously we reported oxidized proteins in AD are critical for some vital functions (Butterfield, Drake et al., 2001; Butterfield and Lauderback, 2002; Castegna, Aksenov et al., 2002a; Castegna, Aksenov et al., 2002b; Lauderback, Drake et al., 2003). The results shown in our *in vivo* study are consistent with our *in vitro* results, showing that ADR acts as an oxidant. In the present study there was a significant increase in



protein carbonyl formation and 3-NT levels, markers of protein oxidation and RNS attack on tyrosine residues of protein, and in HNE, a marker of lipid peroxidation, in brain homogenates isolated from ADR-injected mice.

ADR increases superoxide production and enhances formation of nitric oxide (Vasquez-Vivar, Hogg et al., 1999). As a consequence, the balance between superoxide and nitric oxide shifts and could lead to formation of peroxynitrite (van der Vliet, Eiserich et al., 1996; Vasquez-Vivar, Hogg et al., 1999), from which 3-NT can arise (Lauderback, Drake et al., 2003). We have seen a significant increase in 3-NT levels in brain homogenate from ADR-treated mice when compared to those from control mice. This could be due to reaction of peroxynitrite with tyrosine residues on polypeptide chains. The resulting nitration changes protein conformation (Koppal, Drake et al., 1999b) and, consequently, alters their function (Lauderback, Drake et al., 2003).

Lipid peroxidation products such as HNE and acrolein are known to be elevated in brain under oxidative stress in various diseased conditions, including AD (Sayre, Zelasko et al., 1997; Markesbery and Lovell, 1998; Butterfield, Drake et al., 2001; Lauderback, Hackett et al., 2001; Butterfield and Lauderback, 2002). These alkenals react with GSH (Lovell, Xie et al., 1998; Xie, Lovell et al., 1998), and are also known to be involved in apoptosis, which is correlated with GSH depletion (Mark, Lovell et al., 1997). In the current study there was a significant increase in protein bound HNE levels in brain homogenate isolated from ADR-injected mice.

MRP1 is one of the 9-multidrug resistance proteins belonging to the ATP-binding cassette (ABC) transporter family (Nies, Jedlitschky et al., 2004). MRP1 is an integral plasma membrane protein, which mediates ATP-dependent export of cytotoxic organic

anions, glutathione S-conjugates and sulphates (Jedlitschky, Leier et al., 1994; Jedlitschky and Keppler, 2002). MRP1 is expressed in various human tumors. Oxidized glutathione (GSSG) has been recognized as a co-substrate for MRP1 (Loe, Almquist et al., 1996; Loe, Deeley et al., 2000). Translocation of therapeutic drugs into and out of the CNS mediated by MRP1 has been shown (Huai-Yun, Secrest et al., 1998; Rao, Dahlheimer et al., 1999), and others have reported expression of MRP1 in cultured astroglial cells (Decleves, Regina et al., 2000). Involvement of MRP1 in the release of GSSG from brain astrocytes under oxidative stress has also been reported (Hirrlinger, Konig et al., 2001). These studies suggest that MRP1 expression is altered during oxidative stress conditions. Consistent with this suggestion, we reported increased expression of MRP-1 in AD brain (Sultana and Butterfield, 2004), which is under oxidative stress (Stadtman and Berlett, 1997; Markesbery and Lovell, 1998; Butterfield, Drake et al., 2001; Butterfield and Kanski, 2001; Butterfield and Lauderback, 2002; Castegna, Aksenov et al., 2002a; Castegna, Aksenov et al., 2002b).

Studies have shown that MRP1 does not directly transport chemotherapeutic agents such as ADR (Hipfner, Deeley et al., 1999). However, its not clear whether glutathione is either co-transported as a GS-conjugate with ADR or activates MRP1 for ADR transport (Priebe, Krawczyk et al., 1998; Hipfner, Deeley et al., 1999).

In the current study, we observed a significant increase in the levels of MRP1 in brain isolated from ADR-injected mice compared to the level of MRP1 in brain isolated from saline injected control mice. The increased expression could be due to increase in GSSG because of oxidative stress caused by ADR. Since the mechanism of action of

MRP1 is not clear yet, the increased expression could also be result of increased GS-conjugate of ADR, which is transported out of brain with the help of MRP1.

Patients under prolonged treatment with ADR show symptoms of forgetfulness, dizziness and loss of memory, a phenomenon commonly called chemobrain (Abali and Celik, 2002). ADR leads to post-chemotherapeutics problems in children. Often, the symptoms are noticed approximately 10 yrs after treatment. Our current *in vivo* studies show that ADR acts as an oxidant in brain. Our data suggest that ADR or its metabolites likely enter the brain and cause oxidative stress, which may contribute to chemobrain. Further studies are necessary to find the oxidative stress mechanism induced by ADR, which will help in designing therapeutics to reduce the side effects of such anti-cancer drugs in tissues, including chemobrain.

## Chapter 5

### **Alteration in glutathione level and glutathione-related enzyme expression and activity in brain induced by the anti-cancer drug Adriamycin: Implications for oxidative stress-mediated CNS toxicity**

#### **5.1. Overview of study:**

Adriamycin (ADR), a chemotherapeutic agent useful in treating solid cancers, has side effects in various tissues, including brain, apart from its known effects in heart. These side effects limit the successful use of this drug in treatment of cancer. This quinone-containing anthracycline chemotherapeutic is known to produce reactive oxygen species (ROS) in heart. One of the common observations in patients under long-term treatment with ADR is somnolence, often termed as chemobrain by patients. Previously our laboratory has shown significant ADR-induced protein oxidation and lipid peroxidation in cultured neurons and brain, *in vitro* and *in vivo*, respectively. ADR-injected mice also showed an increase in MRP-1 levels, a protein that mediates export of cytotoxic organic anions, glutathione S-conjugates and sulphates. Although, ADR doesn't cross blood brain barrier, we recently showed that the toxicity in the central nervous system (CNS) induced by ADR is mediated by tumor necrosis factor  $\alpha$  (TNF-  $\alpha$ ). Given the oxidative stress in brain induced *in vivo* by ADR, in the current study we measured the levels of brain glutathione (GSH), a major thiol antioxidant, in ADR-injected mice brain. Accordingly, we examined the *in vivo* levels of GSH-related enzyme expression and activity induced by i.p. injection of ADR. The results showed a significantly decreased total GSH levels, increased levels of glutathione peroxidase (GPx), glutathione-S-transferase (GST) and glutathione reductase (GR) and an increased activity

of GPx and GST, but a significant reduction in GR activity in brain isolated from mice, 72 hrs post i.p injection of ADR (20 mg/kg). These results are consistent with brain-resident oxidative stress observed in ADR treated mice and consistent with the hypothesis that *in vivo* administration of ADR causes alterations in antioxidant capacity in brain. Sequelae of ADR may be the cause of chemobrain observed in the patients treated with this redox cycling chemotherapeutic agent. The results suggest that a potential therapeutic intervention towards increasing the antioxidant capacity in brain might alleviate the side effects in brain.

## **5.2. Introduction**

Free radical-mediated oxidative stress has been implicated in many neurodegenerative disorders (Hensley, Hall et al., 1995; Stadtman and Berlett, 1997; Markesbery and Lovell, 1998; Butterfield, Drake et al., 2001; Butterfield and Lauderback, 2002). Reactive oxygen species (ROS) and reactive nitrogen species (RNS) produced as a consequence to oxidative stress leads to a significant protein oxidation (Hensley, Hall et al., 1995; Stadtman and Berlett, 1997), lipid peroxidation (Markesbery and Lovell, 1998; Butterfield and Lauderback, 2002) and DNA and RNA oxidation (Butterfield, Drake et al., 2001).

Glutathione (GSH) is a major tripeptide intracellular antioxidant present ubiquitously in the range of 1-3mM throughout the brain (Cooper, 1997), acting as a high capacity detoxification agent. GSH maintains the cellular redox balance and is involved in various biosynthetic processes as well (Schulz, Lindenau et al., 2000). The level of GSH is reduced in specific regions of the central nervous system in various neurodegenerative disorders and concomitant increase in oxidized glutathione (GSSG)

levels contributes to the oxidative stress-mediated neuronal cell dysfunction and/or loss in these disorders (Benzi and Moretti, 1995a; Cooper, 1997). GSH, in conjugation with glutathione reductase (GR), glutathione peroxidase (GPx), glutathione-S-transferase (GST) and NADPH provide protection against various toxic electrophiles and hydrogen peroxide (Watson, Chen et al., 2003). GST-mediated glutathione-S conjugates are further acted upon by multi drug resistant protein-1 (MRP-1), an ATP-binding cassette (ABC) transporter family protein (Nies, Jedlitschky et al., 2004), for their export out of the cell in an ATP-dependent manner (Sultana and Butterfield, 2004).

Adriamycin (ADR) is a quinone containing cancer chemotherapeutic agent used to treat various solid tumors. ADR intercalates itself into the grooves of DNA and inhibits its replication and synthesis (Cummings, Anderson et al., 1991). Although there are various other mechanism of action of this drug described in literature, enzymatic free radical generation by action of a variety of oxidases, reductases and dehydrogenases on ADR is widely accepted (Kappus, 1987; Gutierrez, 2000) and could be contributing factor towards its toxicity. The quinone in ADR undergoes one electron reduction to produce a semiquinone, which is a free radical itself, and in the presence of oxygen it generates superoxide radical and converts itself back to quinone, a process called redox cycling (Handa and Sato, 1975; Gutteridge, 1984). This property of ADR may be responsible for its serious side effects in heart. A free radical mediated protein oxidation and lipid peroxidation has been reported in cardiomyocytes treated with ADR (DeAtley, Aksenov et al., 1998). Apart from cardiomyopathy, patients under long term treatment with ADR have complained of dizziness, forgetfulness and lack of concentration (somnolence) (Meyers, 2000; Schagen, Hamburger et al., 2001; Freeman and Broshek,

2002). Recently, we showed that systemic administration of ADR induces brain TNF accumulation, causes neuronal mitochondrial dysfunction and may be responsible for consequent CNS injury (Tangpong, Cole et al., 2006b). Although the biochemical basis for ADR-mediated cognitive imbalance is not very well established, ADR is known to cause increased protein oxidation and lipid peroxidation along with increased MRP-1 expression in brain isolated from ADR-injected mice (Joshi, Sultana et al., 2005b). ADR cannot cross the blood brain barrier (Bigotte, Arvidson et al., 1982a; Bigotte, Arvidson et al., 1982b; Tangpong, Cole et al., 2006b) hence, the side effects could be due to ADR-mediated TNF- $\alpha$  production via activation of glia, which can further lead to increased ROS and RNS.

In recent years, GSH and other cellular antioxidant enzyme systems have been studied with reference to redox signaling mechanisms that function in cell regulation and growth control. Among others, one such antioxidant enzyme system is superoxide dismutase (SOD). The primary function of SOD is to convert superoxide radicals to hydrogen peroxide, which is subsequently converted to water and oxygen by action of GPx and/or catalase. Increased expression of certain SOD has shown to be protective against oxidative stress in many disease models (Yen, Oberley et al., 1999). Based on these studies we tested the hypothesis that *in vivo* administration of ADR modulates the GSH antioxidant defense mechanism.

The present study was designed to look at the effect of *in vivo* administration of ADR on certain antioxidant enzyme systems with prime focus on modulation of GSH and its related enzyme expression and activities. The results shown here are discussed with reference to chemobrain induced by free radical-mediated oxidative stress by ADR.

### **5.3. Experimentals**

#### **5.3.1. Animals**

For the studies, male B6C3 mice (2-3 months of age), approximately 30 g in size, housed in the University of Kentucky Central Animal Facility in 12-h light/dark conditions and fed standard Purina rodent laboratory chow *ad libitum*, were used. The animal protocols were approved by the University of Kentucky Animal Care and Use Committee.

#### **5.3.2. Chemicals**

Doxorubicin HCl (ADR) was purchased from Bedford Laboratories. All other chemicals were purchased from Sigma-Aldrich (St. Louis, MO), unless stated otherwise. The primary antibody for GST and GPx were purchased from Chemicon International (Temecula, CA). The primary antibody for GR was purchased from Abcam, Inc (Cambridge, MA). Sodium dodecyl sulfate (SDS) polyacrylamide gels (12.5%) and transfer membranes were purchased from Biorad (Hercules, CA). The GSH assay kit was purchased from Cayman chemicals (Ann Arbor, MI).

#### **5.3.3 Preparation of brain homogenate**

Brains were isolated and dissected following sacrifice by decapitation from mice injected intraperitoneally (i.p.) with ADR (20mg/kg body weight), 72 h post i.p. injection, or from saline treated control mice, and placed in ice cold lysing buffer containing 4µg/ml leupeptin, 4µg/ml pepstatin, 5 µg/ml aprotinin, 2mM ethylenediaminetetraacetic acid (EDTA), 2mM ethylene glycol-bistetraacetic acid (EGTA) and 10mM 4-(2-hydroxyethyl)-1-piperazine-ethanesulfonic acid (HEPES), pH 7.4. The dosage of ADR and time used were chosen based on prior studies (Joshi, Sultana et al., 2005b). The brain



was homogenized by 20 passes of a Wheaton tissue homogenizer, and the resulting homogenate was centrifuged at 1500g for 10 minutes. The pellet (nuclear fraction) was suspended in 1ml phosphate buffered saline (PBS) containing 0.01% (w/v) sodium azide and 0.2% (v/v) Tween 20. The supernatant was retained and centrifuged at 20000g for 10 minutes. The pellet (membrane fraction) was suspended in 1ml PBS and the supernatant (cytosolic fraction) was retained for fluorescence studies, GSH measurement and enzyme activities. All the fractions suspended in PBS were washed twice with PBS at 32000g for 10 min. The resulting fractions were assayed for protein concentration by the Pierce BCA method (Bradford, 1976).

#### **5.3.4. GSH assay**

The supernatant obtained from homogenate was deproteinated with 10% metaphosphoric acid. The subsequent deproteinated supernatant was treated with 4M triethanolmalamine (TEAM) solution. Following TEAM treatment, the GSH assay kit was used according to the manufacturer's direction to assay total GSH.

#### **5.3.5. Western blots**

Samples (100 µg) were incubated with sample loading buffer, and protein samples were denatured and electrophoresed on a 12.5% SDS-polyacrylamide gel. Proteins were transferred to a nitrocellulose membrane at 90 mA/gel for 2 h. The blots were blocked for 1h in fresh wash buffer (10 mM Tris-HCl, pH7.5), 150 mM NaCl, 0.05% Tween 20, pH 7.4, containing 3% bovine serum albumin) and incubated with a 1:1000 dilution of the respective anti GST, GPx and GR monoclonal antibody in phosphate buffered saline containing 0.01% (w/v) sodium azide and 0.2% (v/v) Tween 20 (PBS) for 1h. The membrane was washed three times in PBS and was incubated for 1 h

with an anti-rabbit IgG alkaline phosphatase secondary antibody diluted in PBS in 1:8000 ratio. The membrane was washed for three times in PBS for 5 min and developed in Sigma fast tablets (BCIP/NBT substrate).

In all cases non-specific background labeling by secondary antibody was negligible.

### **5.3.6. Enzyme activity assays**

#### **5.3.6.1. Estimation of glutathione-S-transferase activity**

GST (EC 2.5.1.18) activity was measured using a reaction mixture consisting of 0.1 M phosphate buffer (pH 6.5), 1.0 mM reduced glutathione, 1.0 mM CDNB and 1mg/ml of supernatant protein (Habig, Pabst et al., 1974). The changes in absorbance were recorded at 340 nm in a 96 well microtiter plate, and the enzymatic activity was calculated as nmol of CDNB conjugate formed  $\text{min}^{-1} \text{mg}^{-1}$  protein.

#### **5.3.6.2. Estimation of glutathione peroxidase activity**

GPx (EC 1.11.1.9) was measured using a reaction mixture consisting of 0.2 mM  $\text{H}_2\text{O}_2$ , 1.0 mM GSH, 0.14 U of glutathione reductase (GR), 1.5 mM NADPH, 1.0 mM sodium azide and 0.1M phosphate buffer (pH 7.4) and 1mg/ml of supernatant protein (Wheeler, Salzman et al., 1990). The changes in absorbance were recorded at 340 nm in a 96 well microtiter plate and enzyme activity was calculated as nmol of NADPH oxidized  $\text{min}^{-1} \text{mg}^{-1}$  protein.

#### **5.3.6.3. Estimation of glutathione reductase activity**

The GR (EC 1.6.4.2) activity assay reaction mixture consisted of 0.1 M phosphate buffer (pH 7.6), 0.5 mM EDTA, 1.0 mM oxidized glutathione, 0.1 mM NADPH and 1mg/ml of supernatant protein in a total volume of 200  $\mu\text{l}$  (Carlberg and Mannervik,

1985). The enzyme activity was assayed in a 96-well plate reader by measuring the disappearance of NADPH at 340 nm and was calculated as nmol of NADPH oxidized  $\text{min}^{-1} \text{mg}^{-1}$  protein.

#### **5.3.6.4. Estimation of total SOD activity**

SOD (EC 1.15.1.1) activity assay reaction consisted of 50 mmol/l glycine buffer, pH 10.4, and 1mg/ml supernatant protein. The reaction was initiated by the addition of 20 mg/ml solution of (–)-epinephrine and absorbance was measured at 480 nm (Stevens, Obrosova et al., 2000). SOD activity was expressed as nmol of (–)-epinephrine protected from oxidation  $\text{min}^{-1} \text{mg}^{-1}$  protein.

#### **5.4. Statistical analysis**

A two-tailed Student's t-test was used to assess statistical significance. P values <0.05 were considered significant for comparison between control and experimental data sets.

### **5.5. Results**

#### **5.5.1. GSH assay**

GSH levels in a system are an indication of its cellular redox balance. A more reduced to oxidized ratio is indication of healthy state, whereas a reduction in total GSH levels may be an indication of redox imbalance or oxidative stress (Watson, Chen et al., 2003). Figure 5.1 shows a significantly reduced GSH level in brain isolated from ADR-injected mice when compared to saline-injected control ( $p < 0.05$ ,  $n = 5$ ).

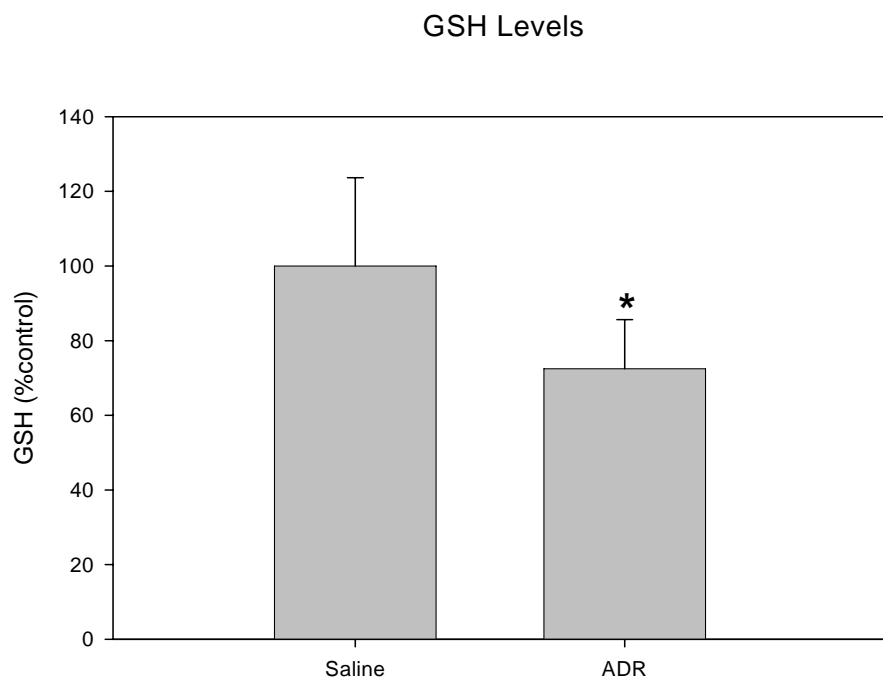
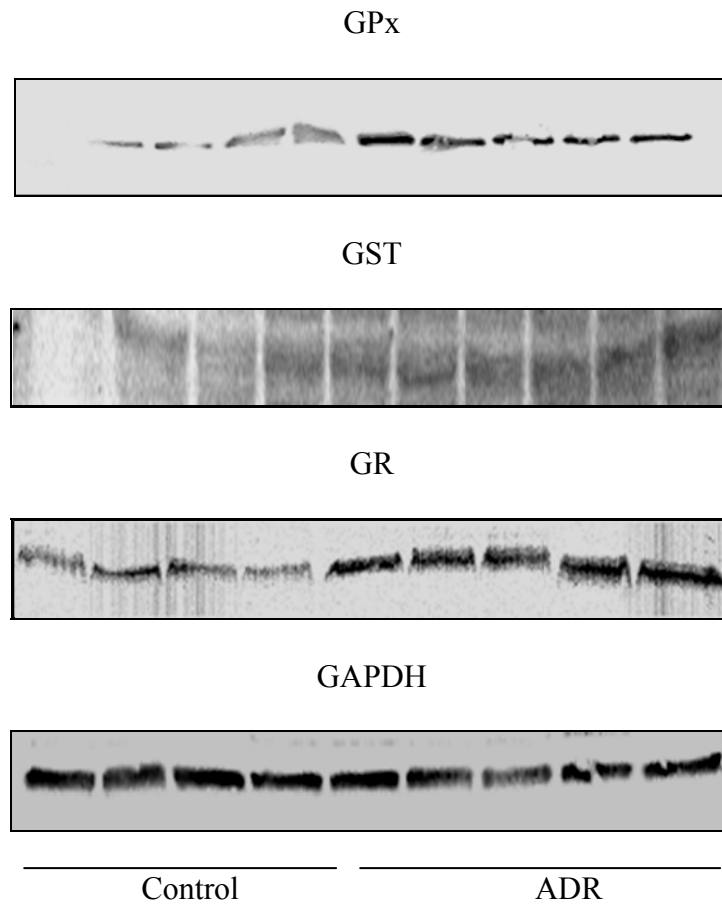


**Figure 5.1:** Brain total GSH level in saline-injected and ADR-injected mice, 72 h post i.p. injections. A significant reduction in GSH level is seen in brain isolated from ADR-injected mice when compared to control. \*  $p < 0.05$ ,  $n = 5$ . The data are presented as mean  $\pm$  SEM expressed as percentage of control.

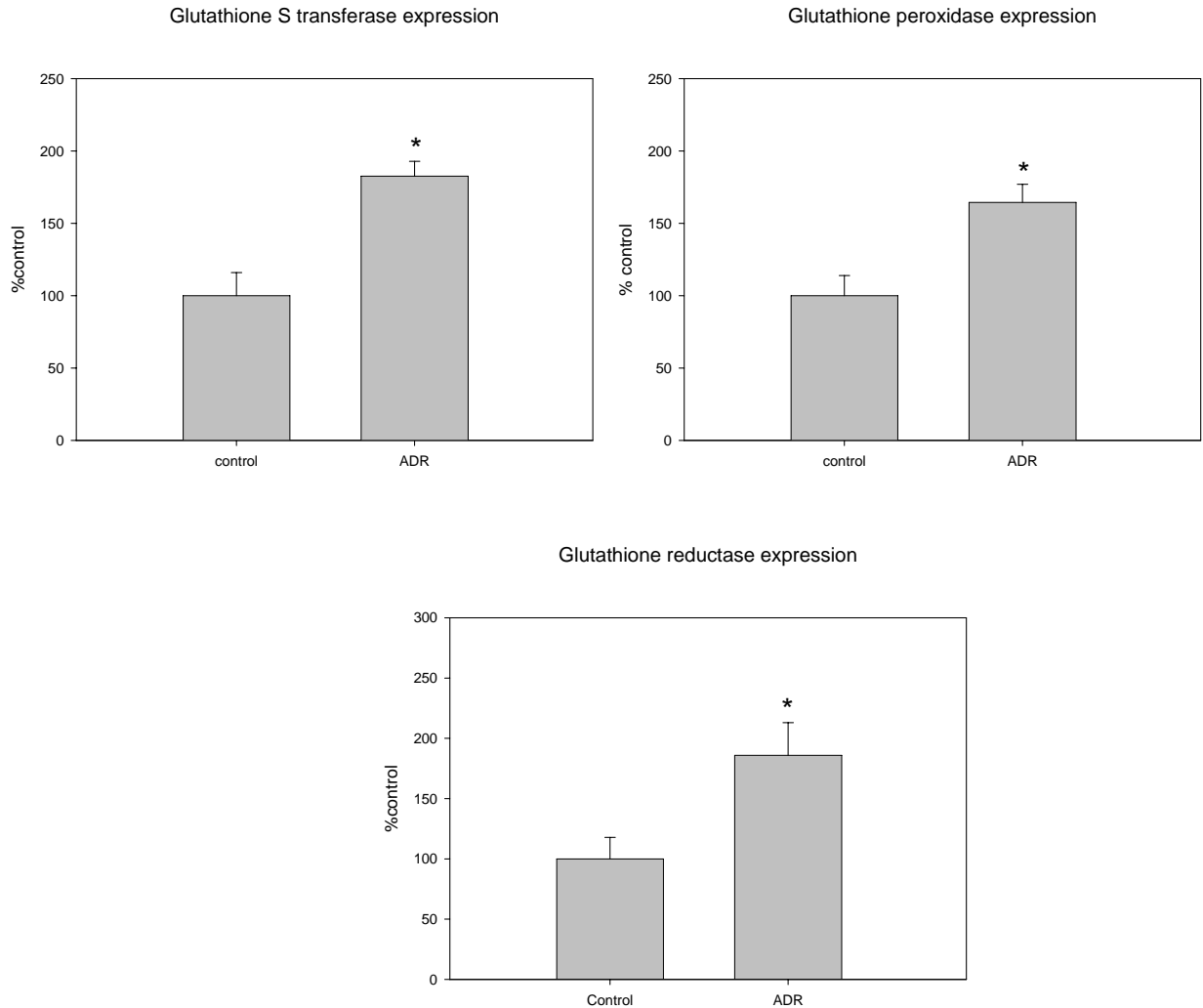
### 5.5.2. Western blot analysis

Figure 5.2 shows the western blots and representative plots of GST, GPx and GR in brain isolated from mice injected i.p. with saline or ADR. GAPDH is used as a loading control. Plots of normalized entity of each enzyme are shown in figure 5.3. As evident from the figures, a significant increased expression of GST, GPx and GR in brain isolated

from ADR-injected mice when compared to saline-injected control is observed ( $p < 0.05$ ,  $n = 5$ ).



**Figure 5.2:** Representative Western blots of brain GPx, GST and GR 72 h post i.p. injection of saline or ADR in mice. GAPDH is used as a loading control.



**Figure 5.3:** Representative plot of GST, GPx and GR levels in saline-injected and ADR-injected mice brain, 72 h post i.p. injections. A significant increase in GST, GPx and GR level is seen in ADR-injected mice brain when compared to control. \*  $p < 0.05$ ,  $n = 5$ . The data are presented as mean  $\pm$  SEM expressed as percentage of control.

### 5.5.3. Enzyme activities

Table 5.1 shows the activity of GSH related enzymes GST, GPx and GR along with the activity of total SOD. There was a significant increase in activity of GPx, whereas a significantly reduced activities of GST, GR and SOD in brain isolated from ADR-injected mice when compared to saline-injected control ( $p < 0.05$ ,  $n = 5$  in each case).

Enzyme	Brain from saline-injected Group	Brain from ADR-injected Group
GST (nmol CDNB conjugate formed $\text{min}^{-1} \text{mg}^{-1}$ protein)	$15.6 \pm 0.3$	$12.1 \pm 0.3^*$
GPx (nmol NADPH oxidized $\text{min}^{-1} \text{mg}^{-1}$ protein)	$83.7 \pm 0.8$	$96.9 \pm 0.7^*$
GR (nmol NADPH oxidized $\text{min}^{-1} \text{mg}^{-1}$ protein)	$34.9 \pm 1.6$	$27.16 \pm 2.0^*$
SOD (nmol of (–)-epinephrine protected from oxidation $\text{min}^{-1} \text{mg}^{-1}$ protein.	$9.4 \pm 1.6$	$7.1 \pm 3.1^*$

**Table 5.1:** GSH-related enzymes and SOD activity in brain homogenate obtained from mice, 72 h post i.p. injection of saline (control) or ADR. The data are presented as mean  $\pm$  SEM ( $n=5$ ), \*  $p < 0.05$ .

## 5.6. Discussion

GSH is the major non-protein thiol antioxidant used in the redox balance of cells and cellular environments. Any kind of imbalance in the ratio of reduced to oxidized GSH may both index and cause oxidative stress that leads to significant protein oxidation and lipid peroxidation. GSH is known to protect against cellular free radical-mediated oxidative damage by functioning as an oxyradical scavenger thereby reducing lipid peroxidation (Meister, 1995; Darley-USmar and Halliwell, 1996; Sies, 1999; Schulz, Lindenau et al., 2000; Hansen, Go et al., 2006). GSH, apart from its endogenous antioxidant activity, also has role in wide range of metabolic processes such as activation of transcription factors, DNA repair, enzyme activity regulation and biosynthetic processes (Meister and Anderson, 1983).

The nervous system is particularly susceptible to oxidative insults because of high level of polyunsaturated fatty acids, high oxygen consumption and low antioxidant capacity. Hence, the brain is dependent on glutathione defense mechanism as a primary endogenous neuroprotectant. GSH helps neurons in detoxification of HNE and other reactive alkenals and damage by peroxynitrite (Mark, Lovell et al., 1997; Koppal, Drake et al., 1999a). HNE, acrolein and other lipid peroxidation product are known to cause damage to proteins and other biomolecules in AD brain (Sayre, Zelasko et al., 1997; Lovell, Xie et al., 1998; Lauderback, Hackett et al., 2001). These alkenals form an immediate substrate for GSH (Xie, Lovell et al., 1998) consequently, GSH depletion may lead to apoptosis initiated by lipid peroxidation products (Mark, Lovell et al., 1997). In the current study, reduced level of brain GSH was found in ADR-injected mice when compared to saline-injected control (Fig. 5.1). We previously reported an increased



protein carbonyls, HNE and 3NT levels in brain isolated from ADR-injected mice (Joshi, Sultana et al., 2005b). We hypothesized that a reduced level of GSH play a role in the observed brain protein oxidation and increased reactive alkenal in ADR-injected mice.

Oxygen is the terminal acceptor of electrons in the electron transport chain that subsequently produces superoxide radical. Superoxide radicals are formed by action of enzyme NADPH oxidase (NOX) on oxygen (Babior, 1999). Superoxide radicals are also increased by ADR that enhances production of NO (Vasquez-Vivar, Hogg et al., 1999). SOD catalyses the dismutation of superoxide free radicals to form  $H_2O_2$ . GPx and GR provide protection to neurons from oxidative stress at the expense of GSH (Sies, 1999; Hansen, Go et al., 2006). GPx converts the  $H_2O_2$  to  $H_2O$  and  $O_2$ . The reducing electrons are provided by GSH which is converted to its disulfide GSSG. GR converts GSSG back to reduced GSH by utilizing NADPH as a cofactor. NADPH also reduces peroxynitrite, thereby providing enzymatic defense against peroxynitrite (Sies, Sharov et al., 1997). GST play a role in neuroprotection by catalyzing the conjugation of GSH to HNE, a lipid peroxidation product, and, formation of other glutathione-S conjugates with various toxic electrophiles. These conjugates are then cleared from neurons by the action of the MRP-1 (Sultana and Butterfield, 2004). Both GST and MRP-1 are oxidatively modified and likely dysfunctional in AD brain (Sultana and Butterfield, 2004). We previously reported increased expression of brain MRP-1 in ADR-injected mice (Joshi, Sultana et al., 2005b). In the present study we found a significantly increased expression of GST, GPx and GR (Fig 5.2 and 5.3). Although increased protein expression is not always indicative of the activity of these enzymes, the activity of GST, GR and SOD in brain isolated from ADR-injected mice is significantly decreased whereas a significant elevated activity of GPx is

observed. A reduced activity in GR may result in increased GSSG levels, thereby altering the GSG/GSSG ratio towards more oxidized form, leading to oxidative stress. A reduced GST activity would lead to less clearance of toxic substances, which may contribute to the observed increased protein-bound HNE levels in brain from ADR-injected mice. A reduced SOD activity leads to an increase in superoxide radical levels. Superoxide radical,  $H_2O_2$  and NO can react directly or indirectly with each other and produce several other toxic ROS and RNS (Halliwell and Gutteridge, 1999), which may contribute to the oxidative stress observed.

*In vivo* ADR induces TNF- $\alpha$  production, and circulating TNF- $\alpha$  in brain triggers apoptotic pathways along with production of ROS/RNS. A neutralizing antibody against TNF eliminates these effects (Tangpong, Cole et al., 2006b). Injection of ADR causes significant increase in protein oxidation and lipid peroxidation (Joshi, Sultana et al., 2005b). The observed elevated oxidative stress could be either a cause or consequence of glutathione depletion and alteration in various antioxidant enzyme defense systems and TNF-mediated processes. Cognitive dysfunction in patients undergoing chemotherapy is elevated (Meyers, 2000; Schagen, Hamburger et al., 2001; Freeman and Broshek, 2002). We suggest that oxidative stress in brain could contribute to somnolence observed in some patients undergoing ADR or other chemotherapy. The current study is the first to show the role of GSH in ADR-mediated chemobrain. The results suggest that increment in brain GSH levels and the activity of its dependent enzymes (GST, GPx and GR) could be a potential therapeutic approach towards eliminating the observed cognitive impairment in patients undergoing chemotherapy. Studies to determine if such an

approach to prevent chemobrain may be useful, without compromising the chemotherapeutic properties of ADR are in progress.

## Chapter 6

### **Proteomic identification of differentially expressed proteins and redox proteomic identification of specifically oxidized proteins in brain isolated from adriamycin-injected mice: Potential targets for therapeutics.**

#### **6.1. Overview of study**

The central nervous system (CNS) toxicity mediated by the anti-cancer drug adriamycin (ADR) has gained considerable importance recently. ADR is a chemotherapeutic agent used in treatment of solid tumors. Its toxic side effects in heart and brain limit successful use of this drug in treating cancer. Many patients report symptoms of somnolence (Chemobrain) following ADR therapy. Systemic administration of ADR leads to significant protein oxidation, lipid peroxidation and glutathione (GSH) depletion along with alteration in GSH dependent enzyme activities in brain. The observed protein oxidation and lipid peroxidation was reduced by *in vivo* administration of GSH precursor,  $\gamma$ -glutamyl cysteine ethyl ester (GCEE). Intra-peritoneal (i.p.) injection of ADR induces production of tumor necrosis factor- $\alpha$  (TNF- $\alpha$ ) and causes mitochondrial dysfunction, leading to apoptosis in brain. Inducible nitric oxide synthase is involved in ADR-mediated CNS injury, since brain mitochondria isolated from iNOS knock-out mice previously treated with ADR are not dysfunctional when compared to mitochondria isolated from ADR-injected wild type mice. ADR does not cross the blood brain barrier (BBB), but ADR-induced cognitive dysfunction by cytokine-mediated pathways appear prominent. Free radical-mediated oxidative stress caused by ADR damages biomolecules such as proteins and membrane lipids, which might lead to neuronal loss followed by cognitive impairment. These damaged

biomolecules lead to antioxidant depletion, mitochondrial dysfunction and loss of function of important metabolic protein. Although ADR-induced CNS toxicity and chemobrain are increasingly recognized, the biochemical basis behind these effects is not clear yet. The current study was aimed at using expression proteomics followed by parallel redox proteomics for unbiased identification of brain proteins that are differentially expressed or specifically oxidized. The results are discussed with reference to ADR-mediated CNS toxicity, cognitive dysfunction and chemobrain.

## **6.2. Introduction**

Free radical-mediated oxidative stress has been implicated in many neurodegenerative conditions. Impaired function of central nervous system (CNS) and its toxicity is caused, in part, by free radical-mediated protein oxidation (Stadtman and Berlett, 1997; Butterfield and Kanski, 2001), lipid peroxidation (Markesbery and Lovell, 1998), DNA/RNA oxidation (Wang, Xiong et al., 2005) and neuronal dysfunction or death. In most of the neurodegenerative conditions, free radicals react with brain biomolecules such as proteins and lipids, resulting in cognitive decline (Butterfield and Lauderback, 2002). Mitochondria, in particular, play an important role in free radical generation. Mitochondrial dysfunction along with damaged mitochondrial enzymes lead to increased free radical generation and increased oxidative stress (Miquel, Economos et al., 1980). Although mitochondria are a source of free radicals, they also become immediate targets for free radical-mediated oxidative stress thereby, causing energy metabolism dysfunction along with triggering apoptotic signals, leading to neuronal death (Ventura, Genova et al., 2002; Sastre, Pallardo et al., 2003).

Adriamycin (ADR), a cancer chemotherapeutic drug used in treating various solid tumors in breast and lung cancer, has shown various side effects in heart and brain. Apart from its known mechanism of action of intercalating itself into the grooves of DNA and inhibiting DNA replication (Cummings, Anderson et al., 1991), a free radical-mediated mechanism of toxicity involving enzymatic electron reduction of ADR by variety of oxidases, reductases and dehydrogenases, is widely accepted (Kappus, 1987; Gutierrez, 2000). The quinone-containing ADR is known to cause cardiomyopathy, a serious side effect that limits its successful use in treating cancer (Steinherz, Steinherz et al., 1991). Cardiomyocytes treated with ADR show significant protein oxidation and lipid peroxidation, and antioxidants are known to prevent these effects (DeAtley, Aksenov et al., 1998; DeAtley, Aksenov et al., 1999). Apart from its known side effects in heart, ADR also induces cognitive decline (chemobrain) in many patients, often lasting years following treatment with this drug (Meyers, 2000; Schagen, Hamburger et al., 2001). ADR does not cross the blood brain barrier (BBB) (Bigotte, Arvidson et al., 1982a; Bigotte, Arvidson et al., 1982b). *In vivo* ADR causes significant elevation in markers of protein oxidation and lipid peroxidation and increased expression of multidrug resistant protein-1 (MRP-1) in brain (Joshi, Sultana et al., 2005b). ADR also causes glutathione (GSH) depletion and alteration in expression and activities of various GSH related enzymes in brain (Joshi, Sultana et al., 2006). *In vivo* delivery of GSH precursor,  $\gamma$ -glutamyl cysteine ethyl ester (GCEE), modulated brain oxidative stress induced by ADR (Joshi, Hardas et al., 2006).

Involvement of mitochondria and mitochondrial enzymes has been reported in ADR mediated toxicity in heart and brain (Yen, Oberley et al., 1999; Tangpong, Cole et

al., 2006a; Tangpong, Cole et al., 2006b). Manganese superoxide dismutase (MnSOD), a key mitochondrial enzyme is involved in catalyzing the dismutation of superoxide radicals to hydrogen peroxide. Increased expression of MnSOD protects mitochondrial complex 1 against ADR-induced cardiomyopathy (Yen, Oberley et al., 1999). We recently showed that systemic administration of ADR caused mitochondrial dysfunction in brain by inducing tumor necrosis factor- $\alpha$  (TNF-  $\alpha$ ), which leads to various apoptotic pathways (Tangpong, Cole et al., 2006b). Inducible nitric oxide synthase, leads to NO, plays a significant role in ADR-induced CNS toxicity, since iNOS knock-out mice treated with ADR show no brain mitochondrial dysfunction (Tangpong, Cole et al., 2006a). An antibody against TNF prevented the mitochondrial dysfunction and apoptosis mediated by ADR *in vivo* (Tangpong, Cole et al., 2006a; Tangpong, Cole et al., 2006b). Based on these previous studies, we hypothesized that *in vivo* ADR cause oxidative stress in brain and ADR-mediated CNS toxicity is involved in chemobrain and subsequent cognitive decline in patients treated with this drug.

### **6.3. Purpose of the study**

Recently, proteomics along with advances in bioinformatics tools has lead to the identification, characterization and sequencing of proteins in various organisms, including humans. Using redox proteomics (Dalle-Donne, Scaloni et al., 2006) our laboratory has shown many key proteins that are oxidized or differentially expressed in various neurodegenerative conditions or models thereof, such as Alzheimer's disease (AD) (Butterfield and Boyd-Kimball, 2004; Tangpong, Cole et al., 2006a), ageing (Poon, Calabrese et al., 2006), amyotrophic lateral sclerosis (ALS) (Poon, Hensley et al., 2005), Parkinson's disease (PD) (Poon, Frasier et al., 2005), mild cognitive impairment (MCI)

(Butterfield, Poon et al., 2006) among others. Although it is clear that *in vivo* ADR increases protein oxidation in brain, it is not clear which specific brain proteins show increased oxidative damage. In the current study we used 2-dimensional gel electrophoresis (2DE) coupled with mass spectrometric analysis (expression proteomics) to identify proteins that are differentially expressed and 2DE followed by western blot coupled with mass spectrometric analysis (redox proteomics) to identify proteins that are oxidized in brain isolated from mice i.p injected with ADR.

## **6.4. Experimentals**

### **6.4.1. Chemicals**

All the chemicals used were purchased from Sigma-Aldrich (St. Louis, MO), unless stated otherwise. Doxorubicin HCl (ADR) was purchased from Bedford Laboratories. All the 2DE gels, stains, buffers and Western blot material were purchased from Bio-Rad (Hercules, CA). The protein oxidation detection kit was purchased from InterGen (Purchase, NY). Trypsin was purchased from Promega (Madison, WI).

### **6.4.2. Animals**

For the studies, male mice (2-3 months of age), approximately 30 g in size, housed in the University of Kentucky Central Animal Facility in 12-h light/dark conditions and fed standard Purina rodent laboratory chow *ad libitum*, were used. The animal protocols were approved by the University of Kentucky Animal Care and Use Committee. The animals were divided into 2 groups. One group received saline and other group received ADR (20mg/kg body weight). 72 h post i.p. injection the mice were sacrificed, brains were isolated and flash frozen in liquid nitrogen till further studies. The dosage and time were chosen based on prior studies (Joshi, Sultana et al., 2005b).



#### **6.4.3. Preparation of brain homogenate**

Brains obtained from mice were thawed and placed in lysing buffer containing 4µg/ml leupeptin, 4µg/ml pepstatin, 5 µg/ml aprotinin, 2mM ethylenediaminetetraacetic acid (EDTA), 2mM ethylene glycol-bis(tetraacetic acid) (EGTA) and 10mM 4-(2-hydroxyethyl)-1-piperazine-ethanesulfonic acid (HEPES), pH 7.4 and homogenized by 20 passes of a Wheaton tissue homogenizer. The resulting homogenate was centrifuged at 15,800g for 10 min to remove debris. The supernatant was retained and suspended in PBS after washing twice with PBS at 32000g for 10 min. The resulting fractions were assayed for protein concentration by the Pierce BCA method (Bradford, 1976).

#### **6.4.4. 2-dimensional gel electrophoresis**

Samples of the proteins from homogenate were prepared as previously described (Poon, Castegna et al., 2004). Briefly, for isoelectric focusing, 200µg of protein were applied to a pH 3–10 ReadyStrip™ IPG strip (Bio-Rad), and Linear Gradient (8– 16%) Precast criterion Tris-HCl gels (Bio-Rad) were used to separate proteins according to their molecular migration rate (MrW). Sypro ruby stain was used to stain the gel for ~ 1 h, after which the gels were placed overnight in deionized water for destaining.

#### **6.4.5. Western blotting**

Western blotting for 2DE gels was performed as previously described (Poon, Castegna et al., 2004). Briefly, 200µg of the brain protein were incubated with 10 mM DNPH solution in 2 N HCl at room temperature (37°C) for 20 min. The gels were prepared in the same manner as for 2DE. The proteins from gels following the second dimension electrophoresis were transferred onto nitrocellulose paper (Bio-Rad) using a Transblot-Blot® SD semi-dry Transfer Cell (Bio-Rad) at 15V for 2 h. The derivatized

carbonyl adduct of the brain proteins were detected immunochemically (Butterfield, 2004).

#### **6.4.6. Image analysis**

The gels and blots were scanned and saved in TIF format using a Storm 860 Scanner (Molecular Dynamics, Sunnyvale, CA) and Scanjet 3300C (Hewlett Packard, Palo Alto, CA), respectively. PDQuest (Bio-Rad) software was used for matching and analyzing visualized protein spots among different gels and oxyblots. After matching all the spots, the normalized intensity of each protein spot from individual gels (or oxyblots) was compared between groups using statistical analysis.

#### **6.4.7. Trypsin digestion**

Statistically significant spots were excised from the gel and were digested as described previously (Poon, Castegna et al., 2004). Briefly, the excised protein spots were washed with ammonium bicarbonate ( $\text{NH}_4\text{HCO}_3$ ) followed by acetonitrile at room temperature. The gel pieces were digested with 20ng/ $\mu\text{l}$  modified trypsin and incubated at 37°C overnight in a shaking incubator.

#### **6.4.8. Mass spectrometry**

1  $\mu\text{l}$  of  $\alpha$ -cyano-4-hydroxy trans-cinnamic acid (10 mg/ml in 0.1% TFA: ACN, 1:1, v/v) was mixed with tryptic digests (1  $\mu\text{l}$ ). The mixture (1  $\mu\text{l}$ ) was deposited onto the surface of a fast evaporation nitrocellulose matrix and analyzed in reflectron mode with a ToFSpec 2E (Micromass, UK) matrix-assisted laser desorption ionization-time of flight (MALDI-TOF) mass spectrometer. The mass axis was adjusted with trypsin autohydrolysis peaks ( $m/z$  2239.14, 2211.10, or 842.51) as lock masses. The MALDI spectra used for protein identification from tryptic fragments were searched against the

Swissprot protein databases using the MASCOT search engine. Peptide mass fingerprinting used the assumption that peptides are oxidized at methionine residues, are monoisotopic and cysteine residues in peptide is carbamidomethylated (Butterfield and Castegna, 2003; Tangpong, Cole et al., 2006a). Up to 1 missed trypsin cleavage was allowed. Window of error allowed for matching the peptide mass values was set at mass tolerance of 150 ppm. We used the probability-based Mowse score, which indicates the probability that the match between the database and a spectrum is a random event to assign a level of confidence to the identification of specific proteins from the mass spectra. This probability equals  $10^{(-\text{Mowse score}/10)}$ . Mowse scores greater than 53 were considered significant.

### **6.5. Statistics**

The expression level of specific proteins and carbonyl levels in specific proteins, measured by the intensity of the carbonyl level divided by the intensity of protein level of an individual spot, were obtained from five individual 2D gels or blot, one each from each animal. The data were analyzed by two-tailed Student's *t* tests. A value of  $p < 0.05$  was considered statistically significant. In proteomics for identification of a smaller member of protein, large-scale statistical analysis such as that used in DNA microarray studies, is not appropriate.

### **6.6. Results**

Previously we reported (Chapter 4) an increased total protein carbonyl levels in brain isolated from ADR-injected mice when compared to brain isolated from saline-injected controls (Joshi, Sultana et al., 2005b). Here we performed expression proteomics

analysis and redox proteomics analysis unbiasedly identify for differentially expressed brain proteins and specifically oxidized proteins respectively, following treatment with ADR.

#### **6.6.1. Expression proteomics**

From Figure 6.1a and b, it is evident that there are proteins that are less expressed in 2D gels of brain proteins of ADR-injected mice when compared to control. Upon image analysis by using PDQest software we identified 6 proteins that showed significantly decreased expression in brain from ADR-injected mice. These proteins were dynamin 1 (DNM1), triose phosphate isomerase (TPI), NADH ubiquinone oxidoreductase, vacuolar ATP synthase (V-ATPase), visinin like protein 1 (VLP 1) and syntaxin 1B2. These proteins are shown on representative gels in Figures 1a and b. Table 6.1 presents the Mowse scores and p values along with molecular migration rate (MrW) and isoelectric point (PI) of the respective proteins. The identification of the proteins was performed by matching the obtained mass spectrum to the spectrum in the Swissprot database. The probability of the match being a random event is indicated by the Mowse score. A higher Mowse score indicates that the match is unlikely to be a random event.

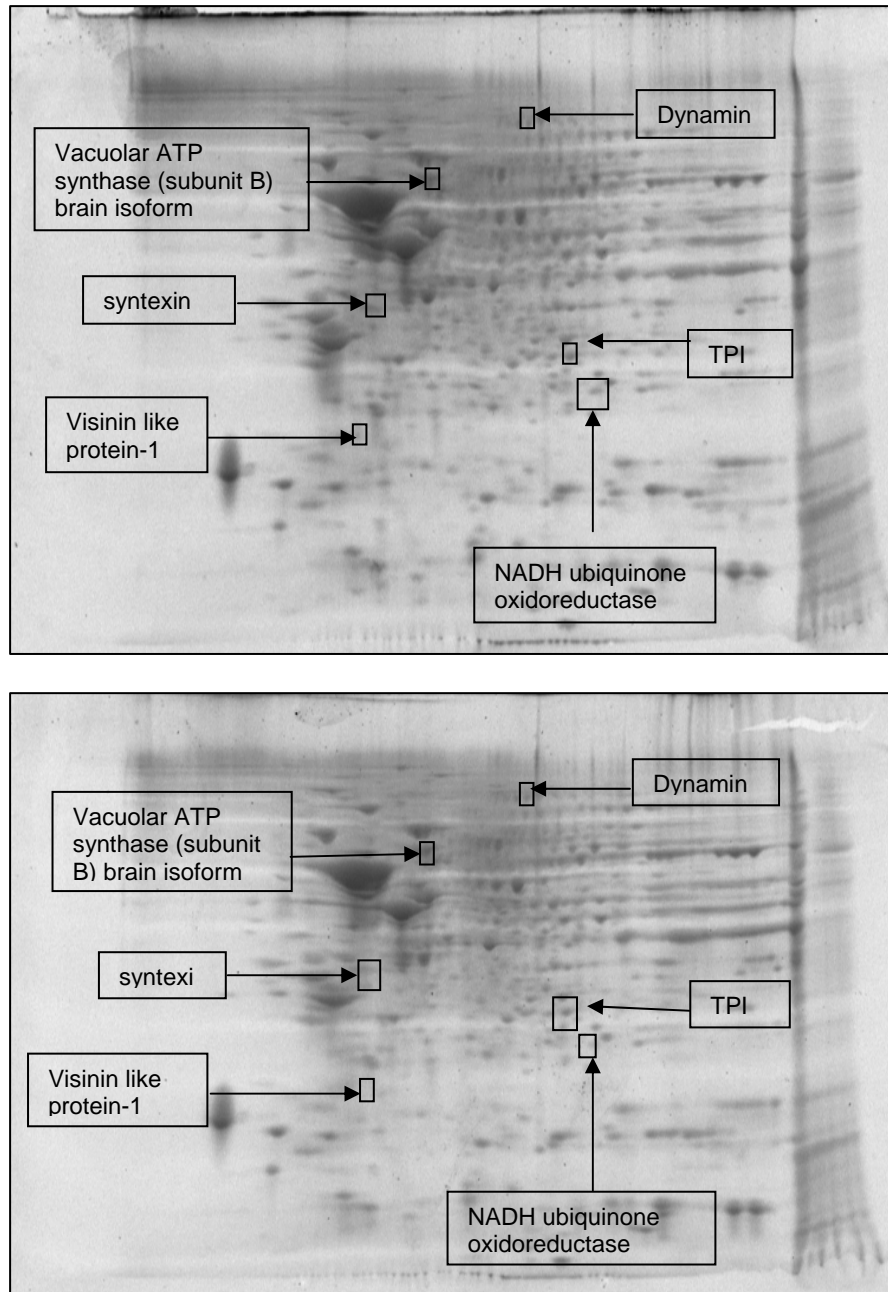


**Figure 6.1a and b:** representative 2DE gels of brain proteins from saline-injected and ADR-injected mice, respectively. The labeled proteins on respective gels showed significantly lower expression in brain isolated from ADR-injected mice when compared to saline-injected control. ( $p < 0.05$ ,  $n = 5$ ).

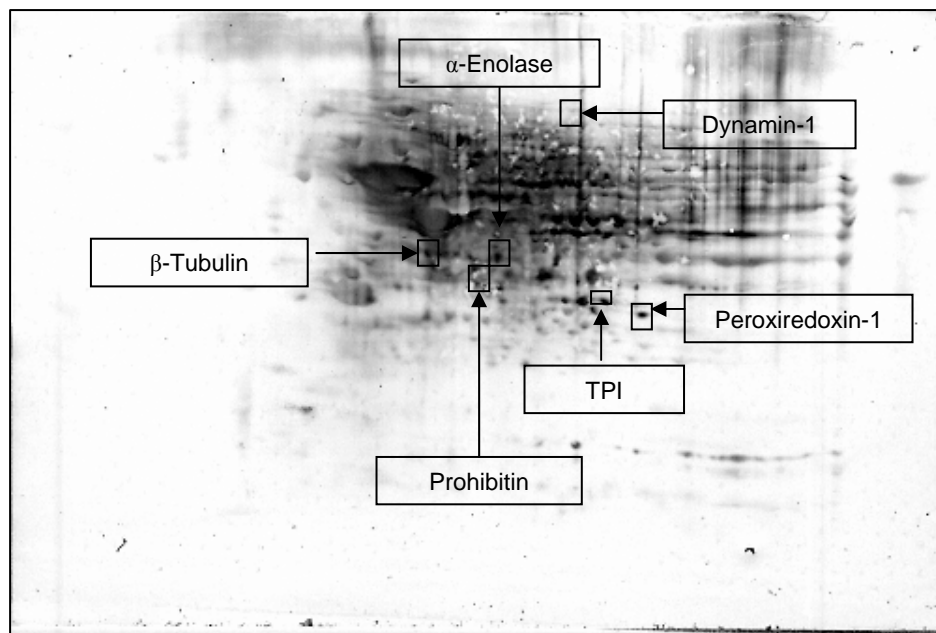
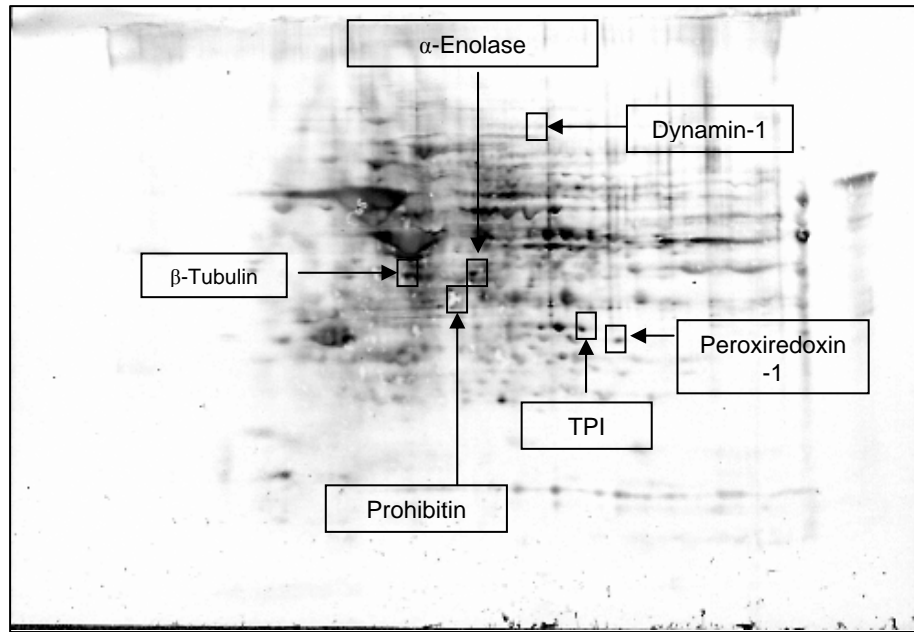


**Figure 6.2a and b:** representative Western blot obtained from 2DE gels of brain proteins from saline-injected and ADR-injected mice, respectively. The labeled proteins on respective blots showed significantly increased oxidation in brain isolated from ADR-injected mice when compared to saline-injected control. ( $p < 0.05$ ,  $n = 5$ ).

### 6.6.2. Redox proteomics

From Figure 6.2a and b, there are proteins that are more oxidized in 2D Western blots of brain proteins from ADR-injected mice when compared to control. Upon image analysis by using PDQest software we identified 6 proteins that showed significantly increased oxidation in brain from ADR-injected mice. These proteins were  $\alpha$ -enolase (ENO1), DNMT1, TPI, peroxiredoxin-1 (Prdx1),  $\beta$ -tubulin and prohibitin. These proteins are shown on representative Western blots in figures 2a and b. Table 6.2 shows the Mowse scores and p values along with MrW and PI of respective proteins. The identification of the proteins was performed by matching the obtained mass spectra of tryptic peptides to the spectra in the Swissprot database. The initial results suggest that the accuracy of protein identification by mass spectrometry is equivalent to immunochemical identification (Castegna, Aksenov et al., 2002a).

Protein	Number of peptides matched	% Sequence coverage	Mowse score	p value	pI	MrW	gi accession number
Dynamin 1	25	26%	156	0.01	7.6	98.14	gi 32172431
TPI	8	39%	77	0.04	7.0	26.90	gi 2851390
NADH ubiquinone oxidoreductase	7	37%	75	0.05	7.0	27.64	gi 20178012
Vacuolar ATP synthase	15	40%	145	0.07	5.5	56.8	gi 51338706
Visinin like protein 1	9	45%	107	0.009	5.0	22.7	gi 51338697
Syntaxin 1B2	8	36%	145	0.05	5.2	33.4	gi 47117767

**Table 6.1:** Proteins showing decreased levels in brain isolated from ADR-injected mice when compared to saline-injected control, as determined by PDQuest analysis on gels obtained from 2DE. Proteins were trypsinized and analyzed by Mass spectrometry in order to ascertain their identities. Proteins with Mowse score > 53 were considered to be identified at statistically significant level.



Protein	Number of peptides matched	% Sequence coverage	Mowse score	p value	pI	MrW	gi accession number
Alpha Enolase	6	19%	61	0.05	6.36	47.322	gi 13637776
Peroxiredoxin 1	9	45%	134	0.05	8.26	22.39	gi 547923
Dynamin 1	25	26%	156	0.01	7.61	98.14	gi 32172431
TPI	8	39%	77	0.04	7.08	26.907	gi 2851390
beta Tubulin	10	24%	95	0.07	4.78	50.095	gi 56754803
Prohibitin	9	48%	133	0.05	5.57	29.859	gi 54038837

**Table 6.2:** Proteins showing increased oxidation levels in brain isolated from ADR-injected mice when compared to saline-injected control, as determined by PDQuest analysis on the blots obtained from 2DE followed by Western blot. The normalized spots were identified and corresponding proteins were trypsinized and analyzed by Mass spectrometry in order to ascertain their identities. Protein with Mowse scores > 53 were considered to be identified at a statistically significant level.

## 6.7. Discussion

Previously we reported an increased protein oxidation and lipid peroxidation in brain isolated from ADR-injected mice when compared to that of saline-injected mice (Joshi, Sultana et al., 2005b). Increased oxidative stress markers may be cause or consequence of a compromised antioxidant defense system. Our laboratory also reported that ADR injection systemically causes increased TNF- $\alpha$  in brain that leads to increased apoptotic bodies and mitochondrial dysfunction (Tangpong, Cole et al., 2006b). We also recently reported that iNOS was involved in ADR-induced modulation of MnSOD and mitochondrial dysfunction, since iNOS knock-out mice injected previously with ADR had no brain mitochondrial dysfunction (Tangpong, Cole et al., 2006a).

The present study was carried out to identify in an unbiased manner differentially expressed and specifically oxidized proteins in the brain isolated from saline- or ADR-injected mice. Using the proteomics approach previously utilized in our laboratories (Castegna, Aksenov et al., 2002a; Castegna, Aksenov et al., 2002b; Poon, Castegna et al., 2004; Poon, Calabrese et al., 2006; Tangpong, Cole et al., 2006a), we determined that the expression levels of DNM 1, TPI, NADH ubiquinone oxidoreductase, V-ATPase, VLP1 and syntaxin 1B2 were significantly decreased in the brains isolated from ADR-injected mice when compared to the brains isolated from saline-injected mice (Figure 6.1a & b). Further, we showed that the total level of protein oxidation increased in the brains isolated from ADR-injected mice when compared to brain from saline-injected mice, and that the specific carbonyl levels of ENO 1, DNM 1, TPI, Prdx1,  $\beta$ -tubulin and prohibitin were significantly increased in the brains of ADR-injected mice (Figure 6.2a & b). Upon examination of the proteomic data, we observed that the proteins that were

differentially expressed in the brain isolated from saline- or ADR-injected mice fell into four broadly defined functional groups, with some placed in more than one of these groups: namely, metabolism, antioxidant defense, transport/motility, cell proliferation and regulation. Interestingly, these processes are known to affect cognitive function.

#### **6.7.1. Transport/mobility and cytoskeleton**

Dynamins are members of a subfamily of GTP-binding proteins. DNM1 is a GTPase that is involved in clathrin-mediated endocytosis and other vesicular trafficking processes (Sontag, Fykse et al., 1994) and is a substrate for protein kinase C (PKC). Phosphorylation of DNM1 by PKC enhances the GTPase activity of DNM1 (Sontag, Fykse et al., 1994). DNM1 also functions in receptor-mediated endocytosis and vesicle formation. DNM1 is believed to assemble around the necks of clathrin-coated pits and assist in pinching vesicles from the plasma membrane (van der Bliek, Redelmeier et al., 1993). It is suggested that DNM1 has a primary role in synaptic vesicle recycling in the nerve terminal (Sontag, Fykse et al., 1994). The formation of complexes between the actin-binding protein profilin and DNM1 at sites of synaptic vesicle recycling has been well-characterized (Witke, Podtelejnikov et al., 1998). An observed significant decrease in DNM1 mRNA and protein levels in AD brains was interpreted to reflect its role in synaptic vesicle endocytosis (Yao, Zhu et al., 2003). Our laboratory recently reported that DNM1 protein is less abundant in the olfactory bulbs of old mice (Poon, Vaishnav et al., 2005). In the current study we showed a decreased expression of DNM1 in brain isolated from ADR-injected mice when compared to brain isolated from saline-injected mice (Fig 6.1a & b). By redox proteomics we showed that DNM1 is significantly oxidized in brain isolated from ADR-injected mice when compared to saline-injected control (Fig 6.2a &

b), Consistent with the notion of altered neurotransmitter reuptake by neuronal synapses and altered synaptic vesicle recycling with ADR injection. Since synaptic remodeling is critical to learning and memory, these alterations could affect neuronal transport/mobility considerably leading to decreased synaptic function, which conceivably could contribute to chemobrain.

Tubulin is a heterodimer consisting of alpha and beta-tubulin subunits present ubiquitously among eukaryotic cells (Chakraborty, Sarkar et al., 1999). Like DNMT1, beta tubulin is a GTPase and forms the structural subunit of microtubules (Tian, Bhamidipati et al., 1999).  $\alpha$ - and  $\beta$ -tubulin polymerize to form microtubules that help in cellular trafficking (Pennisi, 1998). Hence,  $\beta$ -tubulin inactivation may not only alter cytoskeleton and intracellular transport but also alter cell proliferation. The level of  $\alpha$ -tubulin is significantly decreased as a function of age (Nishibayashi, Ogawa et al., 1994; Poon, Calabrese et al., 2006). Recently our laboratory showed oxidation of  $\beta$ -tubulin in a model of AD by using redox proteomics (Boyd-Kimball, Sultana et al., 2005b). In the present study we showed significant oxidation of  $\beta$ -tubulin in brain isolated from ADR-injected mice when compared to brain isolated from saline-injected mice. Oxidation of  $\beta$ -tubulin may implicate altered intracellular trafficking and disruption of the cytoskeleton that may contribute to chemobrain.

### **6.7.2. Energy Metabolism**

NADH ubiquinone oxidoreductase, a component of mitochondrial complex 1, is involved in catalyzing the oxidation of NADH, the reduction of ubiquinone, and the transfer of  $4H^+$ /NADH across the coupling membrane. This protein provides the input to

the oxidative phosphorylation for ATP production from the NAD-linked dehydrogenases of the citric acid cycle (Weiss, Friedrich et al., 1991). Mutation and dysregulation in this complex is associated with many neurodegenerative disorders including AD (Robinson, Luo et al., 1998; Karry, Klein et al., 2004). Dysfunctional NADH ubiquinone oxidoreductase is linked to altered energy metabolism. Consistent with this notion we showed a lower expression of this enzyme in brain isolated from ADR-injected mice when compared to brain isolated from saline-injected mice. An altered energy metabolism may lead to mitochondrial dysfunction, which was observed in the brain isolated from ADR-injected mice when compared to control (Tangpong, Cole et al., 2006a; Tangpong, Cole et al., 2006b) and may be related to cognitive dysfunction following ADR chemotherapy.

V-ATPase, found in the endomembrane of eukaryotic cells and the plasma membrane of some specialized eukaryotic cells, is primarily involved in ATP hydrolysis to drive a proton pump. Apart from its ATPase activity V-ATPase also is involved in active transport of metabolites, protein trafficking, receptor mediated endocytosis and neurotransmitter release (Finbow and Harrison, 1997; Stevens and Forgac, 1997; Nelson and Harvey, 1999; Futai, Oka et al., 2000; Nishi and Forgac, 2002; Wilkens, Inoue et al., 2004). In all cases, V-ATPase carries proton transport from the cytoplasmic compartment to the opposite side of the membrane in an ATP dependent manner (Nishi and Forgac, 2002). The proton gradient generated by V-ATPase is also used to accumulate neurotransmitters in synaptic vesicles by specific vesicular transporters in neurons (Verdier, Huszar et al., 2005). Any alteration in V-ATPase may have consequences in energy production and/or neurotransmitter accumulation in presynaptic vesicles. In the

present study we reported a decreased expression of V-ATPase in brain isolated from ADR-injected mice when compared to brain isolated from saline injected mice. A decreased expression may hence implicate altered functions of V-ATPase that have roles in the various cellular processes described above, which conceivably could be involved in cognitive dysfunction associated with cancer chemotherapy.

ENO1 is a key glycolytic enzyme present in the cytosol. The prime function of ENO1 is to catalyze the formation of phosphoenolpyruvate from 2-phospho-D-glycerate. In the subsequent reaction in glycolysis, phosphoenolpyruvate is converted to pyruvate and ATP by an enzyme, pyruvate kinase. ENO1, also known as  $\alpha$ -enolase [brain-specific subunit of enolase, (Keller, Berod et al., 1994)], hence becomes a key enzyme in the process of ATP synthesis. Previously our lab reported possible post-transcriptional regulation of ENO1 in aging by transcriptional analysis (Poon, Vaishnav et al., 2005), which may indicate reduced proteasomal degradation of this protein possibly being oxidized/nitrated or as a result of decreased proteasomal activity during aging (Keller, Dimayuga et al., 2004). ENO1 is also up-regulated at the protein level in AD brains (Schonberger, Edgar et al., 2001). ENO1 is a specific target of oxidation and is both oxidized and nitrated in brain that is under oxidative stress in AD patients (Castegna, Aksenov et al., 2002a; Castegna, Aksenov et al., 2002b; Castegna, Thongboonkerd et al., 2003; Reverter-Branchat, Cabiscol et al., 2004). In the present study we showed that ENO1 is specifically oxidized in brain isolated from ADR-injected mice when compared to brain isolated from saline-injected mice. Since oxidatively modified protein are generally dysfunctional (Butterfield, Poon et al., 2006; Sultana, Perluigi et al., 2006) the possible implications of oxidative modification of ENO1 may relate to altered energy

metabolism and directly or indirectly might affect mitochondrial dysfunction. Lower ATP production could affect deleteriously the maintenance of ion gradients, the activities of pumps and channels, among others processes related to normal cognition. Hence, altered ENO1 may contribute to the symptoms of cognitive dysfunction or chemobrain.

TPI catalyzes the reversible interconversion of dihydroxyacetone phosphate and glyceraldehyde 3-phosphate during glycolysis. TPI is ubiquitously expressed in cytoplasm. TPI deficiency has been reported in chronic nonspherocytic hemolytic anemia that eventually developed into cerebellar dysfunction and spasticity with hyperreflexia (Chang, Artymiuk et al., 1993). In another study, decreased neuronal ATP production followed by progressive neuronal death was observed upon inhibition of TPI (Sheline and Choi, 1998). Previous studies from our laboratory have reported oxidation/nitration of TPI in AD (Castegna, Thongboonkerd et al., 2003), however, the activity of TPI is not altered in either AD or demented patients (Iwangoff, Armbruster et al., 1980; Meier-Ruge, Iwangoff et al., 1984). In the current study, we observed an increased oxidation and decreased expression of TPI in brain isolated from ADR-injected mice when compared to brain isolated from saline-injected control. A lower expression and increased oxidation may implicate altered energy metabolism, lower ATP production leading to chemobrain as described above.

### **6.7.3. Antioxidant proteins**

Prdx1 is an antioxidant protein that contain essential catalytic cysteine residues and use thioredoxin as an electron donor (Yim, Chae et al., 1994; Neumann, Krause et al., 2003). The primary function of Prdx 1 is to scavenge peroxides and Prdx1 and prdx2 are thought to be involved in the cellular response to ROS. Prdx1 is ubiquitously

expressed predominantly in cytosol and alternatively in nucleus. In brain Prdx1 is localised in astrocytes, whereas Prdx2 is expressed in neurons (Sarafian, Verity et al., 1999). Prdx1 expression can be induced by oxidative stress (Ishii, Yamada et al., 1993; Prosperi, Ferbus et al., 1998). Transfection studies show that Prdx1 can regulate ROS induced by growth factor signalling and can eliminate peroxide *in vivo* (Kang, Chae et al., 1998). Altered expression of various Prdx have been observed in oxidative stress-mediated neurodegenerative disorders including AD (Krapfenbauer, Engidawork et al., 2003). A decreased expression of Prdx1 may lead to increased peroxidative stress. In the current study we observed an increased oxidative modification of Prdx1 in brain isolated from ADR-injected mice when compared to brain isolated from saline-injected control. Increased oxidative modification of the antioxidant protein Prdx1 may decrease the clearance of various peroxides and increase ROS. This alteration may be related to ADR-mediated elevated oxidative stress in brain and to cognitive dysfunction in ADR-treated patients.

#### **6.7.4. Regulation/Homeostasis**

Syntaxin 1B2 is an integral membrane protein belonging to the membrane transport proteins. In neurons it forms an integral part of synaptic vesicles. The primary function of syntaxin 1B2 is docking/priming of synaptic vesicles at presynaptic active zones (Morciano, Burre et al., 2005). It is sometimes also described as a vesicular trafficking protein. Although not much research has been done on this protein, its expression is known to be decreased in neurons of transgenic mice with altered glial fibrillary acidic protein (GFAP), a model of Alexander's disease, a fatal neurodegenerative disorder resulting from missense mutations of the intermediate



filament protein, GFAP (Hagemann, Gaeta et al., 2005). In the present study we observed a decreased protein expression of this protein in brain isolated from ADR-injected mice when compared to brain isolated from saline-injected mice. Lower expression may implicate defective vesicle docking to the presynaptic membrane, leading to dysfunctional neurotransmitter release, which could be related to cognitive dysfunction or chemobrain.

Prohibitin is ubiquitously expressed predominantly in mitochondria, associated with the inner mitochondrial membrane (McClung, Jupe et al., 1995). Prohibitin is a multi-functional protein, ranging from cell proliferation, inhibiting DNA synthesis, serving as a chaperone protein in the mitochondria, tumor suppression or progression in breast cancer cells and their ability to target to lipid rafts (McClung, Jupe et al., 1995; Mishra, Murphy et al., 2006). Prohibitin is also localized in the nucleus and can modulate transcriptional activity by interacting with various transcription factors, including steroid hormone receptors (Mishra, Murphy et al., 2006). Prohibitin may play role in regulating mitochondrial respiration activity and in aging. All these function suggests that altered prohibitin may lead to mitochondrial dysfunction and might also have implication in various neurodegenerative conditions. In the present study we see an increased carbonylation of prohibitin in brain isolated from ADR-injected mice when compared to brain isolated from saline-injected mice. Oxidative modification of this protein may alter its function, which suggests an altered regulation of mitochondrial respiration activity. We previously showed decreased mitochondrial respiration activity in brain upon systemic administration of ADR in mice (Tangpong, Cole et al., 2006a; Tangpong, Cole et al., 2006b).

VLP1 is primarily localized in the plasma membrane, predominantly expressed in brain (Bernstein, Baumann et al., 1999). VLP1 belongs to a family of neuronal  $\text{Ca}^{2+}$  sensor/binding proteins (Braunewell and Gundelfinger, 1999; An, Bowlby et al., 2000). VLP1, upon binding to calcium undergoes a conformational change, a mechanism termed as  $\text{Ca}^{2+}$ -myristoyl switch that facilitates its association with lipid bilayers (Ames, Ishima et al., 1997). VLP1 is also shown to modulate cGMP signaling pathways in transfected neurons, *in vitro* (Braunewell, Brackmann et al., 2001). Possible involvement of VLP1 in pathology and possibly pathophysiology of changed calcium homeostasis in AD has been previously studied (Schnurra, Bernstein et al., 2001). VLP1 showed reduced immunoreactivity in neurons from temporal cortex of AD patients (Schnurra, Bernstein et al., 2001). In the current study we have observed a decreased expression of VLP1 in brain isolated from ADR-injected mice when compared to brain isolated from saline-injected mice. Lower expression may cause  $\text{Ca}^{2+}$  dyshomeostasis that may lead to neuronal apoptosis with subsequent effect on cognition.

The present proteomics identification of differentially expressed brain proteins and specifically oxidized proteins are consistent with our previous *in vivo* (Joshi, Sultana et al., 2005b; Tangpong, Cole et al., 2006a; Tangpong, Cole et al., 2006b). The previously observed ADR-induced increased oxidative stress, altered glutathione and its dependent enzyme expression and activity, TNF- $\alpha$  production, and circulating TNF causing mitochondrial dysfunction and appearance of apoptotic bodies in brain may be related to the observed differential expression or specific oxidation of key protein in brain.

The proteins involved in our study are fall under four major categories that have implication in neurodegeneration: transport/mobility and cytoskeleton, antioxidant, energy metabolism, and regulation/homeostasis. Impairment and alteration in these proteins lead to mitochondrial and cellular dysfunction, increased oxidative stress and apoptotic cascade, ultimately leading to neuronal death as observed in our previous *in vivo* studies. All the previous studies and the present study show that mice injected with ADR are under oxidative stress. The results presented in this study suggest that a therapeutic strategy aimed towards preventing the observed differential expression and oxidative modification of specific proteins may modulate the observed cognitive impairment in patients undergoing chemotherapy. Studies to test this notion are in progress.

## Chapter 7

### **Glutathione elevation by $\gamma$ -glutamyl cysteine ethyl ester as a potential therapeutic strategy towards preventing oxidative stress in brain mediated by *in vivo* administration of adriamycin: Implication for chemobrain.**

#### **7.1. Overview of the study**

Oxidative stress in heart and brain by the cancer chemotherapeutic drug adriamycin (ADR), used for treating solid tumors, is well established. Long-term treatment of ADR in breast cancer patients has shown symptoms of cardiomyopathy. Less well recognized, but increasingly documented, is cognitive dysfunction. Following chemotherapy, free radical-mediated oxidative stress has been reported in both heart and brain. We recently showed a significant increase in protein oxidation and lipid peroxidation in brain isolated from mice injected intraperitoneally (i.p) with ADR. Systemic administration of ADR also induces tumor necrosis factor- $\alpha$  (TNF- $\alpha$ ), that leads to production of reactive oxygen species (ROS) and reactive nitrogen species (RNS) in brain. Circulating TNF also causes mitochondrial dysfunction leading to apoptotic pathways in brain. Inducible nitric oxide synthase also plays a role in ADR-induced TNF-mediated neurotoxicity. We also previously showed a significant decrease in glutathione (GSH) levels in brain isolated from ADR injected mice, along with increased expression of multidrug resistant protein-1 (MRP-1), glutathione-S-transferase (GST), glutathione peroxidase (GPx), and glutathione reductase (GR). There was a significant decrease in activity of brain GST. The present study was designed to test the hypothesis that by elevating brain levels of GSH, the brain would be protected against oxidative stress in ADR-injected mice.  $\gamma$ -Glutamyl cysteine ethyl ester (GCEE), a precursor of glutathione,

injected i.p (150mg/kg body weight) 4 h prior ADR injection (20mg/kg body weight) led to significantly decreased protein oxidation and lipid peroxidation in subsequently isolated mice brain when compared to brain isolated from ADR-injected mice without GCEE. The GSH levels were restored to that of brain isolated from saline-injected mice. Further, the enzyme activity of GST was increased in brain isolated from ADR-injected mice previously injected with GCEE when compared to the brain isolated from ADR-injected mice previously injected with saline. These results are discussed with relevance to potential pharmacological prevention of brain cognitive dysfunction in patients receiving ADR chemotherapy.

## **7.2. Introduction**

Oxidative stress has been implicated in many neurodegenerative disorder conditions including Alzheimer's disease (AD) (Butterfield, Drake et al., 2001; Lauderback, Kanski et al., 2002). In brain, free radical-mediated oxidative stress leads to significantly increased protein oxidation (Hensley, Hall et al., 1995; Stadtman and Berlett, 1997; Butterfield and Kanski, 2001), lipid peroxidation (Markesbery and Lovell, 1998; Butterfield and Lauderback, 2002), DNA and RNA oxidation (Wang, Xiong et al., 2005), neuronal dysfunction and death. Brain is particularly vulnerable to oxidative stress because of the relatively large amount of polyunsaturated fatty acids (PUFA), higher oxygen consumption and relatively low antioxidant capacity. By using redox proteomics, our laboratory has previously identified many key enzymes and proteins that are oxidatively modified in AD subjects and models of AD (Tangpong, Cole et al., 2006a),

aging (Poon, Calabrese et al., 2006) and in the patients with mild cognitive impairment (MCI) (Butterfield, Poon et al., 2006).

Adriamycin (ADR), a cancer chemotherapeutic drug used to treat solid tumors, is known to cause side effects in heart and brain (Steinherz, Steinherz et al., 1991; Joshi, Sultana et al., 2005b; Tangpong, Cole et al., 2006a; Tangpong, Cole et al., 2006b). Cardiomyocytes treated with ADR have elevated levels of protein oxidation and lipid peroxidation (DeAtley, Aksenov et al., 1998). Free radical scavengers are known to protect cardiomyocytes from this effect (DeAtley, Aksenov et al., 1999). Brain isolated from mice treated peripherally with ADR shows evidence of oxidative damage and mitochondrial dysfunction (Joshi, Sultana et al., 2005b; Tangpong, Cole et al., 2006a; Tangpong, Cole et al., 2006b). Patients under long-term treatment with ADR for breast and lung cancer have shown symptoms of cognitive dysfunction such as lack of concentration, forgetfulness and dizziness (Meyers, 2000; Schagen, Hamburger et al., 2001; Freeman and Broshek, 2002). The side effects in heart limit the use of ADR in chemotherapy, while the side effects in brain limit the quality of life of patients undergoing chemotherapy.

ADR intercalates into the major groove of DNA and prevents its replication (Cummings, Anderson et al., 1991). ADR is also known to inhibit topoisomerase II to form a cleavable complex with DNA thereby preventing tumor growth (Chuang and Chuang, 1979; Cheng, Cahill et al., 1992). Apart from these mechanisms of action, the quinone containing ADR is also known to generate superoxide radical ( $O_2^{\cdot-}$ ) (Deres, Halmosi et al., 2005). A free radical-mediated mechanism of toxicity of ADR is widely accepted. The quinone in ADR undergoes one electron reduction to generate

semiquinone, which is a free radical, and in the presence of oxygen converts back to quinone producing  $O_2^{\cdot-}$ , a process known as redox cycling. ADR dependent redox cycling is likely activated by nitric oxide synthase and cytochrome P 450 (Gutierrez, 2000; Deres, Halmosi et al., 2005). Cardiotoxicity mediated by ADR is known to target mitochondria and NADH dehydrogenase, a mitochondrial enzyme, stimulates ADR to form semiquinone radical and  $O_2^{\cdot-}$  (Doroshov and Davies, 1986).  $O_2^{\cdot-}$  radicals are converted to hydrogen peroxide ( $H_2O_2$ ) enzymatically by superoxide dismutase. Overexpression of MnSOD is known to protect complex I of mitochondrial electron transport chain in ADR-mediated cardiomyopathy (Yen, Oberley et al., 1999). Superoxide radical can react with  $H_2O_2$  and other reactive species to generate various other reactive oxygen species/reactive nitrogen species (ROS/RNS) (Halliwell and Gutteridge, 1999).

Apart from SOD, another major antioxidant defense system includes glutathione (GSH) and its dependent enzymes such as glutathione peroxidase (GPx), glutathione reductase (GR) and glutathione-S-transferase (GST). GSH is a non-protein thiol present in millimolar concentrations in brain (Cooper, 1997). GSH provides protection against  $H_2O_2$ -mediated toxicity by providing reduced electrons and is oxidized to glutathione disulfide (GSSG). This reaction is catalyzed by GPx. GSSG is converted to GSH by action of glutathione reductase (GR) with the help of the cofactor NADPH (Cooper, 1997). GPx is also known to reduce peroxynitrite thereby providing protection against peroxynitrite-induced toxicity (Sies, Sharov et al., 1997).

GSH also forms glutathione-S conjugates with xenobiotics and reactive alkenals such as 4-hydroxynonenal (HNE) and acrolein, products of lipid peroxidation, with the

help of GST, and these conjugates are removed from cells by the multidrug resistant protein-1 (MRP-1), an ATP binding cassette (ABC) family protein (Sultana and Butterfield, 2004) MRP-1 is an integral plasma membrane protein that exports glutathione-S conjugates out of the cell in an ATP-dependent manner (Nies, Jedlitschky et al., 2004; Conseil, Deeley et al., 2005). GSH, apart from its endogenous antioxidant properties, is also involved in biosynthetic processes, DNA repair, enzyme activity regulation and activation of transcription factors (Meister and Anderson, 1983). GSH levels are decreased in certain regions of central nervous system (CNS) in various neurodegenerative disorders (Benzi and Moretti, 1995a). An imbalance in the ratio of reduced to oxidized GSH level indexes oxidative stress. Studies also have shown reduced GST activity in brain and ventricular fluids in AD (Lovell, Xie et al., 1998). Increased expression of GST increased resistance towards oxidative stress in neuroblastoma cells and provides protection against HNE mediated toxicity in neuronal cell culture (Lovell, Xie et al., 1998).

### **7.3. Purpose of the study**

Involvement of oxidative stress-mediated toxicity in neurodegenerative events and neuronal cell death has been extensively studied (Good, Werner et al., 1996; Moreira, Smith et al., 2005). Hence, various experimental approaches for effective protection by antioxidants have emerged. In different models of oxidative stress-induced cell death, a number of potential free-radical scavengers and antioxidant have been tested, such as Vitamin E (Behl, Davis et al., 1992), Vitamin C, melatonin (Pappolla, Sos et al., 1997), ginkgo biloba (Smith and Luo, 2003), steroid hormones (Goodman, Bruce et al., 1996; Behl, Skutella et al., 1997), N-acetylcysteine (Adair, Knoefel et al., 2001), etc. Due to



poor blood brain barrier (BBB) permeability of many of these antioxidants, clinical trials largely have been unsuccessful.

Studies have shown that an increase in endogenous GSH levels by dietary or pharmacological intake of GSH precursors or GSH mimetic or substrates for GSH synthesis protects brain against oxidative stress (Anderson and Luo, 1998; Halliwell, 2001; Pocernich, Cardin et al., 2001; Butterfield, Castegna et al., 2002a; Joshi, Sultana et al., 2005a; Pocernich, Sultana et al., 2005). Considering the importance of developing new antioxidant compounds and their relevance in the treatment of neurodegenerative conditions, we examined  $\gamma$ -glutamyl cysteine ethyl ester (GCEE), a GSH precursor. Cysteine is the limiting substrate in the synthesis of GSH (Anderson and Luo, 1998). Additionally,  $\gamma$ -glutamylcysteine ligase (GCL) is the rate-limiting enzyme for GSH synthesis, the enzyme that catalyzes the ligation of the substrate glutamate to cysteine. GCL is feedback inhibited by the excess production of GSH. Based on this concept, we hypothesized that GCEE administered to the cell would avoid feedback inhibition and the limiting substrate for GSH synthesis would be provided to the process (Drake, Kanski et al., 2002). The ethyl ester moiety on  $\gamma$ -glutamylcysteine would further increase the efficacy of  $\gamma$ -glutamylcysteine to cross the plasma membrane and upregulate GSH biosynthesis.

Previous studies from our laboratory have shown protection against peroxynitrite-induced oxidative stress in brain following *in vivo* administration of GCEE (Drake, Kanski et al., 2002). GSH up-regulation by GCEE also protects mitochondria against peroxynitrite, *in vivo* (Drake, Sultana et al., 2003). Furthermore, elevation of GSH by GCEE protects neurons against A $\beta$ (1-42)-mediated oxidative stress and neurotoxicity

(Boyd-Kimball, Sultana et al., 2005a). The present study was carried out to test the hypothesis that *in vivo* GCEE elevates GSH levels in brain and thereby prevents oxidative stress mediated by *in vivo* ADR.

## **7.4. Experimentals**

### **7.4.1. Animals**

For this study, male B6C3 mice (2-3 months of age), approximately 30 g in size, housed in the University of Kentucky Central Animal Facility in 12-h light/dark conditions and fed standard Purina rodent laboratory chow *ad libitum*, were used. The animal protocols were approved by the University of Kentucky Animal Care and Use Committee.

### **7.4.2. Chemicals**

All the chemicals were purchased from Sigma-Aldrich (St. Louis, MO), unless stated otherwise. Doxorubicin HCl (ADR) was purchased from Bedford Laboratories. GCEE was purchased from Bachem (Torrance, CA). The OxyBlot kit used for protein carbonyl determination was purchased from Intergen (Purchase, NY). The GSH assay kit was purchased from Cayman Chemicals (Ann Arbor, MI). The primary antibody for 4-hydroxynonenal was purchased from Alpha Diagnostics (San Antonio, TX).

### **7.4.3. Treatments**

Mice were divided into 4 groups. Two groups received saline and another two groups were given 150 mg/kg bodyweight of GCEE. One of the saline-injected and GCEE-injected group received 20 mg/kg bodyweight ADR, i.p., 4 h after saline or GCEE injection. The dose and time for GCEE and ADR used were chosen based on prior studies (Drake, Kanski et al., 2002; Joshi, Sultana et al., 2005b). Following 72 h post-i.p.

injections of ADR, mice were sacrificed and brain was isolated and flash frozen in liquid nitrogen.

#### **7.4.4. Preparation of brain homogenate**

Brains were isolated, thawed and dissected from all the treatment groups and placed in ice cold lysing buffer containing 4µg/ml leupeptin, 4µg/ml pepstatin, 5 µg/ml aprotinin, 2mM ethylenediaminetetraacetic acid (EDTA), 2mM ethylene glycol-bistetraacetic acid (EGTA) and 10mM 4-(2-hydroxyethyl)-1-piperazine-ethanesulfonic acid (HEPES), pH 7.4. The brain was homogenized by 20 passes of a Wheaton tissue homogenizer, and the resulting homogenate was centrifuged at 20000g for 10 minutes. The pellet was suspended in 1ml phosphate buffered saline (PBS) containing 0.01% (w/v) sodium azide and 0.2% (v/v) Tween 20. The supernatant (cytosolic fraction) was retained for fluorescence studies, GSH measurement and enzyme activities. All the fractions suspended in PBS were washed twice with PBS at 32000g for 10 min. The resulting fractions were assayed for protein concentration by the Pierce BCA method (Bradford, 1976).

#### **7.4.5. GSH assay**

A known volume of supernatant obtained from homogenate was deproteinated with 10% meta phosphoric acid. The subsequent deproteinated supernatant was treated with 4M triethanolamine (TEAM) solution. Following TEAM treatment, the GSH assay kit was used according to the manufacturer's direction to determine GSH levels as described in chapter 3.

#### **7.4.6. Protein Carbonyls**

Samples (5µl) of brain homogenate, 12% sodium dodecyl sulfate (SDS) (5µl), and 10µl of 10 times diluted 2,4-dinitrophenylhydrazine (DNPH) from 200mM stock were incubated at room temperature for 20 min, followed by neutralization with 7.5µl neutralization solution (2M Tris in 30% glycerol). Protein (250ng) was loaded in each well on a nitrocellulose membrane under vacuum using a slot blot apparatus. The membrane was blocked in blocking buffer (3% bovine serum albumin) in PBS 0.01% (w/v) sodium azide and 0.2% (v/v) Tween 20 for 1h and incubated with a 1:100 dilution of anti-DNP polyclonal antibody in PBS containing 0.01% (w/v) sodium azide and 0.2% (v/v) Tween 20 for 1h. The membrane was washed in PBS following primary antibody incubation three times at intervals of 5 min each. The membrane was incubated following washing with an anti-rabbit IgG alkaline phosphatase secondary antibody diluted in PBS in a 1:8000 ratio for 1h. The membrane was washed three times in PBS for 5 min and developed in Sigma fast tablets, [5-bromo-4-chloro-3-indolyl phosphate/Nitro blue tetrazolium substrate (BCIP/NBT substrate)]. Blots were dried, scanned with Adobe Photoshop, and quantified with Scion Image (PC version of Macintosh compatible NIH image). No non-specific binding of antibody to the membrane was observed.

#### **7.4.7. 4-Hydroxynonenal (HNE)**

Sample (5µl) of brain homogenate, 12% SDS (5µl), and 5µl of modified Laemmli buffer containing 0.125 M Tris base pH 6.8, 4% (v/v) SDS, and 20% (v/v) glycerol were incubated for 20 min at room temperature and were loaded (250ng) in each well on a nitrocellulose membrane in a slot blot apparatus under vacuum. The membrane was treated as above and incubated with a 1: 5000 dilution of anti-HNE polyclonal antibody

in PBS for 1h 30min. The membranes were further developed and quantified as above. A faint background staining due to the antibody alone was observed, but since each sample had a control, this minor effect was controlled.

#### **7.4.8. 3-Nitrotyrosine (3-NT)**

Samples (5µl) of brain homogenate, 12% SDS (5µl), and 5µl of modified Laemmli buffer containing 0.125 M Tris base pH 6.8, 4% (v/v) SDS, and 20% (v/v) glycerol were incubated for 20 min at room temperature and were loaded (250ng) in each well on a nitrocellulose membrane in slot blot apparatus under vacuum. The membrane was treated as above and incubated with a 1: 2000 dilution of anti-3-nitrotyrosine (3NT) polyclonal antibody in PBS for 1h 30min. The membranes were developed further and quantified as described above. No non-specific binding of antibody to the membrane was observed.

#### **7.4.9. Enzyme activity assays**

##### *Estimation of glutathione-S-transferase activity*

GST (EC 2.5.1.18) activity was measured using a reaction mixture consisting of 0.1 M phosphate buffer (pH 6.5), 1.0 mM reduced glutathione, 1.0 mM CDNB and 1mg/ml of supernatant protein (Habig, Pabst et al., 1974). The changes in absorbance were recorded at 340 nm in a 96 well microtiter plate, and the enzymatic activity was calculated as nmol of CDNB conjugate formed  $\text{min}^{-1} \text{mg}^{-1}$  protein.

#### **7.5. Statistical analysis**

Two-way ANOVA followed by a multiple comparisons test (Turkey HSD) was used to assess statistical significance. P values <0.05 were considered significant for comparison between control and experimental data sets.

## **7.6. Results**

### **7.6.1. GSH assay**

As shown in Figure 7.1, there were significant reductions in GSH levels in brain isolated from ADR-injected mice when compared to the levels in brain isolated from saline or GCEE-injected mice. Administration of GCEE elevated the levels of GSH significantly ( $p < 0.05$ ,  $n = 5$ ) in brain isolated from mice injected with GCEE followed by saline or ADR, although the GSH level in the latter case did not reach the level of the saline control.

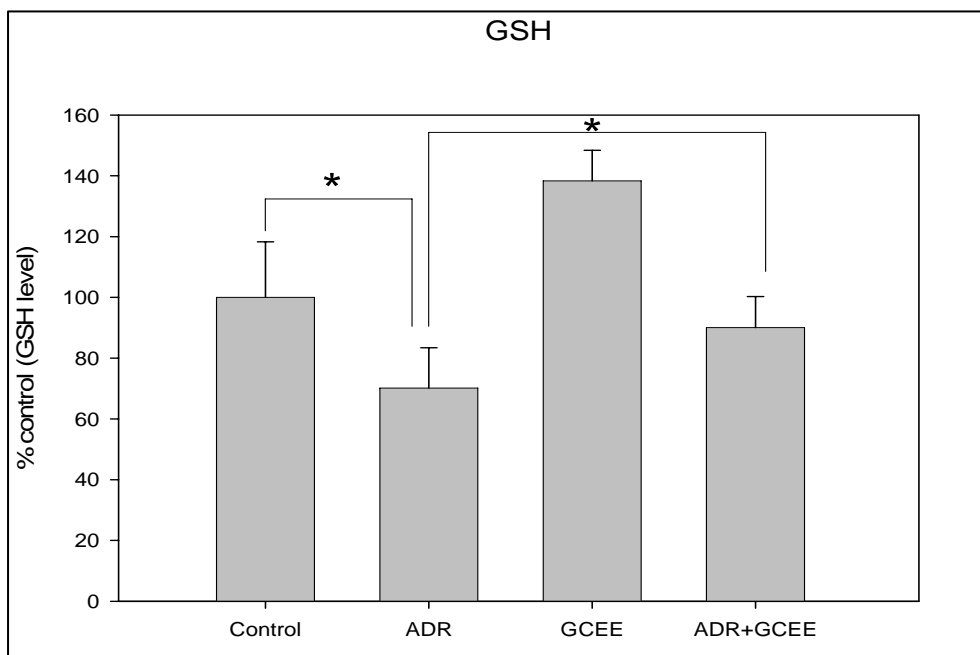


**Figure 7.1:** Levels of GSH in all the treatment groups. There is a significant decrease in GSH level in brain isolated from ADR-injected mice when compared to control (\*  $p < 0.05$ ,  $n = 5$ ). I.p injection of GCEE increases GSH level significantly in brain. The brain isolated from GCEE-injected mice followed by ADR injection shows a significant increase in GSH levels when compared to the levels in brain isolated from ADR injected mice that were previously injected with saline (\*  $p < 0.05$ ,  $n = 5$ ). The data are presented as mean  $\pm$  SEM expressed as percentage of control.

#### **7.6.2. Protein carbonyl, 3 nitrotyrosine and 4-hydroxynonenal**

Figures 7.2, 7.3 and 7.4 show the levels of protein carbonyls, 3-NT (markers of protein oxidation) and protein bound HNE (a lipid peroxidation product) levels, respectively, in all the treatment groups. There was significant elevation in protein carbonyl, 3-NT and protein bound HNE levels in brain isolated from ADR-injected mice when compared to the levels in brain isolated from saline or GCEE-injected mice ( $p <$

0.05,  $n = 5$ ), confirming our previous findings (Joshi, Sultana et al., 2005b). Administration of GCEE reduced the levels of protein carbonyls, 3-NT and protein-bound HNE significantly ( $p < 0.05$ ,  $n = 5$ ) in brain isolated from mice injected with GCEE followed by saline or ADR.

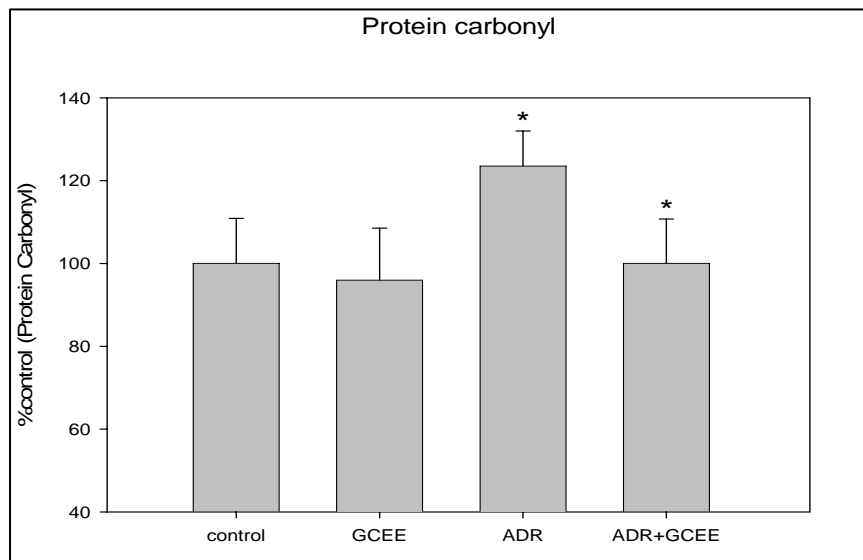


**Figure 7.2:** Levels of protein carbonyl in all the treatment groups. There is a significant increase in protein carbonyl level in brain isolated from ADR-injected mice when compared to control (\*  $p < 0.05$ ,  $n = 5$ ). I.p injection of GCEE decreases protein carbonyl level significantly in brain. The brain isolated from GCEE-injected mice followed by ADR injection shows a significant decrease in protein carbonyl levels when compared to the levels in brain isolated from ADR injected mice that were previously injected with saline (\*  $p < 0.05$ ,  $n = 5$ ). The data are presented as mean  $\pm$  SEM expressed as percentage of control.



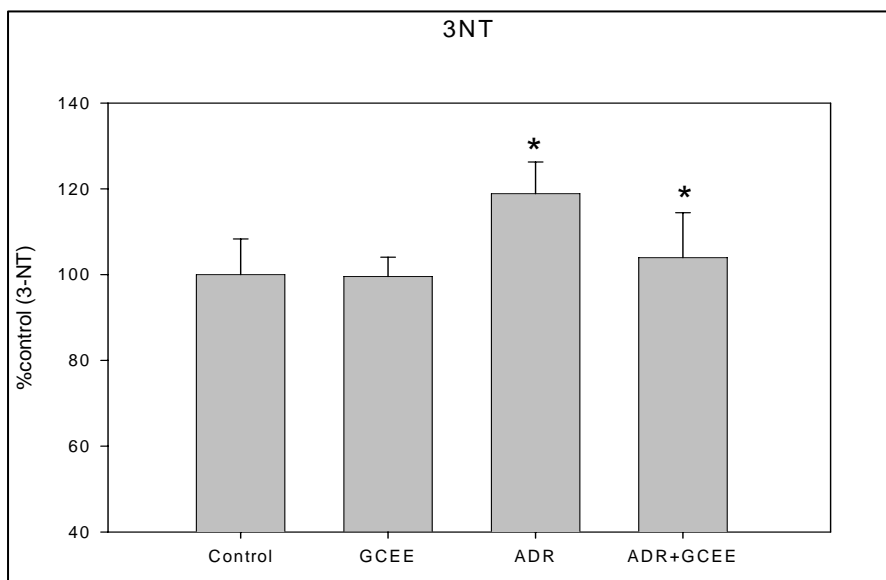


**Figure 7.3:** Levels of 3NT in all the treatment groups. There is a significant increase in 3NT level in brain isolated from ADR-injected mice when compared to control (\*  $p < 0.05$ ,  $n = 5$ ). I.p injection of GCEE decreases 3NT level significantly in brain. The brain isolated from GCEE-injected mice followed by ADR injection shows a significant decrease in 3NT levels when compared to the levels in brain isolated from ADR injected mice that were previously injected with saline (\*  $p < 0.05$ ,  $n = 5$ ). The data are presented as mean  $\pm$  SEM expressed as percentage of control.

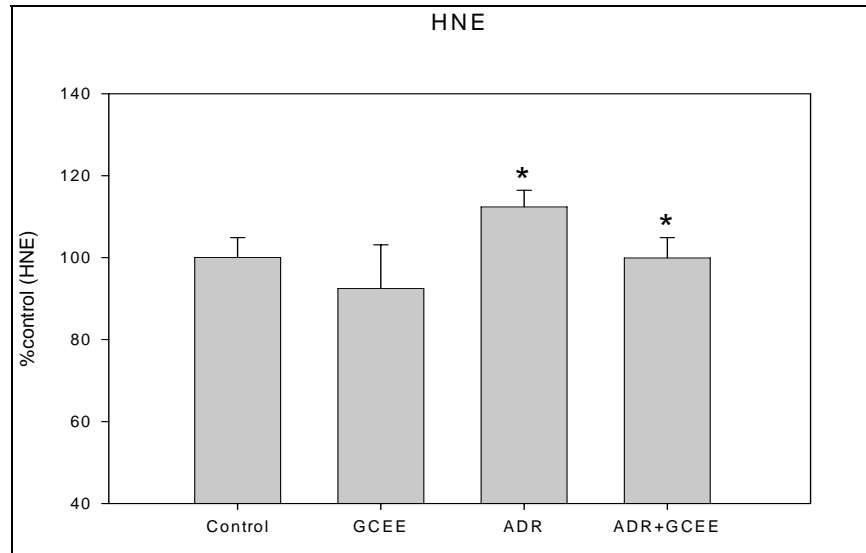


**Figure 7.4:** Levels of HNE in all the treatment groups. There is a significant increase in HNE level in brain isolated from ADR-injected mice when compared to control (\*  $p < 0.05$ ,  $n = 5$ ). I.p injection of GCEE decreases HNE level significantly in brain. The brain isolated from GCEE-injected mice followed by ADR injection shows a significant decrease in HNE levels when compared to the levels in brain isolated from ADR injected mice that were previously injected with saline (\*  $p < 0.05$ ,  $n = 5$ ). The data are presented as mean  $\pm$  SEM expressed as percentage of control.

### **7.6.3. GST activity**

Figure 7.5 shows the activity of GST in all the treatment groups. There was significant reduction in GST activity in brain isolated from ADR-injected mice when compared to the activities in brain isolated from saline or GCEE-injected mice ( $p < 0.05$ ,  $n = 5$ ). Administration of GCEE elevated the GST activity significantly ( $p < 0.05$ ,  $n = 5$ ) in brain isolated from mice injected with GCEE followed by ADR. Injection of GCEE alone significantly increased GST activity when compared to saline-injected control.

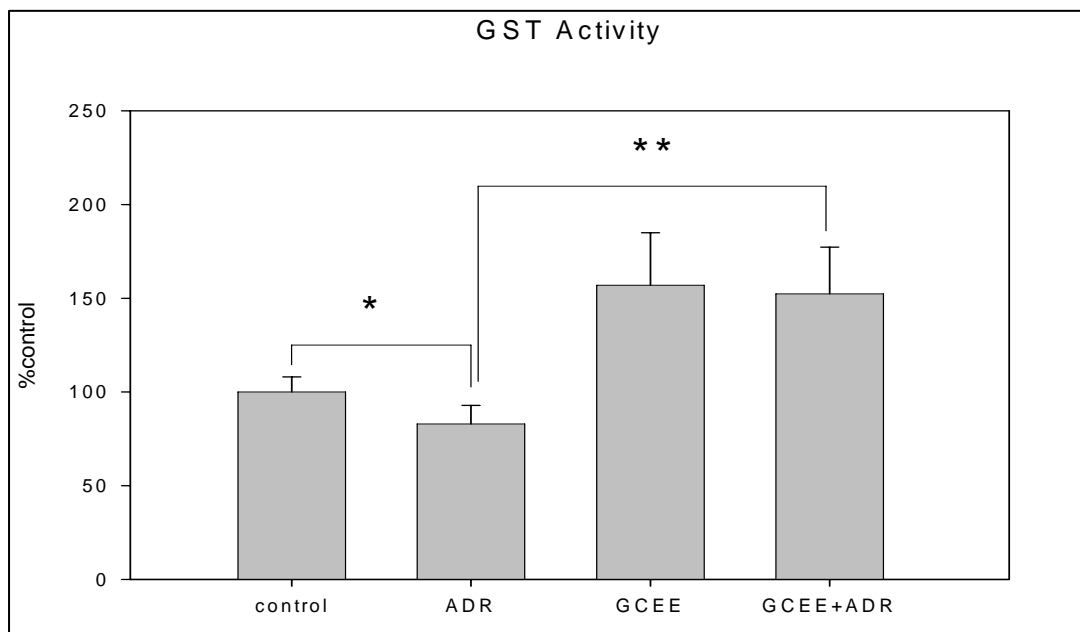


**Figure 7.5:** Plot of activity of GST in all the treatment groups. There is a significant decrease in GST activity in brain isolated from ADR-injected mice when compared to control (\*  $p < 0.05$ ,  $n = 5$ ). I.p injection of GCEE increases GST activity significantly in brain. The brain isolated from GCEE-injected mice followed by ADR injection shows a significant increase in GST activity when compared to the activity in brain isolated from ADR injected mice that were previously injected with saline (\*\*  $p < 0.01$ ,  $n = 5$ ). The data are presented as mean  $\pm$  SEM expressed as percentage of control.

## 7.7. Discussion

ADR-mediated oxidative stress in brain has gained increasing importance recently (Joshi, Sultana et al., 2005b; Joshi, Sultana et al., 2006; Tangpong, Cole et al., 2006a; Tangpong, Cole et al., 2006b). Free radical-mediated protein oxidation and lipid peroxidation in cardiomyocytes and involvement of ADR in cardiomyopathy has been extensively studied by various groups (Doroshov and Davies, 1986; Sarvazyan, 1996; Vasquez-Vivar, Martasek et al., 1997; Yen, Oberley et al., 1999). We previously showed increased protein oxidation and lipid peroxidation in brain isolated from ADR-injected mice that conceivably could be involved in the symptoms of chemobrain observed in patients treated with ADR (Joshi, Sultana et al., 2005b). ADR does not cross the BBB (Bigotte, Arvidson et al., 1982a; Bigotte, Arvidson et al., 1982b; Tangpong, Cole et al., 2006b). The first investigation of potential biochemical pathways for ADR-mediated CNS toxicity was recently reported by our group (Tangpong, Cole et al., 2006b). Systemic administration of ADR significantly elevated the level of circulating TNF- $\alpha$ , which crossed the blood brain barrier to reside in neurons. Neuronal-resident TNF- $\alpha$  caused brain mitochondrial dysfunction leading to activation of apoptotic pathways. Pro-apoptotic p53 migrates to brain mitochondria to interact with anti-apoptotic Bcl-xL. The evidence of apoptosis in brain following ADR suggest p53 interacts with Bcl-xL inhibited the function of the latter protein. A neutralizing antibody against TNF abrogated these effects in brain (Tangpong, Cole et al., 2006b). More recently, we showed a role of iNOS in these effects. ADR given to mice lacking iNOS did not demonstrate a brain mitochondrial dysfunction (Tangpong, Cole et al., 2006a). ADR was shown to lead to nitrated and dysfunctional MnSOD, a mitochondrial-resident protective enzyme.

We recently showed a role for GSH, a major endogenous cellular thiol antioxidant, and its related enzyme expression and activity, in ADR-mediated oxidative stress in brain (Joshi, Sultana et al., 2006). There was a significant depletion in GSH levels in brain isolated from ADR-injected mice (Joshi, Sultana et al., 2006). GCEE, a precursor of GSH, is known to elevate GSH levels in brain by providing the rate limiting substrate,  $\gamma$ -glutamylcysteine (Drake, Kanski et al., 2002). *In vivo* administration of GCEE elevated the GSH level significantly in brain isolated from saline- or ADR-injected mice (Fig 1). The increase in GSH levels in GCEE followed by ADR injection in mice was almost that of control mice. GCEE alone showed a significantly increased GSH levels when compared to all the treatment groups. Moreover, the protection of brain against peroxynitrite by prior GCEE administration (Drake, Sultana et al., 2003) is concomitant with GSH scavenging of NO to form nitrosothiol functionality on GSH.

Increasing GSH levels by pharmacological or dietary intervention has been shown to reduce oxidative stress in models of various neurodegenerative conditions (Pocernich, Cardin et al., 2001; Boyd-Kimball, Sultana et al., 2005a). *In vivo* GCEE administration followed by ADR injection to mice reduced the protein oxidation (Figs. 7.2 and 7.3) and lipid peroxidation (Fig 4) in brain when compared to brain isolated from ADR-injected mice previously injected i.p. with saline. Increasing GSH by GCEE suggests increased antioxidant capacity of brain, hence improved protection against free radical-mediated oxidative stress caused by ADR.

GST is a major detoxification enzyme that works with MRP-1 to remove toxicants from the cell (Sultana and Butterfield, 2004). We showed ADR caused elevation of expression of MRP-1 (Joshi, Sultana et al., 2005b), an ATP binding cassette

(ABC) family protein in brain. MRP-1 in conjugation with GST is known to transport glutathione-S conjugates of electrophiles, anions and other xenobiotics out of the cell. We previously showed a significant elevation in expression of GST in brain isolated from ADR-injected mice (Joshi, Sultana et al., 2006). Although the expression of GST was increased, there was a significant decrease in its activity of brain GST in ADR-injected mice (Joshi, Sultana et al., 2006). *In vivo* GCEE elevated the activity of GST in brain isolated from ADR-injected mice previously injected with GCEE when compared to brain isolated from saline- or ADR-injected mice (Fig 5). Increased activity of GST may result in improved formation of glutathione-S- conjugates and these conjugates including GS-HNE conjugate are cleared from cell by action of MRP1 from the cell, putatively leading to less toxicity and reduced oxidative stress. As noted above, elevated GSH could serve as a substrate for NO, produced in response to oxidative stress to form nitrosothiol adduct. This would have the effect of decreasing peroxynitrite and therefore 3-NT formation as observed in Fig 3. These results are consistent with the notion that brain accessible GCEE may protects brain from oxidative stress induced by ADR via TNF- or iNOS-mediated processes.

In conclusion, the protection of brain against the oxidative damage caused by *in vivo* ADR by GCEE is consistent with previous other studies in which GCEE protected neurons against AD-related amyloid beta-peptide (Boyd-Kimball, Sultana et al., 2005c). Further studies on an animal model could form the basis for eventual treatment strategy for preventing oxidative stress mediated by ADR. The current results suggest that GCEE-mediated increment in brain GSH levels and the activity of GST could be a potential

therapeutic approach towards modulating cognitive impairment in patients undergoing chemotherapy.



## Chapter 8

### ***In Vivo* Protection of Synaptosomes from Oxidative Stress Mediated by $\text{Fe}^{2+}/\text{H}_2\text{O}_2$ or 2,2-Azobis (2-amidino-propane) dihydrochloride (AAPH) by the Glutathione Mimetic Tricyclodecan-9-yl-xanthogenate (D609)**

#### **8.1. Overview of the study**

D609 (tricyclodecan-9-yl-xanthogenate) is a phosphatidylcholine- specific phospholipase C inhibitor that also has been reported to protect rodents against oxidative damage caused by lethal doses of ionizing radiation. We previously showed that D609 mimics glutathione. D609 has a free thiol group, which upon oxidation forms a disulfide. The resulting dioxanthate is a substrate for glutathione reductase, regenerating D609. Recent studies from our laboratory have also shown that D609 reduces the Alzheimer's amyloid  $\beta$  peptide [ $\text{A}\beta$  (1-42)]-induced oxidative stress and cytotoxicity in neuronal cell culture. The present study was undertaken to test the hypothesis that D609 would provide neuroprotection against free radical oxidative stress *in vivo*. Synaptosomes isolated from gerbils, previously injected intraperitoneally (i.p.) with D609, were treated with the oxidants,  $\text{Fe}^{2+}/\text{H}_2\text{O}_2$  or 2,2- Azobis (2-amidino-propane) dihydrochloride (AAPH), which produce free radicals. Synaptosomes isolated from the gerbils i.p. injected with D609 and treated with  $\text{Fe}^{2+}/\text{H}_2\text{O}_2$  and AAPH showed significant reduction in reactive oxygen species (ROS), levels of protein carbonyl, protein bound hydroxynonenal (HNE, a lipid peroxidation product) and 3-nitrotyrosine (3NT, another marker of protein oxidation formed by reaction of tyrosine residues with peroxynitrite) when compared to oxidative stress in synaptosomes isolated from gerbils that were injected with saline, but treated with  $\text{Fe}^{2+}/\text{H}_2\text{O}_2$  and AAPH. These results are discussed with reference to potential use of

this brain accessible glutathione mimetic in the treatment of oxidative stress related neurodegenerative disorders.

## **8.2. Introduction**

Alzheimer's disease (AD) is an age-associated dementing disorder characterized by loss of synapses and the presence of senile plaques and neurofibrillary tangles, affecting more than four million Americans (Katzman and Saitoh, 1991). Oxidative stress has been implicated in many neurodegenerative disorders including AD (Hensley, Hall et al., 1995; Stadtman and Berlett, 1997; Markesbery and Lovell, 1998; Butterfield, Drake et al., 2001; Butterfield and Lauderback, 2002). Reactive oxygen species (ROS) leads to protein oxidation (Hensley, Hall et al., 1995; Stadtman and Berlett, 1997), lipid peroxidation (Markesbery and Lovell, 1998; Butterfield and Lauderback, 2002), DNA and RNA oxidation (Butterfield, Drake et al., 2001) and neuronal dysfunction or death. ROS generation hence becomes important in understanding oxidative stress and oxidative stress related disorders. Many antioxidant therapies for neurological disorder are under investigation.

Glutathione (GSH) is an intracellular antioxidant that maintains redox balance in cell. GSH is the major thiol participating in various cellular redox functions and biosynthesis (Schulz, Lindenau et al., 2000). Reduced levels of GSH have been observed in oxidative stress related disorders (Bains and Shaw, 1997). Reduced levels of GSH in specific regions of the central nervous system of AD patients contribute to the oxidative stress mediated neuronal cell dysfunction and/or loss (Benzi and Moretti, 1995a). In AD, increased levels of oxidized glutathione (GSSG) have been observed (Cooper, 1997). Studies have shown that an increase in endogenous GSH levels by dietary or

pharmacological intake of GSH precursors or GSH mimetics or substrates for GSH synthesis protects brain against oxidative stress (Anderson and Luo, 1998; Halliwell, 2001; Butterfield, Castegna et al., 2002a). Previously, our lab showed that endogenous elevation of GSH by i.p. injection of N-acetyl cysteine (NAC) or gamma- glutamyl-cysteine ethyl ester (GCEE) reduced oxidative stress markers in synaptosomes treated with various oxidants (Pocernich, Cardin et al., 2001; Drake, Kanski et al., 2002; Drake, Sultana et al., 2003). Recently, we showed that tricyclodecan-9-yl-xanthogenate (D609), a glutathione mimetic, protects primary neuronal culture against amyloid  $\beta$ -peptide (1-42) [A $\beta$  (1-42)]-induced oxidative stress and neurotoxicity (Sultana, Shelley et al., 2004).

D609 (Figure 8.1) is a phosphatidylcholine-specific phospholipase C inhibitor (Monick, Carter et al., 1999) that has been shown to trap hydroxyl free radical and to reduce oxidative stress induced by ionizing radiation (Zhou, Lauderback et al., 2001). D609 has antiviral and antitumor activity (Amtmann, 1996). Previously we showed that D609 mimics glutathione (GSH) function in that it has a free thiol group, which upon oxidation forms a disulfide. The resulting dioxanthate is a substrate for glutathione reductase, regenerating D609 (Lauderback, Drake et al., 2003). D609 has the ability to scavenge hydrogen peroxide and hydroxyl free radicals. In addition, D609 can bind to reactive alkenals formed due to peroxidation of lipids and detoxifies their effect, thereby preventing these alkenals from damaging synaptosomes (Lauderback, Drake et al., 2003). Based on these studies we tested the hypothesis that D609 delivered *in vivo*, modulates oxidative stress in brain induced by various oxidants.

### 8.3. Purpose of the study

Our study was aimed at determining the effects of intraperitoneally (i.p). injected D609 in gerbils against oxidative stress in subsequently isolated synaptosomes induced by  $\text{Fe}^{2+}/\text{H}_2\text{O}_2$  (hydroxyl radical formation) and AAPH (alkoxyl and peroxy radical formation).

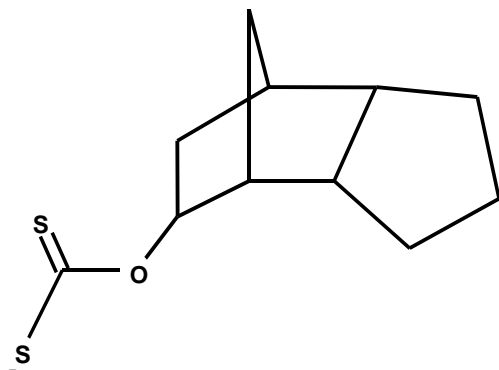


**Figure 8.1:** Tricyclodecan-9-yl-xanthogenate (D609)

### 8.4. Experimentals

#### 8.4.1. Animals

For all the studies male Mongolian gerbils (2-3 months of age), approximately 100 g in size, housed in the University of Kentucky Central Animal Facility in 12-h light/dark conditions and fed standard Purina rodent laboratory chow *ad libitum*, were used. The animal protocols were approved by the University of Kentucky Animal Care and Use Committee.

#### 8.4.2. Chemicals

D609 was purchased from Biomol (Plymouth Meeting, PA) and all other chemicals were purchased from Sigma-Aldrich (St. Louis, MO), unless stated otherwise. Fresh 10 mM stock solution of 2,7-dichlorofluorescein diacetate (DCFH-DA) was

prepared in ethanol for DCF fluorescence assay. Fresh D609 (50mg/kg bodyweight) was prepared in phosphate-buffered saline (PBS). The protein oxidation detection kit was purchased from Interger (Purchase, NY) and primary antibody for HNE and 3NT were purchased from Chemicon International.

#### **8.4.3. Preparation of Synaptosomes**

Synaptosomes were isolated from gerbils injected i.p. with saline (control) or with D609 (50mg/kg body weight), 60min after injection. This level was chosen based on previous experiments conducted at various concentrations (Figure 2). The synaptosomal isolation procedure has been described elsewhere (Whittaker, 1993). Briefly, the gerbils were sacrificed by decapitation and the brain was isolated on a cold plate and placed in 0.32M sucrose isolation buffer containing 4µg/ml leupeptin, 4µg/ml pepstatin, 5 µg/ml aprotinin, 2mM ethylenediaminetetraacetic acid (EDTA), 2mM ethylene glycol-bis(tetraacetic acid (EGTA) and 20mM 4-(2-hydroxyethyl)-1-piperazine-ethanesulfonic acid (HEPES), 20µg/ml trypsin inhibitor and 0.2mM phenylmethanesulfonyl fluoride (PMSF), pH 7.4. The whole brain was homogenized by 20 passes with a Wheaton tissue homogenizer. The homogenate was centrifuged at 1500 g for 10 min. The pellet was discarded and the supernatant was retained and centrifuged at 20000 g for 10 min. The resulting pellet was resuspended in approximately 1ml of 0.32M sucrose isolation buffer and layered over discontinuous sucrose gradient (0.85M pH 8.0, 1.0M pH8.0, 1.18M pH8.5 sucrose solutions each containing 2mM EDTA, 2mM EGTA and 10mM HEPES) and spun at 82500g for 1h at 4° C. The purified synaptosomes were collected from the sucrose gradient interface at the 1.0/1.18M interface and washed with phosphate buffered saline containing 0.01% (w/v) sodium azide and 0.2% (v/v) Tween 20 (PBS), twice and

centrifuged at 32000 g. The resulting synaptosomal membranes were assayed for protein concentration by Pierce BCA method (Bradford, 1976). The synaptosomes obtained were divided in two aliquots. One part was incubated with 30 mM FeSO<sub>4</sub> and 10 mM H<sub>2</sub>O<sub>2</sub>, and the other aliquot was incubated with 1mM AAPH for 1h at 37° C. The synaptosomal samples were washed following incubation and suspended in PBS.

#### **8.4.4. DCF fluorescence**

10 µM DCFH-DA was incubated with synaptosomes (1mg/ml) for 30 minutes at 37° C. Intracellular esterases convert DCFH-DA into anionic DCFH, which because of its negative charge is trapped in the synaptosomes. Upon oxidation with ROS, DCFH is converted to 2,7- dichlorofluoroscein (DCF), a fluorescent compound. Synaptosomes were spun at 3000 g in a tabletop Eppendorf centrifuge for 5 minutes at 4° C. Synaptosomes were resuspended in 500 µl of PBS and loaded in triplicate (100 µl per well) in a black microtiter plate and fluorescence was measured in a Spectramax microtiter plate reader ( $\lambda_{\text{ex}} = 495\text{nm}$ ,  $\lambda_{\text{em}} = 530\text{nm}$ ) and quantified using softPro max software. To verify that ester cleavage and efflux of the dye were not contributing to changes in fluorescence, similar studies were done with an oxidation-insensitive dye CDCF-DA (C369).

#### **8.4.5. Protein carbonyls**

Protein carbonyls are the markers of protein oxidation and were assayed by following the standard protocol described elsewhere (Stadtman and Berlett, 1997). Sample (5 µl) (normalized to 4mg/ml), 5µl of 12% sodium dodecyl sulfate (SDS) and 10µl of 10 times diluted 2,4-dinitrophenylhydrazine (DNPH) from 200mM stock were incubated at room temperature for 20 min. Samples were neutralized with 7.5µl

neutralization solution (2M Tris in 30% glycerol). The resulting solution was solution was loaded in each well on nitrocellulose membrane under vacuum using a slot blot apparatus. The membrane was blocked in blocking buffer (3% bovine serum albumin) in phosphate buffered saline containing 0.01% (w/v) sodium azide and 0.2% (v/v) Tween 20 (PBS) for 1 h and incubated with a 1:100 dilution of anti DNP polyclonal antibody in phosphate buffered saline containing 0.01% (w/v) sodium azide and 0.2% (v/v) Tween 20 (PBS) for 1h. The membrane was washed three times in PBS and was incubated for 1 h with an anti-rabbit IgG alkaline phosphatase secondary antibody diluted in PBS in a 1:8000 ratio. The membrane was washed for three times in PBS for 5 min and developed in Sigma fast tablets (BCIP/NBT substrate). Blots were dried, scanned with Adobe Photoshop, and quantified with Scion Image (PC version of Macintosh compatible NIH image).

#### **8.4.6. 4-Hydroxynonenal (HNE)**

Sample (5 µl) (normalized to 4mg/ml), 5µl of 12% sodium dodecyl sulfate (SDS) and 5µl of modified Laemmli buffer containing 0.125 M tris base pH 6.8, 4% (v/v) SDS, and 20% (v/v) glycerol were incubated for 20 minutes at room temperature. Sample (250 ng) was loaded in each well on nitrocellulose membrane in slot blot apparatus under vacuum. The membrane was blocked in blocking buffer (3% bovine serum albumin) in phosphate buffered saline containing 0.01% (w/v) sodium azide and 0.2% (v/v) Tween 20 (PBS) for 1 hr and incubated with a 1: 5000 dilution of anti-HNE polyclonal antibody in PBS for 1 h 30 min. The membrane was washed in PBS for 5 min three times after incubation. The membrane was incubated for 1 h, following washing, with an anti-rabbit IgG alkaline phosphatase secondary antibody diluted in PBS in 1:8000 ratio. The

membrane was washed three times in PBS for 5 min and developed in Sigma fast tablets (BCIP/NBT substrate). Blots were dried, scanned with Adobe Photoshop, and quantified with Scion Image as above.

#### **8.4.7. 3-Nitrotyrosine (3NT)**

Sample (5  $\mu$ l) (normalized to 4mg/ml), 5 $\mu$ l of 12% sodium dodecyl sulfate (SDS) and 5 $\mu$ l of modified Laemmli buffer containing 0.125 M tris base pH 6.8, 4% (v/v) SDS, and 20% (v/v) glycerol were incubated for 20 minutes at room temperature. Sample (250 ng) was loaded in each well on nitrocellulose membrane in slot blot apparatus under vacuum. The membrane was blocked in blocking buffer (3% bovine serum albumin) in phosphate buffered saline containing 0.01% (w/v) sodium azide and 0.2% (v/v) Tween 20 (PBS) for 1 hr and incubated with a 1: 2000 dilution of anti-3-nitrotyrosine (3NT) polyclonal antibody in PBS for 1 h 30 min. The membrane was washed in PBS for 5 min three times after incubation. The membrane was incubated for 1 h, following washing, with an anti-rabbit IgG alkaline phosphatase secondary antibody diluted in PBS in 1:8000 ratio. The membrane was washed for three times in PBS for 5 minutes and developed in Sigma fast tablets. Blots were dried, scanned with Adobe Photoshop, and quantified with Scion Image as above.

#### **8.4.8. Western blot for Protein oxidation**

Samples (100  $\mu$ g) were incubated with DNPH at room temperature for 30 min and then precipitated with trichloro acetic acid (TCA) following incubation. The pellet was washed with 1:1 Ethanol: Ethyl acetate for three times. After addition of sample loading buffer, protein sample were denatured and electrophoresed on a 10% SDS-polyacrylamide gel. Proteins were transferred to nitrocellulose at 90 mA/gel for 2 h. The



blots were blocked for 1h in fresh wash buffer (10 mM tris-HCl 9pH7.5), 150 mM NaCl, 0.05% Tween 20, pH 7.4, containing 3% bovine serum albumin) and incubated with a 1:100 dilution of anti DNP polyclonal antibody in phosphate buffered saline containing 0.01% (w/v) sodium azide and 0.2% (v/v) Tween 20 (PBS) for 1h. The membrane was washed three times in PBS and was incubated for 1 h with an anti-rabbit IgG alkaline phosphatase secondary antibody diluted in PBS in a 1:8000 ratio. The membrane was washed for three times in PBS for 5 min and developed in Sigma fast tablets (BCIP/NBT substrate). The blot was stripped and reprobed for GAPDH to show equal loading of protein.

### **8.5. Statistical analysis**

Analysis of variance (ANOVA) was used for comparison among the groups and statistical evaluation. Results are presented as means  $\pm$  SEM. P values  $< 0.05$  were considered significant.

## **8.6. Results**

### **8.6.1. DCF fluorescence**

The DCF assay is useful to monitor ROS generation. DCF is sensitive to many oxidative stress-inducing compounds including hydroxyl radical, ONOO-, AAPH and A $\beta$  (Wang and Joseph, 1999; Keller, Lauderback et al., 2000; Lauderback, Kanski et al., 2002). Figure 8.2 shows the ROS levels in synaptosomes isolated from saline-injected gerbils (control), synaptosomes isolated from saline-injected gerbils treated with Fe<sup>2+</sup>/H<sub>2</sub>O<sub>2</sub> or AAPH and Fe<sup>2+</sup>/H<sub>2</sub>O<sub>2</sub> or AAPH treated synaptosomes isolated from gerbils previously injected i.p. with D609, respectively. There was a significant increase in ROS

generation in synaptosomes isolated from control gerbils treated with  $\text{Fe}^{2+}/\text{H}_2\text{O}_2$  or AAPH ( $p < 0.0001$ ) when compared to control. Synaptosomes isolated from D609 injected gerbils and subsequently treated with  $\text{Fe}^{2+}/\text{H}_2\text{O}_2$  or AAPH showed significant decrease in ROS levels when compared to synaptosomes treated with  $\text{Fe}^{2+}/\text{H}_2\text{O}_2$  or AAPH, isolated from gerbils injected i.p. with saline ( $p < 0.005$ ).

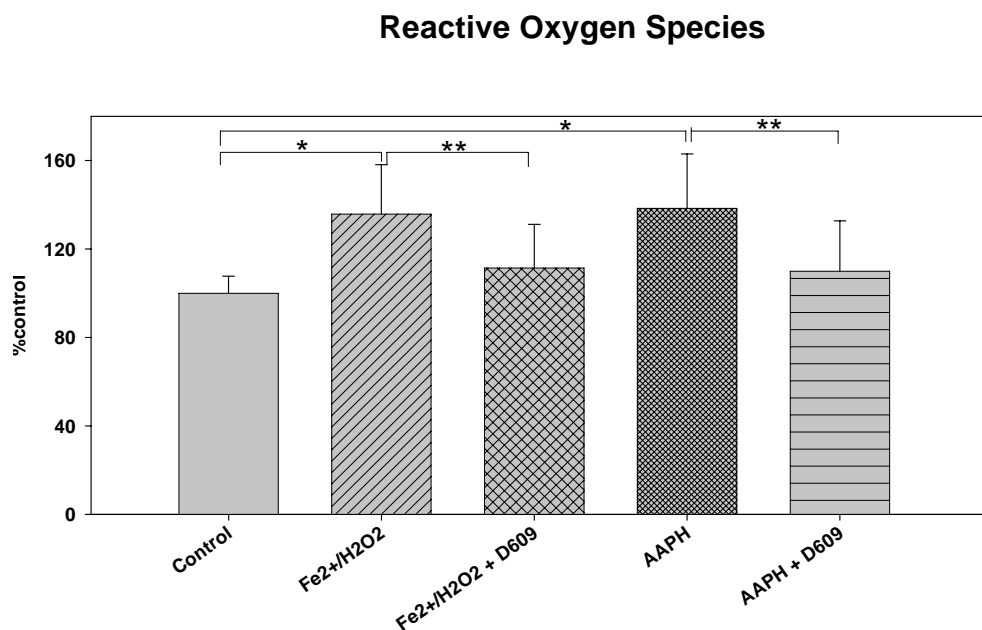


**Figure 8.2:** Significant increase in ROS in synaptosomes isolated from saline injected gerbils and subsequently treated with Fe<sup>2+</sup>/H<sub>2</sub>O<sub>2</sub> or AAPH compared to ROS in synaptosomes isolated from saline-injected gerbils, \*  $p < 0.005$ . Decreased ROS in synaptosomes isolated from gerbils injected i.p. with D609 subsequently treated with Fe<sup>2+</sup>/H<sub>2</sub>O<sub>2</sub> or AAPH relative to ROS in synaptosomes isolated from gerbils injected with saline and subsequently treated with Fe<sup>2+</sup>/H<sub>2</sub>O<sub>2</sub> or AAPH, \*\*  $p < 0.005$ ; the data are the mean  $\pm$  SEM expressed as percentage of control values, (n = 6).

To ensure that ester cleavage or efflux of the DCFH, prior to the reaction with ROS, was not contributing to changes in fluorescence, the oxidation-insensitive dye (C369) was used in similar studies and was used as control. No difference in fluorescence was found in all the studies, confirming that a change in fluorescence shown in Figure 8.3 was due to oxidation of the dye and not because of some other parameter.

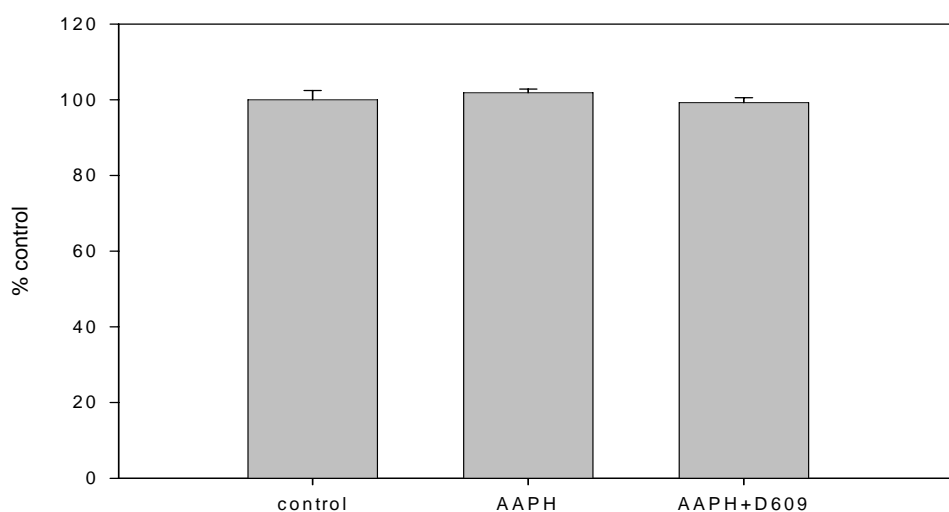
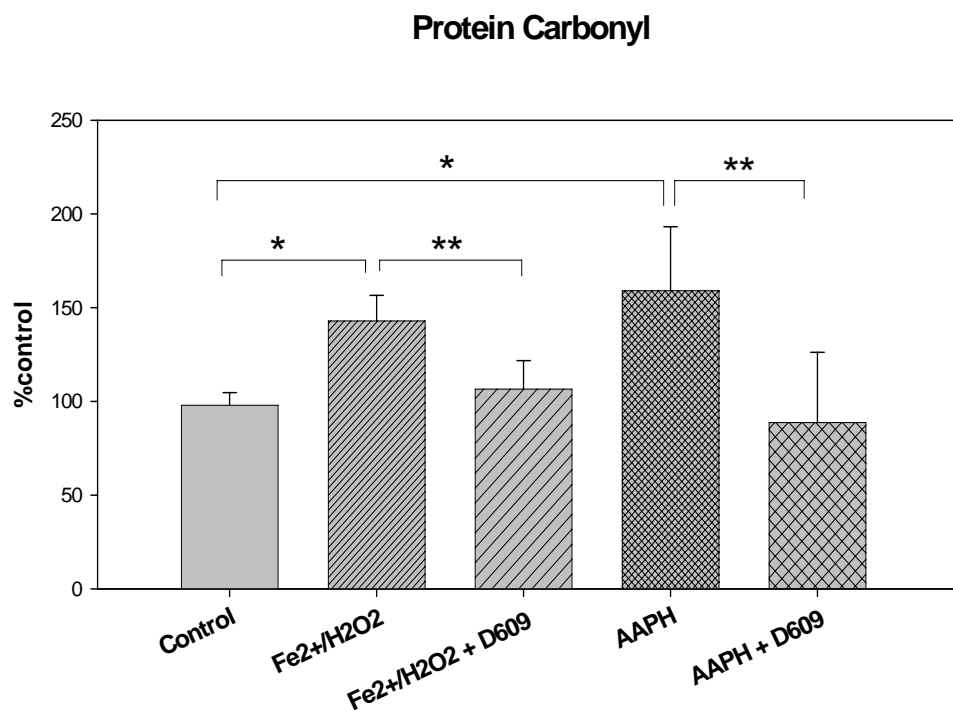


**Figure 8.3:** Measurement of ROS generation using the oxidation-insensitive probe C369. The oxidation-insensitive fluorescence probe C369 was used as control to show esterase activity and drug efflux changes of DCFH-DA.

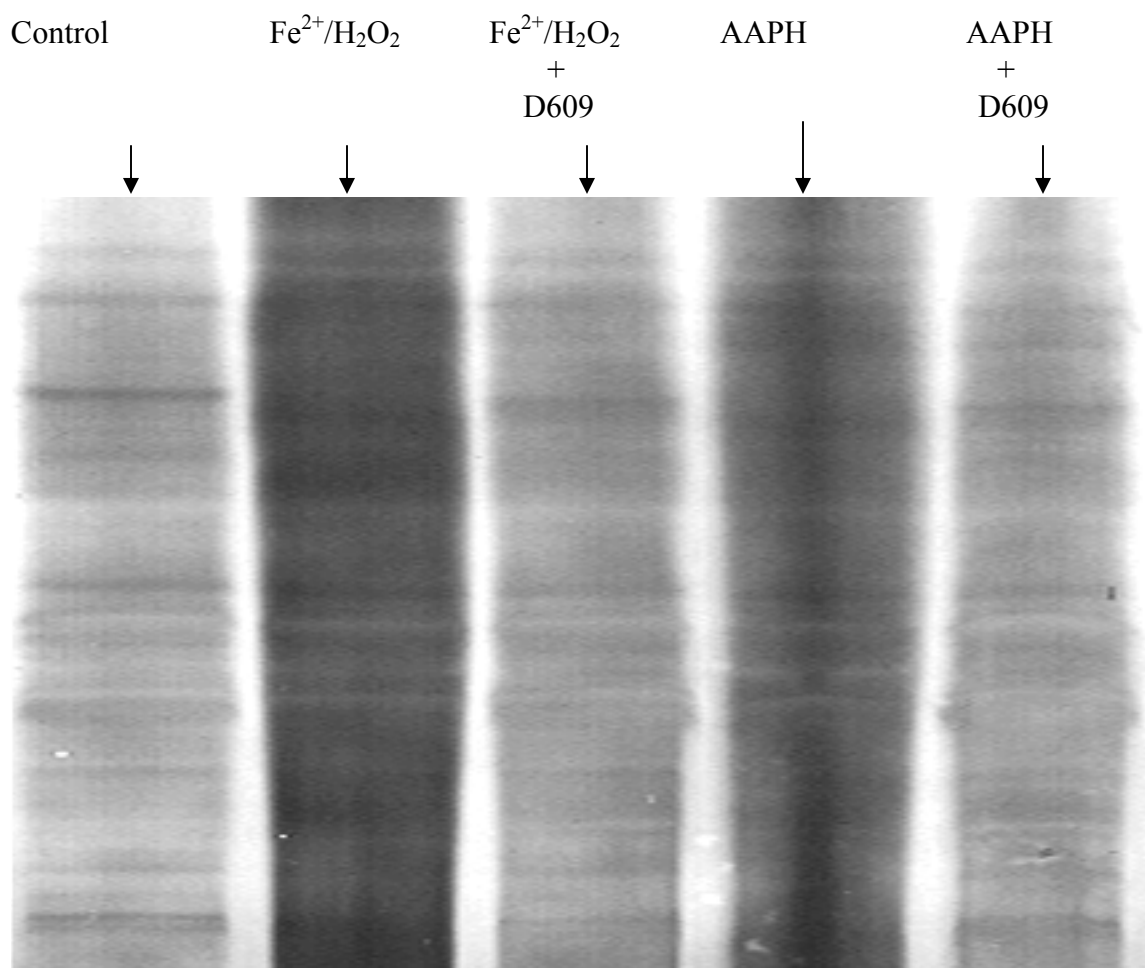
### 8.6.2. Protein carbonyl

Figure 8.4 shows the protein carbonyl levels in synaptosomes isolated from saline injected gerbils (control), synaptosomes isolated from control gerbils subsequently treated with  $\text{Fe}^{2+}/\text{H}_2\text{O}_2$  or AAPH and  $\text{Fe}^{2+}/\text{H}_2\text{O}_2$  - or AAPH-treated synaptosomes isolated from gerbils previously injected i.p. with D609. There was a significant increase in protein carbonyl levels in synaptosomes isolated from control gerbils treated with  $\text{Fe}^{2+}/\text{H}_2\text{O}_2$  or AAPH ( $p < 0.000001$ ) when compared to control. Synaptosomes isolated from D609 injected gerbils subsequently treated with  $\text{Fe}^{2+}/\text{H}_2\text{O}_2$  and AAPH showed significantly decreased protein carbonyl levels when compared to synaptosomes isolated from saline-injected gerbils and subsequently treated with  $\text{Fe}^{2+}/\text{H}_2\text{O}_2$  or AAPH ( $p < 0.00005$ ).

Figure 8.5 show representative western blots for total protein oxidation. It is clear that decreased protein oxidation is found in  $\text{Fe}^{2+}/\text{H}_2\text{O}_2$  or AAPH treated synaptosomes isolated from gerbils previously injected with D609.



**Figure 8.4:** Significant increase in protein carbonyl levels in synaptosomes isolated from saline injected gerbils and subsequently treated with Fe<sup>2+</sup>/H<sub>2</sub>O<sub>2</sub> or AAPH compared to protein carbonyls in synaptosomes isolated from saline injected gerbils, \* p < 0.005. Decreased protein carbonyl level in synaptosomes isolated from gerbils injected i.p. with D609 subsequently treated with Fe<sup>2+</sup>/H<sub>2</sub>O<sub>2</sub> or AAPH relative to protein carbonyl level in synaptosomes isolated from gerbils injected with saline and subsequently treated with Fe<sup>2+</sup>/H<sub>2</sub>O<sub>2</sub> or AAPH, \*\* p < 0.005; the data are the mean ± SEM expressed as percentage of control values, (n = 6).



**Figure 8.5:** Representative western blot showing protein carbonyl levels from various treatments.

### 8.6.3. HNE

Arachidonic acid from phospholipids, on attack by free radicals, produces reactive alkenals, such as HNE. HNE binds to proteins by Michael addition (Butterfield and Stadtman, 1997) and inactivates them by changing their conformation (Subramaniam, Roediger et al., 1997; Zhou, Lauderback et al., 2001) Figure 8.6 shows the protein-bound HNE levels in synaptosomes isolated from saline-injected gerbils (control), synaptosomes isolated from control gerbils treated with  $\text{Fe}^{2+}/\text{H}_2\text{O}_2$  or AAPH and  $\text{Fe}^{2+}/\text{H}_2\text{O}_2$ - or AAPH-treated synaptosomes isolated from gerbils previously injected i.p. with D609. There was a significant increase in protein-bound HNE levels in synaptosomes isolated from control gerbils treated with  $\text{Fe}^{2+}/\text{H}_2\text{O}_2$  or AAPH ( $p < 0.0001$ ) when compared to control. Synaptosomes isolated from D609 injected gerbils subsequently treated with  $\text{Fe}^{2+}/\text{H}_2\text{O}_2$  or AAPH showed significant decrease in protein bound HNE levels when compared to synaptosomes isolated from saline-injected gerbils treated with  $\text{Fe}^{2+}/\text{H}_2\text{O}_2$  or AAPH ( $p < 0.001$ ).

### 8.6.4. 3NT

Figure 8.7 shows levels of 3-NT in synaptosomes isolated from saline injected gerbils (control), synaptosomes isolated from control gerbils treated with  $\text{Fe}^{2+}/\text{H}_2\text{O}_2$  or AAPH and  $\text{Fe}^{2+}/\text{H}_2\text{O}_2$ - and AAPH-treated synaptosomes isolated from gerbils previously injected i.p. with D609 . There was a significant increase in 3-NT levels in synaptosomes isolated from saline-injected gerbils treated with  $\text{Fe}^{2+}/\text{H}_2\text{O}_2$  or AAPH ( $p < 0.001$ ) when compared to control. Synaptosomes isolated from D609 injected gerbils subsequently treated with  $\text{Fe}^{2+}/\text{H}_2\text{O}_2$  and AAPH showed a significant decrease in 3-NT levels when



compared to synaptosomes isolated from saline injected gerbils treated with  $\text{Fe}^{2+}/\text{H}_2\text{O}_2$  or AAPH ( $p < 0.001$ ).

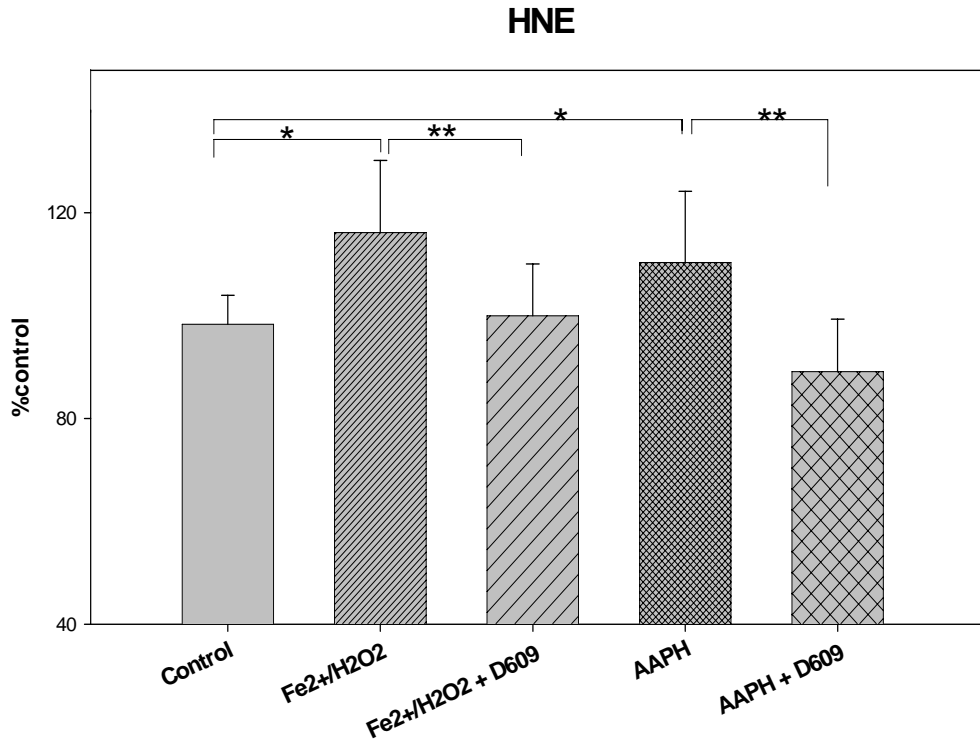


**Figure 8.6:** Significant increase in protein bound HNE levels in synaptosomes isolated from saline injected gerbils and subsequently treated with  $\text{Fe}^{2+}/\text{H}_2\text{O}_2$  or AAPH compared to protein carbonyls in synaptosomes isolated from saline injected gerbils, \*  $p < 0.005$ . Decreased protein bound HNE level in synaptosomes isolated from gerbils injected i.p. with D609 subsequently treated with  $\text{Fe}^{2+}/\text{H}_2\text{O}_2$  or AAPH relative to protein carbonyl level in synaptosomes isolated from gerbils injected with saline and subsequently treated with  $\text{Fe}^{2+}/\text{H}_2\text{O}_2$  or AAPH, \*\*  $p < 0.005$ ; the data are the mean  $\pm$  SEM expressed as percentage of control values, ( $n = 6$ ).

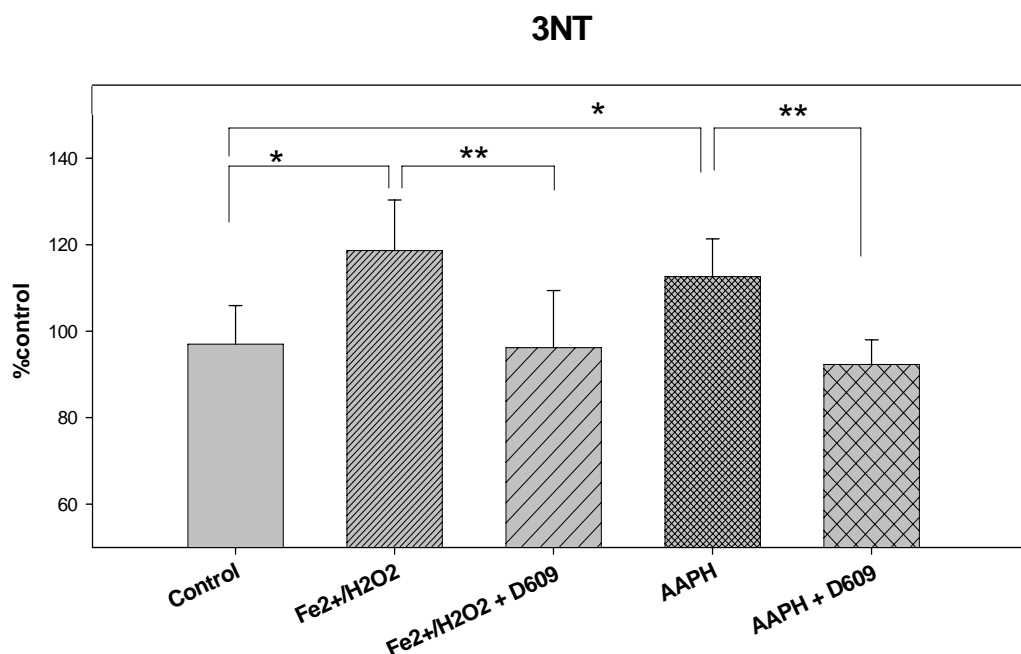


**Figure 8.7:** Significant increase in 3NT levels in synaptosomes isolated from saline-injected gerbils and subsequently treated with Fe<sup>2+</sup>/H<sub>2</sub>O<sub>2</sub> or AAPH compared to 3-NT levels in synaptosomes isolated from saline-injected gerbils, \*  $p < 0.005$ . Decreased 3NT levels in synaptosomes isolated from gerbils injected i.p. with D609 subsequently treated with Fe<sup>2+</sup>/H<sub>2</sub>O<sub>2</sub> or AAPH relative to protein carbonyl level in synaptosomes isolated from gerbils injected with saline and subsequently treated with Fe<sup>2+</sup>/H<sub>2</sub>O<sub>2</sub> or AAPH, \*\*  $p < 0.005$ ; the data are the mean  $\pm$  SEM expressed as percentage of control values, (n = 6).

## 8.7. Discussion

Oxidative stress has been implicated in many neurodegenerative disorders including AD (Butterfield, Drake et al., 2001). Oxidative stress arises due to an imbalance in the antioxidant system and generation of oxidants such as free radicals (Yu, 1994). In AD, synaptic membranes are known to show increased oxidative stress (Hensley, Carney et al., 1994; Hensley, Hall et al., 1995). Synaptosomes were selected for our studies for the following reasons. Synaptic membranes have receptors for glutamate which mediate increase in intracellular  $\text{Ca}^{2+}$  and excitotoxicity and cause production of ROS and RNS including peroxynitrite and lead to subsequent protein oxidation (Hensley, Carney et al., 1994; Mattson, 1996). Elevation in  $\text{Ca}^{2+}$  level also causes change in mitochondrial potential and lead to production of superoxide ion radicals. Due to more energy usage in the synaptic region of neuron, mitochondria are concentrated in these areas of cell. Hence, the synaptic region of neurons becomes more vulnerable to oxidative stress.

There are increasing evidence to demonstrate that AD brain is under oxidative stress (Butterfield, Drake et al., 2001). Oxidative damage to protein, lipids and DNA lead to cellular dysfunction and also cell death (Yu, 1994; Butterfield, 2002; Butterfield and Lauderback, 2002; Castegna, Aksenov et al., 2002a; Castegna, Aksenov et al., 2002b; Castegna, Thongboonkerd et al., 2003). Due to relatively poor antioxidant defense available in brain, the high content of polyunsaturated fatty acids and the high oxygen utilization in brain, vulnerability of neurons towards oxidative stress is increased. Among the antioxidants present in brain, glutathione (GSH) is the most abundant and is present ubiquitously (Cooper, 1997).

A well known antioxidant and is a free radical scavenger, GSH is also involved in maintenance of cellular redox status, DNA synthesis and repair, protein synthesis, amino acid transport, binding of heavy metals and other functions (Cooper, 1997). Normally, in most cells the GSH/GSSG ratio is vastly shifted to the reduced form of GSH except under oxidative stress conditions. These two forms are interconvertible by the action of glutathione peroxidase and glutathione reductase (Hayes and McLellan, 1999).

Many studies have shown that GSH protects the brain against various oxidants found in AD (Bains and Shaw, 1997). GSH is known to detoxify HNE, a lipid peroxidation product found to be elevated in AD brain (Sayre, Zelasko et al., 1997; Lovell, Xie et al., 1998; Xie, Lovell et al., 1998). It has also been shown that GSH protects cultured neurons against oxidative damage resulting from amyloid  $\beta$ -peptide, iron and HNE (Mark, Lovell et al., 1997; Mark, Pang et al., 1997). In addition, GSH can also protect brain from damage by peroxynitrite, hydroxyl free radicals or reactive alkenals (Koppal, Drake et al., 1999a; Koppal, Drake et al., 1999b; Pocernich, La Fontaine et al., 2000; Pocernich, Cardin et al., 2001; Drake, Kanski et al., 2002; Drake, Sultana et al., 2003). Low levels of GSH are associated with aging and many diseased conditions including AIDS, amyotrophic lateral sclerosis, AD (Bains and Shaw, 1997). The diminution of GSH levels in these conditions could be due to malfunctioning of enzymes required for GSH synthesis or due to insufficient supply of substrate involved in GSH metabolism.

Tricyclodecan-9-yl-xanthogenate (D609) is a derivative of xanthic acid (Rao, 1971) that has been reported as a phosphatidylcholine-specific phospholipase C inhibitor (Sauer, Amtmann et al., 1984; Monick, Carter et al., 1999). In performing this function,

D609 protects brain from ceramide-induced apoptosis and transcription of inflammatory molecules mediated by NF- $\kappa$ B (Schutze, Potthoff et al., 1992; Cifone, Roncaioli et al., 1995; Li, Maher et al., 1998; Sortino, Condorelli et al., 1999). Since oxidative stress is involved in these processes, the antioxidant property of D609 was studied. Our lab demonstrated that D609 scavenges H<sub>2</sub>O<sub>2</sub> (Lauderback, Drake et al., 2003). These studies suggested that D609 mimics glutathione (GSH) function in that it has a free thiol group, which upon oxidation forms a disulfide. The resulting dithiolane formed acts as a substrate for glutathione reductase, regenerating D609 (Lauderback, Drake et al., 2003). In addition, D609 binds to reactive alkenals formed due to peroxidation of lipids and detoxifies their effect, thereby preventing these alkenals from damaging synaptosomes (Lauderback, Drake et al., 2003).

Intracellular elevation of glutathione has been used as therapeutics in many diseases (Anderson and Luo, 1998). Previously, our lab showed that i.p. injection of N-acetyl cysteine (NAC) and gamma-glutamyl-cysteine ethyl ester (GCEE) reduced the oxidative stress markers in synaptosomes (Pocernich, Cardin et al., 2001; Drake, Kanski et al., 2002) by elevating the endogenous GSH levels. The i.p. injection of NAC protects synaptosomes against hydroxyl radical and acrolein and is also shown to protect *in vitro* oxidative stress caused by peroxynitrite (Koppal, Drake et al., 1999a; Pocernich, Cardin et al., 2001). Similar results have been shown with GCEE (Drake, Kanski et al., 2002). D609 reduces oxidative stress markers *in vitro* (Lauderback, Drake et al., 2003). Recent studies have also shown that D609 reduces the A $\beta$  (1-42) induced oxidative stress and cytotoxicity in neuronal cell culture (Sultana, Shelley et al., 2004).

Protein oxidation is elevated in AD brain (Butterfield and Lauderback, 2002). Oxidation of protein leads to deactivation of enzymes critical for cell functioning, and recently our lab showed some of the critical proteins that are oxidized in AD by proteomics studies (Castegna, Aksenov et al., 2002a; Castegna, Aksenov et al., 2002b; Castegna, Thongboonkerd et al., 2003).  $\text{Fe}^{2+}/\text{H}_2\text{O}_2$  (hydroxyl radical formation) and AAPH (alkoxyl and peroxy radical formation) are known to induce protein oxidation (Pocernich, La Fontaine et al., 2000; Kanski, Lauderback et al., 2001). We previously demonstrated by using Fenton chemistry ( $\text{Fe}^{2+}/\text{H}_2\text{O}_2$ ), D609 inhibits the formation of a PBN spin adduct, which shows hydroxyl radical scavenging property (Lauderback, Drake et al., 2003). Decreased protein oxidation was observed in neuronal cell culture pretreated with D609 on incubation with  $\text{A}\beta$  (1-42) (Sultana, Shelley et al., 2004). The results shown in this *in vivo* study are in consistent with the *in vitro* data, showing that D609 acts as an antioxidant. There was a significant reduction in protein carbonyl formation and 3NT levels, both markers of protein oxidation, in synaptosomes isolated from D609 injected gerbils subsequently treated with  $\text{Fe}^{2+}/\text{H}_2\text{O}_2$  or AAPH in comparison with synaptosomes isolated from saline injected gerbils and subsequently treated with  $\text{Fe}^{2+}/\text{H}_2\text{O}_2$  or AAPH.

Lipid peroxidation products such as HNE and acrolein are known to be elevated in AD brain (Sayre, Zelasko et al., 1997; Lauderback, Hackett et al., 2001). These alkenals form the immediate substrate for GSH (Lovell, Xie et al., 1998; Xie, Lovell et al., 1998) and these lipid peroxidation products are known to be involved in apoptosis, which is seen as a consequence of GSH depletion (Mark, Lovell et al., 1997). Lipid peroxidation induced by Fenton chemistry was reduced by D609 in synaptosomes

(Lauderback, Drake et al., 2003). Decreased lipid peroxidation was observed in neuronal cell culture pretreated with D609 on incubation with A $\beta$  (1-42) (Sultana, Shelley et al., 2004) . We demonstrated previously that treatment of neuronal cultures with D609 prevents apoptosis induced by A $\beta$  (1-42) mediated oxidative stress (Sultana, Shelley et al., 2004). In the present study, there was a significant reduction in protein bound HNE levels in synaptosomes isolated from D609 injected gerbils subsequently treated with Fe<sup>2+</sup>/H<sub>2</sub>O<sub>2</sub> and AAPH in comparison with synaptosomes isolated from saline injected gerbils and subsequently treated with Fe<sup>2+</sup>/H<sub>2</sub>O<sub>2</sub> and AAPH.

All the *in vitro* studies and studies on cultures show that D609 acts as an antioxidant. Our *in vivo* data are consistent with previously observed results. There was a reduction in ROS levels in synaptosomes isolated from gerbils injected i.p with D609 and subsequently treated with Fe<sup>2+</sup>/H<sub>2</sub>O<sub>2</sub> or AAPH when compared to synaptosomes isolated from saline-injected gerbils and subsequently treated with Fe<sup>2+</sup>/H<sub>2</sub>O<sub>2</sub> or AAPH. These results are consistent with the notion that D609 or its key metabolites may cross the blood brain barrier (BBB) and protect synaptosomes from oxidative stress induced by Fe<sup>2+</sup>/H<sub>2</sub>O<sub>2</sub> or AAPH. In some of the data presented, the level of oxidative stress markers are below the control level in synaptosomes isolated from D609-treated rodent. This could be due to the presence of D609 in the system that could prevent oxidation of synaptosomes due to environmental oxidants, the kind of protection that is lacking in controls.

In conclusion, the protection of synaptosomes, *in vivo*, by D609 is consistent with previous *in vitro* and cell culture studies. The presence of the thiol group in D609 is the basis for its antioxidant property, since the methylated derivative of D609 is inactive

(Sultana, Shelley et al., 2004). Xanthates in general are known to be the strong reducing agents (Rao, 1971). The thiol group in D609 could react with lipid peroxidation products and form Michael adducts and prevent these reactive lipid peroxidation products from causing neurotoxicity. These studies on an animal model could form the basis for eventual treatment strategies for oxidative stress related disorders, although additional studies are required to determine if this notion has merit. Studies on the effect of D609 on animal models of oxidative stress-related disorders are on progress.



## Chapter 9

### ***In vivo* protection by the xanthate D609 against amyloid $\beta$ -peptide (1-42)-induced**

#### **oxidative stress: Implications for Alzheimer's disease**

##### **9.1. Overview of the study**

Considerable evidence supports the role of oxidative stress in the pathogenesis of Alzheimer's disease (AD). One hallmark of AD is the accumulation of amyloid  $\beta$ -peptide ( $A\beta$ ), which invokes a cascade of oxidative damage to neurons that can eventually result in neuronal death.  $A\beta$  is the main component of senile plaques and generates free radicals ultimately leading to neuronal damage of membrane lipids, proteins and nucleic acids. Therefore, interest in the protective role of different antioxidant compounds has been growing for treatment of AD and other oxidative stress-related disorders. Among different antioxidant drugs, much interest has been devoted to "thiol-delivering" compounds. Tricyclodecan-9-yl-xanthogenate (D609) is an inhibitor of phosphatidylcholine specific phospholipase (PC-PLC), and recent studies reported its ability to act as a glutathione-mimetic compound. In the present study, we investigate the *in vivo* ability of D609 to protect synaptosomes against  $A\beta$ -induced oxidative stress. Gerbils were injected intraperitoneally (i.p.) with D609 or with saline solution, and synaptosomes were isolated from the brain. Synaptosomal preparations isolated from D609 injected gerbils and treated *ex vivo* with  $A\beta$ (1-42) showed a significant decrease of oxidative stress parameters: reactive oxygen species (ROS) levels, protein oxidation (protein carbonyl and 3-nitrotyrosine levels) and lipid peroxidation (4-hydroxy-2-nonenal levels). Our results are consistent with the hypothesis that modulation of free radicals generated by amyloid  $\beta$ -peptide might represent an efficient therapeutic strategy for

treatment of AD and other oxidative-stress related disorders. Based on the above data, we suggest that D609 is a potent antioxidant and could be of importance for the treatment of AD and other oxidative stress-related disorders.

## **9.2. Introduction**

Alzheimer's disease (AD) is a progressive neurological disorder characterized by loss of memory cognition. Major pathological hallmarks of AD include loss of synapses and the presence of senile plaques and neurofibrillary tangles. The major protein component of the core of senile plaques is amyloid  $\beta$ -peptide ( $A\beta$ ).  $A\beta$  is formed upon proteolytic processing, by  $\beta$ - and  $\gamma$ -secretases (Haass and De Strooper, 1999), of the larger amyloid precursor protein (APP), a ubiquitously expressed transmembrane glycoprotein (Glenner and Wong, 1984; Glenner, Eanes et al., 1988). The amyloid  $\beta$ -cascade hypothesis, suitably updated, postulates that  $A\beta$  is likely central to the pathogenesis of AD (Hardy and Allsop, 1991; Smith, Chen et al., 1999; Selkoe, 2001). The mechanisms involved in the  $A\beta$ -mediated neurotoxicity are unknown, but there is evidence suggesting that oxidative stress plays a key role (Butterfield, Drake et al., 2001; Butterfield and Lauderback, 2002; Canevari, Abramov et al., 2004). Growing attention has been focused to investigate the oxidative mechanism of  $A\beta$  toxicity and as well in the search for novel neuroprotective agents. Previous studies from our laboratory and others reported that  $A\beta$  peptide induces *in vitro* reactive oxygen species production, protein oxidation, DNA and RNA oxidation and lipid peroxidation (Butterfield, 2002).

Because of the involvement of oxidative stress-mediated toxicity in neurodegenerative events and neuronal cell death (Good, Werner et al., 1996; Moreira, Smith et al., 2005), various experimental approaches for effective protection by

antioxidants have emerged. In addition, antioxidant therapy is being discussed for Parkinson's disease (Ebadi, Srinivasan et al., 1996; Prasad, Cole et al., 1999), ischemia (Marczin, El-Habashi et al., 2003) as well as for AD (Grundman and Delaney, 2002; Gilgun-Sherki, Melamed et al., 2003) and other age-related disorders (Ames, 2004). Numerous potential free-radical scavengers have been tested in different experimental paradigms of oxidative stress-induced cell death, such as Vitamin E (Behl, Davis et al., 1992), Vitamin C, melatonin (Pappolla, Sos et al., 1997), ginkgo biloba (Smith and Luo, 2003), steroid hormones (Goodman, Bruce et al., 1996; Behl, Skutella et al., 1997), N-acetylcysteine (Adair, Knoefel et al., 2001), etc. However, many clinical trials are still unsuccessful because all the antioxidants tested are poorly active in crossing the blood brain barrier (BBB).

Glutathione is one of the major intracellular defense systems, and depletion of GSH is known to be involved in several neurodegenerative disorders (Benzi and Moretti, 1995b; Markesbery, 1997; Butterfield, Castegna et al., 2002a). Many attempts have been made to develop antioxidant compounds able to “mimic” GSH as scavenger of reactive oxygen species (ROS) and to maintain the intracellular redox state. Increase in endogenous GSH levels by dietary or pharmacological intake of GSH precursor or GSH mimetic protects brain against oxidative stress (Anderson and Luo, 1998; Butterfield, Drake et al., 2001; Halliwell, 2001). Considering the importance of developing new antioxidant compounds and the relevance of their application in the treatment of neurodegenerative diseases, we focused our attention on tricyclodecan-9-yl-xanthogenate (D609). D609 is an inhibitor of phosphatidylcholine-specific phospholipase C (PC-PLC) (Schutze, Potthoff et al., 1992; Wiegmann, Schutze et al., 1994) and sphingomyelinase

(Yu, Nikolova-Karakashian et al., 2000; Meng, Luberto et al., 2004). D609 exhibits a variety of potent biological properties, including antitumor (Amtmann and Sauer, 1987), antiviral (Amtmann, Muller-Decker et al., 1987; Villanueva, Navarro et al., 1991) and anti-inflammatory activities (Machleidt, Kramer et al., 1996). The xanthate D609 is a reducing agent and it has been reported to protect rodents against UV-induced oxidative damage (Zhou, Lauderback et al., 2001). Previous studies from our laboratory have shown that D609 exerts its antioxidant properties acting as a glutathione (GSH)-mimetic compound (Lauderback, Drake et al., 2003). The free thiol group of the xanthate is oxidized to the corresponding disulfide (dixanthate) that is a substrate for GSH-reductase, regenerating D609 active form (xanthate). D609 can scavenge hydrogen peroxide and hydroxyl free radicals. In addition, D609 can bind directly to reactive alkenals, providing detoxification of these lipid peroxidation end-products thereby preventing oxidative damage of synaptic membranes (Lauderback, Drake et al., 2003). Recently, Sultana et al. demonstrated that D609 is protective against A $\beta$ -induced toxicity in primary neuronal cultures (Sultana, Newman et al., 2004).

### **9.3. Purpose of the study**

Based upon the mechanisms by which D609 scavenges free radicals, the aim of the present study was to investigate the ability of D609 to provide *in vivo* neuroprotection against A $\beta$ -induced oxidative stress. The results are consistent with the hypothesis that D609 is a potent antioxidant and could be beneficial in the treatment of AD and other oxidative stress-related disorders.

## **9.4. Experimentals**

### **9.4.1. Chemicals**

D09 was purchased from Biomol Inc (Plymouth Meeting, PA) and most other chemicals were purchased from Sigma-Aldrich (St. Louis, MO, USA). The fluorescent indicator for ROS measurement, 2,7-dichlorofluorescein diacetate (DCFH-DA), was obtained from Molecular Probes (Eugene, OR, U.S.A.), and a fresh 10 mM stock solution was prepared in ethanol. Fresh D609 was dissolved in phosphate-buffered saline (PBS). The OxyBlot oxidized protein kit was obtained from Intergen, Inc. (Purchase, NY). Amyloid- $\beta$  peptide (1-42) (HPLC and MS certified quality) was purchased from Anaspec, Inc. (San Jose, CA). For all experiments, A $\beta$  was incubated for 24 hr in PBS at 37 °C before application to synaptosomes. Primary antibodies for 4-hydroxynonenal (HNE) and 3-nitrotyrosine were obtained from Chemicon.

### **9.4.2. Animals**

For the present study, three month-old male Mongolian gerbils, approximately 100 g in size, were used to isolate synaptosomes. All the following protocols were approved by the University of Kentucky Animal Care and Use Committee. All the animals were kept under twelve hours light/dark condition at University of Kentucky Animal Facility, and fed with standard Purina rodent laboratory chow ad libitum. The gerbils (n=12, 12 separate sets of experiments) were injected i.p. with freshly prepared D609 (50 mg/Kg body weight) 1 hr before sacrifice. The dose and the time were chosen according to previous experiments performed in our laboratory (Joshi, Sultana et al., 2005a). Control animals were injected with saline solution for the same time (n=12). The animals were euthanized with sodium pentobarbital before sacrifice.

#### **9.4.3. Synaptosomal preparation**

Synaptosomes were prepared according to the procedure described by Keller et al. (Keller, Lauderback et al., 2000). The brain was isolated immediately after decapitation and placed in a 0.32M sucrose isolation buffer containing 4 µg/mL leupeptin, 4 µg/mL pepstatin, 5 µg/mL aprotinin, 20 µg/mL trypsin inhibitor, 0.2 mM PMSF, 2 mM EDTA, 2mM EGTA, 20 mM HEPES pH 7.4. Samples were homogenized with a Wheaton tissue homogenizer and centrifuged at 1,500 x g for 10 minutes. The supernatant was collected and centrifuged at 20,000 x g for 10 min. The pellet was resuspended in 1mL of 0.32 sucrose isolation buffer and layered onto discontinuous sucrose density gradients of 10 mL each of 0.85M, pH 8.0; 1.0M, pH 8.0; 1.18M, pH 8.5 sucrose solution each containing 10mM Hepes, 2mM EDTA and 2mM EGTA. The gradients were spun in a Beckman L7-55 ultracentrifuge at 82,550 x g for 1 hr at 4 C. The synaptosomal layer was collected at the 1/1.18M sucrose interface, washed twice with PBS for 10 min at 32000g, yielding synaptosomes. Protein concentrations of the purified synaptosomes were determined by the BCA assay (Pierce, Rockford, IL). Synaptosomal preparations (1mg/mL) were incubated with 10 µM Aβ(1-42) for 6 hr at 37°C.

#### **9.4.4. Reactive oxygen species (ROS) measurements**

ROS levels were measured by dichlorofluorescein (DCF) assay. After incubation with Aβ(1-42), synaptosomes (1mg/mL) were washed with PBS and incubated with 10 µM of non-fluorescent dichlorofluorescein diacetate (DCFH-DA) for 30 min. Cytosolic esterases cleaved DCFH-DA, forming the anion DCFH that is trapped within the synaptosomes. The reaction of intracellular ROS with DCFH yields the fluorescent dye DCF. Synaptosomes were spun at 3,000 x g in a tabletop Eppendorf centrifuge for 5 min

at 4°C. Synaptosomes were resuspended in 500 µL of PBS and run in triplicate (100 µL per well) in a black microtiter plate. The measurements were performed on a Molecular Devices SpectraMax microtiter plate reader with  $\lambda_{\text{ex}} = 495 \text{ nm}$  and  $\lambda_{\text{em}} = 530 \text{ nm}$ . Data are given as percentage of corresponding controls and are the mean of at least six independent experiments.

#### **9.4.5. Protein carbonyl measurement**

Protein carbonyls are an index of protein oxidation and were determined as described previously (Berlett and Stadtman, 1997). Briefly, 5 µL of synaptosome preparations (4 mg/mL) were incubated at room temperature with 10 mM 2,4-dinitrophenylhydrazine in the presence of 5 µL of 12% SDS for 20 min at room temperature. The samples were neutralized with 7.5 µL of the neutralization solution (2 M Tris in 30% glycerol). 250 ng of protein sample was loaded into the wells of the slot blot apparatus. Proteins were transferred directly to nitrocellulose paper under vacuum pressure and standard immunochemical techniques were performed. Membranes were blocked in the presence of 3% bovine serum albumin (BSA) in TBS-T (10 mM Tris-HCl, pH 7.5, 150 mM NaCl, 0.05% Tween 20) for 1 h, followed by incubation with rabbit polyclonal antibody anti-DNP (1:100) for 1 h. The membrane were washed three times with TBS-T and incubated with alkaline-phosphatase (AP)-conjugated secondary antibody for 1 h. The specificity of primary antibodies has been previously demonstrated by experiments performed in our laboratory (Aksenov, Aksenova et al., 2001). Samples were developed using SigmaFast Tablets (BCIP/NBT) substrate), and blots were scanned into Adobe Photoshop (Adobe System, Inc., Mountain View, CA) and quantitated with Scion Image (PC version of Macintosh compatible NIH Image).

#### **9.4.6. 3NT**

Nitrotyrosine contents were determined by incubating 5  $\mu$ L of synaptosomes preparations with Laemmli buffer (0.125 M Trizma base, pH 6.8, 4% SDS, 20% glycerol) for 20 min. 250 ng of protein were blotted onto nitrocellulose membranes and immunochemical methods were performed. The rabbit anti-3-NT primary antibody was incubated 1:200 in blocking buffer (BSA 3% in TBS-T) for 2 h. The membranes were washed three times with TBS-T and incubated with alkaline phosphatase-conjugated goat anti-rabbit secondary antibody (1: 10,000). Densitometric analysis of bands in images of the blots was used to calculate levels of 3-NT.

#### **9.4.7. HNE**

Protein-bound HNE levels were measured as markers of lipid peroxidation. The samples (5  $\mu$ L) were incubated with 10  $\mu$ L Laemmli buffer for 20 min at room temperature. 250 ng of protein samples were loaded in each well on nitrocellulose membrane in a slot blot apparatus under vacuum. The membranes were incubated with anti-HNE rabbit polyclonal antibody (1: 5000) for 2 h, washed three times with TBS-T and then incubated with an anti-rabbit IgG alkaline phosphatase-conjugated secondary antibody (1:10,000). Controls in which the primary antibody was reacted with free HNE resulted in faint and non-specific binding of the antibody (data not shown). In addition, the specificity of primary and secondary antibodies was demonstrated by experiments previously performed in our laboratory (Sultana, Newman et al., 2004; Perluigi, Fai Poon et al., 2005). Samples were developed using SigmaFast Tablets (BCIP/NBT substrate), and blots were scanned into Adobe Photoshop (Adobe System, Inc., Mountain View, CA) and quantitated with Scion Image (PC version of Macintosh compatible NIH Image).



#### **9.4.8. GSH assay**

GSH levels were measured by a GSH Assay Kit (Cayman Chemical Company, Ann Harbor, MI). Briefly, the cytosolic fraction isolated from brain homogenates was precipitated with 10% (w/v) metaphosphoric acid and then centrifuged for 5 min at 5,000 X g. The supernatants were neutralized with 4M triethanolamine and then analyzed according to manufacturer instructions. GSH concentration in the samples was calculated using the kinetic method by measuring the absorbance at 405 nm with a Bio-Tek Powerwave X Microtiter Plate Reader (Bio, Inc.). A plot of the corrected absorbance vs the concentration of GSH standards ( $\mu\text{M}$ ) was utilized to calculate the average concentration of GSH present in the samples.

#### **9.4.9. iNOS expression levels**

Synaptosome samples (50  $\mu\text{g}$ ) were mixed with sample loading buffer, denatured for 5 min at 100 °C and then loaded on 10% SDS-polyacrylamide gels. Proteins were transferred to nitrocellulose membrane in 25 mM Tris, 192 mM glycine containing 20% (v/v) at 80 mA/gel for 2 h. For iNOS detection, membranes were probed first with 10 ml of blocking buffer (3% BSA in TBS-T) containing rabbit anti-iNOS polyclonal antibody (Santa Cruz Biotechnology Inc., CA 1:1000) for 2 h at 27 °C, followed by 10 ml of blocking buffer containing alkaline phosphatase (AP)-conjugated goat anti-rabbit IgG from Sigma Chemical Co. (St. Louis, MO, 1:5000) for 1 h at 27 °C. Membranes were washed three times with T-TBS (0.5% tween in TBS) and the bands were visualized using SigmaFast Tablets (BCIP/NBT) substrate). iNOS protein levels were normalized relative to the  $\beta$ -actin level in each sample.

## 9.5. Statistical analysis

ANOVA was used for statistical evaluation of data followed by Student's *t*-test. P values < 0.05 were considered significant for comparison between control and experimental data.

## 9.6. Results

### 9.6.1. D609 prevents *in vivo* ROS accumulation

The DCFH-DA method was used to monitor the ROS levels generated by A $\beta$ (1-42) in our experimental model. Figure 9.1 shows the levels of ROS in synaptosomes isolated from saline/D609 injected gerbils (CTR), in synaptosomes isolated from saline injected gerbils and treated *in vitro* with A $\beta$ (1-42) and in synaptosomes isolated from D609 injected gerbils and treated *in vitro* with A $\beta$ (1-42). In the absence of 10  $\mu$ M A $\beta$ (1-42), levels of ROS in synaptosomes from saline injected gerbils did not show any significant difference compared with the levels measured in synaptosomes from D609 injected gerbils. Hence, both these groups can be referred as CTR. Thus, D609 itself does not reduce basal oxidation levels. Synaptosomes isolated from saline injected gerbils and treated with 10  $\mu$ M A $\beta$ (1-42) for 6 hrs displayed an increased fluorescence, about 20% compared to control synaptosomes (untreated) ( $p < 0.005$ ). Synaptosomes isolated from D609 injected gerbils were not affected by A $\beta$ (1-42)-induced ROS accumulation ( $p < 0.002$ ). Thus, D609 is able to prevent ROS accumulation in synaptosomes.

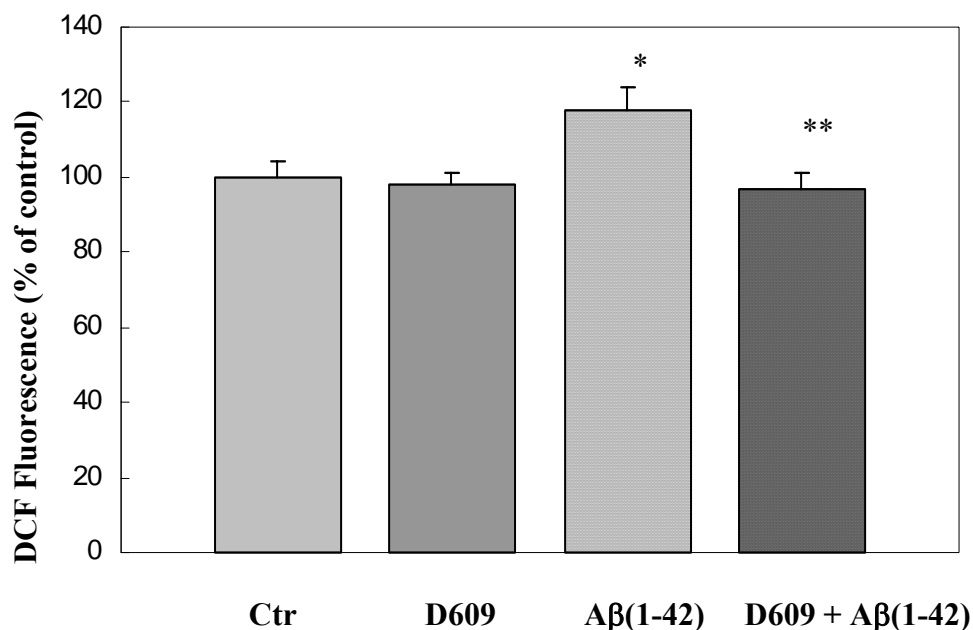


**Figure 9.1:** D609 prevents A $\beta$ (1-42)-induced ROS production. ROS levels were determined by the DCF fluorescence assay. Ctrl = synaptosomes isolated from saline injected gerbils with no further treatment (n=6, six separate sets of experiments); D609 = synaptosomes isolated from D609 injected gerbils with no further treatment (n=6); A $\beta$ (1-42) = synaptosomes isolated from saline injected gerbils and treated with 10  $\mu$ M A $\beta$ (1-42) for 6 hrs (n=6); A $\beta$ (1-42) + D609 = synaptosomes isolated from D609 injected gerbils and treated with 10  $\mu$ M A $\beta$ (1-42) for 6hrs (n=6). The data are the mean  $\pm$  S.E.M of six independent experiments, expressed as percentage of control values. Statistical comparison was made using ANOVA test (n=6 for each group). (\*)  $p < 0.005$ , A $\beta$ (1-42) vs Control; (\*\*)  $p < 0.002$ , A $\beta$ (1-42) vs A $\beta$ (1-42) + D609.

### **9.6.2. D609 in vivo protects against A $\beta$ (1-42)-induced protein oxidation and lipid peroxidation**

Protein carbonyls and 3-NT levels were measured as markers of protein oxidation (Stadtman and Berlett, 1997). Collectively, ROS can lead to the oxidation of amino acid residue side chains, formation of protein-protein cross-linkages and oxidation of the protein backbones resulting in protein fragmentation. The presence of carbonyl groups in proteins has therefore been used as a marker of ROS-mediated protein oxidation. Fig. 9.2a shows the carbonyl levels in synaptosomes isolated from saline injected gerbils and from D609 injected gerbils, and then treated in vitro with A $\beta$ (1-42). The level of carbonyls was found to be significantly higher ( $p < 0.001$ ) in synaptosomes obtained from saline injected gerbils and treated with A $\beta$ (1-42). D609 treatment protects synaptosomes against A $\beta$ (1-42)-induced oxidative protein damage ( $p < 0.004$ ).

In order to demonstrate the specificity of D609, two other A $\beta$  peptides, A $\beta$ (1-40) and control reverse of A $\beta$  peptide (A $\beta$  (42-1)) were used. Figure 9.2b shows the carbonyl levels in Various A $\beta$  peptide treated synaptosomes and in synaptosomes isolated from D609 injected gerbils subsequently treated with A $\beta$ (1-42), A $\beta$ (1-40) and A $\beta$ (42-1) respectively. As shown in figure, D609 treatment protects synaptosomes against A $\beta$ (1-42) and A $\beta$ (1-40)-induced oxidative protein damage ( $p < 0.05$ ). There was no significant increase in protein carbonyl levels in synaptosomes isolated from saline injected and D609 injected gerbils subsequently treated with A $\beta$ (42-1).

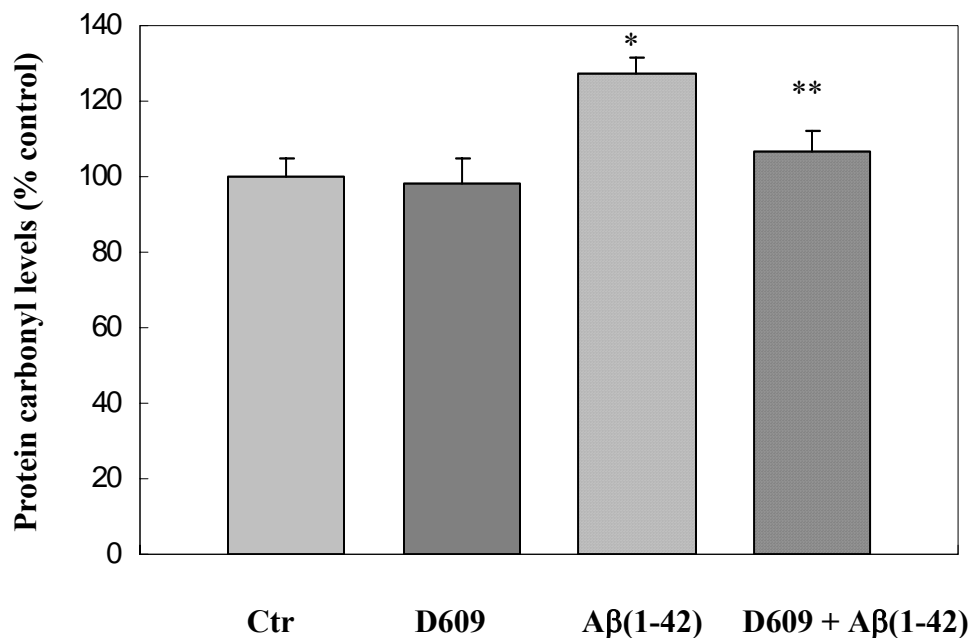


**Figure 9.2a:** Protective effects of D609 on Aβ-induced protein oxidation. Synaptosomes isolated from saline injected gerbils and treated with 10μM Aβ(1-42) demonstrate a higher level of protein carbonyls than that of untreated controls (Ctrl and D609). (\*)  $p < 0.001$ , Aβ(1-42) vs Control. Synaptosomes isolated from D609 injected gerbils were completely protected from Aβ-induced oxidative modifications [Aβ(1-42) + D609]. (\*\*)  $p < 0.004$ , Aβ(1-42) vs Aβ(1-42) + D609. (Data collected in collaboration with Dr. Marzia Perluigi)

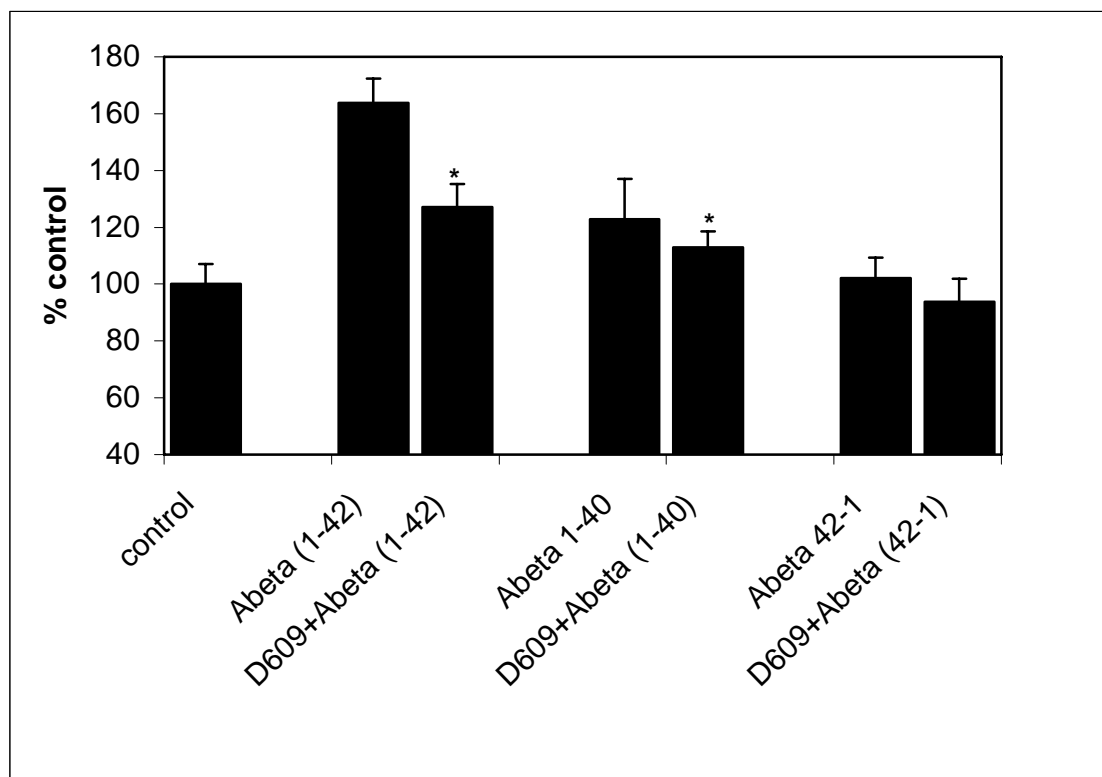


**Figure 9.2b:** Protective effects of D609 on A $\beta$ -induced protein oxidation. Synaptosomes isolated from saline injected gerbils and treated with 10 $\mu$ M A $\beta$ (1-42) and 10 $\mu$ M A $\beta$ (1-40) demonstrate a higher level of protein carbonyls than that of untreated controls, whereas 10 $\mu$ M A $\beta$ (42-1) did not show any significant increase in protein carbonyls. Synaptosomes isolated from D609 injected gerbils were completely protected from A $\beta$ (1-42) and A $\beta$  (1-40) induced oxidative modifications. (\*)  $p < 0.05$ ,  $n = 5$ .

The antioxidant properties of D609 were further confirmed by measuring 3NT levels, formed by reaction of reactive nitrogen species (RNS) with proteins (Castegna, Thongboonkerd et al., 2003). Figure 9.3 shows the protective effects of D609 on A $\beta$ (1-42)-induced formation of 3NT. Synaptosomes isolated from saline injected gerbils

showed increased levels of 3NT ( $p < 0.005$ ) when treated in vitro with A $\beta$ (1-42), while synaptosomes isolated from D609 injected gerbils were completely protected ( $p < 0.05$ ).

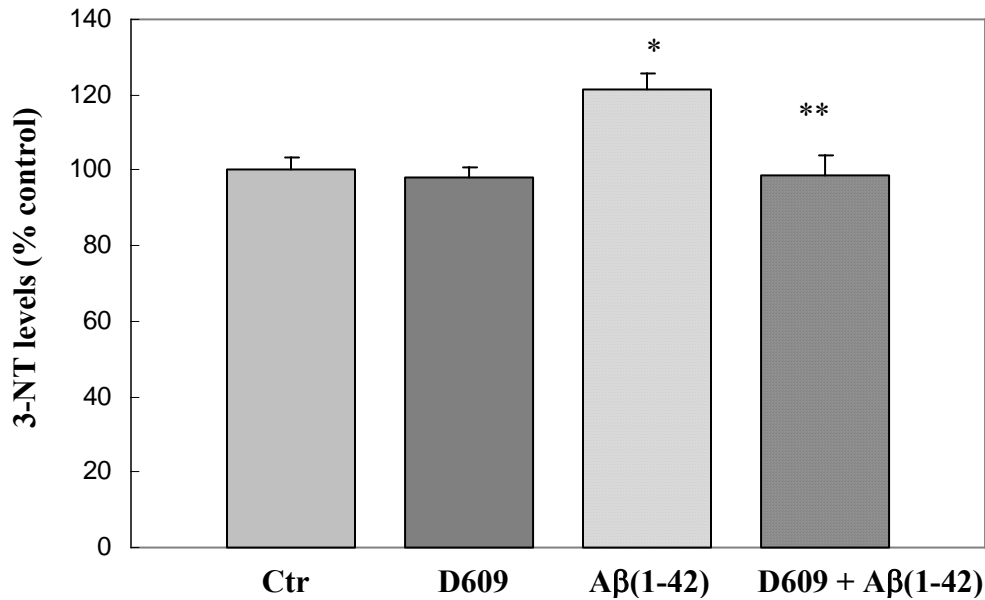


**Figure 9.3:** Protective effect of D609 on A $\beta$ -induced 3-NT formation. 3-NT levels were determined as described in the “Material and Methods” section. Ctr = synaptosomes isolated from saline or D609 injected gerbils with no further treatment; D609 = synaptosomes isolated from D609 injected gerbils with no further treatment; A $\beta$ (1-42) = synaptosomes isolated from saline injected gerbils and treated with 10  $\mu$ M A $\beta$ (1-42) for 6 hrs; A $\beta$ (1-42) + D609 = synaptosomes isolated from D609 injected gerbils and treated with 10  $\mu$ M A $\beta$ (1-42) for 6 hrs. The data are the mean  $\pm$  S.E.M expressed as percentage of control values (n=6). (\*)  $p < 0.005$ , A $\beta$ (1-42) vs Control; (\*\*)  $p < 0.05$ , A $\beta$ (1-42) vs A $\beta$  (1-42) + D609. (Data collected in collaboration with Dr. Marzia Perluigi)

Free radical attack on phospholipids PUFA leads to the formation of reactive aldehydes, among which one of the most neurotoxic is HNE (Esterbauer, Schaur et al., 1991). This alkenal reacts with proteins forming stable covalent adducts to histidine, lysine and cysteine residues via Michael addition. The extent of this reaction can be measured immunochemically by quantifying the levels of HNE-bound proteins. Figure 9.4 shows the HNE-bound protein levels in synaptosomes isolated from gerbils previously injected with D609 or with saline solution and incubated *in vitro* with 10  $\mu$ M A $\beta$ (1-42) for 6 hrs. Consistent with the protein oxidation results showed above, we observed *in vivo* protection by D609 against 10  $\mu$ M A $\beta$ -induced lipid peroxidation. HNE levels were found to be higher in A $\beta$ (1-42)-treated synaptosomes isolated from saline injected gerbils, while A $\beta$ (1-42)-treated synaptosomes isolated from D609 injected gerbils showed reduced levels of HNE-bound proteins. These results are consistent with recent *in vitro* data obtained on primary neuronal cultures (Sultana, Newman et al., 2004), indicating that D609 acts as a potent antioxidant thus preventing protein oxidation and lipid peroxidation.



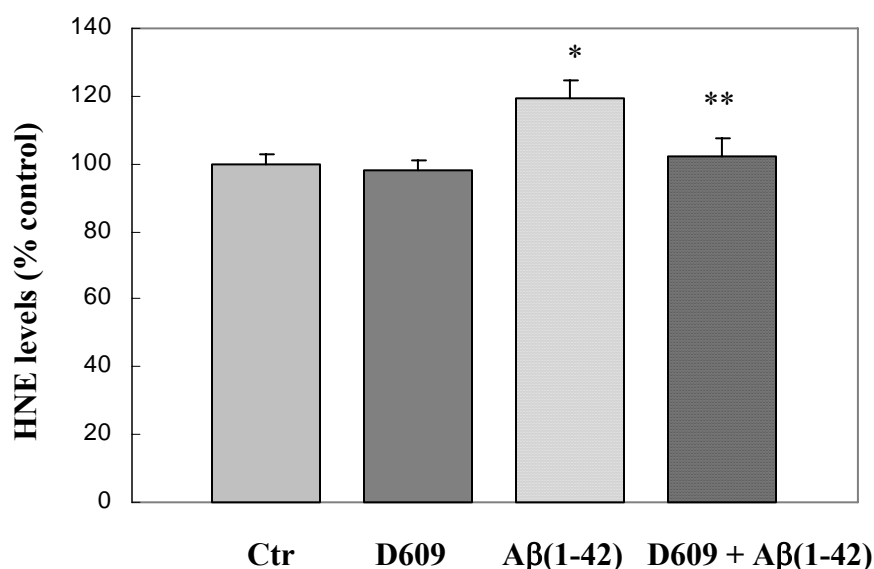


**Figure 9.4:** Protective effect of D609 on Aβ-induced lipid peroxidation (HNE levels). HNE levels were determined as described in the “Material and Methods” section. Ctr = synaptosomes isolated from saline/D609 injected gerbils; D609 = synaptosomes isolated from D609 injected gerbils with no further treatment; Aβ(1-42) = synaptosomes isolated from saline injected gerbils and treated with 10 μM Aβ(1-42) for 6 hrs; Aβ(1-42) + D609 = synaptosomes isolated from D609 injected gerbils and treated with 10 μM Aβ(1-42) for 6 hrs. The data are the mean ± SEM expressed as percentage of control values (n=6). (\*) p < 0.005, Aβ(1-42) vs Control; (\*\*) p < 0.05, Aβ(1-42) vs Aβ (1-42) + D609. (Data collected in collaboration with Dr. Marzia Perluigi)

### **9.6.3. D609 modulates A $\beta$ (1-42)-induced iNOS expression levels**

As shown in Fig. 9.5, iNOS levels were significantly increased (40%) in synaptosomes isolated from DMSO-injected gerbils treated with A $\beta$ (1-42) when compared with controls ( $p < 0.01$ ). In contrast, we observed a decrease in expression of iNOS in synaptosomes isolated from D609-injected gerbils ( $p < 0.05$ ) and subsequently treated with A $\beta$ (1-42), a result that is consistent with our findings of decreased levels of 3-NT. Several lines of evidence show that iNOS expression is induced by oxidative stress and that antioxidant compounds suppress its expression either at gene level or at protein level (Ayasolla, Khan et al., 2004; Calabrese, Stella et al., 2004). In the present study, we observed that both iNOS and 3NT levels were increased in A $\beta$ (1-42)-treated synaptosomes and that D609 treatment showed protection against the A $\beta$ (1-42)-induced increase of iNOS and 3-NT levels.

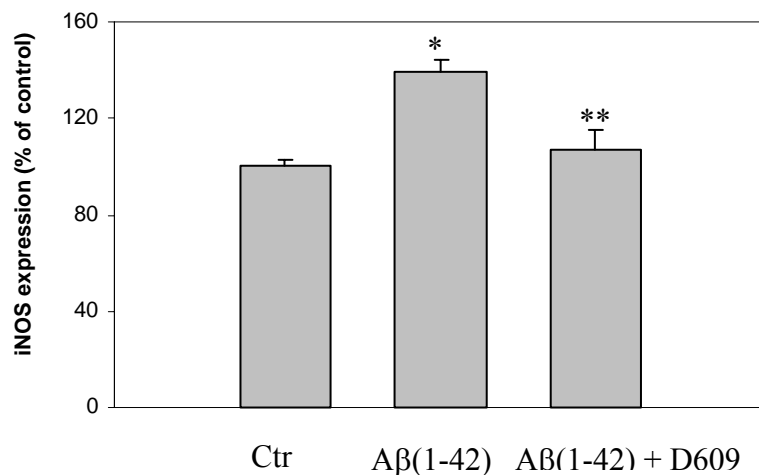


**Figure 9.5:** Western blot analysis of synaptosomes for iNOS protein expression levels. Samples containing 50 µg of protein were loaded onto 10% SDS-PAGE gels, and the blots were probed with the polyclonal anti-iNOS antibody (1:1000) for 2 h. Immunoblots were scanned by densitometry and all values were normalized to β-actin. A representative immunoblot (A) and densitometric values (B) are shown. Densitometric values represent the mean ± S.E.M. obtained from three independent experiments. Significant differences were assessed by ANOVA. \*  $p < 0.01$ , control vs Aβ(1-42); \*\*  $p < 0.05$ , Aβ(1-42) + D609. (Data collected in collaboration with Dr. Marzia Perluigi)

## 9.7. Discussion

Oxidative damage is present in the brains of patients with AD, and is observed within every class of biomolecules, including nucleic acids, proteins, lipids and carbohydrates (Butterfield, Drake et al., 2001; Butterfield and Lauderback, 2002; Castegna, Thongboonkerd et al., 2003). Our laboratory has suggested a comprehensive model for neurodegeneration in AD combining two established notions: i) elevated oxidative stress in AD brain; ii) centrality of A $\beta$  in the cause and consequences of this dementing disorder (Butterfield and Lauderback, 2002; Castegna, Thongboonkerd et al., 2003). Many additional studies from different labs have supported the view that oxidative stress may be central to the A $\beta$ -driven neurodegeneration. Based on these notions, treatment with brain accessible antioxidants may be a promising approach for slowing disease progression to the extent that oxidative damage may be responsible for the cognitive and functional decline observed in AD.

Previous studies from our laboratory and others have shown that A $\beta$ (1-42) is associated with free radical generation leading to oxidative damage of proteins, lipids, DNA and RNA (Varadarajan, Yatin et al., 2000; Butterfield, Drake et al., 2001; Butterfield and Lauderback, 2002). The oxidation of proteins by free radicals or free radical oxidation products may be responsible for damaging enzymes critical in neuronal function (Varadarajan, Yatin et al., 2000; Butterfield, Boyd-Kimball et al., 2003).

In the present study, we showed the ability of *in vivo*-injected D609 to provide neuroprotection against oxidative stress induced by A $\beta$ (1-42) on subsequently isolated synaptosomes. A variety of well established and new potential antioxidant compounds are under investigation to prevent A $\beta$ -induced toxic effects (Behl, 2002; Grundman and

Delaney, 2002). Among different classes of antioxidant drugs, much interest has been devoted to “thiol-delivering” compounds. Because decreased levels of GSH are associated with aging and neurodegeneration (Liu and Choi, 2000; Butterfield, Castegna et al., 2002a), therapeutic strategies based on elevation of GSH levels have been shown to be protective against oxidative stress conditions of the brain (Butterfield, Castegna et al., 2002a). The age-related decrease of GSH may represent a key factor in the aging process and may underlie a number of changes occurring in normal aging and the onset of various diseases.

We have previously shown that the antioxidant properties of D609 are associated with the free thiol group of the xanthate (Lauderback, Drake et al., 2003). For example, methylated D609 is unable to protect cultured neurons from damage by A $\beta$ (1-42) (Sultana et al., 2004). D609 in its reduced form is oxidized to the corresponding disulfide (dixanthate) that is converted back to the xanthate by GSH reductase (Lauderback et al., 2003). D609 has been reported to protect against glutamate toxicity and ionizing radiation-induced oxidative stress in lymphocytes by maintaining intracellular GSH homeostasis (Zhou, Lauderback et al., 2001). The results presented in this paper demonstrated that *in vivo* injection of D609 was effective in reducing protein oxidation, lipid peroxidation and ROS production induced by A $\beta$ (1-42) treatment.

The concept that A $\beta$  induces lipid peroxidation is a key component of the A $\beta$ (1-42)-associated free radical model for neurodegeneration in AD (Butterfield, 1997; Varadarajan, Yatin et al., 2000; Lauderback, Hackett et al., 2001). HNE alters the conformation of transmembrane and cytoskeletal synaptosomal proteins (Esterbauer, Schaur et al., 1991; Subramaniam, Roediger et al., 1997). GSH blocks the damaging

effects of this unsaturated aldehyde on synaptosomal proteins (Pocernich, La Fontaine et al., 2000; Pocernich, Cardin et al., 2001). As noted above, D609 binds to  $\alpha,\beta$ -unsaturated aldehydes to prevent their toxicity (Lauderback, Drake et al., 2003). Taken together, these data support the notion that the ability of D609 to exert its protective effects against A $\beta$ -associated lipid peroxidation involves its direct binding to HNE thus providing an efficient tool for detoxication. Consistent with the A $\beta$ -associated free radical process, A $\beta$ (1-42) induces protein oxidation, indexed by the increase of carbonyl levels and of nitrotyrosine residues. Oxidative modification of crucial proteins results in alteration of their structural and functional properties, eventually leading to synapse loss and neurodegeneration.

There is compelling evidence supporting that enhanced pro-inflammatory activities induced by A $\beta$  are associated with the pathogenesis and/or progression of AD, and that some anti-inflammatory agents protect neurons against A $\beta$ -induced neurotoxicity (Breitner, 1996). One of the principal enzymes that play a pivotal role in mediating an inflammatory response is inducible nitric oxide synthase (iNOS). iNOS is mainly localized in astrocytes and microglia, and catalyzes the oxidative deamination of L-arginine to produce nitric oxide (NO), a potent pro-inflammatory mediator. In Alzheimer's tissue, pro-inflammatory iNOS is notably up-regulated and colocalized in A $\beta$  plaques. Several studies have demonstrated that A $\beta$  stimulates microglial and astrocytic iNOS induction and subsequent NO production (Akama and Van Eldik, 2000). We observed an increase in 3NT levels in synaptosomes isolated from DMSO-injected gerbils and treated with A $\beta$ (1-42) that coincides with a parallel increase in iNOS levels. Pre-treatment with D609 reduced significantly the levels of iNOS and of nitrated

proteins. iNOS induction may reflect the degree of inflammation associated to A $\beta$ (1-42), and the ability of D609 to block this effect may represent a further additional protective mechanism in addition to the antioxidant potential of this xanthate.

The levels of oxidized glutathione are consistently elevated in Alzheimer's patients as compared to their age-matched controls and correlate with cognitive dysfunction (Vina, Lloret et al., 2004). Recent findings suggested that A $\beta$  could initiate a cascade of events resulting in a severe depletion of glutathione (Abramov, Canevari et al., 2003). Alteration of glutathione homeostasis impairs neuronal viability because GSH depletion leaves the neurons vulnerable to damage by oxidative stress. Here, we demonstrated that D609 is able to provide neuroprotection against A $\beta$ -induced neurotoxicity acting as a glutathione-mimetic compound, thus modulating the effects of GSH depletion. Previous studies from our laboratory have shown that i.p. administration of N-acetylcysteine and of gamma-glutamyl-cysteine ethyl ester (GCEE) protected synaptosomes against oxidative stress (Pocernich, Cardin et al., 2001; Butterfield, Castegna et al., 2002a; Boyd-Kimball, Sultana et al., 2005a). These compounds led to an increase of brain glutathione by serving as precursor for GSH biosynthesis. Because glutathione itself penetrates the blood-brain barrier only poorly and cannot be taken up by neurons directly, other treatment options to increase brain concentration of glutathione including glutathione analogs, mimetic or precursors have been used in patients or animal models. Based on the results presented in the current paper and on our previous studies (Sultana, Newman et al., 2004), we hypothesized that D609 is a potential brain-accessible GSH-mimetic compound. This hypothesis that D609 is a GSH mimetic that is itself not

GSH is further supported by the finding that D609 treatment does not lead to an increase of brain GSH levels (Table 9.1).

Injection	GSH (mM) $\pm$ S.E.M
Control	4.27 $\pm$ 0.87
D609	3.98 $\pm$ 0.54

**Table 9.1:** D609 does not influence total brain GSH levels. Results presented are the mean  $\pm$  S.E.M, n=6. Total GSH levels, following i.p D609 injection, were measured by a GSH assay kit as described in the Chapter 3.

The ability of *in vivo* D609 to prevent A $\beta$ -induced oxidative stress could also be related to its property as an inhibitor of PC-PLC and sphingomyelinase. Most of D609 biological activities (antitumor, antiviral, anti-inflammatory) have been largely attributed to the inhibition of PC-PLC and sphingomyelinase. However, the identification of D609 as a potent antioxidant implies that D609 may exert some of the reported activities by its antioxidant properties. The biological activity of PC-PLC and sphingomyelinase involves regulation of Ca<sup>+2</sup> homeostasis through the production of ceramide. Since A $\beta$  may lead to altered Ca<sup>+2</sup> homeostasis in neurons (Mattson, Barger et al., 1993), it is reasonable to argue that the protective effects of D609 could rely also on its inhibitory activity on PC-PLC or sphingomyelinase. Thus, we suggest that multiple biological functions of D609 could potentially contribute to counteract A $\beta$ -driven neurotoxicity in the brain. The presence of the free thiol group in the molecule confers to the xanthate a strong reducing



property (Rao, 1971; Lauderback, Drake et al., 2003; Sultana, Newman et al., 2004) that is undoubtedly responsible for the antioxidant activity of D609.

Considering that A $\beta$ (1-42) is a potent inducer of oxidative stress and that the deposition of this peptide can induce the cascade of pathological changes occurring in AD, many attempts to test effective protection by antioxidants are currently under investigation. However, many clinical trials are unsuccessful due to a low brain-accessible capability of the antioxidant compounds tested. Based on these notions, searches for new potential antioxidant compounds could be of relevance for future directions of AD treatments.

In conclusion, the present study demonstrated the ability of D609 to act as a potent antioxidant *in vivo*, thereby providing neuroprotection against A $\beta$ -induced oxidative stress. Further studies are required to gain insight into the potential use of D609 in the treatment of AD and other oxidative stress-related disorders. Investigations of the use of D609 on animal models of AD are in progress.

**Note:** A part of this study was carried out by Dr. Marzia Perluigi in Prof. Butterfield's laboratory that has been supported by a post-doc grant of the University of Rome "La Sapienza".

## Chapter 10

### ***In vivo* administration of D609 leads to protection of subsequently isolated gerbil brain mitochondria subjected to *in vitro* oxidative stress inducers: Relevance to Alzheimer's disease and other oxidative stress related neurodegenerative disorders**

#### **10.1. Overview of the study**

Tricyclodecan-9-yl-xanthogenate (D609) has *in vivo* and *in vitro* antioxidant properties. D609 mimics glutathione (GSH), has a free thiol group, which upon oxidation forms a disulfide. The resulting dioxanthate is a substrate for glutathione reductase, regenerating D609. Recent studies have also shown that D609 protects brain *in vivo* and neuronal cultures *in vitro* against the potential Alzheimer's disease (AD) causative factor, A $\beta$  (1-42)-induced oxidative stress and cytotoxicity. Mitochondria are important organelles with both pro- and anti-apoptotic factor proteins. The present study was undertaken to test the hypothesis that i.p. injection of D609 would provide neuroprotection against free radical-induced, mitochondria-mediated apoptosis, *in vitro*. Brain mitochondria were isolated from gerbils 1 h post injection intraperitoneally (i.p.) with D609 and subsequently treated *in vitro* with the oxidants Fe<sup>2+</sup>/H<sub>2</sub>O<sub>2</sub> (hydroxyl free radicals), 2,2-azobis-(2-amidinopropane) dihydrochloride (AAPH, alkoxyl and peroxy free radicals) and AD-relevant amyloid  $\beta$ -peptide 1-42 [A $\beta$  (1-42)]. Brain mitochondria isolated from the gerbils previously injected i.p. with D609 and subjected to these oxidative stress inducers, *in vitro*, showed significant reduction in levels of protein carbonyls, protein-bound hydroxynonenal (HNE) [a lipid peroxidation product], 3-nitrotyrosine (3-NT), and cytochrome-c release compared to oxidant-treated brain mitochondria isolated from saline-injected gerbils. D609 treatment significantly

maintains the GSH/GSSG ratio in oxidant-treated mitochondria. Increased activity of glutathione-S-transferase (GST), glutathione peroxidase (GPx) and glutathione reductase (GR) in brain isolated from D609-injected gerbils is consistent with the notion that D609 acts like GSH. These anti-apoptotic findings are discussed with reference to the potential use of this brain-accessible glutathione mimetic in the treatment of oxidative stress-related neurodegenerative disorders, including AD.

## **10.2. Introduction**

Oxidative stress has been implicated in many neurodegenerative disorders, including Alzheimer's disease (AD) (Hensley, Hall et al., 1995; Markesbery and Lovell, 1998; Butterfield, Drake et al., 2001; Butterfield and Lauderback, 2002), AD is characterized clinically by progressive dementia and pathologically by extracellular amyloid protein deposits, intracellular neurofibrillary tangles (NFTs) (composed mostly of hyperphosphorylated tau protein), loss of synapses, mitochondrial dysfunction and programmed cell death (PCD) (Katzman and Saitoh, 1991; Bosetti, Brizzi et al., 2002). The reduced energy metabolism in AD may be due to oxidative dysfunction of some of the key metabolic or mitochondrial enzymes (Castegna, Aksenov et al., 2002a; Castegna, Thongboonkerd et al., 2003; Butterfield, 2004; Castegna, Thongboonkerd et al., 2004; Sultana, Boyd-Kimball et al., 2006b; Sultana, Poon et al., 2006b), which may lead to increased reactive oxygen species (ROS) production.

It is well known that mitochondria are the major cellular site of energy production, and these organelles also play a key role in the ROS generation, resulting in oxidative damage to neurons. Amyloid deposition, oxidative stress, mitochondria DNA deletion and mitochondrial structural and functional abnormalities are prominent in AD

(Bosetti, Brizzi et al., 2002; Huang, Zhang et al., 2004; Aliyev, Chen et al., 2005). Many pro-apoptotic signals and anti-apoptotic defenses converge in the mitochondria (Antonsson, 2004). Protein factors (cytochrome-C, Apaf1, AIF and SMAC/DIBLO) and  $\text{Ca}^{2+}$  released from mitochondria during oxidative stress activate caspase dependent and/or caspase independent mechanisms that lead to apoptotic cell death (Antonsson, 2004). The role of mitochondria is not only as ATP producers but also as regulators of intracellular  $\text{Ca}^{2+}$  homeostasis and endogenous producers of ROS. Increased mitochondrial  $\text{Ca}^{2+}$  overload has been associated with the generation of superoxide and the release of pro-apoptotic mitochondrial proteins leading to cell death (Zamzami, Marchetti et al., 1995; Sheehan, Swerdlow et al., 1997). The alterations in  $\text{Ca}^{2+}$  homeostasis and ROS generation lead to increased susceptibility to cell death under circumstances that are otherwise not ordinarily toxic (Sheehan, Swerdlow et al., 1997).

In AD brain ROS lead to protein oxidation (Hensley, Hall et al., 1995; Castegna, Aksenov et al., 2002a; Castegna, Thongboonkerd et al., 2003; Butterfield, 2004; Castegna, Thongboonkerd et al., 2004; Sultana, Boyd-Kimball et al., 2006b; Sultana, Poon et al., 2006b), lipid peroxidation (Markesbery and Lovell, 1998; Butterfield and Lauderback, 2002), DNA and RNA oxidation (Mecocci, MacGarvey et al., 1993; Lovell, Gabbita et al., 1999; Nunomura, Perry et al., 1999), and neuronal dysfunction or death. Recent studies indicate that protein oxidation and lipid peroxidation in brain from mild cognitive impairment subjects (Butterfield, Poon et al., 2006; Butterfield, Reed et al., 2006), suggesting oxidative stress is an early event in the pathogenesis of AD. ROS generation from mitochondria and its impact on neuronal systems hence becomes

important in understanding oxidative stress and oxidative stress-related disorders, including AD.

Mitochondrial electron transport is a potential source of ROS production (Ide, Tsutsui et al., 1999). It is now well known that ROS such as superoxide anion ( $O_2^-$ ), hydroxyl radical (OH), hydrogen peroxide ( $H_2O_2$ ), and peroxynitrite ( $ONOO^-$ ) contribute to neurodegeneration (Zhang, Dawson et al., 1994; Rego and Oliveira, 2003; Ansari, Ahmad et al., 2004; Butterfield, Reed et al., 2006; Tangpong, Cole et al., 2006a). Mitochondrial membrane potential depolarization induces cytochrome-c release into the cytoplasm and elevates the activity of caspase-3, suggesting a role for mtDNA-derived mitochondrial dysfunction in AD degeneration (Bosetti, Brizzi et al., 2002).

Glutathione is widely recognized as an endogenous nonenzymatic antioxidant, an oxyradical scavenger, thereby useful in protecting against oxidative damage by free radicals and inhibiting lipid peroxidation and DNA damage (Meister, 1995; Darley-Usmar and Halliwell, 1996; Sies, 1999; Schulz, Lindenau et al., 2000; Hansen, Go et al., 2006). Glutathione has been implicated in a wide range of metabolic processes, including cell division, DNA repair, regulation of enzyme activity, activation of transcription factors, modulation of anion and cation homeostasis and protection against oxidative damage (Meister and Anderson, 1983). The nervous system is particularly susceptible to oxidative insults, and dependent on its glutathione defense.

Tricyclodecan-9-yl-xanthogenate (D609) exhibits a variety of potent biological functions, including antiviral (Amtmann, 1996) and anti-inflammatory (Amtmann and Sauer, 1987; Sauer, Amtmann et al., 1990; Tschakowsky, Schmidt et al., 1998) activities. Most of these activities have been linked to the inhibitory effect of D609 on

phosphatidylcholine-specific phospholipase C (PC-PLC) (Schutze, Potthoff et al., 1992; Amtmann, 1996). Such inhibition decreases production of the secondary messenger diacylglycerol (DAG) that activates protein kinase C (PKC) and acidic sphingomyelinase (aSMase) (Cifone, Roncaioli et al., 1995). However, with a free thiol group, D609 may also possess strong antioxidant activity (Rao, 1971) with *in vitro* and *in vivo* radical scavenging properties and inhibition of free radical-induced oxidative stress (Zhou, Lauderback et al., 2001; Lauderback, Drake et al., 2003; Sultana, Newman et al., 2004; Joshi, Sultana et al., 2005a; Perluigi, Joshi et al., 2006).

### **10.3. Purpose of the study**

The particular species of ROS that D609 can effectively scavenge is not clear, but this xanthate has ability to scavenge hydroxyl radicals (Zhou, Lauderback et al., 2001; Lauderback, Drake et al., 2003; Sultana, Newman et al., 2004; Joshi, Sultana et al., 2005a; Perluigi, Joshi et al., 2006). The reaction with other ROS is also possible since xanthates generally have high reductive potential (Rao, 1971). D609 may protect intracellular GSH, which is important intracellular defense molecule against oxidative stress in neurons and has been shown to play an important role in radiation protection (Anderson and Luo, 1998; Halliwell, 2001; Zhou, Lauderback et al., 2001). Recently, we showed that D609, a glutathione mimetic (Lauderback, Drake et al., 2003), protects primary neuronal culture against amyloid  $\beta$ -peptide (1-42) [ $A\beta$  (1-42)]-induced oxidative stress and neurotoxicity *in vitro* (Sims, 1990) and in synaptosomes *in vivo* (Perluigi, Joshi et al., 2006).

We performed the current study to test the hypothesis that the D609-mediated *in vivo* protection of brain mitochondria against subsequent *in vitro* treatment of various

oxidants, including A $\beta$  (1-42), is associated with D609-mediated modulation of GSH and GSH related enzyme activities.

## **10.4. Experimentals**

### **10.4.1. Animals**

For all studies male Mongolian gerbils (2–3 months of age), approximately 100 g in size, housed in the University of Kentucky Central Animal Facility under 12-h light/dark conditions and fed standard Purina rodent laboratory chow ad libitum, were used. The animal protocols were approved by the University of Kentucky Animal Care and Use Committee.

### **10.4.2. Chemicals**

D609 was purchased from Biomol (Plymouth Meeting, PA, USA) and all other chemicals were purchased from Sigma–Aldrich (St. Louis, MO, USA). Fresh D609 (50 mg/ kg body wt) was prepared in phosphate-buffered saline (PBS). The primary anti body for 4-hydroxy-nonenal (HNE) and 3-nitrotyrosine (3-NT) were purchased from Chemicon International.

### **10.4.3. Preparation of mitochondria**

Brain mitochondria were isolated from gerbils previously injected i.p. with saline (control) or with D609 (50 mg/ kg body wt), 60 min after injection. This time and level of D609 were chosen based on previous (Joshi, Sultana et al., 2005a) dose-response experiments. The brain mitochondria were isolated according to the procedure of Sims et al. (Sims, 1990) with minor modifications. Gerbils were decapitated and the whole brain was isolated on ice. Whole brain was homogenized in ice-cold isolation buffer (250 mM sucrose, 10 mM HEPES, and 1 mM potassium EDTA, pH 7.2, 4  $\mu$ g/ml leupeptin, 4

μg/ml pepstatin, 5 μg/ml aprotinin 20 μg/ml trypsin inhibitor) with 6 passes of a Wheaton tissue homogenizer. The homogenate was centrifuged for 3 min at 1,330× *g* at 4°C, and the resulting pellet was resuspended in isolation buffer and centrifuged at 1,330× *g* for 3 min. The supernatants from both spins were combined and spun at 21,200× *g* for 10 min at 4°C. The pellet was resuspended in 15% Percoll solution (v/v in isolation buffer) and layered onto discontinuous Percoll gradients of 23 and 40% Percoll (v/v in isolation buffer). Gradients were centrifuged at 30,700× *g* for 5 min at 4°C. At the 23-40% Percoll interface, mitochondria were isolated and resuspended in respiration buffer (250 mM sucrose, 2 mM magnesium chloride, 20 mM HEPES, and 2.5 mM phosphate buffer, pH 7.2) and centrifuged at 16,700× *g* for 10 min at 4°C. The pellet was resuspended in respiration buffer, centrifuged at 6,900× *g* for 10 min at 4°C, and the resulting pellet was washed in PBS at 6,900× *g* for 10 min at 4°C.

#### **10.4.4. Protein estimation and treatment**

The pellet was resuspended in 250 μl PBS and protein concentration determined by the Pierce BCA method (Bradford, 1976), using bovine serum albumin (BSA) as a standard. The mitochondrial samples were divided into six aliquots and incubated at 37 °C. The first sample set was incubated without treatment of any oxidant for 1 h; the second set of mitochondria was incubated with 30 μM Fe SO<sub>4</sub> and 2.0 mM H<sub>2</sub>O<sub>2</sub>, a process that induces hydroxyl radical formation (Halliwell and Gutteridge, 1999), the third and fourth set of samples were also incubated in same manner with/or without the oxidant AAPH (1 mM) for 1 h at 37 °C. The fifth sample set was incubated without treatment of any oxidant for 6 h and the sixth sample set was incubated with Aβ(1-42) for



6 h. The mitochondrial samples were washed after incubation and resuspended in PBS/Tween.

#### **10.4.5. Protein carbonyls**

Protein carbonyls are markers of protein oxidation and were assessed by following the standard protocol described previously (Joshi, Sultana et al., 2005a). Samples (5 µl) (normalized to 4 mg/ml), 5 µl of 12% sodium dodecyl sulfate (SDS), and 10 µl of 10 times diluted 2,4-dinitrophenyl hydrazine (DNPH) from 200 mM stock were incubated at room temperature for 20 min. Samples were neutralized with 7.5 µl neutralization solution (2 M Tris in 30% glycerol). The resulting solution was loaded into each well on nitrocellulose membrane under vacuum using a slot-blot apparatus. The membrane was blocked in blocking buffer (3% bovine serum albumin) in PBS/Tween for 1 h and incubated with a 1:100 dilution of anti-DNP polyclonal antibody in PBS/Tween for 1 h. The membrane was washed three times in PBS/Tween and was incubated for 1 h with an anti-rabbit IgG alkaline phosphatase secondary antibody diluted in PBS/ Tween in a 1:8000 ratio. The membrane was washed three times in PBS/ Tween for 5 min and developed in Sigma Fast tablets (BCIP/ NBT substrate). Blots were dried, scanned with Adobe PhotoShop, and quantified with Scion Image (PC version of Macintosh-compatible NIH Image). No non-specific binding of antibody to the membrane was observed.

#### **10.4.6. 3NT**

Samples (5 µl) (normalized to 4 mg/ml), 5 µl of 12% SDS, and 5 µl of modified Laemmli buffer containing 0.125 M Tris base, pH 6.8, 4% (v/v) SDS, and 20% (v/v) glycerol were incubated for 20 min at room temperature. Sample (250 ng) was loaded

into each well on a nitrocellulose membrane in a slot blot apparatus under vacuum. The membrane was blocked in blocking buffer (3% bovine serum albumin) in PBS/Tween for 1 h and incubated with a 1:2000 dilution of anti-3-N T polyclonal antibody in PBS/Tween for 1 h 30 min. The membrane was washed in PBS/Tween for 5 min three times after incubation. The membrane was incubated for 1 h, after washing, with an anti-rabbit IgG alkaline phosphatase secondary anti body diluted in PBS/Tween in a 1:8000 ratio. The membrane was washed three times in PBS/Tween for 5 min and developed in Sigma Fast tablets. Blots were dried, scanned with Adobe PhotoShop, and quantified with Scion Image as above. No non-specific binding of antibody to the membrane was observed.

#### **10.4.7. HNE**

Sample (5  $\mu$ l) (normalized to 4 mg/ml), 5  $\mu$ l of 12% SDS, and 5  $\mu$ l of modified Laemmli buffer containing 0.125 M Tris base, pH 6.8, 4% (v/v) SDS, and 20% (v/v) glycerol were incubated for 20 min at room temperature. Sample (250 ng) was loaded into each well on a nitrocellulose membrane in a slot blot apparatus under vacuum. The membrane was blocked in blocking buffer (3% bovine serum albumin) in PBS/Tween for 1 h and incubated with a 1:5000 dilution of anti-HNE polyclonal antibody in PBS/Tween for 1 h 30 min. The membrane was washed in PBS/Tween for 5 min three times after incubation. The membrane was incubated for 1 h, after washing, with an anti-rabbit IgG alkaline phosphatase secondary antibody diluted in PBS/Tween in a 1:8000 ratio. The membrane was washed three times in PBS/Tween for 5 min and developed in Sigma Fast tablets. Blots were dried, scanned with Adobe PhotoShop, and quantified with Scion

Image as above. A faint background staining due to the antibody alone was observed, but since each sample had a control, this minor effect was well controlled.

#### **10.4.8. Estimation of cytochrome-c release**

Cytochrome c release was detected by the method of Yang et al., (1997) (Yang, Liu et al., 1997) with slight modification. After incubation and spun of mitochondrial samples, supernatant was used for Western blot analysis to cytochrome c release. The membrane was blocked in blocking buffer (3% bovine serum albumin) in PBS/Tween for 1 h and incubated with a 1:2000 dilution of anti-cytochrome-c polyclonal antibody (C-5723; anti-sheep; Sigma) in PBS/Tween for 1 h 30 min. The membrane was washed in PBS/Tween for 5 min three times after incubation. The membrane was incubated for 1 h, after washing, with an anti-sheep IgG alkaline phosphatase secondary anti body diluted in PBS/Tween in a 1:8000 ratio. The membrane was washed three times in PBS/Tween for 5 min and developed in Sigma Fast tablets. Blots were dried, scanned with Adobe PhotoShop, and quantified with Scion Image as above.

#### **10.4.9. Estimation of reduced glutathione (GSH)**

Determination of GSH was performed by the method of Hissin and Hilf (Hissin and Hilf, 1976). The reaction mixture containing 0.1 M sodium phosphate buffer (pH-8.0), 5.0 mM EDTA, 10  $\mu$ l *O*-phthaldehyde (1.0 mg/ml) and 10  $\mu$ l of sample. After incubation for 15 min at room temperature, fluorescence at emission 420 nm was recorded by excitation at 350nm.

#### **10.4.11. Estimation of oxidized glutathione (GSSG)**

The estimation of GSSG was performed by the method of Hissin and Hilf (Hissin and Hilf, 1976). The samples were incubated first with 0.04 M N-ethyleimide (NEM) for

30 min to interact with GSH present in sample. The reaction mixture containing 0.1 N NaOH, 5.0 mM EDTA, 10  $\mu$ l *O*-phthaldehyde (1.0 mg/ml) and 10  $\mu$ l of sample. After incubation for 15 min at room temperature, fluorescence at emission 420 nm was recorded by excitation at 350nm.

#### **10.4.12. Enzyme activities**

##### **10.4.12.1. Estimation of glutathione-S-transferase activity**

GST (EC 2.5.1.18) activity was measured in a 96-well plate reader, with the reaction mixture consisting of 0.1 M phosphate buffer (pH 6.5), 1.0 mM reduced glutathione, 1.0 mM CDNB and 0.1  $\mu$ l of PMS in a total volume of 200  $\mu$ l (Habig, Pabst et al., 1974). The changes in absorbance were recorded at 340 nm, and the enzymatic activity was calculated as nmol CDNB conjugate formed  $\text{min}^{-1} \text{mg}^{-1}$  protein.

##### **10.4.12.2. Estimation of glutathione peroxidase activity**

GPx (EC 1.11.1.9) activity was measured in a 96-well plate reader at 37 °C by a coupled assay system (Wheeler, Salzman et al., 1990). The reaction mixture consisted of 0.2 mM  $\text{H}_2\text{O}_2$ , 1.0 mM GSH, 0.14 U of GR, 1.5 mM NADPH, 1.0 mM sodium azide and 0.1M phosphate buffer (pH 7.4) and 10  $\mu$ l PMS in a total volume of 200  $\mu$ l. The enzyme activity was calculated as nmol NADPH oxidized  $\text{min}^{-1} \text{mg}^{-1}$  protein.

##### **10.4.12.3. Estimation of glutathione reductase activity**

The assay system to estimate GR (EC 1.6.4.2) activity consisted of 0.1 M phosphate buffer (pH 7.6), 0.5 mM EDTA, 1.0 mM oxidized glutathione, 0.1 mM NADPH and 10  $\mu$ l PMS in a total volume of 200  $\mu$ l (Carlberg and Mannervik, 1985). The

enzyme activity was assayed in a 96-well plate reader by measuring the disappearance of NADPH at 340 nm and was calculated as nmol NADPH oxidized  $\text{min}^{-1} \text{mg}^{-1}$  protein.

### 10.5. Statistical analysis

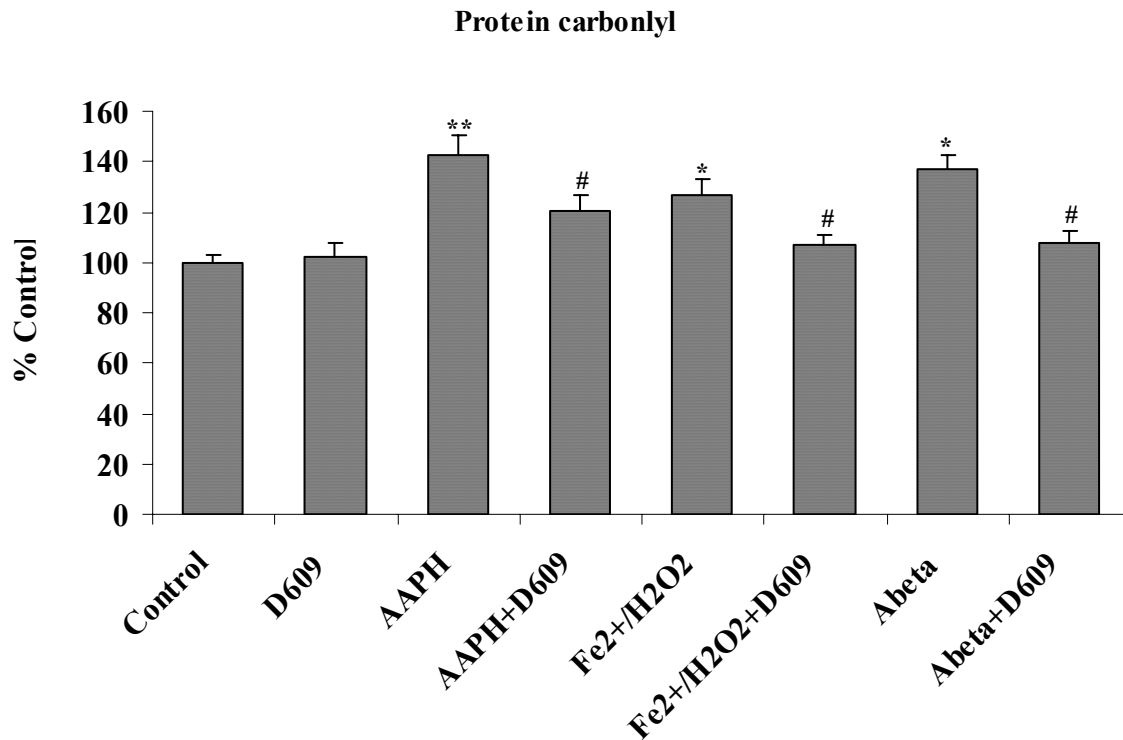
ANOVA was used for statistical evaluation of data followed by Student's *t*-test. Results are presented as mean  $\pm$  SEM. P-values less than 0.05 were considered significant.

### 10.6. Results

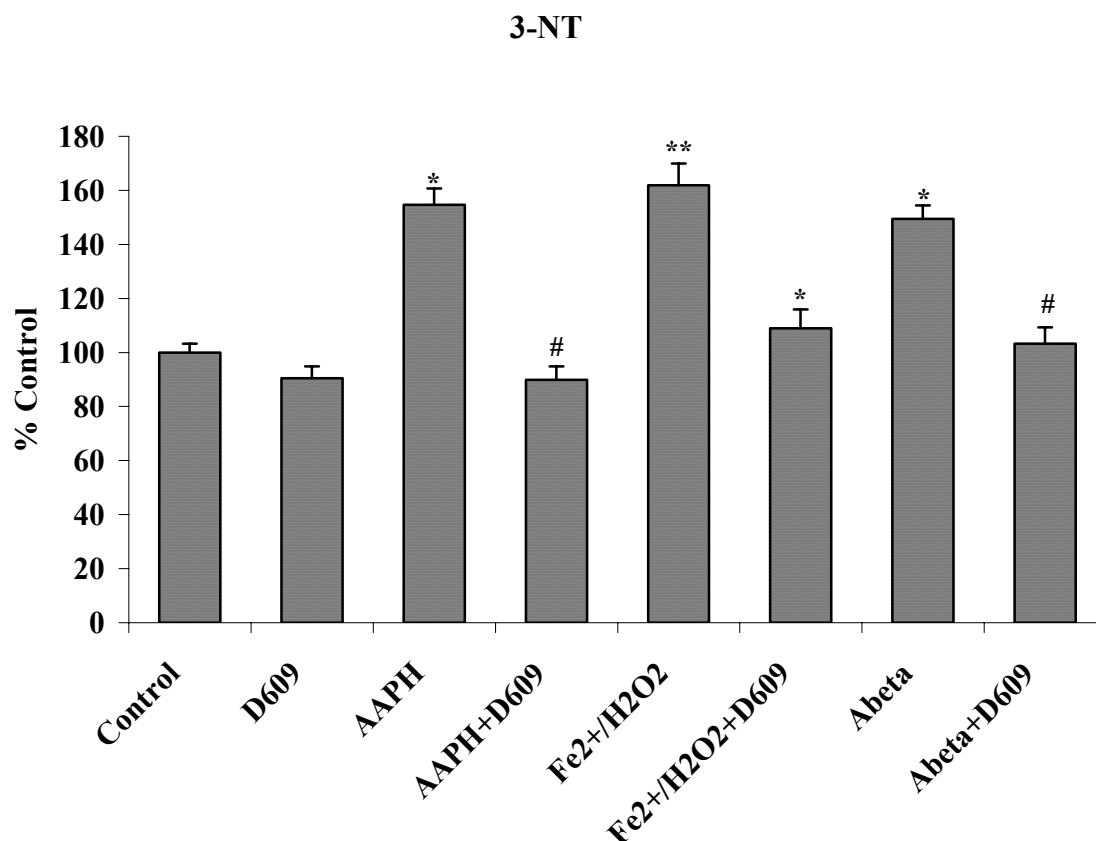
#### 10.6.1. Protein Oxidation and Lipid Peroxidation

Fig. 10.1, 10.2 and 10.3 show the levels of protein carbonyl, 3NT and HNE respectively in mitochondria isolated from brain of gerbils that had been previously injected i.p. with saline or D609. These isolated brain mitochondrial samples were subsequently treated with  $\text{Fe}^{2+}/\text{H}_2\text{O}_2$ , AAPH or  $\text{A}\beta$  (1-42), *in vitro*. The concentrations of these oxidants were chosen based on prior dose-response studies of the agents in *in vivo* investigations (Joshi, Sultana et al., 2005a; Perluigi, Joshi et al., 2006). The levels of protein carbonyl, 3NT and HNE were found significantly increased in mitochondria isolated from saline-injected gerbils brain and subsequently treated with oxidants, *in vitro*, compared to control (without treatment of oxidants). Brain mitochondria isolated from gerbils previously injected i.p. with D609 and subsequent *in vitro* treatment with  $\text{Fe}^{2+}/\text{H}_2\text{O}_2$ , AAPH and  $\text{A}\beta$  (1-42) showed significantly decreased protein carbonyl, 3NT and HNE levels as compared to brain mitochondria isolated from gerbils previously injected i.p. with saline and subsequently treated with  $\text{Fe}^{2+}/\text{H}_2\text{O}_2$ , AAPH and  $\text{A}\beta$  (1-42), *in vitro*. The D609-alone sample had no significant effect on the levels of protein

carbonyls, 3NT or HNE in brain mitochondria. It is clear that less protein oxidation and lipid peroxidation product, HNE was found in  $\text{Fe}^{2+}/\text{H}_2\text{O}_2$ , AAPH and  $\text{A}\beta$  (1-42) treated mitochondria isolated from gerbils previously injected with D609.



**Figure 10.1:** Shows the increment in protein carbonyl formation in brain mitochondria isolated from saline-injected gerbils and treated with various oxidants compared to control. The protective effects of D609 against protein carbonyl formation in brain mitochondria isolated from gerbils injected i.p. 1h before sacrifice with D609 and treated with AAPH,  $\text{Fe}^{2+}/\text{H}_2\text{O}_2$  and  $\text{A}\beta$  (1-42) also are shown. \* $p < 0.01$  and \*\* $p < 0.001$  compared to control and #  $p < 0.01$  compared to oxidant treatment. The data are presented as mean  $\pm$  SEM expressed as percentage of control (n=6). (Data collected in collaboration with Dr Mubeen Ansari)



**Figure 10.2:** Shows the increment in 3-NT levels in brain mitochondria isolated from saline-injected gerbils and subsequently treated with AAPH, Fe<sup>2+</sup>/H<sub>2</sub>O<sub>2</sub> or A $\beta$  (1-42) compared to 3NT levels in brain mitochondria isolated from saline-injected gerbil that received no treatment of any oxidant, \*p<0.01 and \*\*p<0.001. This figure also shows decreased 3NT levels shows in brain mitochondria isolated from gerbils previously injected i.p. with D609 1 h before sacrifice and treated with AAPH, Fe<sup>2+</sup>/H<sub>2</sub>O<sub>2</sub> or A $\beta$  (1-42) compared to the oxidant treatment but no prior injection of D609, # p<0.01. The data are presented as mean  $\pm$  SEM expressed as percentage of control (n=6). (Data collected in collaboration with Dr Mubeen Ansari)

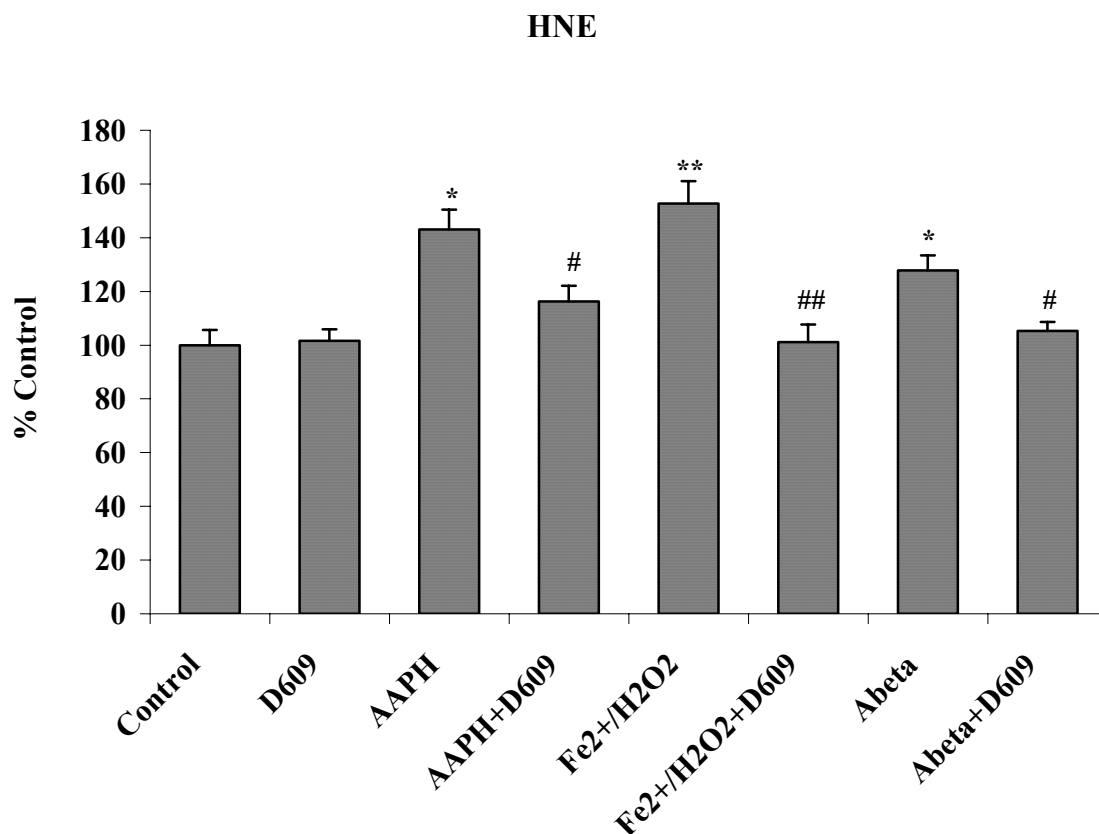


**Figure 10.3:** Shows the significantly elevated protein-bound HNE content in brain mitochondria isolated from saline-injected gerbils and treated with different oxidants [AAPH, Fe<sup>2+</sup>/H<sub>2</sub>O<sub>2</sub> or Aβ (1-42)]. The protective effects of D609 against HNE formation of protein-bound HNE in brain mitochondria isolated from gerbil injected i.p. with D609 1 h before sacrifice and treated with AAPH, Fe<sup>2+</sup>/H<sub>2</sub>O<sub>2</sub> or Aβ (1-42) also are shown. \*p<0.01 and \*\*p<0.001 compared to control, # p<0.01 and ## p<0.001 compared to oxidant treatment. The data are presented as mean ± SEM expressed as percentage of control (n=6). (Data collected in collaboration with Dr Mubeen Ansari)



### 10.6.2. Reduced glutathione (GSH)

Fig. 10.4a shows the levels of GSH in mitochondria isolated from gerbil brain from saline- as well as D609-injected rodents. These brain mitochondrial samples were subsequently treated with  $\text{Fe}^{2+}/\text{H}_2\text{O}_2$ , AAPH or  $\text{A}\beta$  (1-42), *in vitro*. The levels of GSH were found significantly decreased in mitochondria isolated from saline-injected gerbils brain and treated *in vitro* with oxidants compared to control. In contrast, brain mitochondria isolated from D609-injected gerbils and subsequently treated *in vitro* with  $\text{Fe}^{2+}/\text{H}_2\text{O}_2$ , AAPH or  $\text{A}\beta$  (1-42) showed increased levels of GSH.

### 10.6.3. Oxidized Glutathione (GSSG)

Fig. 10.4b shows significantly increased GSSG levels in brain mitochondria treated with different oxidants [ $\text{Fe}^{2+}/\text{H}_2\text{O}_2$ , AAPH or  $\text{A}\beta$  (1-42)] that were isolated from saline-injected gerbils (control). In contrast, there were significantly decreased GSSG levels in mitochondria isolated from gerbils previously injected i.p. with D609 and treated with  $\text{Fe}^{2+}/\text{H}_2\text{O}_2$ , AAPH or  $\text{A}\beta$  (1-42), *in vitro*.

### 10.6.4. The Ratio of Reduced and Oxidized Glutathione (GSH/GSSG)

Fig.10.4c shows the significantly decreased GSH/GSSG ratio in brain mitochondria isolated from saline-injected gerbils (control) and treated with different oxidants, *in vitro*. This GSH/GSSG ratio was significantly increased in brain mitochondria isolated from gerbils previously injected i.p. with D609 and treated with  $\text{Fe}^{2+}/\text{H}_2\text{O}_2$ , AAPH or  $\text{A}\beta$  (1-42), *in vitro*.

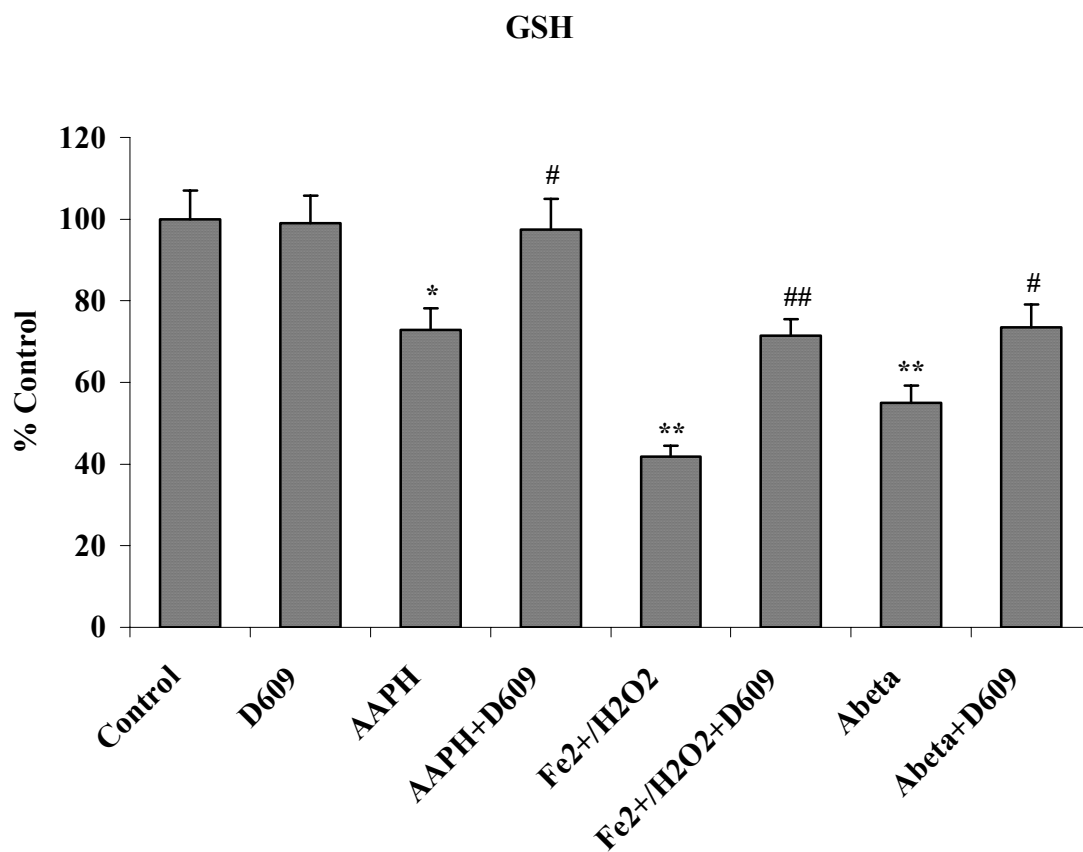


**Figure 10.4a:** Shows a significant decrement in GSH levels in brain mitochondria isolated from saline-injected gerbils and subsequently treated with AAPH, Fe<sup>2+</sup>/H<sub>2</sub>O<sub>2</sub> or Aβ (1-42) compared to GSH levels in brain mitochondria isolated from saline-injected gerbils not subjected to treatment of any oxidant. Also shown is the protection of GSH levels in brain mitochondria isolated from gerbils previously injected i.p. with D609 1 h before sacrifice and treated with AAPH, Fe<sup>2+</sup>/H<sub>2</sub>O<sub>2</sub> or Aβ (1-42) compared to GSH levels in brain mitochondria isolated from saline-treated gerbils and then treated with oxidants. \*p<0.01 and \*\*p<0.001 compared to control, # p<0.01 and ## p<0.01 compared to oxidant treatment. The data are presented as mean ± SEM expressed as percentage of control (n=6).

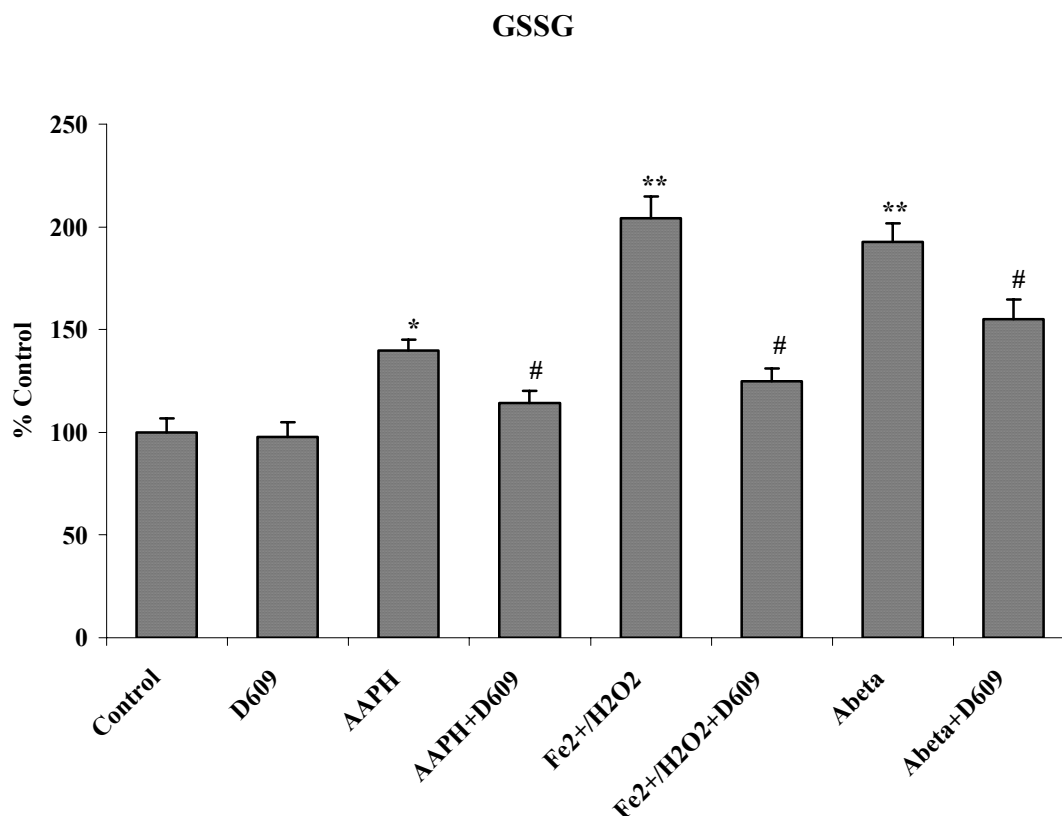


**Figure 10.4b:** Shows the increased level of GSSG in brain mitochondria isolated from saline-injected gerbils and subsequently treated with AAPH, Fe<sup>2+</sup>/H<sub>2</sub>O<sub>2</sub> or A $\beta$  (1-42) as compared to GSSG levels in brain mitochondria isolated from saline-injected gerbils but not subjected to treatment of any oxidant. The reduction in GSSG level shows in brain mitochondria isolated from gerbils previously injected i.p. with D609 1 h before sacrifice and treated with AAPH, Fe<sup>2+</sup>/H<sub>2</sub>O<sub>2</sub> or A $\beta$  (1-42) compared to GSSG levels in brain mitochondria isolated from saline-treated gerbil and then treated with oxidants. \*p<0.01 and \*\*p<0.001 compared to control, # p<0.01 and ## p<0.01 compared to oxidant treatment. The data are presented as mean  $\pm$  SEM expressed as percentage of control (n=6).

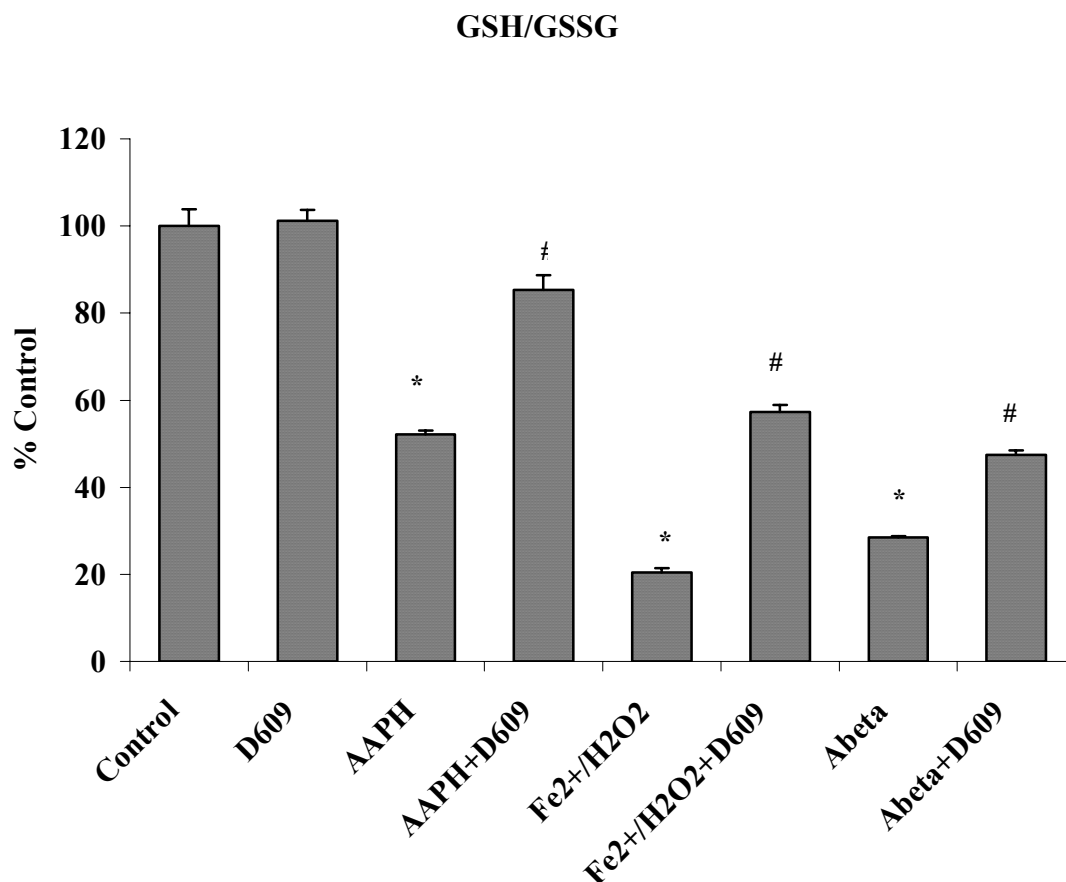


**Figure 10.4c:** Shows the ratio of GSH/GSSG, decreased in brain mitochondria isolated from saline-injected gerbils and subsequently treated with AAPH, Fe<sup>2+</sup>/H<sub>2</sub>O<sub>2</sub> or Aβ (1-42), compared to the GSH/GSSG ratio in brain mitochondria isolated from saline-injected gerbils but not subjected to treatment of any oxidant. The increment in the ratio of GSH/GSSG in brain mitochondria isolated from gerbils previously injected i.p. with D609 1 h before sacrifice and then treated with AAPH, Fe<sup>2+</sup>/H<sub>2</sub>O<sub>2</sub> or Aβ (1-42) compared to this ratio determined in brain from mice treated with oxidant but no pre-injection of gerbils with D609 is also shown. \*p<0.01 and \*\*p<0.001 compared to control, # p<0.01 and ## p<0.01 compared to oxidant treatment. The data are presented as mean ± SEM expressed as percentage of control (n=6).

#### 10.6.5. Cytochrome-c Release

Reactive oxygen species are produced by mitochondria that can cause the release of cytochrome-c from the mitochondrial membrane. Figure 11.5 shows the level of cytochrome-c released from brain mitochondria isolated from saline- as well as D609-injected gerbils and subsequently treated with different oxidants, *in vitro*. There was a significant reduction in cytochrome-c release from brain mitochondria by prior i.p. D609 treatment compared to that in brain mitochondria isolated from saline-injected gerbils. Increased cytochrome-c release from brain mitochondria isolated from control gerbils with subsequent *in vitro* treatment of  $\text{Fe}^{2+}/\text{H}_2\text{O}_2$ , AAPH or  $\text{A}\beta$  (1-42) compared to control was discussed. Brain mitochondria isolated from D609-injected gerbils and subsequently treated with  $\text{Fe}^{2+}/\text{H}_2\text{O}_2$ , AAPH or  $\text{A}\beta$  (1-42), *in vitro*, showed a significant decrease in cytochrome-c release compared to mitochondria isolated from saline-injected gerbils treated with oxidants (Figure 11.5).

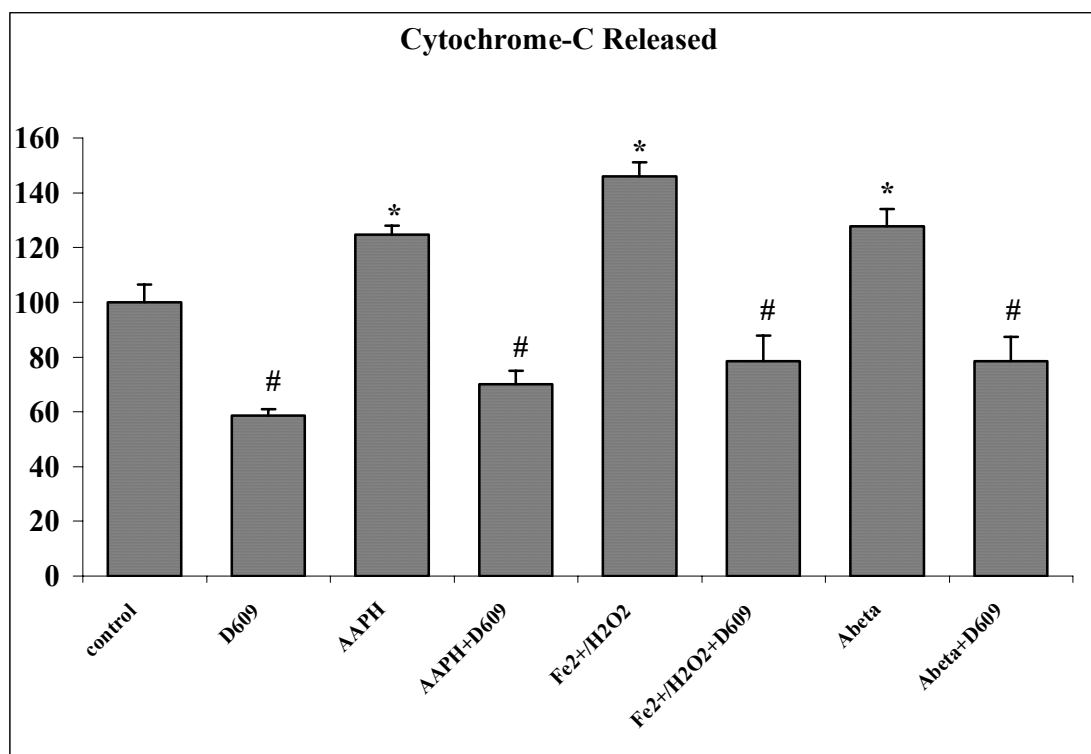


**Figure 10.5:** Shows the increased level of cytochrome-c released from brain mitochondria isolated from saline-injected gerbils and treated with various oxidants (AAPH, Fe<sup>2+</sup>/H<sub>2</sub>O<sub>2</sub> or Aβ (1-42) as compared to cytochrome-c released from brain mitochondria isolated from saline-injected gerbils but not subjected to treatment of any oxidant. Also shown is the decrement of cytochrome-c release from brain mitochondria isolated from gerbils previously injected i.p. with D609 1 h before sacrifice and treated with AAPH, Fe<sup>2+</sup>/H<sub>2</sub>O<sub>2</sub> or Aβ (1-42) compared to that released from brain mitochondria isolated from gerbils subjected to oxidant treatment. The D609 only treatment shows significantly less cytochrome-c release compared control. \*p<0.01 as compared to control, # p<0.01 compared to oxidant treatment. The data are presented as mean ± SEM expressed as percentage of control (n=5). (Data collected in collaboration with Dr Mubeen Ansari)

#### 10.6.6. The Activity of GSH-relevant Enzymes

Table 10.1 shows the activity of some GSH-relevant enzymes in gerbil brain from which mitochondria were isolated. The activities of glutathione-S-transferase (GST) and glutathione peroxidase (GPx) were increased significantly in post mitochondrial supernatant from D609-injected gerbils. The activity of glutathione reductase (GR) also was increased, but non-significantly. Thus, these results suggest that D609 has a role in the redox cycle of GSH (oxidation and reduction of GSH) and in the neuroprotection against free radicals.

Enzyme	Brain from Control Group	Brain from D609 Treated Group
GST (nmol CDNB conjugate formed $\text{min}^{-1} \text{mg}^{-1}$ protein)	38.4 $\pm$ 3.44	61.5 $\pm$ 4.74 <sup>*</sup>
GPx (nmol NADPH oxidized $\text{min}^{-1} \text{mg}^{-1}$ protein)	34.5 $\pm$ 2.87	43.1 $\pm$ 3.41 <sup>#</sup>
GR (nmol NADPH oxidized $\text{min}^{-1} \text{mg}^{-1}$ protein)	23.4 $\pm$ 2.89	26.6 $\pm$ 3.10

**Table 10.1:** Activities of some GSH-related enzymes in post mitochondrial supernatant obtained from gerbil brain mitochondria that were previously injected i.p. with saline (control) or D609. The data are presented as mean  $\pm$  SEM expressed as percentage of control (n=6). <sup>\*</sup>p<0.01 and <sup>#</sup>p<0.05 compared to control. (Data collected in collaboration with Dr Mubeen Ansari).

### 10.7. Discussion

Oxidative stress reflects a marked imbalance between ROS and their removal by anti-oxidant systems. This imbalance may originate from an overproduction of ROS or from a reduction in antioxidant defenses or both (Butterfield and Stadtman, 1997). An inverse relationship between lipid peroxidation and GSH and its dependent enzymes, along with the activities of catalase and superoxide dismutase is well known (Sies, 1999; Hansen, Go et al., 2006). A reduction in GSH may impair H<sub>2</sub>O<sub>2</sub> clearance and promote hydroxyl radical formation, thus increasing the free radical load, which triggers oxidative stress. Conversely, GSH is converted to GSSG, a process that in conjunction with the cofactor NADPH can reduce lipid peroxides, free radicals and H<sub>2</sub>O<sub>2</sub>. NADPH also acts as a peroxynitrite reductant, thereby providing enzymatic defense against peroxynitrite (Sies, Sharov et al., 1997). Glutathione peroxidase (GPx) and glutathione reductase (GR) protect the neurons from oxidative stress by catalyzing the reduction of H<sub>2</sub>O<sub>2</sub> at the expense of glutathione (Sies, 1999; Hansen, Go et al., 2006). Glutathione-S-transferase (GST) play a role in neuroprotection by catalyzing the formation of the GSH-HNE conjugate, which is then removed from neurons by the action of the multidrug resistant protein-1 (Sultana and Butterfield, 2004). In AD brain, both GST and MRP-1 are oxidatively modified and likely dysfunctional (Sultana and Butterfield, 2004). In our results GST (Table I) and GPx have higher activities following *in vitro* oxidant treatment of brain homogenate isolated from previously D609-injected gerbils. GR activity in brain (Table I) of D609-injected animals was not significantly elevated following subsequent *in vitro* oxidant treatment to isolated mitochondria relative to control.

Reduced levels of GSH (Fig. 4A) have been observed in oxidative stress-related disorders (Bains and Shaw, 1997) in specific regions of the central nervous system of AD



patients, and thus reduced GSH may contribute to the neuronal cell dysfunction and/or loss. In AD, increased levels of GSSG (Cooper, 1997) have been observed. Studies have shown that an increase in endogenous GSH levels by dietary or pharmacological intake of GSH precursors or GSH mimetics or substrates for GSH synthesis protects the brain against oxidative stress (Anderson and Luo, 1998; Fontaine, Geddes et al., 2000; Pocernich, La Fontaine et al., 2000; Halliwell, 2001; Pocernich, Cardin et al., 2001; Drake, Kanski et al., 2002; Drake, Sultana et al., 2003). The increase in the content of GSH and decrease in the extent of GSSG in mitochondria isolated from gerbil brain previously injected with D609 in our study is in agreement with earlier reports (Perluigi, Joshi et al., 2006).

We earlier showed that D609 could effectively scavenge hydroxyl radicals (Zhou, Lauderback et al., 2001). The identification of D609 as a potent antioxidant implies that D609 may exert some of the reported activities that have been largely attributed to the inhibition of phosphatidyl choline-specific phospholipase C (PC-PLC) by its antioxidant properties. Among these activities are inhibition of LPS-and TNF-induced NF-kB activation and inflammatory cytokine production (Schutze, Potthoff et al., 1992; Amtmann, 1996). ROS activated NF-kB causes a differential change in gene expression between neurons and astrocytes in the AD brain (Tanaka, Takehashi et al., 2002; Onyango, Bennett et al., 2005). We earlier reported the anticarcinogenic activity of D609 might be due to its antioxidant property (Zhou, Lauderback et al., 2001). *In vitro*, D609 kills a variety of tumor cells but has limited toxic effects on normal cells (Sauer, Amtmann et al., 1990). Although D609 might be involved in alternate biochemical pathways, its glutathione mimetic property cannot be ignored. The free thiol group in

D609 may act as substrate for hydroxyl radicals, or may act as electron acceptor from hydrogen peroxide to form a dixanthate, which forms the substrate for glutathione reductase to convert it back to xanthate. This property of D609 is yet to be explored.

Protein carbonyls, 3NT and HNE levels are elevated in AD and MCI brains (Butterfield, Drake et al., 2001; Butterfield and Lauderback, 2002; Castegna, Aksenov et al., 2002a; Castegna, Thongboonkerd et al., 2003; Butterfield, 2004; Castegna, Thongboonkerd et al., 2004; Butterfield, Poon et al., 2006; Butterfield, Reed et al., 2006; Sultana, Poon et al., 2006a; Sultana, Poon et al., 2006b). HNE is a highly reactive product of arachidonic acid metabolism that is believed to interfere with normal cellular functions (Butterfield and Lauderback, 2002). During oxidative stress several lipid peroxidation products are formed, including HNE, one of the most abundant and toxic lipid-derived aldehydes, and which can induce oxidative stress (Esterbauer, Schaur et al., 1991; Lauderback, Hackett et al., 2001). Lipid peroxidation products such as HNE and acrolein are known to cause damage to biomembranes, proteins and other biomolecules in AD brain (Sayre, Zelasko et al., 1997; Lovell, Xie et al., 1998; Lauderback, Hackett et al., 2001). These alkenals form an immediate substrate for GSH (Xie, Lovell et al., 1998) and these lipid peroxidation products are known to be involved in apoptosis, which can be initiated as a consequence of GSH depletion (Mark, Lovell et al., 1997).

GSH is known to detoxify HNE and protect cultured neurons against oxidative damage resulting from amyloid  $\beta$ -peptide, iron, and HNE (Mark, Lovell et al., 1997). GSH can also protect brain from damage by peroxynitrite, hydroxyl free radicals, or reactive alkenals (Koppal, Drake et al., 1999b; Pocernich, La Fontaine et al., 2000; Pocernich, Cardin et al., 2001; Drake, Kanski et al., 2002; Drake, Sultana et al., 2003).

D609 may binds to reactive alkenals formed due to peroxidation of lipids and detoxifies their effects (Lauderback, Drake et al., 2003).

HNE can alter pyruvate dehydrogenase (PD) (Pocernich and Butterfield, 2003), decrease cell survival (decrease MTT reduction) and cause inhibition of  $\text{Na}^+\text{K}^+$  ATPase (Mark, Lovell et al., 1997). The activity of the adenine nucleotide transporter in mitochondria is inhibited by HNE, which directly results in ATP depletion (Chen, Bertrand et al., 1995).  $\text{A}\beta$  increases lipid derived free radical production (Chen, Bertrand et al., 1995; Mark, Lovell et al., 1997; Butterfield, Drake et al., 2001; Butterfield and Lauderback, 2002; Boyd-Kimball, Mohmmad Abdul et al., 2004). HNE rapidly leads to decline in multiple sites of the mitochondrial respiratory chain and modified specific mitochondrial target proteins lead to apoptosis and cell death in AD (Picklo, Amarnath et al., 1999).

Recently, we showed that the xanthate D609, a glutathione mimetic (Lauderback, Drake et al., 2003), protects primary neuronal culture against  $\text{A}\beta$  (1-42)-induced oxidative stress and neurotoxicity *in vitro* (Sultana, Newman et al., 2004) and against  $\text{A}\beta$  (1-42) *in vivo* (Perluigi, Joshi et al., 2006). D609 has the ability to scavenge hydrogen peroxide and hydroxyl free radicals (Lauderback, Drake et al., 2003). D609 can bind to reactive alkenals and detoxify their effect, thereby preventing these alkenals from damaging mitochondria (Lauderback, Drake et al., 2003; Joshi, Sultana et al., 2005a). AAPH is known to induce protein carbonylation and nitration (Kanski, Lauderback et al., 2001) in mitochondria. In the current study, we report that *in vivo* delivery of D609 inhibits the damage to brain mitochondria caused by production of hydroxyl free radicals,

alkoxyl and peroxy radicals and A $\beta$  (1-42)-induced *in vitro* oxidative stress to decrease protein oxidation and lipid peroxidation.

A $\beta$  disrupts Ca<sup>2+</sup> homeostasis in neurons (Mattson, Barger et al., 1993), and increased intracellular Ca<sup>2+</sup> level can increase sphingomyelinase activity to produce ceramide (Di Paola, Zaccagnino et al., 2004). Activation of the apoptogenic sphingomyelin-dependent signaling pathway is mediated by ceramide (Di Paola, Zaccagnino et al., 2004) during oxidative stress to play role in the pathogenesis of neuronal disease (Michel, Lambeng et al., 1999). Apoptosis induced by the membrane-permeable second messenger ceramide, followed by the release of cytochrome-c and Ca<sup>2+</sup> from the mitochondria with the loss of mitochondrial transmembrane potential has been observed (Michel, Lambeng et al., 1999). Both cytochrome-c release and rise of intracellular Ca<sup>2+</sup> cause caspase-3 activation and nuclear condensation (Michel, Lambeng et al., 1999). ROS-dependent and independent pathways are initiated by caspase-8 activation and contribute to ceramide formation via the activation of both neutral and acid sphingomyelinases (SMases) in TNF-alpha-induced apoptosis of human glioma cells (Michel, Lambeng et al., 1999). In one study, D609 has also been shown to inhibit sphingomyelin synthase in SV40-transformed human lung fibroblasts, but ceramide and DAG levels evolved in opposite directions (Luberto and Hannun, 1998) and partially protected against apoptosis (Denis, Lecomte et al., 2002).

In conclusion, this study has demonstrated that, similar to the case with elevated cytosolic GSH protecting brain mitochondria (Drake, Kanski et al., 2002), i.p. injection of D609 protects brain mitochondria (anti-apoptotic) against oxidative stress induced *in vitro* by different oxidants, such as AAPH, Fe<sup>2+</sup>/H<sub>2</sub>O<sub>2</sub> or A $\beta$ (1–42). *In vivo* delivery of

D609 showed significant protection against protein oxidation, lipid peroxidation and cytochrome-c release in gerbil brain mitochondria. While a role for inhibition of PC-PLC by D609 in the protection of brain mitochondria cannot be excluded, based on the data from the present and previous studies (Joshi, Sultana et al., 2005a; Perluigi, Joshi et al., 2006), the increment in the GSH level and the activity of its dependent enzymes (GST, GPx and GR), are strong indications to suggest that D609 has neuroprotective effects to brain mitochondria due in significant part to its antioxidant properties. Thus, in brain mitochondria, the antioxidant properties of *in vivo* delivery of D609 conceivably could be beneficial in the treatment of diseases related to oxidative stress that involve mitochondria (AD, Huntington disease, Parkinson's disease, for example). This xanthate compound protects against *in vitro* treatment of A $\beta$  (1-42); consequently, we suggest D609 may be part of a promising therapeutic strategy for Alzheimer's disease. Studies to test this notion in rodent models of AD are in progress.

## Chapter 11

### **N-Acetyl cysteine-mediated protection against oxidative stress in APP/PS-1 mouse:**

### **A pilot study towards therapeutic modulation of mild cognitive impairment (MCI)**

#### **11.1. Overview of the Study**

N-acetyl cysteine (NAC) is a glutathione (GSH) precursor. It provides the limiting substrate in GSH synthesis, cysteine. The mechanism by which it does is not very well known. NAC is commonly used in treatment of acetaminophen poisoning. NAC is one of the most widely used in antioxidant therapy. Previously our laboratory showed an increase in GSH levels post i.p. injection of NAC. NAC reduces the protein oxidation and lipid peroxidation in synaptosomes treated with acrolein. The present study was undertaken to test the hypothesis that NAC would provide *in vivo* neuroprotection against free radical oxidative stress-mediated by A $\beta$  (1-42) in APP/PS-1 mice, a model of Alzheimer's disease (AD). In the present study, NAC was administered orally (2mg/kg body weight/day) in drinking water for 5 months beginning at 4 months of age for both APP/PS-1 mice and wild type aged matched control. Another group of APP/PS-1 and wild type mice were given normal drinking water. Brain isolated from APP/PS-1 mice given NAC in water at 9 month of age showed significant reduction in the levels of protein oxidation and lipid peroxidation when compared to the brain isolated from APP/PS-1 mice given normal drinking water. Additionally, increased expression of a key antioxidant enzymes expression levels, GPx, was also observed in brain isolated from APP/PS-1 given NAC when compared to APP/PS-1 mice given normal drinking water. We also observed an increased expression of Pin 1, a key cell cycle protein in brain isolated from APP/PS-1 mice that were given NAC when compared to APP/PS-1 mice

given normal drinking water. These results are discussed with reference to potential use of this brain accessible glutathione precursor in the treatment of oxidative stress-mediated AD.

### **11.2. Introduction**

Oxidative stress has implication in various neurodegenerative disorders including Alzheimer's disease (AD) (Hensley, Hall et al., 1995; Markesbery and Lovell, 1998; Butterfield, Drake et al., 2001; Butterfield and Lauderback, 2002). As described in Chapter 1, AD affects more than 4 million Americans and is one of the leading causes of death in US. There is no efficient therapy towards treatment of this dreaded disorder. Pathological characteristics of AD includes the presence of senile plaques comprised of aggregated A $\beta$ , neurofibrillary tangles consisting of hyperphosphorylated tau, and synapse loss (Katzman and Saitoh, 1991; Bosetti, Brizzi et al., 2002). Etiologically, a free radical-mediated oxidative stress hypothesis in AD has gained considerable importance (Butterfield, Drake et al., 2001). In AD brain, oxidative stress leads to significant protein oxidation (Butterfield and Lauderback, 2002), DNA and RNA oxidation (Mecocci, MacGarvey et al., 1993; Lovell, Gabbita et al., 1999; Nunomura, Perry et al., 1999; Wang, Xiong et al., 2005), lipid peroxidation (Markesbery and Lovell, 1998; Lauderback, Hackett et al., 2001), and neuronal dysfunction or death. Increased production of reactive oxygen species (ROS) along with depletion in antioxidant capacity is observed in AD (Beckman and Ames, 1998) and consistent with this observation  $\alpha$ -tocopherol (vitamin E) administration in AD patients delayed its progression when compared to placebo treated control (Sano, Ernesto et al., 1997), suggesting that oxidative stress-mediated AD progression may possibly be delayed by antioxidant therapy.

Mild cognitive impairment (MCI) is generally referred as the transitional zone between normal aging and early dementia or clinically probable Alzheimer's disease (AD) (Winblad, Palmer et al., 2004). Most individuals with MCI eventually develop AD or other forms of dementia, which may suggest that MCI could be the early phase in the development of AD (Almkvist, Basun et al., 1998; Morris, Storandt et al., 2001). MCI is a general term used to describe a slight but measurable memory disorder. A person with MCI has memory problems greater than normally expected with aging, but does not show other symptoms of dementia, such as impaired reasoning or judgment. A person with MCI is at higher risk for developing AD. Although some of the MCI cases become stable or become resolved, most persons with MCI develop AD. A direct relationship between MCI and AD is yet to be established. Recently our laboratory showed an overlap in the oxidized proteins in MCI and AD subjects (Butterfield, Poon et al., 2006). Oxidation of these proteins may play a significant role in development of MCI to AD (Butterfield, Poon et al., 2006). Oxidative stress has been implicated in MCI (Keller, Schmitt et al., 2005; Butterfield, Reed et al., 2006). Our laboratory recently showed elevated protein-bound 4-hydroxy-2-nonenal (HNE) levels, a lipid peroxidation product, in brain from persons with mild cognitive impairment (Butterfield, Reed et al., 2006). By using redox proteomics, our laboratory showed some key proteins to be oxidized in MCI brain, suggesting oxidative stress play an important role in MCI and may be the reason for progression of MCI to AD (Butterfield, Poon et al., 2006). Since MCI is potentially reversible, and oxidative stress plays a key role in development and progression of this disease, it is imperative to look at a potential therapeutic strategy involving antioxidants to prevent MCI and eventually stop its progression to AD.



Among the genetic risk factors for AD, includes mutations in the presenilin 1 (PS1) (Sherrington, Rogaev et al., 1995), presenilin 2 (PS2) (Rogaev, Sherrington et al., 1995), or the APP gene (Chartier-Harlin, Crawford et al., 1991). Approximately 30% familial Alzheimer's disease (FAD) cases have mutations in PS1 (Schellenberg, 1995). PS1 is a part of  $\gamma$ -secretase complex that cleaves APP to release A $\beta$ (1-42). Mutation in PS1 has been shown to alters APP processing to enhance the generation of A $\beta$ (1-42) peptides (Jarrett, Berger et al., 1993). Synaptosomal proteins from PS-1 mutant mice showed increased oxidative stress and alteration in synaptosomal protein structure when compared to wild type (LaFontaine, Mattson et al., 2002).

Several line of evidence shows that A $\beta$ (1-42) plays a central role in AD pathogenesis and is well documented. Our laboratory was instrumental in hypothesizing A $\beta$ (1-42)-mediated oxidative stress in AD brain (Butterfield, Drake et al., 2001). Based on these studies a mouse model showing accelerated A $\beta$ (1-42) deposition was used to study the oxidative stress parameter and antioxidant therapeutic intervention towards MCI or AD. As described in Chapter 2, this mouse model was developed by Borchelt et al., which had FAD mutant human PS1-A246E and a chimeric mouse/human (Mo/Hu) APP695 harboring a Hu A $\beta$  domain and mutations (K595N, M596L) linked to Swedish FAD (APP swe) coexpressed (APP/PS-1 human knock-in mouse) (Borchelt, Ratovitski et al., 1997). The APP/PS-1 mice showed increased A $\beta$  production and accelerated amyloid deposition in the brain (Borchelt, Ratovitski et al., 1997). Previous studies from our laboratory have shown that neurons from APP/PS1 mice have increased basal protein oxidation and lipid peroxidation, and are more vulnerable to oxidation by various exogenous oxidants when compared to wild type (Mohammad Abdul, Sultana et al.,

2006). All these studies suggest that APP/PS1 mice can be used as a model of FAD, which is characterized by A $\beta$ (1–42)-mediated oxidative stress.

Depletion of glutathione (GSH), an intracellular antioxidant, is known to be involved in several neurodegenerative disorders (Benzi and Moretti, 1995b; Markesbery, 1997; Butterfield, Castegna et al., 2002a). Many attempts have been made to develop antioxidant compounds that can act as precursor of GSH or mimic GSH as scavenger of reactive oxygen species (ROS) and to maintain the intracellular redox state. Increase in the endogenous GSH levels by dietary or pharmacological intake of GSH precursor or GSH mimetic protects brain against oxidative stress (Anderson and Luo, 1998; Butterfield, Drake et al., 2001; Halliwell, 2001). Considering the importance of developing new antioxidant compounds and the relevance of their application in the treatment of neurodegenerative diseases, we focused our attention on glutathione precursor, N-acetyl cysteine (NAC).

NAC is an FDA-approved drug used in the treatment of acetaminophen-mediated liver toxicity (Prescott, Park et al., 1977) or heavy metal poisoning. NAC acts as an indirect precursor of GSH. It is thought to provide cysteine, a rate limiting substrate in GSH synthesis (Dringen and Hamprecht, 1999). NAC acts as antioxidant by raising intracellular levels of cysteine or by the scavenging ROS itself. NAC is also used in treatment of HIV infection (Droge, 1993), and cancer chemotherapy (Holoye, Duelge et al., 1983). Apart from its antioxidant properties, NAC is known to improve neuron survival in the CA1 region of the hippocampus following ischemic-reperfusion injury (Zhang, Tian et al., 2003). NAC can acts as transcription factor and can rescue neurons from apoptotic death by activation of the Ras-ERK pathway (Yan and Greene, 1998).

NAC reduces the inflammatory symptoms in brain by direct inhibition of NF- $\kappa$ B and blocking iNOS from producing inflammatory cytokines (Pahan, Sheikh et al., 1998).

### **11.3. Purpose of the study**

Previous studies from our laboratory have shown that NAC can partially protect brain-derived membrane proteins against peroxynitrite-induced damage (Koppal, Drake et al., 1999a). NAC significantly increased endogenous glutathione levels, *in vivo*, in cortical synaptosome cytosol and prevented protein oxidation caused by hydroxyl radicals (Pocernich, La Fontaine et al., 2000). NAC protected mitochondria against oxidative damage induced by 3-nitropropionic acid and significantly reduce striatal lesion volumes (La Fontaine, Geddes et al., 2000). We also showed that NAC protected synaptosomal membranes against acrolein-induced protein damage by elevating GSH levels, *in vivo* (Pocernich, Cardin et al., 2001). We recently showed reversal of memory impairment and brain oxidative stress by NAC in aged SAMP8 mice (Farr, Poon et al., 2003). The current study was designed to determine if *in vivo* NAC would protect brain from APP/PS-1 mice against inherent A $\beta$ (1–42)-mediated oxidative stress-induced protein oxidation and lipid peroxidation.

### **11.4. Experimentals**

#### **11.4.1. Chemicals**

All the chemicals were purchased from Sigma-Aldrich (St. Louis, MO), unless stated otherwise. The OxyBlot kit used for protein carbonyl determination was purchased from InterGen (Purchase, NY). The primary antibody for HNE was purchased from Alpha Diagnostics (San Antonio, TX). The primary antibody for GPx was purchased from

Chemicon International (Temecula, CA). Transfer membranes for western blot and slot blot were purchased from Biorad (Hercules, CA).

#### **11.4.2. Animals**

For this study, male Wild type (WT) and APP/PS-1 mice, approximately 30 g in size, housed in the University of Kentucky Central Animal Facility in 12-h light/dark conditions and fed standard Purina rodent laboratory chow *ad libitum*, were used. The animal protocols were approved by the University of Kentucky Animal Care and Use Committee. The APP/PS-1 mice used are the APP<sup>NLh</sup>/APP<sup>NLh</sup> × PS-1<sup>P264L</sup>/PS-1<sup>P264L</sup> double mutant generated by using the Cre-loc<sup>©</sup> knock-in technology (Cephalon, Inc., Westchester, PA, USA) to humanize the mouse A $\beta$  sequence and to create a PS-1 mutation identified in human AD (Reaume, Howland et al., 1996; Siman, Reaume et al., 2000).

#### **11.4.3. Treatments**

Mice were divided into 4 groups. A group of WT and APP/PS-1 mice received normal drinking water and another group of WT and APP/PS-1 mice received water containing NAC (2mg/kg/day) for a period of 5 months. A 1% solution of NAC in water (pH adjusted to 7.2 by NaOH) was prepared and given to mice. Water was changed every alternate day for 5 months. Approximately 4 to 5 ml of water was consumed per mice per day, which gives a cumulative dose of 2mg/kg per mice per day, not accounting for spills. The NAC treatment was started at 4 month age. The dose of NAC was chosen based on prior studies (Andreassen, Dedeoglu et al., 2000). Following 5 months of NAC treatment, mice were sacrificed and brains were isolated and flash frozen in liquid nitrogen.

#### **11.4.4. Preparation of brain homogenate**

Brains were thawed and placed in ice cold lysing buffer containing 4µg/ml leupeptin, 4µg/ml pepstatin, 5 µg/ml aprotinin, 2mM ethylenediaminetetraacetic acid (EDTA), 2mM ethylene glycol-bis(tetraacetic acid (EGTA) and 10mM 4-(2-hydroxyethyl)-1-piperazine-ethanesulfonic acid (HEPES), pH 7.4. The brains were homogenized by 20 passes of a Wheaton tissue homogenizer, and the resulting homogenate was centrifuged at 20000g for 10 minutes. The pellet was suspended in 1ml phosphate buffered saline (PBS) and the supernatant (cytosolic fraction) was retained for fluorescence studies, GSH measurement and enzyme activities. All the fractions suspended in PBS were washed twice with PBS at 32000g for 10 min. The resulting fractions were assayed for protein concentration by the Pierce BCA method (Bradford, 1976).

#### **11.4.5. Protein Carbonyls**

Samples (5µl) of brain homogenate, 12% sodium dodecyl sulfate (SDS) (5µl), and 10µl of 10 times diluted 2,4-dinitrophenylhydrazine (DNPH) from 200mM stock were incubated at room temperature for 20 min, followed by neutralization with 7.5µl neutralization solution (2M Tris in 30% glycerol). Protein (250ng) was loaded in each well on a nitrocellulose membrane under vacuum using a slot blot apparatus. The membrane was blocked in blocking buffer (3% bovine serum albumin) in PBS 0.01% (w/v) sodium azide and 0.2% (v/v) Tween 20 for 1h and incubated with a 1:100 dilution of anti-DNP polyclonal antibody in PBS containing 0.01% (w/v) sodium azide and 0.2% (v/v) Tween 20 for 1h. The membrane was washed in PBS following primary antibody incubation three times at intervals of 5 min each. The membrane was incubated following

washing with an anti-rabbit IgG alkaline phosphatase secondary antibody diluted in PBS in a 1:8000 ratio for 1h. The membrane was washed three times in PBS for 5 min and developed in Sigma fast tablets, [5-bromo-4-chloro-3-indolyl phosphate/Nitro blue tetrazolium substrate (BCIP/NBT substrate)]. Blots were dried, scanned with Adobe Photoshop, and quantified with Scion Image (PC version of Macintosh compatible NIH image). No non-specific binding of antibody to the membrane was observed.

#### **11.4.6. HNE**

Sample (5 $\mu$ l) of brain homogenate, 12% SDS (5 $\mu$ l), and 5 $\mu$ l of modified Laemmli buffer containing 0.125 M Tris base pH 6.8, 4% (v/v) SDS, and 20% (v/v) glycerol were incubated for 20 min at room temperature and were loaded (250ng) in each well on a nitrocellulose membrane in a slot blot apparatus under vacuum. The membrane was treated as above and incubated with a 1: 5000 dilution of anti-HNE polyclonal antibody in PBS for 1h 30min. The membranes were further developed and quantified as above. A faint background staining due to the antibody alone was observed, but since each sample had a control, this minor effect was controlled.

#### **11.4.7. 3NT**

Samples (5 $\mu$ l) of brain homogenate, 12% SDS (5 $\mu$ l), and 5 $\mu$ l of modified Laemmli buffer containing 0.125 M Tris base pH 6.8, 4% (v/v) SDS, and 20% (v/v) glycerol were incubated for 20 min at room temperature and were loaded (250ng) in each well on a nitrocellulose membrane in slot blot apparatus under vacuum. The membrane was treated as above and incubated with a 1: 2000 dilution of anti-3-nitrotyrosine (3NT) polyclonal antibody in PBS for 1h 30min. The membranes were developed further and

quantified as described above. No non-specific binding of antibody to the membrane was observed.

#### **11.4.8. Western blots**

Samples (100 µg from cytosolic fraction) were incubated with sample loading buffer, and protein samples were denatured and electrophoresed on a 12.5% SDS-polyacrylamide gel. Proteins were transferred to a nitrocellulose membrane at 90 mA/gel for 2 h. The blots were blocked for 1h in fresh wash buffer (10 mM Tris-HCl, pH7.5), 150 mM NaCl, 0.05% Tween 20, pH 7.4, containing 3% bovine serum albumin) and incubated with a 1:1000 dilution of GPx monoclonal antibody in PBS for 1h. The membrane was washed three times in PBS and was incubated for 1 h with an anti-rabbit IgG alkaline phosphatase secondary antibody diluted in PBS in 1:8000 ratio. The membrane was washed for three times in PBS for 5 min and developed in Sigma fast tablets (BCIP/NBT substrate).

In all cases non-specific background labeling by secondary antibody was negligible.

#### **11.4.9. Enzyme activity assay**

##### **11.4.9.1. Estimation of glutathione peroxidase activity**

GPx (EC 1.11.1.9) was measured using a reaction mixture consisting of 0.2 mM H<sub>2</sub>O<sub>2</sub>, 1.0 mM GSH, 0.14 U of glutathione reductase (GR), 1.5 mM NADPH, 1.0 mM sodium azide and 0.1M phosphate buffer (pH 7.4) and 1mg/ml of supernatant protein (Wheeler, Salzman et al., 1990). The changes in absorbance were recorded at 340 nm in a 96 well microtiter plate and enzyme activity was calculated as nmol of NADPH oxidized min<sup>-1</sup> mg<sup>-1</sup> protein.

### **11.5. Statistical analysis**

Two-way ANOVA followed by a multiple comparisons test (Turkey HSD) was used to assess statistical significance. P values <0.05 were considered significant for comparison between control and experimental data sets.

### **11.6. Results**

The reason for starting NAC treatment at the 4 month age was chosen based on previous pathological studies. The A $\beta$ (1-42) deposition starts at the age of 5-6 months. These mice develop elevated levels of A $\beta$ (1-42) at about 6 months of age (Borchelt, Thinakaran et al., 1996; van Groen, Kiliaan et al., 2006). The A $\beta$ (1-42) aggregation as in senile plaques is seen at the age of 9 months (van Groen, Liu et al., 2003). The brain pathology at 7-9 months age is reminiscent of that of an MCI or early AD brain. Based on this observation we hypothesized that administration of NAC at an early age (4-5mo) for a period of 5 months (time by which amyloid plaques are formed) can reduce the A $\beta$ (1-42)-mediated oxidative stress in APP/PS-1 mice at later age (9 mo) and can prevent MCI like pathology.

#### **11.6.1. NAC protects APP/PS-1 mice brains against protein oxidation and lipid peroxidation**

Figures 11.1, 11.2 and 11.3 show the levels of protein carbonyls, 3-NT (markers of protein oxidation) and protein-bound HNE (a lipid peroxidation product) levels, respectively, in all the treatment groups. There was significant elevation in protein carbonyl, 3-NT and protein bound HNE levels in brain isolated from 9 month-old APP/PS-1 mice that were given normal water when compared to the levels in brain isolated from 9 month-old WT mice given normal drinking water or NAC containing



water ( $p < 0.05$ ,  $n = 6$ ). Administration of water containing NAC to APP/PS-1 mice reduced the levels of protein carbonyls, 3-NT and protein-bound HNE significantly compared to the levels in brain isolated from APP/PS-1 mice given normal drinking water ( $p < 0.05$ ,  $n = 6$ ).

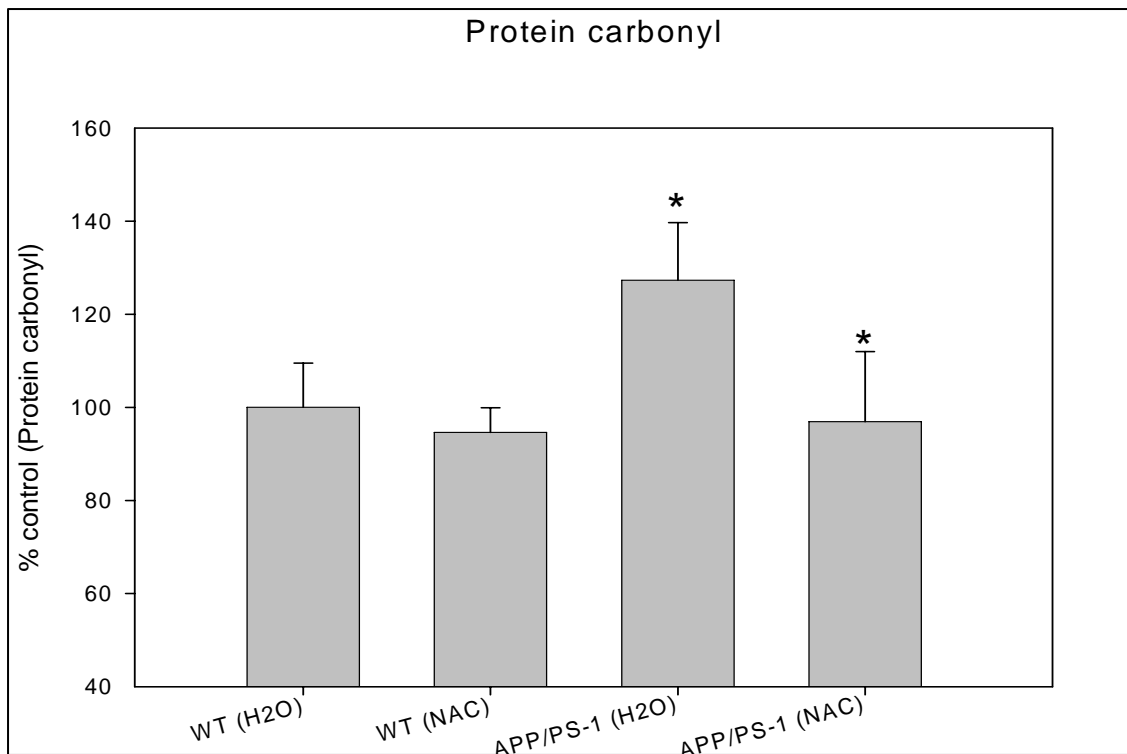


**Figure 11.1:** Levels of protein carbonyl in all the treatment groups. There is a significant increase in protein carbonyl level in brain isolated from APP/PS-1 mice that were given normal drinking water when compared to WT groups (\*  $p < 0.05$ ,  $n = 6$ ). Administration of NAC in drinking water to APP/PS-1 mice decreases protein carbonyl level significantly in brain. The brain isolated from APP/PS-1 mice treated with NAC in water shows a significant decrease in protein carbonyl levels when compared to the levels in brain isolated from APP/PS-1 mice that were given normal drinking water (\*  $p < 0.05$ ,  $n = 6$ ). The data are presented as mean  $\pm$  SEM expressed as percentage of control.

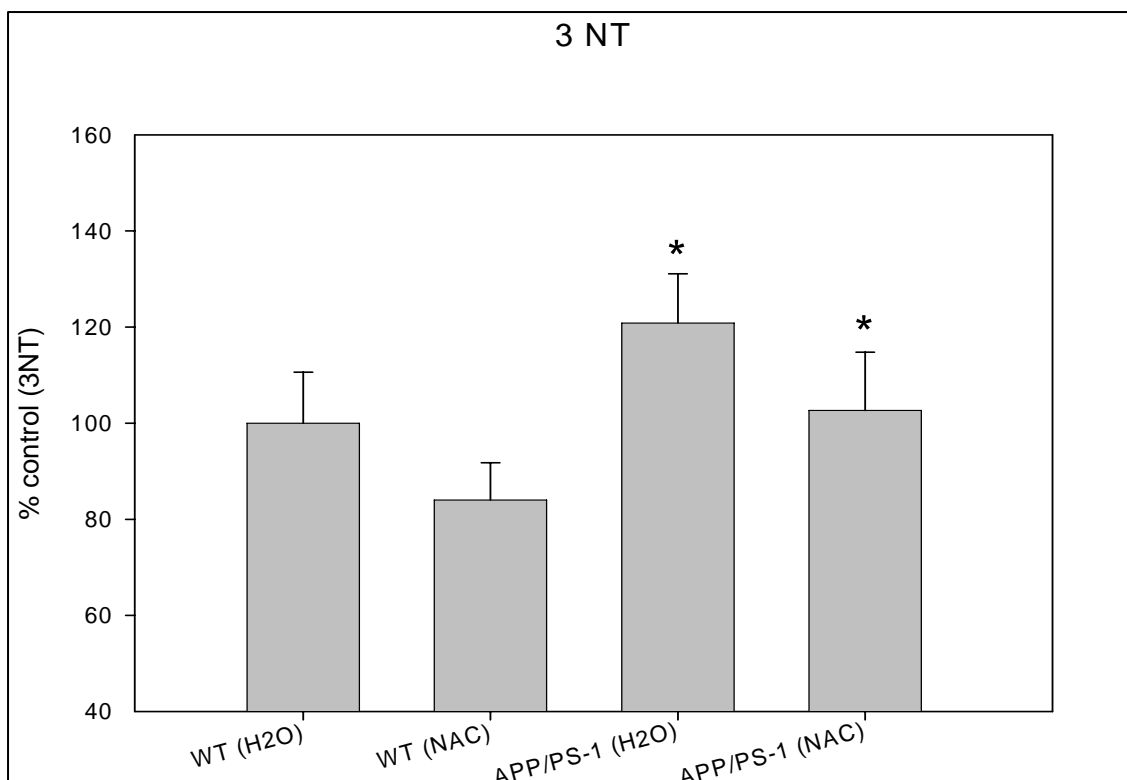


**Figure 11.2:** Levels of 3NT in all the treatment groups. There is a significant increase in 3NT level in brain isolated from APP/PS-1 mice that were given normal drinking water when compared to WT groups (\*  $p < 0.05$ ,  $n = 6$ ). Administration of NAC in drinking water to APP/PS-1 mice decreases 3NT level significantly in brain. The brain isolated from APP/PS-1 mice treated with NAC in water shows a significant decrease in 3NT levels when compared to the levels in brain isolated from APP/PS-1 mice that were given normal drinking water (\*  $p < 0.05$ ,  $n = 6$ ). The data are presented as mean  $\pm$  SEM expressed as percentage of control.

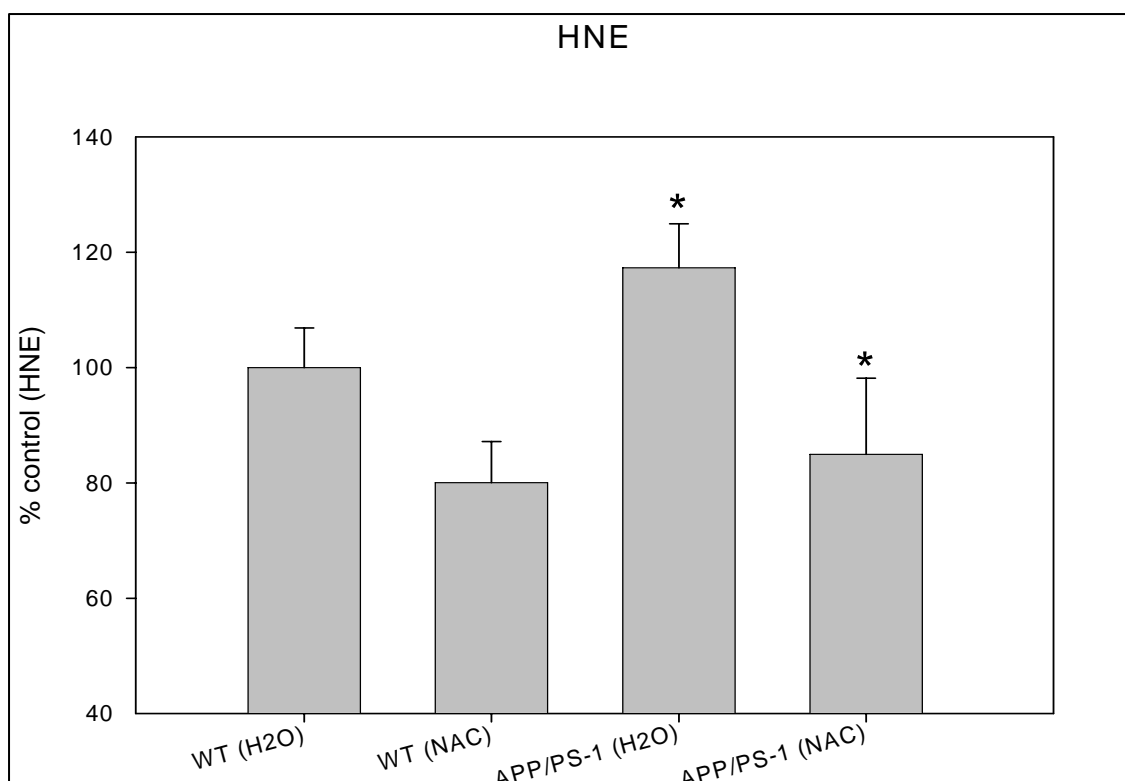


**Figure 11.3:** Levels of protein-bound HNE in all the treatment groups. There is a significant increase in protein-bound HNE level in brain isolated from APP/PS-1 mice that were given normal drinking water when compared to WT groups (\*  $p < 0.05$ ,  $n = 6$ ). Administration of NAC in drinking water to APP/PS-1 mice decreases protein-bound HNE level significantly in brain. The brain isolated from APP/PS-1 mice treated with NAC in water shows a significant decrease in protein-bound HNE levels when compared to the levels in brain isolated from APP/PS-1 mice that were given normal drinking water (\*  $p < 0.05$ ,  $n = 6$ ). The data are presented as mean  $\pm$  SEM expressed as percentage of control.

#### **11.6.2. NAC increased GPx expression and activity in APP/PS-1 mice brain**

Figure 11.4a, b and 11.5 shows the expression and activity of GPx in all the treatment groups. There was significant reduction in GPx expression and activity in brain isolated from 9 month-old APP/PS-1 mice that were given normal water when compared to the GPx expression and activity in brain isolated from 9 month-old WT mice given normal drinking water or NAC containing water ( $p < 0.05$ ,  $n = 6$ ). Administration of water containing NAC to APP/PS-1 mice significantly increased the protein expression and activity of GPx when compared to the levels in brain isolated from 9 month-old APP/PS-1 mice given normal drinking water ( $p < 0.05$ ,  $n = 6$ ).

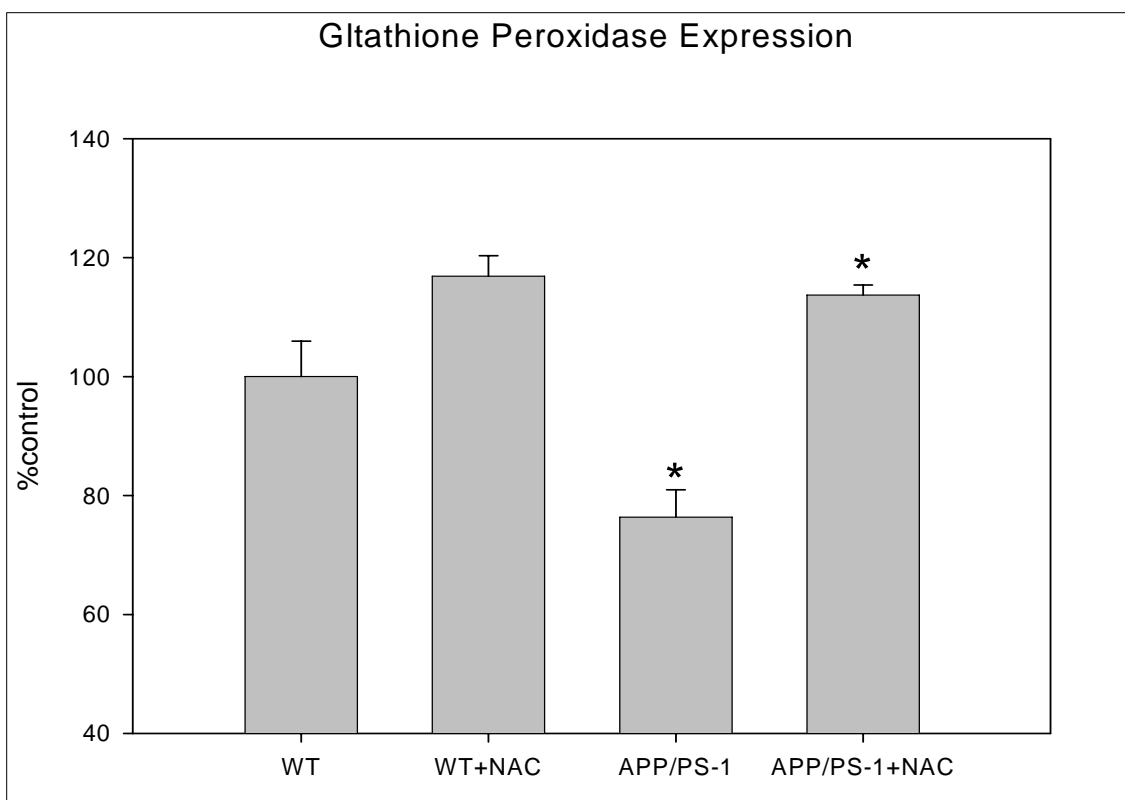


**Figure 11.4a:** Levels of GPx in all the treatment groups. There is a significant decrease in GPx level in brain isolated from APP/PS-1 mice that were given normal drinking water when compared to WT groups (\*  $p < 0.05$ ,  $n = 3$ ). Administration of NAC in drinking water to APP/PS-1 mice increased GPx level significantly in brain. The brain isolated from APP/PS-1 mice treated with NAC in water shows a significant increase in GPx levels when compared to the levels in brain isolated from APP/PS-1 mice that were given normal drinking water (\*  $p < 0.05$ ,  $n = 3$ ). The data are presented as mean  $\pm$  SEM expressed as percentage of control.

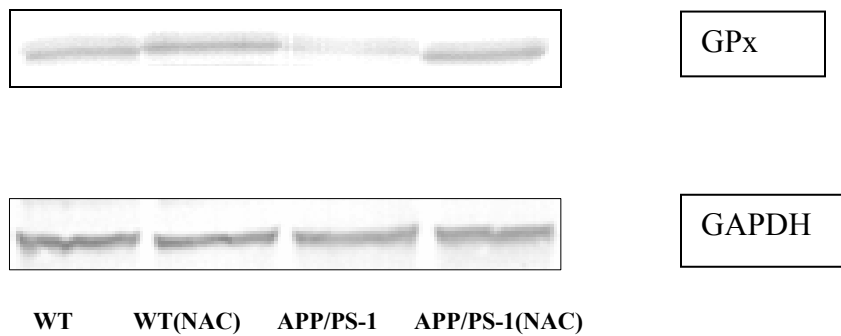


**Figure 11.4b:** A representative western blot showing levels of GPx in various treatment groups. GAPDH was used as loading control.

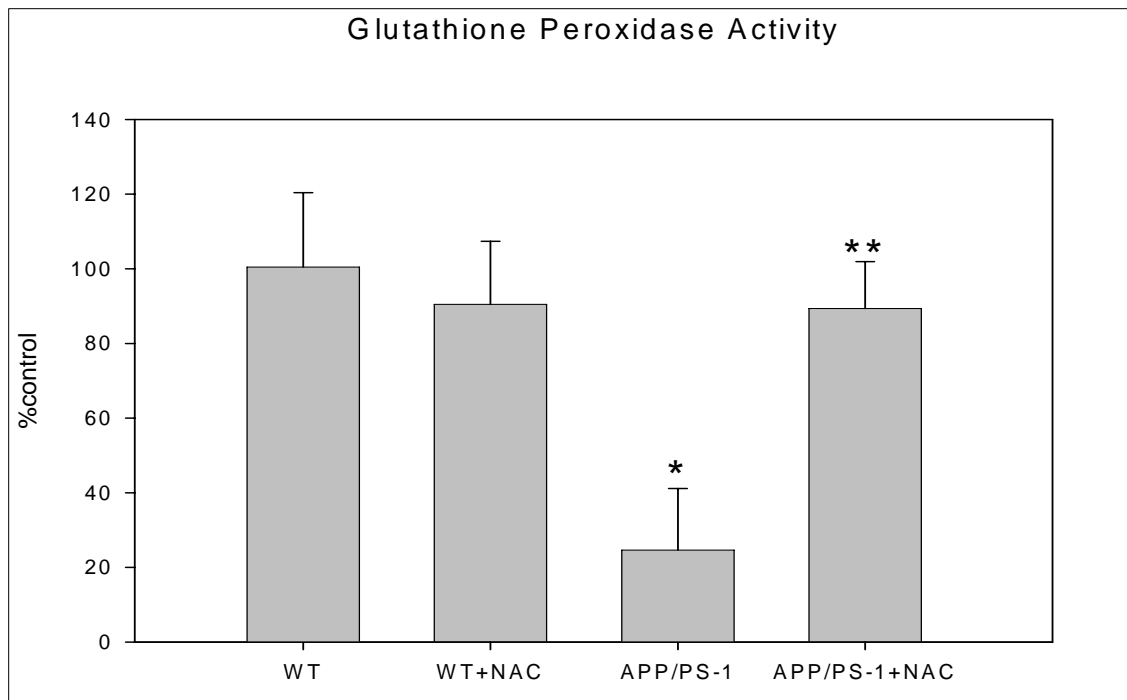


**Figure 11.5:** Activity of GPx in all the treatment groups. There is a significant decrease in GPx activity in brain isolated from APP/PS-1 mice that were given normal drinking water when compared to WT groups (\*  $p < 0.05$ ,  $n = 6$ ). Administration of NAC in drinking water to APP/PS-1 mice increased GPx activity significantly in brain. The brain isolated from APP/PS-1 mice treated with NAC in water shows a significant increase in GPx activity when compared to the activity in brain isolated from APP/PS-1 mice that were given normal drinking water (\*  $p < 0.05$ ,  $n = 6$ ). The data are presented as mean  $\pm$  SEM expressed as percentage of control.

### 11.7. Discussion

Oxidative stress has been implicated in MCI and AD (Butterfield, Drake et al., 2001; Keller, Schmitt et al., 2005; Butterfield, Poon et al., 2006; Butterfield, Reed et al.,

2006). Previous studies from our laboratory and others have shown that A $\beta$ (1-42) is associated with free radical generation leading to proteins and lipids oxidation (Varadarajan, Yatin et al., 2000; Butterfield, Drake et al., 2001; Butterfield and Lauderback, 2002). A comprehensive model for neurodegeneration in AD combining two established notions, *viz.*, elevated oxidative stress in AD brain and centrality of A $\beta$  in the cause and consequences of this dementing disorder (Butterfield and Lauderback, 2002; Castegna, Thongboonkerd et al., 2003) was developed by our laboratory. Based on these and several other well documented notions that support that oxidative stress may be central to the A $\beta$ -driven neurodegeneration, treatment with brain accessible antioxidants may be a promising approach for slowing disease progression and oxidative damage that may be responsible for the cognitive and functional decline observed in MCI or AD.

The oxidation of proteins by free radicals-mediated protein oxidation may be responsible for damaging enzymes critical in neuronal function (Varadarajan, Yatin et al., 2000; Butterfield, Boyd-Kimball et al., 2003). By using proteomics, our laboratory showed some of the critical proteins that are oxidized in AD and MCI (Castegna, Aksenov et al., 2002a; Castegna, Aksenov et al., 2002b; Castegna, Thongboonkerd et al., 2003; Butterfield, Poon et al., 2006). One such protein was peptidyl-prolyl cis/trans isomerase (Pin 1). Pin 1 is oxidatively dysfunctional in AD (Sultana, Boyd-Kimball et al., 2006a) and MCI (Butterfield, Poon et al., 2006) and is down-regulated in AD brain (Sultana, Boyd-Kimball et al., 2006a). The present results demonstrate elevated levels of Pin 1 in 9 month-old APP/PS-1 mice treated with NAC in drinking water compared to the levels in 9 month-old APP/PS-1 mice given drinking water. The oxidative modification of proteins either by introduction of carbonyl functionality or by nitration of tyrosine



residues leads to formation of protein-protein cross-linked aggregates that often changes the conformation, including protein unfolding of functional protein, thereby rendering a protein inactive (Butterfield and Stadtman, 1997; Stadtman and Berlett, 1997). In the present study, we showed the ability of *in vivo* NAC to provide neuroprotection against protein oxidation as indexed by protein carbonyls and 3NT (Stadtman and Berlett, 1997), in APP/PS-1 mice on subsequently isolated brain. There was a significant reduction in protein oxidation in brain isolated from AAP/PS-1 mice that were given NAC in drinking water when compared to the protein oxidation in brain isolated from APP/PS-1 mice that were given normal drinking water. This implicate the efficacy of NAC in preventing A $\beta$ (1-42)-mediated protein oxidation in he model of MCI or early AD.

Elevated level of lipid peroxidation products, such as HNE and acrolein are observed in AD and MCI brain and in a model of MCI (Sayre, Zelasko et al., 1997; Lauderback, Hackett et al., 2001; Butterfield, Reed et al., 2006; Mohmmad Abdul, Sultana et al., 2006). These reactive alkenals form the immediate substrate for GSH (Lovell, Xie et al., 1998; Xie, Lovell et al., 1998). These lipid peroxidation products are also known to be involved in apoptosis, which is seen as a consequence of GSH depletion (Mark, Lovell et al., 1997). HNE and other reactive alkenals can bind to the functional protein and render them inactive (Lauderback, Hackett et al., 2001). In the present study we looked at the levels of protein-bound HNE in all the groups. There was a significant reduction in protein-bound HNE levels in brain isolated from AAP/PS-1 mice that were given NAC in drinking water when compared to the protein-bound HNE levels in brain isolated from APP/PS-1 mice that were given normal drinking water (Figure 11.3). The increase in endogenous GSH levels following *in vivo* administration of NAC (Pocernich,

La Fontaine et al., 2000) may be the reason behind decreased HNE levels. Reduce the level of lipid peroxidation product implicate less oxidative stress (Butterfield and Lauderback, 2002).

Decreased levels of GSH are associated with aging and neurodegeneration (Liu and Choi, 2000; Butterfield, Castegna et al., 2002a) and therapeutic interventions based on elevation of GSH levels have been shown to be protective against oxidative stress conditions of the brain (Koppal, Drake et al., 1999a; Pocernich, Cardin et al., 2001). A variety of well established potential antioxidant compounds are under investigation to prevent A $\beta$ -induced toxic effects (Anderson and Luo, 1998; Behl, 2002; Grundman and Delaney, 2002; Boyd-Kimball, Sultana et al., 2005c). Previously our laboratory showed elevated GSH levels in NAC injected mice and its protective effect on protein and lipid oxidation against hydroxyl radical and peroxynitrite-mediated oxidative stress (Koppal, Drake et al., 1999a; Pocernich, La Fontaine et al., 2000). In the present study we measured the expression and activity of one of the key GSH related enzyme, GPx. GPx protects the neurons from oxidative stress by catalyzing the reduction of H<sub>2</sub>O<sub>2</sub> at the expense of GSH (Sies, 1999; Hansen, Go et al., 2006). There was a significant elevation in protein expression levels of GPx in brain isolated from AAP/PS-1 mice that were given NAC in drinking water when compared to the levels in brain isolated from APP/PS-1 mice that were given normal drinking water. Consistent with the increased GPx expression, we also observed an increased activity of GPx enzyme in brain isolated from AAP/PS-1 mice that were given NAC in drinking water when compared to the GPx activity in brain isolated from APP/PS-1 mice that were given normal drinking water. A lower expression and activity of GPx in APP/PS-1 mice implicate less clearance of H<sub>2</sub>O<sub>2</sub>

and increased ROS. NAC increases the activity and expression of GPx, *in vivo*, thereby more clearance of H<sub>2</sub>O<sub>2</sub> and less ROS-mediated protein oxidation and lipid peroxidation as observed in this study.

The ability of *in vivo* NAC to prevent inherent oxidative stress, possibly due to increased A $\beta$ (1-42), in this APP/PS-1 mouse model of MCI and AD could also be related to its other properties, such as its function as anti-inflammatory and as activator of several other protective signaling pathways as discussed earlier. Thus, we suggest that multiple biological functions of NAC could potentially contribute to counteract A $\beta$ -driven neurotoxicity in the APP/PS-1 mice brain. Preliminary result also suggest that NAC increases the expression of Pin 1 (data not shown), a cell cycle protein, that is known to be oxidatively modified and down-regulated in AD brain (Sultana, Boyd-Kimball et al., 2006a). However, its potential antioxidant property and role as GSH precursor is clear. Consistent with this notion, we showed decreased protein oxidation and lipid peroxidation in APP/PS-1 mice administered NAC, *in vivo* (Figure 11.1-11.3). The study also suggests that administration of lower concentration of NAC over a period of time could act as a preventive measure towards oxidative stress-mediated neurodegenerative disorders, such as MCI. In conclusion, the present study demonstrated the ability of NAC to act as a potent antioxidant *in vivo*, thereby providing neuroprotection against A $\beta$ -induced inherent oxidative stress in model of MCI or AD, although additional studies are required to determine if this notion has merit. Studies to elucidate the mechanistic aspects of neuroprotection by NAC in APP/PS-1 mouse model of AD are on progress.

## Chapter 12

### Conclusion and future studies

#### 12.1 Conclusions

The work in this dissertation examined antioxidant properties of a GSH mimetic and GSH precursor against oxidative stress-mediated neurodegenerative disorders. Specifically, the role of *in vivo* D609 protection against  $\text{Fe}^{2+}/\text{H}_2\text{O}_2$ , AAPH and  $\text{A}\beta$  (1-42)-mediated oxidative stress in brain synaptosomes or mitochondria, the ability of *in vivo* GCEE to reduce ADR-mediated oxidative stress in brain, and *in vivo* NAC-mediated protection against oxidative stress in APP/PS-1 mouse model of AD were examined.

The protection of synaptosomes and mitochondria, *in vivo*, by D609 is arguably due to presence of the thiol group in D609 that forms basis for its antioxidant property. Our group previously showed that the methylated derivative of D609 is inactive against oxidative stress-mediated by  $\text{A}\beta$  (1-42) in neuronal cultures (Sultana, Shelley et al., 2004). The thiol group in D609 could react with lipid peroxidation products and form Michael adducts and prevent these reactive lipid peroxidation products from causing neurotoxicity. Intraperitoneal (i.p.) injection of D609 (50mg/kg) to gerbils, followed by isolation of synaptosomes and mitochondria from brain showed protection against oxidative stress-mediated by  $\text{Fe}^{2+}/\text{H}_2\text{O}_2$ , AAPH and  $\text{A}\beta$  (1-42) when compared to their respective control that were injected i.p. with saline. Furthermore, a significant alteration of the GSH/GSSG ratio towards more oxidized form was observed in brain mitochondria isolated from saline-injected gerbils that were subsequently treated with  $\text{Fe}^{2+}/\text{H}_2\text{O}_2$ , AAPH and  $\text{A}\beta$  (1-42). D609 maintained the GSH/GSSG ratio towards the more reduced form in mitochondria isolated from D609-injected gerbils subsequently treated with

$\text{Fe}^{2+}/\text{H}_2\text{O}_2$ , AAPH and  $\text{A}\beta$  (1-42) when compared to control. These studies on an animal model could form the basis for eventual treatment strategies for oxidative stress related neurodegenerative disorders.

GCEE, a GSH precursor, was used to study its antioxidant properties against ADR-mediated oxidative stress. We observed that ADR, a cancer chemotherapeutic drug, is involved in oxidative stress in brain. Injection (i.p.) of ADR (20 mg/kg) causes significant protein oxidation and lipid peroxidation in brain. ADR also increases the expression of detoxification enzyme and protein, GST and MRP-1, respectively, in brain and alters GSH levels and GSH-dependent enzyme activities. By using redox proteomics we identified several important proteins that were oxidized in brain isolated from ADR-injected mice when compared to control. *In vivo* GCEE (150 mg/kg) showed protection against ADR-mediated alteration in GSH levels and significantly decreased protein oxidation and lipid peroxidation in brain isolated from ADR-injected mice that were previously injected with GCEE. The protection of brain against the oxidative damage caused by *in vivo* ADR by GCEE is consistent with previous other studies in which GCEE protected neurons *in vitro* AD-related amyloid beta-peptide (Boyd-Kimball, Sultana et al., 2005c) or brain *in vivo* against peroxynitrite-induced oxidative stress (Drake, Kanski et al., 2002). Further studies on an animal model could form the basis for an eventual treatment strategy for preventing oxidative stress mediated by ADR. The results shown in this dissertation research suggest that GCEE-mediated increment in brain GSH levels and the activity of GST could be a potential therapeutic approach towards modulating cognitive impairment in patients undergoing chemotherapy.

Lastly, NAC, a GSH precursor, was examined in the APP/PS-1 mouse model of AD. NAC was given to the mice in their drinking water (2mg/kg/day) over a period of five months and oxidative stress parameters were studied. The results reported in this dissertation research showed that NAC has ability to reduce brain protein oxidation and lipid peroxidation in APP/PS-1 mice that our group had shown was due to A $\beta$  (1-42) (Mohammad Abdul, Sultana et al., 2006). APP/PS-1 mice are known to show an accelerated A $\beta$  production in brain and have pathology reminiscent of that AD brain. Apart from protecting brain from protein oxidation and lipid peroxidation, NAC also increased the protein expression levels of several antioxidants and the key modulatory protein, Pin 1, in brain isolated from APP/PS-1 mice when compared to wild type. NAC is a FDA-approved drug and has been used in several studies involving neurodegeneration, such as ALS, AD among others. The findings of this dissertation study is particularly relevant to AD brain because of several lines of evidence involving A $\beta$  (1-42)-mediated oxidative stress in AD brain.

## **12.2 Future studies**

Based on the findings in this dissertation, the following experiments may warrant exploration:

1. Because many neurodegenerative disorders involve mitochondrial dysfunction and our study showed that D609 can protect brain mitochondria from various oxidative stress inducers, it would be useful to look for its effect in mice models of various neurodegenerative disorders, such as AD, PD and ALS. Further, using a redox proteomics approach that can identify specifically oxidized protein, one can determine the identity of proteins specifically protected by D609 *in vivo*.

2. It is now clear from studies described in this dissertation that ADR causes oxidative stress in brain and GCEE protects against ADR-mediated oxidative stress. We used proteomics to identify proteins that are specifically oxidized and differentially expressed in brain isolated from ADR-injected mice. A similar kind of study can be useful to determine if these ADR-mediated oxidized proteins are protected by *in vivo* administration of GCEE. Further, compounds that can elevate the GSH level and have similar action as GCEE should be examined in the mice injected with ADR.

3. Preliminary studies described in this dissertation show that NAC can reduce oxidative stress in the APP/PS-1 mouse model of AD. Further studies are required to investigate the mechanistic aspects of the mode of action of NAC in its ability to protect against oxidative stress. One of the key parameters that will be useful is to examine is the levels of GSH and GSSG and their ratio in NAC-treated mice. GSH elevation could be the important factor towards NAC's ability towards protection against oxidative stress in APP/PS-1 mice. Proteomics can be used to investigate the proteins that are specifically protected from oxidation in these mouse models and should be correlated with proteomics studies conducted on human AD samples already reported from our laboratory.

## Appendix I

### ***In Vivo* Protection of Synaptosomes from Oxidative Stress Mediated by 2,2-Azobis (2-amidino-propane) Dihydrochloride (AAPH) or $\text{Fe}^{2+}/\text{H}_2\text{O}_2$ by Ferulic Acid Ethyl Ester (FAEE): Insight into Mechanisms of Neuroprotection and Relevance to Oxidative Stress Related neurodegenerative Disorders**

#### **A.1. Overview of the study**

Ferulic acid ethyl ester (FAEE) is an ester derivative of ferulic acid, the latter known for its anti-inflammatory and antioxidant properties. Previous studies from our laboratory have shown that ferulic acid protects synaptosomal membrane system and neuronal cell culture systems against hydroxyl and peroxyl radical oxidation. FAEE is lipophilic and is able to penetrate lipid bilayer. Previous studies reported that FAEE reduces Alzheimer's amyloid  $\beta$  peptide  $\text{A}\beta$  (1-42)-induced oxidative stress and cytotoxicity in neuronal cell culture by direct radical scavenging and by inducing certain antioxidant proteins. In the present study we tested the hypothesis that FAEE would provide neuroprotection against free radical oxidative stress *in vivo*. Synaptosomes were isolated from the gerbils that were previously injected intraperitoneally (i.p.) with FAEE or DMSO and were treated with oxidants,  $\text{Fe}^{2+}/\text{H}_2\text{O}_2$  or 2,2- Azobis (2-amidino-propane) dihydrochloride (AAPH). Synaptosomes isolated from the gerbil previously injected i.p. with FAEE and treated with  $\text{Fe}^{2+}/\text{H}_2\text{O}_2$  and AAPH showed significant reduction in reactive oxygen species (ROS), levels of protein carbonyl, protein bound 4-hydroxynonenal (HNE, a lipid peroxidation product), and 3-nitrotyrosine (3NT, another marker of protein oxidation formed by reaction of tyrosine residues with peroxynitrite) compared to  $\text{Fe}^{2+}/\text{H}_2\text{O}_2$  or AAPH induced oxidative stress in synaptosomes isolated from



the brain of gerbils that were previously injected with DMSO. The synaptosomes isolated from gerbil pre-injected with FAEE and subsequently treated with AAPH or  $\text{Fe}^{2+}/\text{H}_2\text{O}_2$  showed induction of heme oxygenase (HO-1) and heat shock protein 70 (HSP-70) but reduced inducible nitric oxide synthase (iNOS) levels. These results are discussed with reference to potential use of this lipophilic antioxidant phenolic compound in the treatment of oxidative stress related neurodegenerative disorders.

## **A.2. Introduction**

Alzheimer's disease (AD), an age-associated dementing disorder, and many other neurodegenerative disorders, are characterized by free radical mediated oxidative stress in brain (Hensley, Hall et al., 1995; Markesbery, 1997; Stadtman and Berlett, 1997; Butterfield, Drake et al., 2001; Kanski, Lauderback et al., 2001; Butterfield and Lauderback, 2002). AD, characterized by the presence of senile plaques, neurofibrillary tangles and loss of synapses, affects more than four million Americans and is one of the leading causes of death in United States (Katzman and Saitoh, 1991). The free radical-mediated reactive oxygen species (ROS) and reactive nitrogen species (RNS) generated in brain can lead to protein oxidation (Hensley, Hall et al., 1995; Stadtman and Berlett, 1997), DNA and RNA oxidation (Gabbita, Lovell et al., 1998; Lovell, Gabbita et al., 1999; Butterfield, Drake et al., 2001), lipid peroxidation (Sayre, Zelasko et al., 1997; Markesbery and Lovell, 1998; Butterfield and Lauderback, 2002) and neuronal dysfunction or death. Increased production of ROS and RNS along with depletion in antioxidant capacity is observed in AD and other neurodegenerative disorders (Butterfield, 1997; McIntosh, Trush et al., 1997; Omar, Chyan et al., 1999; Varadarajan, Yatin et al., 2000). Proteomics analysis of protein from AD brain and from models

thereof, demonstrates oxidative modification of key proteins that are involved in metabolism, excitotoxicity, proteosomal function, lipid asymmetry and redox balance in brain (Castegna, Aksenov et al., 2002a; Castegna, Aksenov et al., 2002b; Calabrese, Stella et al., 2004; Poon, Calabrese et al., 2004). Several lines of evidence show that in models of AD, oxidative stress leads to lipid peroxidation, which releases reactive alkenals that binds to proteins and cause their dysfunction (Mark, Lovell et al., 1997; Sayre, Zelasko et al., 1997; Subramaniam, Roediger et al., 1997; Markesbery and Lovell, 1998; Butterfield and Lauderback, 2002). It has also been reported that ROS and RNS mediated oxidative stress leads to apoptosis in neuronal cell cultures (Butterfield, Castegna et al., 2002b; Butterfield and Lauderback, 2002). Hence, ROS and RNS generation becomes important in understanding oxidative stress and oxidative stress related disorders.

Antioxidant intervention is gaining significance as a promising therapeutic strategy in treating neurological disorders, and many antioxidants and chemicals that mimic antioxidants in the free radical scavenging properties are under investigation (Xie, Lovell et al., 1998; Halliwell, 2001; Pocernich, Cardin et al., 2001; Drake, Kanski et al., 2002; Boyd-Kimball, Sultana et al., 2005c; Joshi, Sultana et al., 2005a). Natural plant products are been studied in great deal with reference to antioxidant therapy for neurodegenerative disorders as they have minimal pathological and toxic side effects associated with oxidative stress (Halliwell, 2001; Butterfield, Castegna et al., 2002a) in contrast to side effects of a number of synthetic drugs.

Ferulic acid (4-hydroxy-3-methoxycinnamic acid) is a phenolic compound and a component of fruits and vegetables, such as tomatoes. Ferulic acid has *in vitro* free

radical scavenging properties toward hydroxyl radical, peroxynitrite and oxidized low-density lipoprotein (Yu, Hong et al., 1999; Kanski, Aksenova et al., 2002; Kikuzaki, Hisamoto et al., 2002; Ogiwara, Satoh et al., 2002). *In vivo* protection against [A $\beta$  (1-42)]-induced toxicity in brain and also suppression of [A $\beta$  (1-42)]-mediated immunoreactivities of the astrocyte marker glial fibrillary acidic protein (GFAP) and interleukin-1 beta (IL-1 beta) in the hippocampus have been reported (Kim, Cho et al., 2004). Studies from our lab showed protective effects of ferulic acid towards hydroxyl and peroxy free radical-mediated oxidative stress in synaptosomes and neuronal cell culture (Kanski, Aksenova et al., 2002).

Ferulic acid ethyl ester (FAEE) (Ethyl 4-hydroxy-3-methoxycinnamate) (Figure A.1) is the ethyl ester, derivative of ferulic acid, the latter known for its anti-inflammatory and antioxidant properties as noted above (Yan, Cho et al., 2001; Kikuzaki, Hisamoto et al., 2002). The ester group of FAEE make the compound more hydrophobic and lipophilic when compared to ferulic acid and hence a better potential antioxidant with respect to brain (Scapagnini, Butterfield et al., 2004). FAEE induces expression of heme oxygenase (HO-1) in astrocytes at both the message and protein levels (Scapagnini, Butterfield et al., 2004; Sultana, Ravagna et al., 2005) produces biliverdin and eventually bilirubin, both known for their antioxidant activity (Scapagnini, Butterfield et al., 2004; Sultana, Ravagna et al., 2005). Recently, our laboratory characterized the protective effect of FAEE on the *in vitro* oxidative stress induced by A $\beta$  (1-42) in rat primary neuronal cell culture by inducing HO-1 and heat shock protein 72 (HSP-72) and by suppressing inducible nitric oxide synthase (iNOS) (Sultana, Ravagna et al., 2005).

### A.3. Purpose of the study

The present study was designed to test the hypothesis that FAEE *in vivo* would protect synaptosomes subsequently isolated from gerbils against oxidative stress induced by  $\text{Fe}^{2+}/\text{H}_2\text{O}_2$  (hydroxyl radical formation) and AAPH (alkoxyl and peroxy radical formation). We examined whether the *in vivo* protective effect of FAEE on oxidative damage in synaptosomes might be mediated by increased expression of HO-1 and HSP-70 and decreased expression of iNOS, as is the case *in vitro* (Sultana, Ravagna et al., 2005).

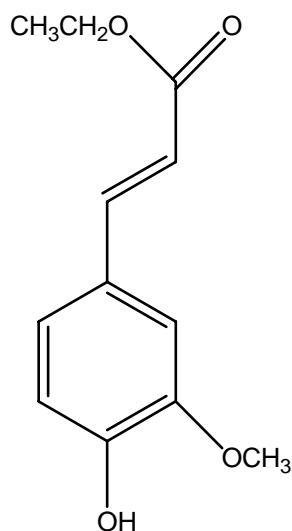


**Figure A.1:** Ethyl 4-hydroxy-3-methoxycinnamate or Ferulic acid ethyl ester (FAEE)

### A.4. Experimentals

#### A.4.1. Animals

For all the studies male Mongolian gerbils (2-3 months of age), approximately 80 g in size, housed in the University of Kentucky Central Animal Facility in 12-h

light/dark conditions and fed standard Purina rodent laboratory chow *ad libitum*, were used. The University of Kentucky Animal Care and Use Committee approved the animal protocols. The animals were divided in three groups. One group was injected i.p. with 150-mg/kg bodyweight of FAEE (dissolved in dimethyl sulfoxide [DMSO]) one hour prior to decapitation and the other groups were given equivalent amount of DMSO at the same time. The concentration and time of FAEE were based on dose-dependent and time-dependent responses (data not shown).

#### **A.4.2. Chemicals**

All chemicals, including FAEE, were purchased from Sigma-Aldrich (St. Louis, MO), unless stated otherwise. Fresh 10 mM stock solution of 2,7-dichlorofluorescein diacetate (DCFH-DA) was prepared in ethanol for the DCF fluorescence assay. Fresh FAEE was prepared in DMSO. The protein oxidation detection kit was purchased from InterGen (Purchase, NY) and primary antibody for HNE and 3NT were purchased from Chemicon International. Anti-HO-1, anti-iNOS, anti-HSP-70 and anti- $\beta$ -actin primary antibodies and alkaline phosphatase-conjugated secondary antibodies were purchased from Santa Cruz Biotechnology (Santa Cruz, CA).

#### **A.4.3. Preparation of Synaptosomes**

Synaptosomes were isolated from gerbils injected i.p. with DMSO (control) or with FAEE (150mg/kg body weight), 1h after injection. The synaptosomal isolation procedure has been described elsewhere (Whittaker, 1993). Briefly, the gerbils were sacrificed by decapitation and the brain was isolated on a cold plate and placed in 0.32M sucrose isolation buffer containing 4 $\mu$ g/ml leupeptin, 4 $\mu$ g/ml pepstatin, 5  $\mu$ g/ml aprotinin, 2mM ethylenediaminetetraacetic acid (EDTA), 2mM ethylene glycol-bis(tetraacetic acid

(EGTA) and 20mM 4-(2-hydroxyethyl)-1-piperazine-ethanesulfonic acid (HEPES), trypsin inhibitor (20 $\mu$ g/ml), and 0.2mM phenylmethanesulfonyl fluoride (PMSF), pH 7.4. The whole brain was homogenized by 20 passes with a Wheaton tissue homogenizer. The homogenate was centrifuged at 1500 g for 10 min. The pellet was discarded and the supernatant was retained and centrifuged at 20000 g for 10 min. The resulting pellet was resuspended in approximately 1ml of 0.32M sucrose isolation buffer and layered over a discontinuous sucrose gradient (0.85M pH 8.0, 1.0M pH8.0, 1.18M pH8.5 sucrose solutions each containing 2mM EDTA, 2mM EGTA and 10mM HEPES) and spun at 82500 g for 1h at 4° C. The purified synaptosomes were collected from the sucrose gradient interface at the 1.0/1.18M interface and twice washed with phosphate buffered saline containing 0.01% (w/v) sodium azide and 0.2% (v/v) Tween 20 (PBS) and centrifuged at 32000 g. The resulting synaptosomal membranes were assayed for protein concentration by Pierce BCA method (Bradford, 1976). The synaptosomes obtained were divided in two aliquots. One aliquot was incubated with 30  $\mu$ M FeSO<sub>4</sub> and 10 mM H<sub>2</sub>O<sub>2</sub>, and the other aliquot was incubated with 1mM AAPH for 1h at 37° C. Both the concentrations were based on prior studies (Joshi, Sultana et al., 2005a). The synaptosomes isolated from DMSO-injected gerbils were treated with equal volume of buffer. The synaptosomal samples were washed following incubation and suspended in PBS for further studies.

#### **A.4.4. DCF fluorescence**

The DCF fluorescence procedure has been described elsewhere (Wang and Joseph, 1999). Briefly, 10  $\mu$ M DCFH-DA was incubated with synaptosomes (1mg/ml) for 30 minutes at 37° C. Intracellular esterases convert DCFH-DA into anionic DCFH,

which because of its negative charge is trapped in the synaptosomes. Upon oxidation with ROS, the non-fluorescent DCFH is converted to fluorescent 2,7- dichlorofluoroscein (DCF). Synaptosomes were spun at 3000 g in a tabletop Eppendorf centrifuge for 5 minutes at 4° C. Synaptosomes were suspended in 500 µl of PBS and loaded in triplicate (100 µl per well) in a black microtiter plate and the fluorescence was measured in a Spectramax microtiter plate reader ( $\lambda_{\text{ex}} = 495\text{nm}$ ,  $\lambda_{\text{em}} = 530\text{nm}$ ) and quantified using softPro max software. Similar studies were performed with an oxidation-insensitive dye CDCF-DA (C369) to determine whether ester cleavage or efflux of the dye might contribute to changes in fluorescence.

#### **A.4.5. Protein carbonyls**

Protein carbonyls are the markers of protein oxidation and were assessed by following the standard protocol described elsewhere (Stadtman and Berlett, 1997). Samples (5 µl), 12% sodium dodecyl sulfate (SDS) and 10 times diluted 2,4-dinitrophenylhydrazine (DNPH) (10µl) from a 200 mM stock solutions, were incubated at room temperature for 20 min. Samples were neutralized with 7.5µl neutralization solution (2M Tris in 30% glycerol). The resulting solution was loaded in each well on a nitrocellulose membrane under vacuum using a slot blot apparatus. The membrane was blocked in blocking buffer (3% bovine serum albumin) for 1h and incubated with a 1:100 dilution of anti DNP polyclonal antibody in phosphate buffered saline containing 0.01% (w/v) sodium azide and 0.2% (v/v) Tween 20 (PBS) for 1h. The membrane was washed three times in PBS and was incubated for 1 h with an anti-rabbit IgG alkaline phosphatase secondary antibody diluted in PBS in a 1:8000 ratio. The membrane was washed for three times in PBS for 5 min and developed in Sigma Fast tablets (BCIP/NBT

substrate). Blots were dried, scanned with Adobe Photoshop, and quantified with Scion Image (PC version of Macintosh compatible NIH image).

#### **A.4.6. HNE**

Samples (5  $\mu$ l) (normalized to 4mg/ml), 5 $\mu$ l of 12% sodium dodecyl sulfate (SDS) and 5 $\mu$ l of modified Laemmli buffer containing 0.125 M Tris base pH 6.8, 4% (v/v) SDS, and 20% (v/v) glycerol were incubated for 20 minutes at room temperature. Samples (250 ng) were loaded in each well on a nitrocellulose membrane in a slot blot apparatus under vacuum. The membrane was blocked as above and incubated with a 1: 5000 dilution of anti-HNE polyclonal antibody in PBS for 1 h 30 min. The membrane was developed as described above.

#### **A.4.7. 3NT**

Sample (5  $\mu$ l) (normalized to 4mg/ml), 5 $\mu$ l of 12% sodium dodecyl sulfate (SDS) and 5 $\mu$ l of modified Laemmli buffer containing 0.125 M tris base pH 6.8, 4% (v/v) SDS, and 20% (v/v) glycerol were incubated for 20 minutes at room temperature, and the membranes were developed as described above except a 1:2000 dilution of anti-3-NT polyclonal antibody was used.

#### **A.4.8. Specificity of HNE and 3-NT antibodies**

The specificity for both HNE and 3NT primary antibodies was checked as described elsewhere (Scapagnini, Butterfield et al., 2004). For example, the samples were treated with either the HNE or 3NT primary antibody reacted with free HNE or free 3-NT, respectively. Very faint, non-specific binding was seen on the HNE blot (data not shown) that was accounted in the background for each blot. No staining was seen on the



3-NT blot, suggesting that there was no non-specific binding of the primary 3-NT antibody (data not shown).

#### **A.4.9. Western blots**

Mixtures of loading buffer and synaptosome samples (100 µg) were denatured and electrophoresed on a 10% SDS-polyacrylamide gel. Proteins were transferred to nitrocellulose at 90 mA/gel for 2 h. The blots were blocked for 1 h in fresh wash buffer (10 mM tris-HCl [pH7.5], 150 mM NaCl, 0.05% Tween 20, pH 7.4, containing 5% nonfat dried milk) and incubated with primary antibodies for 1 h (dilutions (1:1000) of primary anti-HSP 70, iNOS, and HO-1 antibodies were made in wash buffer with 3% nonfat dry milk). The membrane was washed three times in PBS and was incubated for 1 h with horse radish peroxidase-conjugated secondary antibodies in wash blot at room temperature. The membrane was washed again for three times in PBS for 5 min and the bands were visualized using an Amersham chemiluminiscence kit.

#### **A.5. Statistical analysis**

Analysis of variance (ANOVA) was used for comparison among the groups and statistical evaluation. Results are presented as means  $\pm$  SEM. P values < 0.05 were considered significant.

#### **A.6. Results**

##### **A.6.1. FAEE reduces ROS generation in synaptosomes**

ROS generation was measured by using the DCF assay. DCF is formed by reaction of DCFH with ROS (Wang and Joseph, 1999; Keller, Lauderback et al., 2000;

Lauderback, Kanski et al., 2002). Figure A.2a shows the ROS levels in synaptosomes isolated from DMSO-injected gerbils (control), synaptosomes isolated from DMSO-injected gerbils and subsequently treated with  $\text{Fe}^{2+}/\text{H}_2\text{O}_2$  or AAPH and synaptosomes isolated from gerbils injected i.p. previously with FAEE and subsequently treated with  $\text{Fe}^{2+}/\text{H}_2\text{O}_2$  or AAPH. As reported previously (Joshi, Sultana et al., 2005a), there was a significant increase in ROS generation in synaptosomes isolated from control gerbils that were treated with  $\text{Fe}^{2+}/\text{H}_2\text{O}_2$  or AAPH ( $p < 0.005$ ) when compared to control. Synaptosomes isolated from the FAEE-injected gerbils and subsequently treated with  $\text{Fe}^{2+}/\text{H}_2\text{O}_2$  or AAPH showed a significant decrease in ROS levels when compared to synaptosomes treated with  $\text{Fe}^{2+}/\text{H}_2\text{O}_2$  ( $p < 0.001$ ) or AAPH ( $p < 0.005$ ), which were isolated from DMSO-injected gerbils.

The oxidation-insensitive dye, CDCF-DA (C369) was used in similar studies and was used as a control experiment to ensure that ester cleavage or efflux of the DCFH was not contributing to changes in fluorescence. Figure A.2b shows that there was no change observed in the fluorescence in all the groups, confirming that changes in fluorescence shown in Figure A.2a were due to oxidation of the dye and not because of drug efflux changes or ester cleavage.

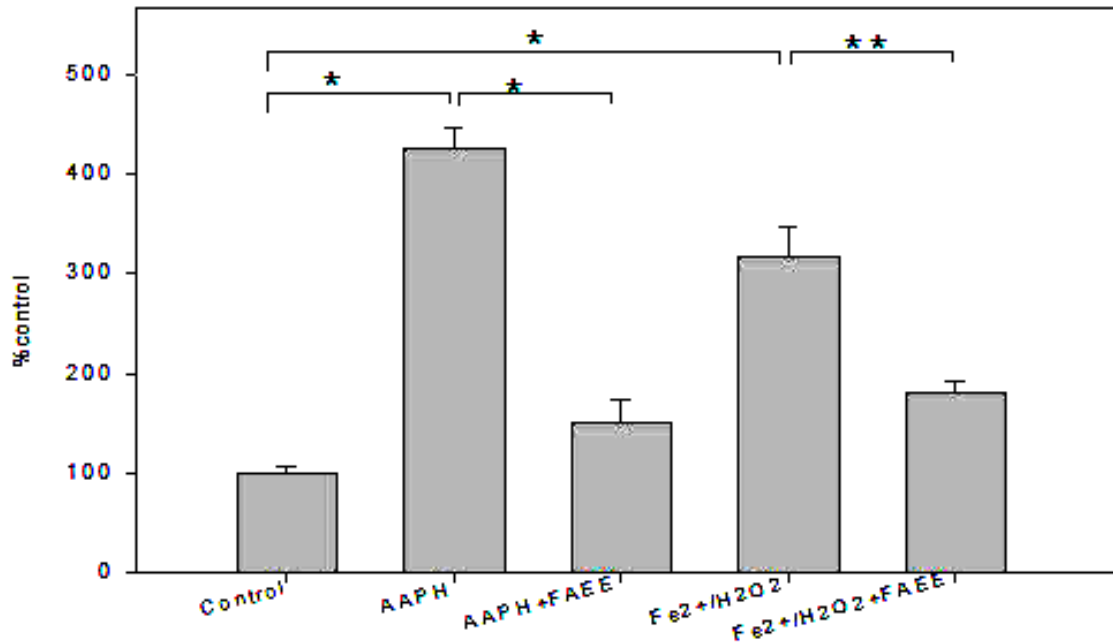


**Figure A.2a:** Significant increase in ROS in synaptosomes isolated from DMSO-injected gerbils and subsequently treated with Fe<sup>2+</sup>/H<sub>2</sub>O<sub>2</sub> or AAPH compared to ROS in synaptosomes isolated from DMSO-injected gerbils. Decreased ROS in synaptosomes isolated from gerbils injected i.p. with FAEE subsequently treated with Fe<sup>2+</sup>/H<sub>2</sub>O<sub>2</sub> or AAPH relative to ROS in synaptosomes isolated from gerbils injected with DMSO and subsequently treated with Fe<sup>2+</sup>/H<sub>2</sub>O<sub>2</sub> or AAPH, \*  $p < 0.005$ , and \*\*  $P < 0.001$ ; the data are the mean  $\pm$  SEM expressed as percentage of control values, (n = 6).

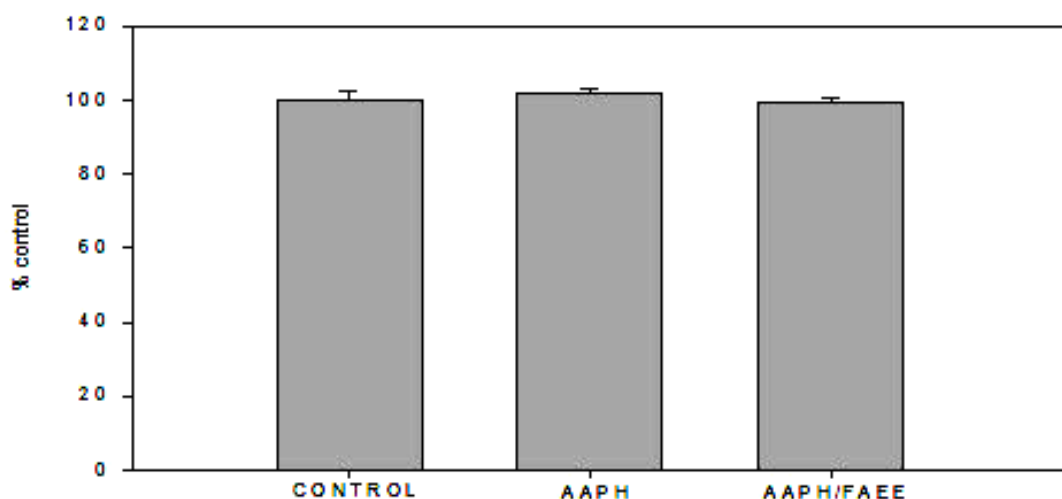


**Figure A.2b:** Measurement of ROS generation using the oxidation-insensitive probe C369. The oxidation-insensitive fluorescence probe C369 was used as control to demonstrate the results of Figure 2a are due to oxidation of DCFH and not due to drug efflux of DCFH-DA with reaction outside the synaptosomes.

#### **A.6.2. FAEE *in vivo* inhibits protein oxidation**

Protein carbonylation is one of the markers of protein oxidation (Butterfield and Stadtman, 1997). Protein carbonyl levels in synaptosomes isolated from brains of DMSO-injected gerbils (control), synaptosomes isolated from control gerbils and subsequently treated with  $\text{Fe}^{2+}/\text{H}_2\text{O}_2$  or AAPH, and  $\text{Fe}^{2+}/\text{H}_2\text{O}_2$  - or AAPH-treated synaptosomes isolated from brains of gerbils previously injected i.p. with FAEE are shown in Figure A.3a. A significant increase in protein carbonyl levels is observed in synaptosomes isolated from control gerbils and subsequently treated with  $\text{Fe}^{2+}/\text{H}_2\text{O}_2$  or AAPH ( $p < 0.005$ ) when compared to untreated control. Synaptosomes isolated from FAEE-injected gerbils and subsequently treated with  $\text{Fe}^{2+}/\text{H}_2\text{O}_2$  and AAPH showed significantly decreased protein carbonyl levels when compared to synaptosomes isolated

from DMSO-injected gerbils and subsequently treated with  $\text{Fe}^{2+}/\text{H}_2\text{O}_2$  or AAPH ( $p < 0.005$ ).

#### **A.6.3. FAEE *in vivo* prevents nitration of tyrosine residues**

3-nitrotyrosine (3-NT) is another marker of protein oxidation (Butterfield and Stadtman, 1997; Castegna, Thongboonkerd et al., 2003). Levels of 3-NT in synaptosomes isolated from the brains of DMSO-injected gerbils (control), synaptosomes isolated from control gerbils and then treated with  $\text{Fe}^{2+}/\text{H}_2\text{O}_2$  or AAPH and  $\text{Fe}^{2+}/\text{H}_2\text{O}_2$ - and AAPH-treated synaptosomes isolated from gerbils previously injected i.p. with FAEE is shown in Figure A.3b. There was a significant increase in 3-NT levels in synaptosomes isolated from DMSO-injected gerbils and subsequently treated with  $\text{Fe}^{2+}/\text{H}_2\text{O}_2$  or AAPH ( $p < 0.005$ ) when compared to those of control. Synaptosomes isolated from FAEE-injected gerbils and subsequently treated with  $\text{Fe}^{2+}/\text{H}_2\text{O}_2$  or AAPH showed a significant decrease in 3-NT levels when compared to synaptosomes isolated from DMSO-injected gerbils and then treated with  $\text{Fe}^{2+}/\text{H}_2\text{O}_2$  or AAPH ( $p < 0.005$ ).

#### **A.6.4. FAEE *in vivo* inhibits HNE formation**

Free radical attack on arachidonic acid produces reactive alkenals, such as 4-hydroxynonenal (HNE). HNE binds to proteins by Michael addition (Butterfield and Stadtman, 1997), altering their conformation, and thereby reducing their activity (Subramaniam, Roediger et al., 1997; Lauderback, Hackett et al., 2001; Zhou, Lauderback et al., 2001). Figure A.3c shows the protein-bound HNE levels in synaptosomes isolated from DMSO-injected gerbils (control), synaptosomes isolated from control gerbils and subsequently treated with  $\text{Fe}^{2+}/\text{H}_2\text{O}_2$  or AAPH, and  $\text{Fe}^{2+}/\text{H}_2\text{O}_2$ - or AAPH-treated synaptosomes isolated from gerbils previously injected i.p. with FAEE.

A significant increase in protein-bound HNE levels is observed in synaptosomes isolated from control gerbil brains treated with  $\text{Fe}^{2+}/\text{H}_2\text{O}_2$  or AAPH ( $p < 0.005$ ) when compared to control. Synaptosomes isolated from FAEE-injected gerbils and subsequently treated with  $\text{Fe}^{2+}/\text{H}_2\text{O}_2$  or AAPH showed a significant decrease in protein bound HNE levels when compared to synaptosomes isolated from DMSO-injected gerbils subsequently treated with  $\text{Fe}^{2+}/\text{H}_2\text{O}_2$  or AAPH ( $p < 0.005$ ).

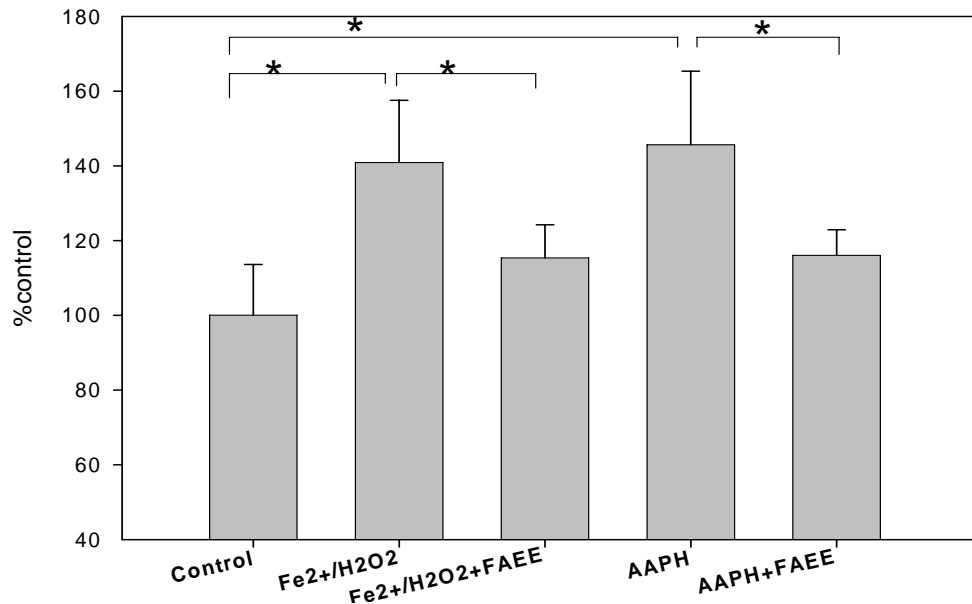


**Figure A.3a:** Significant increase in protein carbonyl levels in synaptosomes isolated from DMSO-injected gerbils and subsequently treated with Fe<sup>2+</sup>/H<sub>2</sub>O<sub>2</sub> or AAPH compared to protein carbonyls in synaptosomes isolated from DMSO-injected gerbils. Decreased protein carbonyl level in synaptosomes isolated from gerbils injected i.p. with FAEE and subsequently treated with Fe<sup>2+</sup>/H<sub>2</sub>O<sub>2</sub> or AAPH relative to protein carbonyl level in synaptosomes isolated from gerbils, injected i.p with DMSO and subsequently treated with Fe<sup>2+</sup>/H<sub>2</sub>O<sub>2</sub> or AAPH, \* p < 0. 005; the data are the mean ± SEM expressed as percentage of control values, (n = 6).

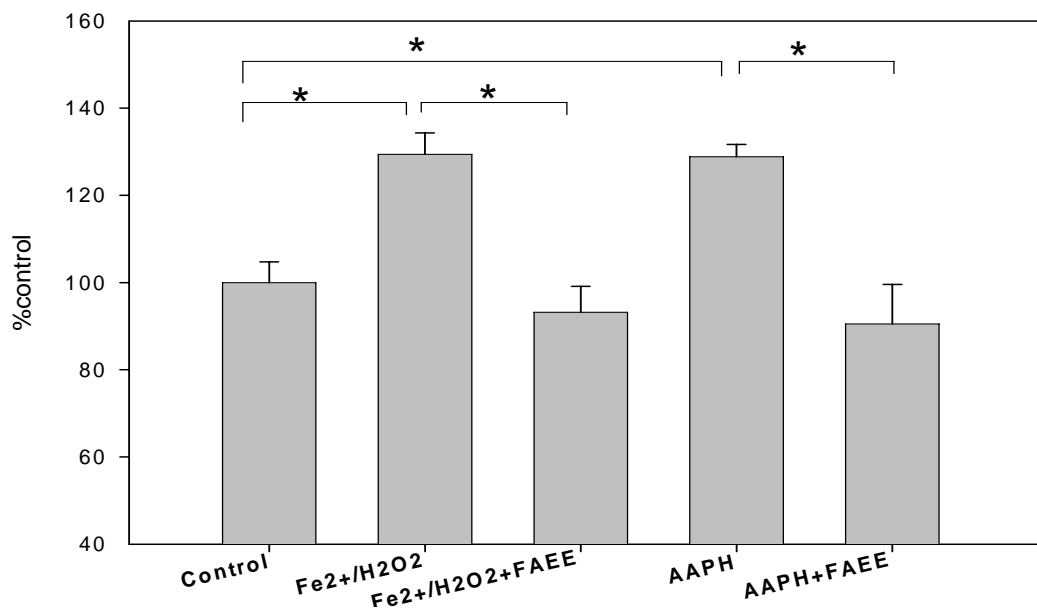


**Figure A.3b:** Significant increase in 3-NT levels in synaptosomes isolated from DMSO-injected gerbils and subsequently treated with Fe<sup>2+</sup>/H<sub>2</sub>O<sub>2</sub> or AAPH compared to 3-NT in synaptosomes isolated from DMSO-injected gerbils. Decreased 3-NT level in synaptosomes isolated from gerbils injected i.p. with FAEE and subsequently treated with Fe<sup>2+</sup>/H<sub>2</sub>O<sub>2</sub> or AAPH relative to 3-NT level in synaptosomes isolated from gerbils, injected i.p with DMSO and subsequently treated with Fe<sup>2+</sup>/H<sub>2</sub>O<sub>2</sub> or AAPH, \* p < 0. 005; the data are the mean ± SEM expressed as percentage of control values, (n = 6).



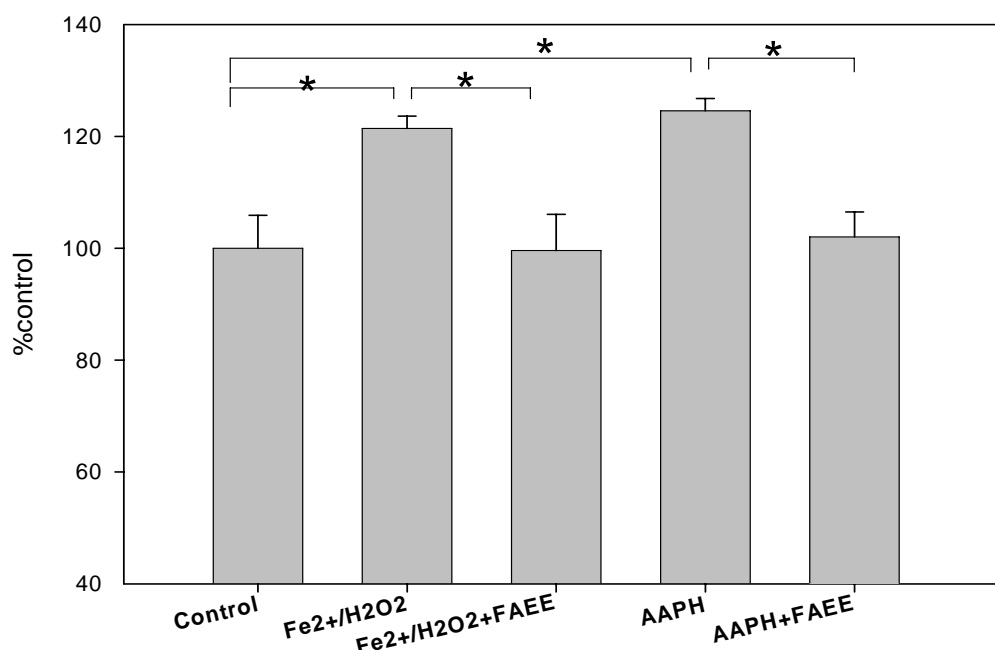


**Figure A.3c:** A significant increase in protein bound HNE levels in synaptosomes isolated from DMSO-injected gerbils and subsequently treated with Fe<sup>2+</sup>/H<sub>2</sub>O<sub>2</sub> or AAPH compared to protein bound HNE in synaptosomes isolated from DMSO-injected gerbils. Decreased protein bound HNE level in synaptosomes isolated from gerbils injected i.p. with FAEE and subsequently treated with Fe<sup>2+</sup>/H<sub>2</sub>O<sub>2</sub> or AAPH relative to protein bound HNE level in synaptosomes isolated from gerbils, injected i.p with DMSO and subsequently treated with Fe<sup>2+</sup>/H<sub>2</sub>O<sub>2</sub> or AAPH, \* p < 0. 005; the data are the mean ± SEM expressed as percentage of control values, (n = 6).

#### **A.6.5. FAEE *in vivo* induces HO-1 and HSP-70 expression**

Previous studies from our laboratory and those of others have shown induction of HO-1 and HSP-72 at both the gene and protein levels in cell culture as a protective response to oxidative challenge (Calabrese, Stella et al., 2004; Scapagnini, Butterfield et al., 2004; Sultana, Ravagna et al., 2005). In the current study we demonstrated an increase in expression of HO-1 (Figure A.4a and b) and HSP-70 (Figure A.4c and d) in synaptosomes isolated from FAEE-injected gerbils, extending the previous *in vitro* studies. We also observed a significant increase in HO-1 and HSP-70 expression levels in synaptosomes isolated from FAEE-injected gerbils and subsequently treated with  $\text{Fe}^{2+}/\text{H}_2\text{O}_2$  or AAPH ( $p < 0.005$ ) when compared to synaptosomes isolated from control gerbils and compared to synaptosomes isolated from DMSO-injected gerbils subsequently treated with  $\text{Fe}^{2+}/\text{H}_2\text{O}_2$  or AAPH, consistent with the observation that both oxidative stress and FAEE synergistically increased HO-1 expression.

#### **A.6.6. FAEE *in vivo* suppresses iNOS expression**

Several lines of evidence show that iNOS expression increases with oxidative stress and several antioxidants suppresses its expression either at gene level or at protein level (Luth, Munch et al., 2002; Ayasolla, Khan et al., 2004). We previously showed that FAEE suppresses the expression of iNOS in neuronal cell culture exposed to  $\text{A}\beta$  (1-42)-induced oxidative stress (Sultana, Ravagna et al., 2005). Figure A.6 show a decrease in expression of iNOS in synaptosomes isolated from FAEE-injected gerbils, extending the *in vitro* studies. There was a significant increase in iNOS expression levels in synaptosomes isolated from DMSO-injected gerbils subsequently treated with AAPH ( $p < 0.005$ ) when compared to control. In contrast, synaptosomes isolated from FAEE-

injected gerbils subsequently treated with AAPH showed a significant decrease in iNOS expression levels when compared to synaptosomes isolated from DMSO-injected gerbils and then treated with AAPH ( $p < 0.005$ ). A decreased iNOS expression was observed in synaptosomes isolated from FAEE-injected gerbils subsequently treated with  $\text{Fe}^{2+}/\text{H}_2\text{O}_2$  when compared to synaptosomes isolated from DMSO-injected gerbils subsequently treated with the same oxidant. However the difference was not statistically significant (data not shown). This is likely due to a larger scatter of the data.

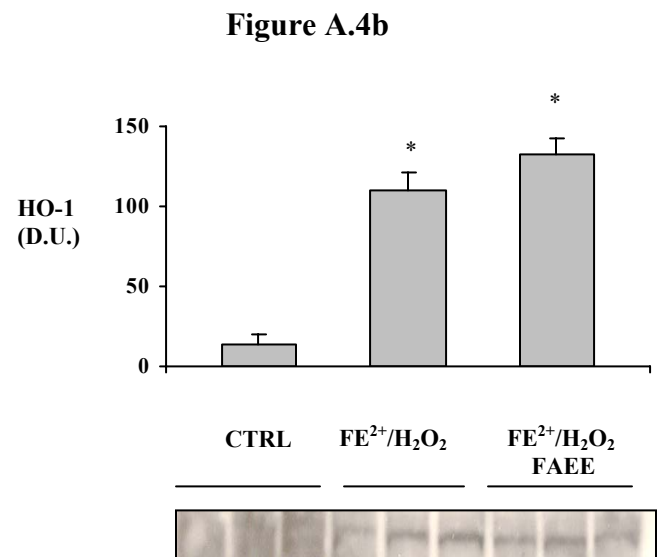
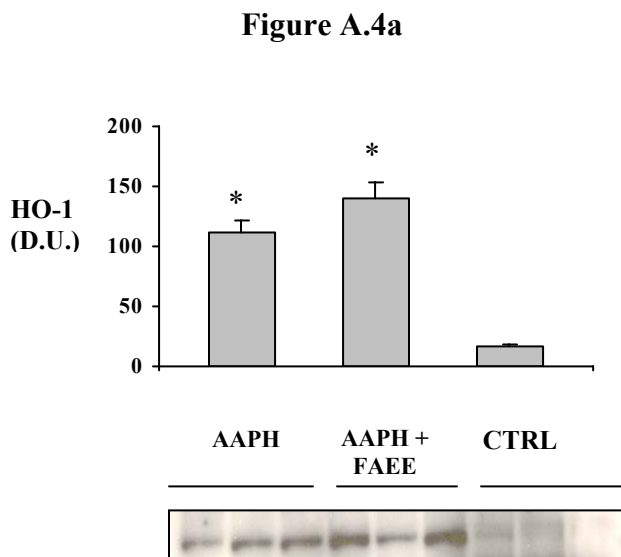


**Figure A.4a and b:** Representative Western blot and plot showing a significant increase in HO-1 expression in synaptosomes isolated from gerbils injected i.p with FAEE and then treated with AAPH or  $\text{Fe}^{2+}/\text{H}_2\text{O}_2$  compared with untreated synaptosomes isolated from DMSO-injected gerbils (control) and control synaptosomes treated with AAPH or  $\text{Fe}^{2+}/\text{H}_2\text{O}_2$  respectively, \*  $p < 0.005$  Vs Control, ( $n = 5$ ).

**Figure A.4c**

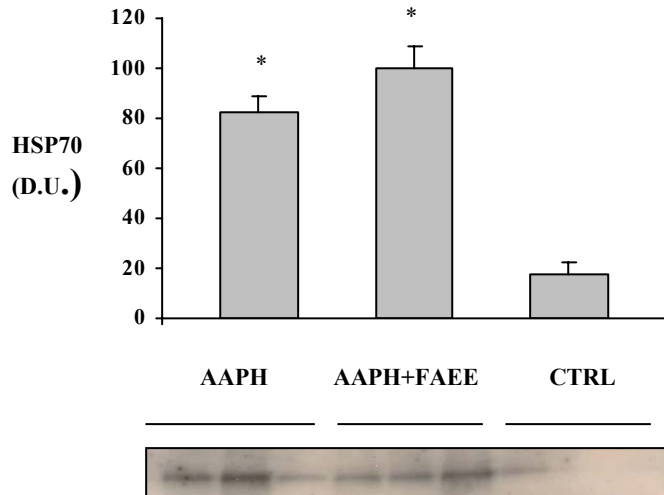


**Figure A.4d**

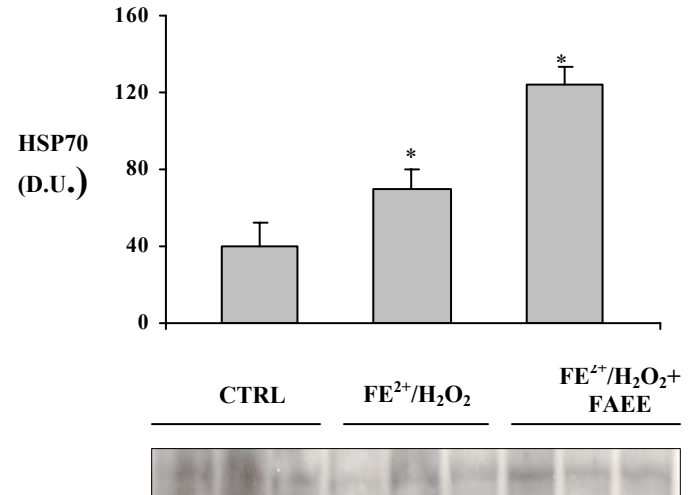


**Figure A.4c and d:** Representative western blot and plot showing a significant increase in HSP-70 expression in synaptosomes isolated from gerbils injected i.p with FAEE and then treated with AAPH and  $Fe^{2+}/H_2O_2$  respectively compared with untreated synaptosomes isolated from DMSO-injected gerbils (control) and control synaptosomes treated with AAPH or  $Fe^{2+}/H_2O_2$  respectively \*  $p < 0.005$  Vs Control, (n = 5).

**Figure A.5**

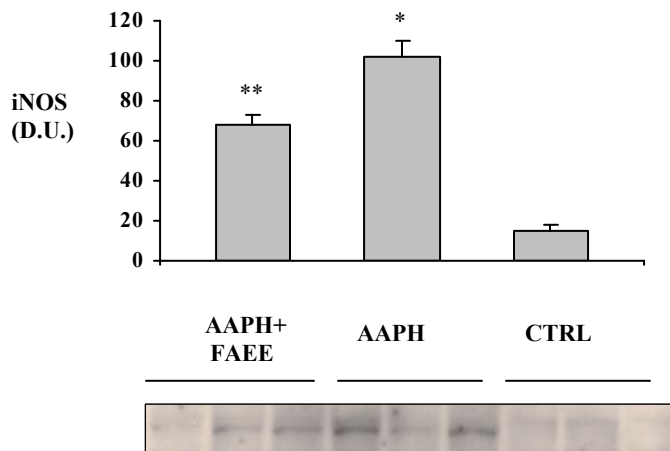


**Figure A.5:** Representative Western blot and plot showing a significant decrease in iNOS expression in synaptosomes isolated from gerbils injected i.p with FAEE and then treated with AAPH compared with control synaptosomes treated with AAPH. There was a significant increase in iNOS expression in control synaptosomes treated with AAPH when compared with control showing induction of iNOS in response to oxidative stress, \*  $p < 0.005$  Vs Control, \*\*  $p < 0.005$  Vs AAPH alone, (n = 5).

### **A.7. Discussion**

High content of polyunsaturated fatty acids, significant oxygen utilization, and relatively poor antioxidant capacity make the brain particularly vulnerable towards oxidative stress (Halliwell, 2001; Butterfield and Lauderback, 2002). Due to an imbalance in the antioxidant system and generation of oxidants such as free radical-mediated ROS and RNS, there is oxidative stress (Yu, 1994; Butterfield, 2002;

Butterfield and Lauderback, 2002). In AD brain, synaptic membranes in particular are vulnerable to oxidative damage (Lauderback, Kanski et al., 2002). Receptors for glutamate are concentrated in synaptic membranes and these receptors mediate increase in intracellular  $\text{Ca}^{2+}$  and excitotoxicity, both of which cause ROS and RNS generation that lead to subsequent protein oxidation (Hensley, Carney et al., 1994; Hensley, Hall et al., 1995; Mattson, 1996). Mitochondrial potential change due to increased  $\text{Ca}^{2+}$  levels lead to release of superoxide ion radicals. Since mitochondria are concentrated in the synaptic region of neurons because of high-energy usage (Mattson, 1996), the synaptic region of neurons becomes particularly more vulnerable to oxidative stress. Therefore, synaptosomes were chosen for our studies to evaluate oxidative stress parameters and investigate likely mechanisms of action of FAEE *in vivo*.

ROS generation and oxidative stress has been implicated in many neurodegenerative disorders including AD (Butterfield, Drake et al., 2001). DCF fluorescence is a useful and reliable technique in quantifying overall oxidative stress in cells. This method can also be used to evaluate the efficacy of antioxidants against oxidative stress in cells (Wang and Joseph, 1999). Previously, our lab showed that ferulic acid scavenges hydroxyl and peroxy radical in synaptosomes (Kanski, Aksenova et al., 2002). Ferulic acid can form a resonance-stabilized phenoxy radical with free radicals, which accounts for its potent antioxidant activity. Recently, we also showed that FAEE scavenges hydroxyl and peroxy radical generated in neuronal cultures in response to  $\text{A}\beta$  (1-42)-induced oxidative stress (Sultana, Ravagna et al., 2005).

The results shown in Figure A.2a suggest that FAEE has radical scavenging property. There was a decrease in fluorescence intensity in synaptosomes that were

isolated from FAEE-injected gerbils and subsequently treated with  $\text{Fe}^{2+}/\text{H}_2\text{O}_2$  or AAPH when compared to synaptosomes that were isolated from DMSO-injected gerbils and subsequently treated with  $\text{Fe}^{2+}/\text{H}_2\text{O}_2$  or AAPH. Use of an oxidation insensitive dye C369 (Figure A.2b) demonstrated that the fluorescence observed in Figure A.2a is due to ROS only. FAEE has conjugated double bonds in its structure, which makes it a good electrophile (Figure A.1). In response to a free radical it can form a resonance-stabilized phenoxy radical (Lauderback, Kanski et al., 2002). Because of its ester group, FAEE is more lipophilic than ferulic acid (Scapagnini, Butterfield et al., 2004) and can hence cross the membrane and trap electrons. This could be the reason for low intracellular ROS in FAEE-treated rodents, as observed in the DCF assay of this study.

As noted above, free radical mediated oxidative stress leads to protein oxidation in many neurodegenerative disorders (Butterfield and Stadtman, 1997; Butterfield, Drake et al., 2001), and protein carbonyls are one of the chief biomarkers for protein oxidation (Stadtman and Berlett, 1997). Studies from our lab and those of others have shown that oxidative stress leads to oxidative modification of key protein and enzymes that are critical for proper biological functions (Castegna, Aksenov et al., 2002a; Castegna, Aksenov et al., 2002b; Poon, Calabrese et al., 2004). AAPH or  $\text{Fe}^{2+}/\text{H}_2\text{O}_2$  induce protein oxidation by increasing protein carbonyl levels (Kanski, Lauderback et al., 2001; Pocernich, Cardin et al., 2001). Ferulic acid was shown to reduce protein oxidation by reducing protein carbonyl formation in synaptosomes and cultured neurons (Lauderback, Kanski et al., 2002). Supporting the hypothesis of the current study, *in vivo* protection of synaptosomes from  $\text{Fe}^{2+}/\text{H}_2\text{O}_2$  or AAPH- mediated oxidative stress was demonstrated by FAEE. There was a significant reduction in protein carbonyl levels (Figure A.3a) in

synaptosomes isolated from FAEE-injected gerbils and subsequently treated with  $\text{Fe}^{2+}/\text{H}_2\text{O}_2$  or AAPH when compared to synaptosomes isolated from DMSO-injected gerbils and subsequently treated with  $\text{Fe}^{2+}/\text{H}_2\text{O}_2$  or AAPH. Attack of free radicals on some amino acid residues leads to carbonyl formation (Butterfield and Stadtman, 1997). Other direct reactions to produce protein carbonyls include cleavage of the protein polypeptide chain or reaction with sugars (glycation) or their glyoxidation products (Butterfield and Stadtman, 1997). HNE and other lipid peroxidation products such as malondialdehyde and acrolein bind to proteins by Michael addition and introduce carbonyl groups in proteins, leading to oxidative modification of proteins (Butterfield and Stadtman, 1997). As demonstrated in our current study, FAEE *in vivo* can reduce free radical generation by scavenging ROS and RNS and thereby reduce the chance of free radical attack on proteins and hence preventing their oxidative modification.

As in the case of protein oxidation, elevated lipid peroxidation products such as HNE and acrolein have been observed in many neurodegenerative disorders (Sayre, Zelasko et al., 1997; Markesbery and Lovell, 1998; Butterfield and Lauderback, 2002; Zarkovic, 2003; Simpson, Henry et al., 2004). HNE alters the conformation of cortical synaptosomal membrane proteins and reduces their activity (Subramaniam, Roediger et al., 1997; Lauderback, Hackett et al., 2001) following binding to proteins by Michael addition (Butterfield and Stadtman, 1997). Ferulic acid has been shown to modulate the lipid peroxidation in neuronal cultures and synaptosomes (Lauderback, Kanski et al., 2002). As noted, we recently reported that FAEE reduces HNE levels in neuronal cell cultures treated with  $\text{A}\beta$  (1-42) (Sultana, Ravagna et al., 2005). In the present study we demonstrated that FAEE *in vivo* reduces the HNE levels produced by  $\text{Fe}^{2+}/\text{H}_2\text{O}_2$  or



AAPH. HNE and other lipid peroxidation products are involved in apoptosis and protein dysregulation (Subramaniam, Roediger et al., 1997; Butterfield and Lauderback, 2002; Awasthi, Sharma et al., 2003; Zarkovic, 2003). Several studies have demonstrated that reducing HNE levels may reduce cytotoxicity (Butterfield, Castegna et al., 2002a; Joshi, Sultana et al., 2005a; Sultana, Ravagna et al., 2005). In biological systems, several enzymes are involved in scavenging or removing HNE (Xie, Lovell et al., 1998; Sultana and Butterfield, 2004) and the proteasomal systems in neurons are responsible for the removal of HNE-bound oxidized cytosolic and nuclear proteins (Grune and Davies, 2003). The reduced levels of HNE by FAEE *in vivo* might implicate reduced cytotoxicity in synaptosomes caused by hydroxyl or alkoxyl free radicals.

Nitration of tyrosine residues on peptides by RNS has been studied as a biomarker for protein oxidation in many neurodegenerative disorders (Stadtman and Berlett, 1997; Castegna, Thongboonkerd et al., 2003). Nitric oxide (NO) is poorly reactive with most biomolecules (except Fe) but reacts vigorously with free radicals such as superoxide radicals to form peroxynitrite. Peroxynitrite can be protonated to peroxynitrous acid (ONOOH) and subsequently reacts with CO<sub>2</sub> and decompose to nitrogen dioxide radical (\*NO<sub>2</sub>) and hydroxyl radical (\*OH), which possess potent free radical characteristics (Hall, Detloff et al., 2004). These radicals react with biomolecules resulting in tyrosine nitration and DNA damage (Beckman, Beckman et al., 1990). One possible cause of oxidative stress is excessive generation of NO from L-arginine and nitric oxide synthase (NOS) (Park, Krishna et al., 2000). Synthesis of NO from inducible NOS (iNOS) has been correlated with a cytotoxic or inflammatory response in the immune system (Park, Krishna et al., 2000). iNOS is specifically expressed as a response to immunological

stimulus during certain pathophysiological conditions (Bredt, 1999). Hence, study of iNOS expression might provide an insight into the effect of pharmacological agents in response to inflammation. We previously showed increased 3NT levels and iNOS expression in cultured neurons treated with A $\beta$  (1-42), an expression that was attenuated by FAEE treatment (Sultana, Ravagna et al., 2005). Consistent with our *in vitro* data, here we demonstrated *in vivo* reduction in 3NT levels in synaptosomes isolated from FAEE-injected gerbils and subsequently treated with AAPH or Fe<sup>2+</sup>/H<sub>2</sub>O<sub>2</sub> when compared to synaptosomes isolated from DMSO-injected gerbils and subsequently treated with AAPH or Fe<sup>2+</sup>/H<sub>2</sub>O<sub>2</sub> (Figure A.3b). We also demonstrated reduced iNOS expression in synaptosomes isolated from FAEE-injected gerbils and subsequently treated with AAPH compared to that in synaptosomes isolated from DMSO-injected gerbils and subsequently treated with AAPH (Figure A.5). FAEE is known for its anti-inflammatory properties. The data obtained suggest that FAEE may be able to reduce NO production by reducing the expression of iNOS reflecting lower inflammation and nitration of tyrosine residues on proteins.

The involvement of heme oxygenase (HO) or heat shock protein (HSP) responses in oxidative stress-related disorders, including AD, has gained considerable importance in recent years (Poon, Calabrese et al., 2004). The expression of HO-1, an inducible isoform of HO, has been closely related to that of amyloid precursor protein (APP) (Dore, 2002). During various pathophysiological conditions, induction of HO-1 (also called HSP-32) catabolizes heme and generates carbon monoxide (CO) and biliverdin (and subsequently bilirubin), a potent antioxidant and anti-inflammatory agent (Calabrese, Stella et al., 2004). The expression of HO-1 is also reported to be upregulated during oxidative stress,

as well as by GSH depletion (Tyrrell, 1999; Calabrese, Stella et al., 2004). The HO pathway has been shown as an important defense system in neurons under oxidative stress (Le, Xie et al., 1999; Chen, Gunter et al., 2000) and expression of HO-1 is altered at the gene and protein levels in AD and other neurodegenerative disorders seen in some neurodegenerative disorders including AD (Pappolla, Chyan et al., 1998; Schipper, 2000; Takahashi, Dore et al., 2000; Takeda, Perry et al., 2000). Previously we demonstrated that FAEE protects rat neuronal culture against oxidative damage and increases cell viability by inducing HO-1 expression both at m-RNA and protein level (Scapagnini, Butterfield et al., 2004; Sultana, Ravagna et al., 2005). This protective effect was attenuated in the presence of Zinc protoporphyrin IX, an inhibitor of HO activity (Scapagnini, Butterfield et al., 2004; Sultana, Ravagna et al., 2005). Similarly, in the current *in vivo* study we demonstrated protection of synaptosomes isolated from FAEE-injected gerbils against oxidative stress by inducing HO-1 and HSP-70 expression (Figure A.4a, b, c, and d, respectively). Although there was an increase in the expression of HO-1 and HSP-70 in synaptosomes isolated from DMSO-injected gerbils, subsequently subjected to oxidative insult when compared to untreated controls, the further increased expression of HO-1 and HSP-70 in synaptosomes isolated from FAEE-injected gerbils subsequently exposed to oxidative stress is likely due to FAEE in the system (Scapagnini, Butterfield et al., 2004; Sultana, Ravagna et al., 2005), suggesting FAEE acts *in vivo* as a neuroprotective agent against oxidative insult by further inducing expression of heat shock proteins in brain.

FAEE has been used previously as an antioxidant agent that has protective effects in *in vitro* models. We extended these results to an *in vivo* model and validated some of

our previous *in vitro* studies. The probable multifunctional mechanism of action of FAEE involves direct scavenging of radicals, up-regulation of HO-1 and HSP 70 and down-regulation of iNOS (Figure A.6). These *in vivo* studies on an animal model of oxidative stress could form the basis for an eventual therapeutic approach towards oxidative stress-related disorders, although further studies are required to establish merit in this notion. Studies on the effect of FAEE on genetically derived animal models of oxidative stress-related disorders are in progress.

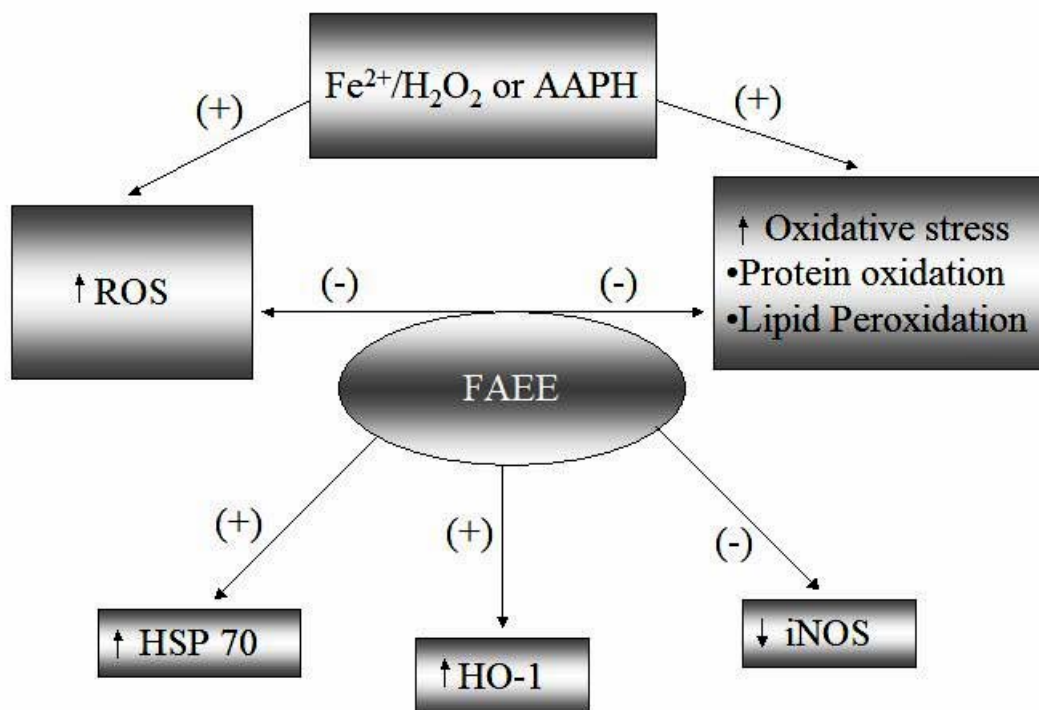


**Figure A.6:** Schematic representation of proposed mechanisms of neuroprotection for FAEE. (+), induction; (-), inhibition; HSP 70, heat shock protein 70; HO-1, heme oxygenase-1; iNOS, inducible nitric oxide synthase.

### A.8. Acknowledgements

This research was supported in part by grants from NIH [AG-10836; AG-05119] to D.A.B.

## Appendix II

### Supporting Data

Figure 4.1

Control	Adr
90.44879	176.985
81.47296	133.2566
110.2417	174.6835
100.3452	159.8
98.73418	168
99.28058	
97.48201	
103.2374	
T value	-8.98478
P value	2.13E-06
Degrees of Freedom	11

Figure 4.2

Control	Adr
102.4715	126
100	128
94.86692	132
98.85932	138.5932
102.2814	
101.5209	
96.77419	
95.28536	
93.79653	
113.1514	
104.5161	
T value	-9.96049
P value	9.81E-08
Degrees of Freedom	14

Figure 4.3

	107.799	147.033
	99.82669	172.7473
	93.58752	139.7802
	110.2253	193.8462
	108.8388	154.9451
	79.7227	188.5714
T value		-6.4098
P value		7.73E-05
Degrees of Freedom		10

Figure 4.4

	control	ADR
	99.89627	300.3112
	78.11203	264.5228
	121.9917	336.0996
Average	100	300.3112
Std Dev	21.94002	35.78838

Figure 5.1

	Control	ADR
1	65.16659	67.74111
2	108.5701	54.22757
3	117.864	85.41019
4	108.3992	69.72808
5		85.24995
average	100	72.47138
std dev	23.63955	13.16665

Figure 5.3

#### Glutathione S transferase

	control	ADR
	64.64498	165.6436
	81.31929	174.5854
	124.8557	222.8493
	129.18	170.7009
		179.1663
avg	100	182.5891
Std Dev	31.98034	23.0496

### Glutathione peroxidase

	Control	ADR
	116.8569	131.9281
	109.1465	158.2046
	115.6774	155.5398
	58.31923	167.7934
		208.726
avg	100	164.4384
Std Dev	27.99333	28.0518

### Glutathione reductase

	Control	ADR
	81.82016	147.2937
	127.2951	146.685
	132.1064	147.4966
	58.77835	203.6954
		284.733
avg	100	185.9807
Std Dev	35.61635	60.38976

Figure 7.1

	Control	ADR	GCEE	ADR+GCEE
1	28.81708	17.98009	38.1673	22.4775
2	18.50748	14.39328	33.15605	20.75295
3	31.2839	22.66988	39.2128	24.7971
4	28.77172	17.29675	40.0967	27.42295
5	28.0154	22.62735	36.62705	26.4817
avg	27.07912	18.99347	37.45198	24.38644
std Dev	4.947606	3.598216	2.726822	2.76701331

Figure 7.2

	control	GCEE	ADR	ADR+GCEE
1	213	271.5	334.5	205.5
2	262	253	319.5	248.5
3	277	189	295.5	260
4	250.5	235.5		272.5
5		253.5	288.5	267
avg	250.625	240.5	309.5	250.7
std Dev	27.3294	31.47817	21.30728	26.81091



Figure 7.3

	Control	GCEE	ADR	ADR+GCEE
1	178.5	177	199	202
2	167.5	170	208	173.5
3	181.5	156	178.5	165.5
4	146	165	208	154.5
5	166.5	168	205	177.5
avg	168	167.2	199.7	174.6
Std Dev	13.95529	7.661593	12.40766	17.65786

Figure 7.4

	control	GCEE	ADR	ADR+GCEE
1	313	349	371	339
2	309	322	340	325
3	329	334	381	318
4	322	343	366	349
5	345	270	373	306
6	350	302	329	309
7	359	302	355	349
8	346	305	340	354
9	314	250	345	334
10	318	261	347	365
AVG	330.5	303.8	354.7	334.8
Std Dev	17.99537	34.47962	17.21143	19.932107

Figure 7.5

	control	ADR	GCEE	ADR+GCEE
1	0.010333	0.008667	0.001521	0.001784
2	0.004667	0.004	0.002259	0.001869
3	0.004	0.007	0.001845	0.002372
4	0.011	0.011667	0.001873	0.001586
5		0.011	0.001466	0.002106
avg	0.0075	0.008467	<b>0.001793</b>	<b>0.001943</b>
Std Dev	0.003677	0.003114	0.000319	0.000304

Figure 8.2

	Control	Fe2+/H2O2	Fe2+/H2O2+D609	AAPH	AAPH+D609
	81.9104	124.26036	122.2316145	150.634	139.4759087
	99.91547	119.69569	135.4184277	156.9738	137.1935757
	92.81488	136.93998	83.68554522	167.6247	142.5190194
	115.131	154.18428	97.12595097	155.7058	135.6720203
	93.57566	149.11243	113.3558749	117.6669	101.310778
	116.6526	161.03128	120.7100592	125.0211	89.6880998
	95.20611	131.54835	126.9891192	101.3284	122.7265765
	99.86591	141.8284	108.2770096	104.1871	104.7964081
	102.8043	172.13134	132.5096399	113.3089	94.33281298
	102.1237	138.39725	136.1234982	107.692	125.5350273
	96.6319	128.94188	112.7096852	136.483	85.61921822
	100.4216	176.91266	137.7301231	125.799	84.27943955
	101.9223	105.59904	90.02759628	163.2685	90.67307928
	101.0242	112.24294	84.88442788	152.8849	85.19814492
	95.32536	110.3616	94.09041905	168.9505	
	102.8842	109.61485	87.11653946	166.2484	
	99.54729				
	102.2432				
Avg	100	135.80014	111.4365957	138.3611	109.9300078
Std Dev	7.721027	22.306731	19.68133688	24.5954	22.75849606

Figure 8.4

	Control	Fe2+/H2O2	Fe2+/H2O2+D609	AAPH	AAPH + D609
	105.6194	157.096	120.7957342	106.3815	107.2093825
	102.1329	145.8162	116.8990976	106.7954	86.23663332
	91.26333	139.2535	107.2600492	214.3791	83.33908244
	100.4922	148.0722	129.4093519	185.2941	91.2038634
	100.4922	130.1313	107.9355609	188.8889	48.69281046
	98.10279	125.8353	109.0095465	174.5098	52.2875817
	98.37875	122.2554	85.7398568	182.3529	46.73202614
	96.58503	144.9881	105.2505967	193.7908	44.77124183
	106.9334	162.5298	77.86396181	150.634	64.37908497
	101.3072	124.2604	100.9546539	156.9738	62.41830065
	106.5359	136.94	122.2316145	167.6247	139.4759087
	90.0358	154.1843	83.68554522	155.7058	137.1935757
	92.00477	149.1124	97.12595097	117.6669	142.5190194
	105.6086	161.0313	113.3558749	125.0211	135.6720203
	99.91547		120.7100592		
avg	99.69385	142.9647	106.548497	159.0014	88.7236094
Std					
Dev	5.454988	13.58106	15.19950997	34.15375	37.53569008

Figure 8.6

	Control	Fe2+/H2O2	Fe2+/H2O2+D609	AAPH	AAPH + D609
	99.94295	118.68	105.3546	116.9768	96.478
	101.0839	119.6701	107.9293	112.4834	98.567
		116.6001	97.20479	116.6001	97.20479
	94.69481	114.0901	102.56	114.0901	95.6578
	104.2784	119.3856	100.1711	114.3562	100.1711
			102.4529		102.4529
avg	100	117.6852	102.6121	114.9013	98.42194
Std Dev	3.984453	2.341087	3.76879	1.870497	2.538917

Figure 8.7

	Control	Fe2+/H2O2	Fe2+/H2O2+D609	AAPH	AAPH+D609
	86.11111	117.9487	91.23931624	109.2469	85.60533842
	102.3504	121.234	101.4957265	115.348	91.70638704
	101.0684	116.547	101.4957265	110.2002	86.9399428
	110.4701	125.768	102.1367521	110.4567	
	102.0019	120.768		104.8618	
	98.57007				
	86.11111				
avg	98.09758	120.4531	99.09188034	110.0227	88.08388942
Std Dev	8.970406	3.552699	5.24375692	3.735478	3.207360122

Figure 9.2b

	control	Abeta 1- 42	Abeta 1- 40	Abeta 42- 1	D609+42	D609+40	D609+42-1
	282	532	314	312	355	317	289
	302	627	316	301	422	385	251
	310	503	350	306	438	375	271
	399	641	543	399	416	420	363
	401	665	592	424	532	438	384
	425	505	487	424	531	456	428
avg	353.1667	578.8333	433.6667	361	449	398.5	331
%control	79.84899	150.6371	88.90986	88.34356	100.5191	89.75932	81.831052
	85.51203	177.5366	89.47617	85.22888	119.4903	109.0137	71.07126
	87.77725	142.4257	99.10335	86.64464	124.0208	106.1822	76.734309
	112.9778	181.5007	153.7518	112.9778	117.7914	118.924	102.78433
	113.5441	188.2964	167.6262	120.0566	150.6371	124.0208	108.73053
	120.3398	142.992	137.8952	120.0566	150.3539	129.1175	121.18924
avg	100	163.8981	122.7938	102.218	127.1354	112.8362	93.723454
std dev	17.49819	20.80923	34.68665	17.18061	19.77531	14.27352	20.024303

Figure 9.5

	control	A beta	A beta+D609
	100	141.341	99.9549
	100	147.3317	121.5408
	100	128.5565	99.26671
avg	100	139.0764	106.9208
Std Dev		9.590267	12.66599

Figure 10.4a

	Control	D609	AAPH	AAPH+D609	F2+/H2O2	F2+/H2O2+D609	Abeta	Abeta+D609
	90.21581	122.5136	56.62763	83.4349495	46.362786	63.64721443	43.87883	55.9243847
	83.7898	86.87442	71.69909	120.055486	46.053098	74.70563567	50.87261	71.7184425
	92.50621	103.0162	92.55782	94.2998161	44.898223	69.58288977	56.13729	62.5504049
	149.2177	76.78957	63.76335	113.461725	37.478628	87.07377657	65.80212	76.0863254
	95.39017	110.9133	83.40914	102.500081	34.033356	74.48627375	68.38285	95.1772638
	88.88029	94.19014	68.90545	71.0861641	42.898223	59.29868705	44.54982	79.2412658
Ave	100	99.04954	72.82708	97.4730368	41.765218	71.46574621	54.93726	73.4496812
stdev	24.42106	16.5795	13.13398	18.4080449	5.0708098	9.756464506	10.45924	13.7223148
sem	9.969854	6.768553	5.361925	7.51505285	2.0701494	3.983059955	4.269966	5.60211157

Figure 10.4b

	Control	D609	AAPH	AAPH+D609	F2+/H2O2	F2+/H2O2+D609	Abeta	Abeta+D609
	110.4802	78.86197	189.0728	103.683899	199.6163	113.4314346	213.857991	122.89732
	121.636	80.09878	180.9907	110.8476029	215.7438	134.689879	182.937731	217.874564
	82.27851	113.8968	133.8204	142.8699716	209.3149	110.0026532	377.66802	158.99749
	96.01812	121.9177	127.8078	109.9536706	196.9223	117.239831	125.199502	134.371492
	80.66208	96.0916	94.70784	108.7291059	220.4951	151.6745923	145.796681	155.0299
	108.925	96.04261	111.7538	109.3046513	182.636	121.9176684	110.076127	141.106598
Ave	100	97.81823	139.6922	114.2314836	204.1214	124.8260098	192.589342	155.046227
Stdv	16.50134	17.42845	37.74618	14.25282222	13.8845	15.70808137	98.3249719	33.5211061
Sem	6.736643	7.115137	15.40981	5.818690307	5.668324	6.412797365	40.1410017	13.6849342

Figure 11.1

	Control	APP/PS-1	WT/NAC	APP/PS-1/NAC
	541	660.5	448	476
	439.5	602	436	382
	470	656.5	427.5	419.5
	433	616	433	420
	524.5	497.5	492.5	493
	453		470	583
avg	476.8333	606.5	451.1667	462.25
%control	113.4568	138.518	93.95316	99.82523593
	92.17057	126.2496	91.43656	80.111849
	98.56693	137.6791	89.65397	87.97623209
	90.80741	129.1856	90.80741	88.08109053
	109.9965	104.3341	103.2856	103.3904229
	95.00175		98.56693	122.2649423
avg	100	127.1933	94.61727	96.9416288
STDEV	9.527396	13.83476	5.299935	15.05524034

Figure 11.2

	Wild (H2O)	Wild (NAC)	APP (H2O)	APP (NAC)
	462	367.5	538	363.5
	424	366.5	556	429
	369	299	487	515
	359.5	348	502	436
	416	325	494.5	409
	462	387.5	434.5	406
ave	415.4166667	348.9166667	502	426.416667
	111.2136409	88.46539619	129.5085256	87.5025075
	102.0661986	88.22467402	133.8415246	103.269809
	88.82647944	71.97592778	117.2316951	123.971916
	86.53961886	83.77131394	120.8425276	104.954865
	100.1404213	78.23470411	119.0371113	98.4553661
	111.2136409	93.27983952	104.5937813	97.7331996
ave	100	83.99197593	120.8425276	102.647944
Std Dev	9.676516268	7.091919293	9.348732869	11.0418676

Figure 11.3

	Wild (H2O)	Wild (NAC)	APP (H2O)	APP (NAC)
	317.5	272.5	401.5	229
	330	259	349	218
	333.5	235	389	243
	309	272.5	341.5	308
	273.5	216	371	286
	316.5	250	353	313
ave	313.3333333	250.8333333	367.5	266.166667
% control	101.3297872	86.9680851	128.1383	73.0851064
	105.3191489	82.6595745	111.38298	69.5744681
	106.4361702	75	124.14894	77.5531915
	98.61702128	86.9680851	108.98936	98.2978723
	87.28723404	68.9361702	118.40426	91.2765957
	101.0106383	79.787234	112.65957	99.893617
ave	100	80.0531915	117.28723	84.9468085
Std Dev	6.272086371	6.47583173	6.9666638	12.0650915

Figure 11.4a

	Wild (H2O)	Wild (NAC)	APP (H2O)	APP (NAC)
	189	209	145	202
	168	201	132	199
	176	213	130	205
Average	177.666667	207.666667	135.66667	202
Std Dev	10.5987421	6.11010093	8.1445278	3
% control	106.378987	117.636023	81.613508	113.69606
	94.5590994	113.133208	74.296435	112.0075
	99.0619137	119.88743	73.170732	115.38462
Average	100	116.885553	76.360225	113.69606

Figure 11.5

	Wild (H2O)	Wild (NAC)	APP (H2O)	APP (NAC)
1	0.000952607	0.000665927	0.00077922	0.001600904
2	0.000178838	0.000533885	7.5812E-05	0.000699285
3	0.001284848	0.000801161	0.00026981	0.000712456
4	0.000684366	0.000779661	7.7922E-05	0.000707156
5	0.000613178	0.000505505	0.00030407	0.000521433
6	0.00071829	0.000723445	0.00127916	
avg	0.000738688	0.000668264	0.00046433	0.000848247
std				
Dev	0.00036786	0.000124635	0.00047474	0.000428321

## Reference

- Abali, H. and I. Celik (2002). "High incidence of central nervous system involvement in patients with breast cancer treated with epirubicin and docetaxel." Am J Clin Oncol **25**(6): 632-3.
- Abd El-Gawad, H. M. and M. M. El-Sawalhi (2004). "Nitric oxide and oxidative stress in brain and heart of normal rats treated with doxorubicin: role of aminoguanidine." J. Biochem. Mol. Toxicol **18**(2): 69-77.
- Abe, K., L. H. Pan, M. Watanabe, T. Kato and Y. Itoyama (1995). "Induction of nitrotyrosine-like immunoreactivity in the lower motor neuron of amyotrophic lateral sclerosis." Neurosci Lett **199**(2): 152-4.
- Abramov, A. Y., L. Canevari and M. R. Duchen (2003). "Changes in intracellular calcium and glutathione in astrocytes as the primary mechanism of amyloid neurotoxicity." J Neurosci **23**(12): 5088-95.
- Adair, J. C., J. E. Knoefel and N. Morgan (2001). "Controlled trial of N-acetylcysteine for patients with probable Alzheimer's disease." Neurology **57**(8): 1515-7.
- Adrain, C. and S. J. Martin (2001). "The mitochondrial apoptosome: a killer unleashed by the cytochrome seas." Trends Biochem Sci **26**(6): 390-7.
- Akama, K. T. and L. J. Van Eldik (2000). "Beta-amyloid stimulation of inducible nitric-oxide synthase in astrocytes is interleukin-1beta- and tumor necrosis factor-alpha (TNFalpha)-dependent, and involves a TNFalpha receptor-associated factor- and NFkappaB-inducing kinase-dependent signaling mechanism." J Biol Chem **275**(11): 7918-24.



- Aksenov, M. Y., M. V. Aksenova, D. A. Butterfield, J. W. Geddes and W. R. Markesbery (2001). "Protein oxidation in the brain in Alzheimer's disease." Neuroscience **103**(2): 373-83.
- Aliyev, A., S. G. Chen, D. Seyidova, M. A. Smith, G. Perry, J. de la Torre and G. Aliev (2005). "Mitochondria DNA deletions in atherosclerotic hypoperfused brain microvessels as a primary target for the development of Alzheimer's disease." J Neurol Sci **229-230**: 285-92.
- Almkvist, O., H. Basun, L. Backman, A. Herlitz, L. Lannfelt, B. Small, M. Viitanen, L. O. Wahlund and B. Winblad (1998). "Mild cognitive impairment--an early stage of Alzheimer's disease?" J Neural Transm Suppl **54**: 21-9.
- Ames, B. N. (2004). "A role for supplements in optimizing health: the metabolic tune-up." Arch Biochem Biophys **423**(1): 227-34.
- Ames, J. B., R. Ishima, T. Tanaka, J. I. Gordon, L. Stryer and M. Ikura (1997). "Molecular mechanics of calcium-myristoyl switches." Nature **389**(6647): 198-202.
- Amici, A., R. L. Levine, L. Tsai and E. R. Stadtman (1989). "Conversion of amino acid residues in proteins and amino acid homopolymers to carbonyl derivatives by metal-catalyzed oxidation reactions." J Biol Chem **264**(6): 3341-6.
- Amtmann, E. (1996). "The antiviral, antitumoural xanthate D609 is a competitive inhibitor of phosphatidylcholine-specific phospholipase C." Drugs Exp Clin Res **22**(6): 287-94.

- Amtmann, E., K. Muller-Decker, A. Hoss, G. Schalasta, C. Doppler and G. Sauer (1987). "Synergistic antiviral effect of xanthates and ionic detergents." Biochem Pharmacol **36**(9): 1545-9.
- Amtmann, E. and G. Sauer (1987). "Selective killing of tumor cells by xanthates." Cancer Lett **35**(3): 237-44.
- An, W. F., M. R. Bowlby, M. Betty, J. Cao, H. P. Ling, G. Mendoza, J. W. Hinson, K. I. Mattsson, B. W. Strassle, J. S. Trimmer and K. J. Rhodes (2000). "Modulation of A-type potassium channels by a family of calcium sensors." Nature **403**(6769): 553-6.
- Anderson, M. E. and J. L. Luo (1998). "Glutathione therapy: from prodrugs to genes." Semin Liver Dis **18**(4): 415-24.
- Andreassen, O. A., A. Dedeoglu, P. Klivenyi, M. F. Beal and A. I. Bush (2000). "N-acetyl-L-cysteine improves survival and preserves motor performance in an animal model of familial amyotrophic lateral sclerosis." Neuroreport **11**(11): 2491-3.
- Ansari, M. A., A. S. Ahmad, M. Ahmad, S. Salim, S. Yousuf, T. Ishrat and F. Islam (2004). "Selenium protects cerebral ischemia in rat brain mitochondria." Biol Trace Elem Res **101**(1): 73-86.
- Antonsson, B. (2004). "Mitochondria and the Bcl-2 family proteins in apoptosis signaling pathways." Mol Cell Biochem **256-257**(1-2): 141-55.
- Awasthi, Y. C., R. Sharma, J. Z. Cheng, Y. Yang, A. Sharma, S. S. Singhal and S. Awasthi (2003). "Role of 4-hydroxynonenal in stress-mediated apoptosis signaling." Mol Aspects Med **24**(4-5): 219-30.

- Ayasolla, K., M. Khan, A. K. Singh and I. Singh (2004). "Inflammatory mediator and beta-amyloid (25-35)-induced ceramide generation and iNOS expression are inhibited by vitamin E." Free Radic Biol Med **37**(3): 325-38.
- Babior, B. M. (1999). "NADPH oxidase: an update." Blood **93**(5): 1464-76.
- Bains, J. S. and C. A. Shaw (1997). "Neurodegenerative disorders in humans: the role of glutathione in oxidative stress-mediated neuronal death." Brain Res Brain Res Rev **25**(3): 335-58.
- Beckman, J. S., T. W. Beckman, J. Chen, P. A. Marshall and B. A. Freeman (1990). "Apparent hydroxyl radical production by peroxynitrite: implications for endothelial injury from nitric oxide and superoxide." Proc Natl Acad Sci U S A **87**(4): 1620-4.
- Beckman, K. B. and B. N. Ames (1998). "The free radical theory of aging matures." Physiol Rev **78**(2): 547-81.
- Behl, C. (2002). "Neuroprotective strategies in Alzheimer's disease." Adv Exp Med Biol **513**: 475-96.
- Behl, C., J. Davis, G. M. Cole and D. Schubert (1992). "Vitamin E protects nerve cells from amyloid beta protein toxicity." Biochem Biophys Res Commun **186**(2): 944-50.
- Behl, C., T. Skutella, F. Lezoualc'h, A. Post, M. Widmann, C. J. Newton and F. Holsboer (1997). "Neuroprotection against oxidative stress by estrogens: structure-activity relationship." Mol Pharmacol **51**(4): 535-41.

- Benzi, G. and A. Moretti (1995a). "Age- and peroxidative stress-related modifications of the cerebral enzymatic activities linked to mitochondria and the glutathione system." Free Radic Biol Med **19**(1): 77-101.
- Benzi, G. and A. Moretti (1995b). "Are reactive oxygen species involved in Alzheimer's disease?" Neurobiol Aging **16**(4): 661-74.
- Berlett, B. S. and E. R. Stadtman (1997). "Protein oxidation in aging, disease, and oxidative stress." J Biol Chem **272**(33): 20313-6.
- Bernstein, H. G., B. Baumann, P. Danos, S. Diekmann, B. Bogerts, E. D. Gundelfinger and K. H. Braunewell (1999). "Regional and cellular distribution of neural visinin-like protein immunoreactivities (VILIP-1 and VILIP-3) in human brain." J Neurocytol **28**(8): 655-62.
- Bigotte, L., B. Arvidson and Y. Olsson (1982a). "Cytofluorescence localization of adriamycin in the nervous system. I. Distribution of the drug in the central nervous system of normal adult mice after intravenous injection." Acta Neuropathol (Berl) **57**(2-3): 121-9.
- Bigotte, L., B. Arvidson and Y. Olsson (1982b). "Cytofluorescence localization of adriamycin in the nervous system. II. Distribution of the drug in the somatic and autonomic peripheral nervous systems of normal adult mice after intravenous injection." Acta Neuropathol (Berl) **57**(2-3): 130-6.
- Borchelt, D. R., T. Ratovitski, J. van Lare, M. K. Lee, V. Gonzales, N. A. Jenkins, N. G. Copeland, D. L. Price and S. S. Sisodia (1997). "Accelerated amyloid deposition in the brains of transgenic mice coexpressing mutant presenilin 1 and amyloid precursor proteins." Neuron **19**(4): 939-45.

- Borchelt, D. R., G. Thinakaran, C. B. Eckman, M. K. Lee, F. Davenport, T. Ratovitsky, C. M. Prada, G. Kim, S. Seekins, D. Yager, H. H. Slunt, R. Wang, M. Seeger, A. I. Levey, S. E. Gandy, N. G. Copeland, N. A. Jenkins, D. L. Price, S. G. Younkin and S. S. Sisodia (1996). "Familial Alzheimer's disease-linked presenilin 1 variants elevate Abeta1-42/1-40 ratio in vitro and in vivo." Neuron **17**(5): 1005-13.
- Bosetti, F., F. Brizzi, S. Barogi, M. Mancuso, G. Siciliano, E. A. Tendi, L. Murri, S. I. Rapoport and G. Solaini (2002). "Cytochrome c oxidase and mitochondrial F1F0-ATPase (ATP synthase) activities in platelets and brain from patients with Alzheimer's disease." Neurobiol Aging **23**(3): 371-6.
- Boyd-Kimball, D., A. Castegna, R. Sultana, H. F. Poon, R. Petroze, B. C. Lynn, J. B. Klein and D. A. Butterfield (2005). "Proteomic identification of proteins oxidized by Abeta(1-42) in synaptosomes: implications for Alzheimer's disease." Brain Res **1044**(2): 206-15.
- Boyd-Kimball, D., H. Mohammad Abdul, T. Reed, R. Sultana and D. A. Butterfield (2004). "Role of phenylalanine 20 in Alzheimer's amyloid beta-peptide (1-42)-induced oxidative stress and neurotoxicity." Chem Res Toxicol **17**(12): 1743-9.
- Boyd-Kimball, D., R. Sultana, H. M. Abdul and D. A. Butterfield (2005a). "Gamma-glutamylcysteine ethyl ester-induced up-regulation of glutathione protects neurons against Abeta(1-42)-mediated oxidative stress and neurotoxicity: implications for Alzheimer's disease." J Neurosci Res **79**(5): 700-6.
- Boyd-Kimball, D., R. Sultana, H. F. Poon, B. C. Lynn, F. Casamenti, G. Pepeu, J. B. Klein and D. A. Butterfield (2005b). "Proteomic identification of proteins

- specifically oxidized by intracerebral injection of amyloid beta-peptide (1-42) into rat brain: implications for Alzheimer's disease." Neuroscience **132**(2): 313-24.
- Boyd-Kimball, D., R. Sultana, H. F. Poon, H. Mohammad-Abdul, B. C. Lynn, J. B. Klein and D. A. Butterfield (2005c). "Gamma-glutamylcysteine ethyl ester protection of proteins from Abeta(1-42)-mediated oxidative stress in neuronal cell culture: a proteomics approach." J Neurosci Res **79**(5): 707-13.
- Bradford, M. M. (1976). "A rapid and sensitive method for the quantitation of microgram quantities of protein utilizing the principle of protein-dye binding." Anal Biochem **72**: 248-54.
- Braunewell, K. H., M. Brackmann, M. Schaupp, C. Spilker, R. Anand and E. D. Gundelfinger (2001). "Intracellular neuronal calcium sensor (NCS) protein VILIP-1 modulates cGMP signalling pathways in transfected neural cells and cerebellar granule neurones." J Neurochem **78**(6): 1277-86.
- Braunewell, K. H. and E. D. Gundelfinger (1999). "Intracellular neuronal calcium sensor proteins: a family of EF-hand calcium-binding proteins in search of a function." Cell Tissue Res **295**(1): 1-12.
- Bredt, D. S. (1999). "Endogenous nitric oxide synthesis: biological functions and pathophysiology." Free Radic Res **31**(6): 577-96.
- Breitner, J. C. (1996). "The role of anti-inflammatory drugs in the prevention and treatment of Alzheimer's disease." Annu Rev Med **47**: 401-11.
- Butterfield, D. (1997). "beta-Amyloid-associated free radical oxidative stress and neurotoxicity: implications for Alzheimer's disease." Chem res Toxicol **10**(5): 495-506.

- Butterfield, D., A. Castegna, C. Pocernich, J. Drake, G. Scapagnini and V. Calabrese (2002a). "Nutritional approaches to combat oxidative stress in Alzheimer's disease." J Nutr Biochem **13**(8): 444.
- Butterfield, D. and E. R. Stadtman (1997). "Protein oxidation processes in aging brain." Advanced Cell Aging and Gerontology **2**: 161–191.
- Butterfield, D. A. (2002). "Amyloid beta-peptide (1-42)-induced oxidative stress and neurotoxicity: implications for neurodegeneration in Alzheimer's disease brain. A review." Free Radic Res **36**(12): 1307-13.
- Butterfield, D. A. (2004). "Proteomics: a new approach to investigate oxidative stress in Alzheimer's disease brain." Brain Res **1000**(1-2): 1-7.
- Butterfield, D. A. and D. Boyd-Kimball (2004). "Proteomics analysis in Alzheimer's disease: new insights into mechanisms of neurodegeneration." Int Rev Neurobiol **61**: 159-88.
- Butterfield, D. A. and D. Boyd-Kimball (2005). "The critical role of methionine 35 in Alzheimer's amyloid beta-peptide (1-42)-induced oxidative stress and neurotoxicity." Biochim Biophys Acta **1703**(2): 149-56.
- Butterfield, D. A., D. Boyd-Kimball and A. Castegna (2003). "Proteomics in Alzheimer's disease: insights into potential mechanisms of neurodegeneration." J Neurochem **86**(6): 1313-27.
- Butterfield, D. A. and A. Castegna (2003). "Proteomic analysis of oxidatively modified proteins in Alzheimer's disease brain: insights into neurodegeneration." Cell Mol Biol (Noisy-le-grand) **49**(5): 747-51.

- Butterfield, D. A., A. Castegna, C. M. Lauderback and J. Drake (2002b). "Evidence that amyloid beta-peptide-induced lipid peroxidation and its sequelae in Alzheimer's disease brain contribute to neuronal death." Neurobiology of Aging **23**(5): 655-64.
- Butterfield, D. A., J. Drake, C. Pocernich and A. Castegna (2001). "Evidence of oxidative damage in Alzheimer's disease brain: central role for amyloid beta-peptide." Trends Mol Med **7**(12): 548-54.
- Butterfield, D. A. and J. Kanski (2001). "Brain protein oxidation in age-related neurodegenerative disorders that are associated with aggregated proteins." Mech Ageing Dev **122**(9): 945-62.
- Butterfield, D. A. and C. M. Lauderback (2002). "Lipid peroxidation and protein oxidation in Alzheimer's disease brain: potential causes and consequences involving amyloid beta-peptide-associated free radical oxidative stress." Free Radic Biol Med **32**(11): 1050-60.
- Butterfield, D. A., M. Perluigi and R. Sultana (2006). "Oxidative stress in Alzheimer's disease brain: new insights from redox proteomics." Eur J Pharmacol **545**(1): 39-50.
- Butterfield, D. A., H. F. Poon, D. St Clair, J. N. Keller, W. M. Pierce, J. B. Klein and W. R. Markesbery (2006). "Redox proteomics identification of oxidatively modified hippocampal proteins in mild cognitive impairment: insights into the development of Alzheimer's disease." Neurobiol Dis **22**(2): 223-32.
- Butterfield, D. A., T. Reed, M. Perluigi, C. De Marco, R. Coccia, C. Cini and R. Sultana (2006). "Elevated protein-bound levels of the lipid peroxidation product, 4-



- hydroxy-2-nonenal, in brain from persons with mild cognitive impairment." Neurosci Lett **397**(3): 170-3.
- Cadenas, E. and K. J. Davies (2000). "Mitochondrial free radical generation, oxidative stress, and aging." Free Radic Biol Med **29**(3-4): 222-30.
- Calabrese, V., A. M. Stella, D. A. Butterfield and G. Scapagnini (2004). "Redox regulation in neurodegeneration and longevity: role of the heme oxygenase and HSP70 systems in brain stress tolerance." Antioxid Redox Signal **6**(5): 895-913.
- Canevari, L., A. Y. Abramov and M. R. Duchen (2004). "Toxicity of amyloid beta peptide: tales of calcium, mitochondria, and oxidative stress." Neurochem Res **29**(3): 637-50.
- Carlberg, I. and B. Mannervik (1985). "Glutathione reductase." Methods Enzymol **113**: 484-90.
- Castegna, A., M. Aksenov, M. Aksenova, V. Thongboonkerd, J. B. Klein, W. M. Pierce, R. Booze, W. R. Markesbery and D. A. Butterfield (2002a). "Proteomic identification of oxidatively modified proteins in Alzheimer's disease brain. Part I: creatine kinase BB, glutamine synthase, and ubiquitin carboxy-terminal hydrolase L-1." Free Radic Biol Med **33**(4): 562-71.
- Castegna, A., M. Aksenov, V. Thongboonkerd, J. B. Klein, W. M. Pierce, R. Booze, W. R. Markesbery and D. A. Butterfield (2002b). "Proteomic identification of oxidatively modified proteins in Alzheimer's disease brain. Part II: dihydropyrimidinase-related protein 2, alpha-enolase and heat shock cognate 71." J Neurochem **82**(6): 1524-32.

- Castegna, A., V. Thongboonkerd, J. Klein, B. C. Lynn, Y. L. Wang, H. Osaka, K. Wada and D. A. Butterfield (2004). "Proteomic analysis of brain proteins in the gracile axonal dystrophy (gad) mouse, a syndrome that emanates from dysfunctional ubiquitin carboxyl-terminal hydrolase L-1, reveals oxidation of key proteins." J Neurochem **88**(6): 1540-6.
- Castegna, A., V. Thongboonkerd, J. B. Klein, B. Lynn, W. R. Markesbery and D. A. Butterfield (2003). "Proteomic identification of nitrated proteins in Alzheimer's disease brain." J Neurochem **85**(6): 1394-401.
- Chakraborty, S., N. Sarkar and B. Bhattacharyya (1999). "Nucleotide-dependent bisANS binding to tubulin." Biochim Biophys Acta **1432**(2): 350-5.
- Chang, M. L., P. J. Artymiuk, X. Wu, S. Hollan, A. Lammi and L. E. Maquat (1993). "Human triosephosphate isomerase deficiency resulting from mutation of Phe-240." Am J Hum Genet **52**(6): 1260-9.
- Chartier-Harlin, M. C., F. Crawford, H. Houlden, A. Warren, D. Hughes, L. Fidani, A. Goate, M. Rossor, P. Roques, J. Hardy and et al. (1991). "Early-onset Alzheimer's disease caused by mutations at codon 717 of the beta-amyloid precursor protein gene." Nature **353**(6347): 844-6.
- Chen, J. J., H. Bertrand and B. P. Yu (1995). "Inhibition of adenine nucleotide translocator by lipid peroxidation products." Free Radic Biol Med **19**(5): 583-90.
- Chen, K., K. Gunter and M. D. Maines (2000). "Neurons overexpressing heme oxygenase-1 resist oxidative stress-mediated cell death." J Neurochem **75**(1): 304-13.

- Chen, Z. and L. H. Lash (1998). "Evidence for mitochondrial uptake of glutathione by dicarboxylate and 2-oxoglutarate carriers." J Pharmacol Exp Ther **285**(2): 608-18.
- Cheng, K. C., D. S. Cahill, H. Kasai, S. Nishimura and L. A. Loeb (1992). "8-Hydroxyguanine, an abundant form of oxidative DNA damage, causes G----T and A----C substitutions." J Biol Chem **267**(1): 166-72.
- Chuang, R. Y. and L. F. Chuang (1979). "Inhibition of chicken myeloblastosis RNA polymerase II activity by adriamycin." Biochemistry **18**(10): 2069-73.
- Cifone, M. G., P. Roncaioli, R. De Maria, G. Camarda, A. Santoni, G. Ruberti and R. Testi (1995). "Multiple pathways originate at the Fas/APO-1 (CD95) receptor: sequential involvement of phosphatidylcholine-specific phospholipase C and acidic sphingomyelinase in the propagation of the apoptotic signal." Embo J **14**(23): 5859-68.
- Conseil, G., R. G. Deeley and S. P. Cole (2005). "Polymorphisms of MRP1 (ABCC1) and related ATP-dependent drug transporters." Pharmacogenet Genomics **15**(8): 523-33.
- Cooper, J. (1997). Glutathione in the brain: disorders of glutathione metabolism. Boston, Butterworth-Heinemann.
- Cummings, J., L. Anderson, N. Willmott and J. F. Smyth (1991). "The molecular pharmacology of doxorubicin in vivo." Eur J Cancer **27**(5): 532-5.
- Dalle-Donne, I., A. Scaloni and D. A. Butterfield (2006). Redox proteomics : from protein modifications to cellular dysfunction and diseases. Hoboken, N.J., Wiley-Interscience.

- Daneshvar, B., H. Frandsen, H. Autrup and L. O. Dragsted (1997). "γ-Glutamyl semialdehyde and 2- amino-adipic semialdehyde: Biomarkers of oxidative damage to proteins." Biomarkers **2**: 117-123.
- Darley-USmar, V. and B. Halliwell (1996). "Blood radicals: reactive nitrogen species, reactive oxygen species, transition metal ions, and the vascular system." Pharm Res **13**(5): 649-662.
- Davies, K. J. and J. H. Doroshov (1986). "Redox cycling of anthracyclines by cardiac mitochondria. I. Anthracycline radical formation by NADH dehydrogenase." J Biol Chem **261**(7): 3060-7.
- Davies, K. J., J. H. Doroshov and P. Hochstein (1983). "Mitochondrial NADH dehydrogenase-catalyzed oxygen radical production by adriamycin, and the relative inactivity of 5-iminodaunorubicin." FEBS Lett **153**(1): 227-30.
- Davies, K. J., S. W. Lin and R. E. Pacifici (1987). "Protein damage and degradation by oxygen radicals. IV. Degradation of denatured protein." J Biol Chem **262**(20): 9914-20.
- DeAtley, S. M., M. Y. Aksenov, M. V. Aksenova, J. M. Carney and D. A. Butterfield (1998). "Adriamycin induces protein oxidation in erythrocyte membranes." Pharmacol Toxicol **83**(2): 62-8.
- DeAtley, S. M., M. Y. Aksenov, M. V. Aksenova, B. Harris, R. Hadley, P. Cole Harper, J. M. Carney and D. A. Butterfield (1999). "Antioxidants protect against reactive oxygen species associated with adriamycin-treated cardiomyocytes." Cancer Lett **136**(1): 41-6.

- Decleves, X., A. Regina, J. L. Laplanche, F. Roux, B. Boval, J. M. Launay and J. M. Scherrmann (2000). "Functional expression of P-glycoprotein and multidrug resistance-associated protein (Mrp1) in primary cultures of rat astrocytes." J Neurosci Res **60**(5): 594-601.
- Denicola, A., B. A. Freeman, M. Trujillo and R. Radi (1996). "Peroxynitrite reaction with carbon dioxide/bicarbonate: kinetics and influence on peroxynitrite-mediated oxidations." Arch Biochem Biophys **333**(1): 49-58.
- Denis, U., M. Lecomte, C. Paget, D. Ruggiero, N. Wiernsperger and M. Lagarde (2002). "Advanced glycation end-products induce apoptosis of bovine retinal pericytes in culture: involvement of diacylglycerol/ceramide production and oxidative stress induction." Free Radic Biol Med **33**(2): 236-47.
- Deres, P., R. Halmosi, A. Toth, K. Kovacs, A. Palfi, T. Habon, L. Czopf, T. Kalai, K. Hideg, B. Sumegi and K. Toth (2005). "Prevention of doxorubicin-induced acute cardiotoxicity by an experimental antioxidant compound." J Cardiovasc Pharmacol **45**(1): 36-43.
- Di Paola, M., P. Zaccagnino, G. Montedoro, T. Cocco and M. Lorusso (2004). "Ceramide induces release of pro-apoptotic proteins from mitochondria by either a Ca<sup>2+</sup> - dependent or a Ca<sup>2+</sup> -independent mechanism." J Bioenerg Biomembr **36**(2): 165-70.
- Dore, S. (2002). "Decreased activity of the antioxidant heme oxygenase enzyme: implications in ischemia and in Alzheimer's disease." Free Radic Biol Med **32**(12): 1276-82.

- Doroshow, J. H. (1983). "Anthracycline antibiotic-stimulated superoxide, hydrogen peroxide, and hydroxyl radical production by NADH dehydrogenase." Cancer Res **43**(10): 4543-51.
- Doroshow, J. H. and K. J. Davies (1986). "Redox cycling of anthracyclines by cardiac mitochondria. II. Formation of superoxide anion, hydrogen peroxide, and hydroxyl radical." J Biol Chem **261**(7): 3068-74.
- Dorr, R. T. (1996). "Cytoprotective agents for anthracyclines." Semin Oncol **23**(4 Suppl 8): 23-34.
- Drake, J., J. Kanski, S. Varadarajan, M. Tsoras and D. A. Butterfield (2002). "Elevation of brain glutathione by gamma-glutamylcysteine ethyl ester protects against peroxynitrite-induced oxidative stress." J Neurosci Res **68**(6): 776-84.
- Drake, J., C. D. Link and D. A. Butterfield (2003). "Oxidative stress precedes fibrillar deposition of Alzheimer's disease amyloid beta-peptide (1-42) in a transgenic *Caenorhabditis elegans* model." Neurobiol Aging **24**(3): 415-20.
- Drake, J., R. Sultana, M. Aksenova, V. Calabrese and D. A. Butterfield (2003). "Elevation of mitochondrial glutathione by gamma-glutamylcysteine ethyl ester protects mitochondria against peroxynitrite-induced oxidative stress." J Neurosci Res **74**(6): 917-27.
- Dringen, R. and B. Hamprecht (1999). "N-acetylcysteine, but not methionine or 2-oxothiazolidine-4-carboxylate, serves as cysteine donor for the synthesis of glutathione in cultured neurons derived from embryonal rat brain." Neurosci Lett **259**(2): 79-82.

- Droge, W. (1993). "Cysteine and glutathione deficiency in AIDS patients: a rationale for the treatment with N-acetyl-cysteine." Pharmacology **46**(2): 61-5.
- Ebadi, M., S. K. Srinivasan and M. D. Baxi (1996). "Oxidative stress and antioxidant therapy in Parkinson's disease." Prog Neurobiol **48**(1): 1-19.
- Eisenhauer, E. A. and J. B. Vermorken (1998). "The taxoids. Comparative clinical pharmacology and therapeutic potential." Drugs **55**(1): 5-30.
- Esterbauer, H. and P. Ramos (1996). "Chemistry and pathophysiology of oxidation of LDL." Rev Physiol Biochem Pharmacol **127**: 31-64.
- Esterbauer, H., R. J. Schaur and H. Zollner (1991). "Chemistry and biochemistry of 4-hydroxynonenal, malonaldehyde and related aldehydes." Free Radic Biol Med **11**(1): 81-128.
- Farr, S. A., H. F. Poon, D. Dogrukol-Ak, J. Drake, W. A. Banks, E. Eyerman, D. A. Butterfield and J. E. Morley (2003). "The antioxidants alpha-lipoic acid and N-acetylcysteine reverse memory impairment and brain oxidative stress in aged SAMP8 mice." J Neurochem **84**(5): 1173-83.
- Finbow, M. E. and M. A. Harrison (1997). "The vacuolar H<sup>+</sup>-ATPase: a universal proton pump of eukaryotes." Biochem J **324 ( Pt 3)**: 697-712.
- Fontaine, M., J. Geddes, A. Banks and D. Butterfield (2000). "Effect of exogenous and endogenous antioxidants on 3-nitropionic acid-induced in vivo oxidative stress and striatal lesions: insights into Huntington's disease." Journal of Neurochemistry **75**(4): 1709-1715.
- Freeman, J. R. and D. K. Broshek (2002). "Assessing cognitive dysfunction in breast cancer: what are the tools?" Clin Breast Cancer **3 Suppl 3**: S91-9.

- Fridovich, I. (1978a). "The biology of oxygen radicals." Science **201**(4359): 875-80.
- Fridovich, I. (1978b). "Superoxide dismutases: defence against endogenous superoxide radical." Ciba Found Symp(65): 77-93.
- Futai, M., T. Oka, G. Sun-Wada, Y. Moriyama, H. Kanazawa and Y. Wada (2000). "Luminal acidification of diverse organelles by V-ATPase in animal cells." J Exp Biol **203**(Pt 1): 107-16.
- Gabbita, S. P., M. A. Lovell and W. R. Markesbery (1998). "Increased nuclear DNA oxidation in the brain in Alzheimer's disease." Journal of Neurochemistry **71**(5): 2034-40.
- Garrett, R. and C. M. Grisham (1995). Biochemistry. Fort Worth, Saunders College Pub.
- Gilgun-Sherki, Y., E. Melamed and D. Offen (2003). "Antioxidant treatment in Alzheimer's disease: current state." J Mol Neurosci **21**(1): 1-11.
- Glenner, G. G., E. D. Eanes and C. A. Wiley (1988). "Amyloid fibrils formed from a segment of the pancreatic islet amyloid protein." Biochem Biophys Res Commun **155**(2): 608-14.
- Glenner, G. G. and C. W. Wong (1984). "Alzheimer's disease: initial report of the purification and characterization of a novel cerebrovascular amyloid protein." Biochem Biophys Res Commun **120**(3): 885-90.
- Good, P. F., A. Hsu, P. Werner, D. P. Perl and C. W. Olanow (1998). "Protein nitration in Parkinson's disease." J Neuropathol Exp Neurol **57**(4): 338-42.
- Good, P. F., P. Werner, A. Hsu, C. W. Olanow and D. P. Perl (1996). "Evidence of neuronal oxidative damage in Alzheimer's disease." Am J Pathol **149**(1): 21-8.



- Goodman, Y., A. J. Bruce, B. Cheng and M. P. Mattson (1996). "Estrogens attenuate and corticosterone exacerbates excitotoxicity, oxidative injury, and amyloid beta-peptide toxicity in hippocampal neurons." J Neurochem **66**(5): 1836-44.
- Griffith, O. W. (1980). "Determination of glutathione and glutathione disulfide using glutathione reductase and 2-vinylpyridine." Anal Biochem **106**(1): 207-12.
- Grundman, M. and P. Delaney (2002). "Antioxidant strategies for Alzheimer's disease." Proc Nutr Soc **61**(2): 191-202.
- Grune, T. and K. J. Davies (2003). "The proteasomal system and HNE-modified proteins." Mol Aspects Med **24**(4-5): 195-204.
- Gutierrez, P. L. (2000). "The role of NAD(P)H oxidoreductase (DT-Diaphorase) in the bioactivation of quinone-containing antitumor agents: a review." Free Radic Biol Med **29**(3-4): 263-75.
- Gutteridge, J. M. (1984). "Lipid peroxidation and possible hydroxyl radical formation stimulated by the self-reduction of a doxorubicin-iron (III) complex." Biochem Pharmacol **33**(11): 1725-8.
- Haass, C. and B. De Strooper (1999). "The presenilins in Alzheimer's disease--proteolysis holds the key." Science **286**(5441): 916-9.
- Habig, W. H., M. J. Pabst and W. B. Jakoby (1974). "Glutathione S-transferases. The first enzymatic step in mercapturic acid formation." J Biol Chem **249**(22): 7130-9.
- Hagemann, T. L., S. A. Gaeta, M. A. Smith, D. A. Johnson, J. A. Johnson and A. Messing (2005). "Gene expression analysis in mice with elevated glial fibrillary acidic protein and Rosenthal fibers reveals a stress response followed by glial activation and neuronal dysfunction." Hum Mol Genet **14**(16): 2443-58.

- Hall, E. D., M. R. Detloff, K. Johnson and N. C. Kupina (2004). "Peroxynitrite-mediated protein nitration and lipid peroxidation in a mouse model of traumatic brain injury." J Neurotrauma **21**(1): 9-20.
- Halliwell, B. (2001). "Role of free radicals in the neurodegenerative diseases: therapeutic implications for antioxidant treatment." Drugs Aging **18**(9): 685-716.
- Halliwell, B. and J. M. C. Gutteridge (1999). Free Radical in Biology and Medicine. Oxford, Oxford University Press.
- Handa, K. and S. Sato (1975). "Generation of free radicals of quinone group-containing anti-cancer chemicals in NADPH-microsome system as evidenced by initiation of sulfite oxidation." Gann **66**(1): 43-7.
- Hansen, J. M., Y. M. Go and D. P. Jones (2006). "Nuclear and mitochondrial compartmentation of oxidative stress and redox signaling." Annu Rev Pharmacol Toxicol **46**: 215-34.
- Hardy, J. and D. Allsop (1991). "Amyloid deposition as the central event in the aetiology of Alzheimer's disease." Trends Pharmacol Sci **12**(10): 383-8.
- Harman, D. (1956). "Aging: a theory based on free radical and radiation chemistry." J Gerontol **11**(3): 298-300.
- Hayes, J. D. and L. I. McLellan (1999). "Glutathione and glutathione-dependent enzymes represent a co-ordinately regulated defence against oxidative stress." Free Radic Res **31**(4): 273-300.
- Hensley, K., J. Carney, N. Hall, W. Shaw and D. A. Butterfield (1994). "Electron paramagnetic resonance investigations of free radical-induced alterations in

- neocortical synaptosomal membrane protein infrastructure." Free Radic Biol Med **17**(4): 321-31.
- Hensley, K., N. Hall, R. Subramaniam, P. Cole, M. Harris, M. Aksenov, M. Aksenova, S. P. Gabbita, J. F. Wu, J. M. Carney and et al. (1995). "Brain regional correspondence between Alzheimer's disease histopathology and biomarkers of protein oxidation." J Neurochem **65**(5): 2146-56.
- Hensley, K., M. L. Maidt, Z. Yu, H. Sang, W. R. Markesbery and R. A. Floyd (1998). "Electrochemical analysis of protein nitrotyrosine and dityrosine in the Alzheimer brain indicates region-specific accumulation." J Neurosci **18**(20): 8126-32.
- Hipfner, D. R., R. G. Deeley and S. P. Cole (1999). "Structural, mechanistic and clinical aspects of MRP1." Biochim Biophys Acta **1461**(2): 359-76.
- Hirrlinger, J., J. Konig, D. Keppler, J. Lindenau, J. B. Schulz and R. Dringen (2001). "The multidrug resistance protein MRP1 mediates the release of glutathione disulfide from rat astrocytes during oxidative stress." J Neurochem **76**(2): 627-36.
- Hissin, P. J. and R. Hilf (1976). "A fluorometric method for determination of oxidized and reduced glutathione in tissues." Anal Biochem **74**(1): 214-26.
- Holoye, P. Y., J. Duelge, R. M. Hansen, P. S. Ritch and T. Anderson (1983). "Prophylaxis of ifosfamide toxicity with oral acetylcysteine." Semin Oncol **10**(1 Suppl 1): 66-71.
- Hoogland, C., J. C. Sanchez, D. Walther, V. Baujard, O. Baujard, L. Tonella, D. F. Hochstrasser and R. D. Appel (1999). "Two-dimensional electrophoresis resources available from ExPASy." Electrophoresis **20**(18): 3568-71.

- Huai-Yun, H., D. T. Secrest, K. S. Mark, D. Carney, C. Brandquist, W. F. Elmquist and D. W. Miller (1998). "Expression of multidrug resistance-associated protein (MRP) in brain microvessel endothelial cells." Biochem Biophys Res Commun **243**(3): 816-20.
- Huang, H. M., H. Zhang, H. C. Ou, H. L. Chen and G. E. Gibson (2004). "alpha-keto-beta-methyl-n-valeric acid diminishes reactive oxygen species and alters endoplasmic reticulum Ca(2+) stores." Free Radic Biol Med **37**(11): 1779-89.
- Ide, T., H. Tsutsui, S. Kinugawa, H. Utsumi, D. Kang, N. Hattori, K. Uchida, K. Arimura, K. Egashira and A. Takeshita (1999). "Mitochondrial electron transport complex I is a potential source of oxygen free radicals in the failing myocardium." Circ Res **85**(4): 357-63.
- Ischiropoulos, H., L. Zhu, J. Chen, M. Tsai, J. C. Martin, C. D. Smith and J. S. Beckman (1992). "Peroxynitrite-mediated tyrosine nitration catalyzed by superoxide dismutase." Arch Biochem Biophys **298**(2): 431-7.
- Ishii, T., M. Yamada, H. Sato, M. Matsue, S. Taketani, K. Nakayama, Y. Sugita and S. Bannai (1993). "Cloning and characterization of a 23-kDa stress-induced mouse peritoneal macrophage protein." J Biol Chem **268**(25): 18633-6.
- Iwangoff, P., R. Armbruster, A. Enz and W. Meier-Ruge (1980). "Glycolytic enzymes from human autaptic brain cortex: normal aged and demented cases." Mech Ageing Dev **14**(1-2): 203-9.
- Jarrett, J. T., E. P. Berger and P. T. Lansbury, Jr. (1993). "The carboxy terminus of the beta amyloid protein is critical for the seeding of amyloid formation: implications for the pathogenesis of Alzheimer's disease." Biochemistry **32**(18): 4693-7.

- Jedlitschky, G. and D. Keppler (2002). "Transport of leukotriene C4 and structurally related conjugates." Vitam Horm **64**: 153-84.
- Jedlitschky, G., I. Leier, U. Buchholz, M. Center and D. Keppler (1994). "ATP-dependent transport of glutathione S-conjugates by the multidrug resistance-associated protein." Cancer Res **54**(18): 4833-6.
- Joshi, G., S. Hardas, R. Sultana, D. St. Clair, M. Vore and D. A. Butterfield (2006). "Glutathione elevation by  $\gamma$ -glutamyl cystein ethyl ester as a potential therapeutic strategy towards preventing oxidative stress in brain mediated by in vivo administration of adriamycin: Implication for chemobrain." J Neurochem Res **Submitted**.
- Joshi, G., R. Sultana, M. P. Cole, D. K. St Clair, M. Vore and D. A. Butterfield (2006). "Alteration in glutathione level and glutathione-related enzyme expression and activity in brain induced by the anti-cancer drug Adriamycin: Implications for oxidative stress-mediated CNS toxicity." Neurochem Int **Submitted**.
- Joshi, G., R. Sultana, M. Perluigi and D. Allan Butterfield (2005a). "In vivo protection of synaptosomes from oxidative stress mediated by  $\text{Fe}^{2+}/\text{H}_2\text{O}_2$  or 2,2-azobis-(2-amidinopropane) dihydrochloride by the glutathione mimetic tricyclodecan-9-yl-xanthogenate." Free Radic Biol Med **38**(8): 1023-31.
- Joshi, G., R. Sultana, J. Tangpong, M. P. Cole, D. K. St Clair, M. Vore, S. Estus and D. A. Butterfield (2005b). "Free radical mediated oxidative stress and toxic side effects in brain induced by the anti cancer drug adriamycin: insight into chemobrain." Free Radic Res **39**(11): 1147-54.

- Kalyanaraman, B., K. M. Morehouse and R. P. Mason (1991). "An electron paramagnetic resonance study of the interactions between the adriamycin semiquinone, hydrogen peroxide, iron-chelators, and radical scavengers." Arch Biochem Biophys **286**(1): 164-70.
- Kang, S. W., H. Z. Chae, M. S. Seo, K. Kim, I. C. Baines and S. G. Rhee (1998). "Mammalian peroxiredoxin isoforms can reduce hydrogen peroxide generated in response to growth factors and tumor necrosis factor-alpha." J Biol Chem **273**(11): 6297-302.
- Kanski, J., M. Aksenova, A. Stoyanova and D. A. Butterfield (2002). "Ferulic acid antioxidant protection against hydroxyl and peroxy radical oxidation in synaptosomal and neuronal cell culture systems in vitro: structure-activity studies." Journal of Nutritional Biochemistry **13**(5): 273-281.
- Kanski, J., C. Lauderback and D. A. Butterfield (2001). "5-Aminosalicylic acid protection against oxidative damage to synaptosomal membranes by alkoxy radicals in vitro." Neurochem Res **26**(1): 23-9.
- Kappus, H. (1987). "Oxidative stress in chemical toxicity." Arch Toxicol **60**(1-3): 144-9.
- Karry, R., E. Klein and D. Ben Shachar (2004). "Mitochondrial complex I subunits expression is altered in schizophrenia: a postmortem study." Biol Psychiatry **55**(7): 676-84.
- Katzman, R. and T. Saitoh (1991). "Advances in Alzheimer's disease." Faseb J **5**(3): 278-86.

- Keller, A., A. Berod, M. Dussaillant, N. Lamande, F. Gros and M. Lucas (1994).  
"Coexpression of alpha and gamma enolase genes in neurons of adult rat brain." J Neurosci Res **38**(5): 493-504.
- Keller, J. N., E. Dimayuga, Q. Chen, J. Thorpe, J. Gee and Q. Ding (2004). "Autophagy, proteasomes, lipofuscin, and oxidative stress in the aging brain." Int J Biochem Cell Biol **36**(12): 2376-91.
- Keller, J. N., C. M. Lauderback, D. A. Butterfield, M. S. Kindy, J. Yu and W. R. Markesbery (2000). "Amyloid beta-peptide effects on synaptosomes from apolipoprotein E-deficient mice." J Neurochem **74**(4): 1579-86.
- Keller, J. N., Z. Pang, J. W. Geddes, J. G. Begley, A. Germeyer, G. Waeg and M. P. Mattson (1997). "Impairment of glucose and glutamate transport and induction of mitochondrial oxidative stress and dysfunction in synaptosomes by amyloid beta-peptide: role of the lipid peroxidation product 4-hydroxynonenal." J Neurochem **69**(1): 273-84.
- Keller, J. N., F. A. Schmitt, S. W. Scheff, Q. Ding, Q. Chen, D. A. Butterfield and W. R. Markesbery (2005). "Evidence of increased oxidative damage in subjects with mild cognitive impairment." Neurology **64**(7): 1152-6.
- Kienzl, E., K. Jellinger, H. Stachelberger and W. Linert (1999). "Iron as catalyst for oxidative stress in the pathogenesis of Parkinson's disease?" Life Sci **65**(18-19): 1973-6.
- Kikuzaki, H., M. Hisamoto, K. Hirose, K. Akiyama and H. Taniguchi (2002).  
"Antioxidant properties of ferulic acid and its related compounds." Journal of Agricultural and Food Chemistry **50**(7): 2161-8.

- Kim, H. S., J. Y. Cho, D. H. Kim, J. J. Yan, H. K. Lee, H. W. Suh and D. K. Song (2004). "Inhibitory effects of long-term administration of ferulic acid on microglial activation induced by intracerebroventricular injection of beta-amyloid peptide (1-42) in mice." Biological & Pharmaceutical Bulletin **27**(1): 120-1.
- Konorev, E. A., M. C. Kennedy and B. Kalyanaraman (1999). "Cell-permeable superoxide dismutase and glutathione peroxidase mimetics afford superior protection against doxorubicin-induced cardiotoxicity: the role of reactive oxygen and nitrogen intermediates." Arch Biochem Biophys **368**(2): 421-8.
- Koppal, T., J. Drake and D. A. Butterfield (1999a). "In vivo modulation of rodent glutathione and its role in peroxynitrite-induced neocortical synaptosomal membrane protein damage." Biochim Biophys Acta **1453**(3): 407-11.
- Koppal, T., J. Drake, S. Yatin, B. Jordan, S. Varadarajan, L. Bettenhausen and D. A. Butterfield (1999b). "Peroxynitrite-induced alterations in synaptosomal membrane proteins: insight into oxidative stress in Alzheimer's disease." J Neurochem **72**(1): 310-7.
- Kotamraju, S., E. A. Konorev, J. Joseph and B. Kalyanaraman (2000). "Doxorubicin-induced apoptosis in endothelial cells and cardiomyocytes is ameliorated by nitron spin traps and ebselen. Role of reactive oxygen and nitrogen species." J Biol Chem **275**(43): 33585-92.
- Krapfenbauer, K., E. Engidawork, N. Cairns, M. Fountoulakis and G. Lubec (2003). "Aberrant expression of peroxiredoxin subtypes in neurodegenerative disorders." Brain Res **967**(1-2): 152-60.



- Kwok, J. C. and D. R. Richardson (2003). "Anthracyclines induce accumulation of iron in ferritin in myocardial and neoplastic cells: inhibition of the ferritin iron mobilization pathway." Mol Pharmacol **63**(4): 849-61.
- La Fontaine, M. A., J. W. Geddes, A. Banks and D. A. Butterfield (2000). "3-nitropropionic acid induced in vivo protein oxidation in striatal and cortical synaptosomes: insights into Huntington's disease." Brain Res **858**(2): 356-62.
- LaFontaine, M. A., M. P. Mattson and D. A. Butterfield (2002). "Oxidative stress in synaptosomal proteins from mutant presenilin-1 knock-in mice: implications for familial Alzheimer's disease." Neurochem Res **27**(5): 417-21.
- Lauderback, C. M., J. Drake, D. Zhou, J. M. Hackett, A. Castegna, J. Kanski, M. Tsoras, S. Varadarajan and D. A. Butterfield (2003). "Derivatives of xanthic acid are novel antioxidants: application to synaptosomes." Free. Radic. Res **37**(4): 355-65.
- Lauderback, C. M., J. M. Hackett, F. F. Huang, J. N. Keller, L. I. Szweda, W. R. Markesbery and D. A. Butterfield (2001). "The glial glutamate transporter, GLT-1, is oxidatively modified by 4-hydroxy-2-nonenal in the Alzheimer's disease brain: the role of Abeta1-42." J. Neurochem **78**(2): 413-6.
- Lauderback, C. M., J. Kanski, J. M. Hackett, N. Maeda, M. S. Kindy and D. A. Butterfield (2002). "Apolipoprotein E modulates Alzheimer's Abeta(1-42)-induced oxidative damage to synaptosomes in an allele-specific manner." Brain Res **924**(1): 90-7.
- Le, W. D., W. J. Xie and S. H. Appel (1999). "Protective role of heme oxygenase-1 in oxidative stress-induced neuronal injury." J Neurosci Res **56**(6): 652-8.

- Lee, M. K., D. R. Borchelt, G. Kim, G. Thinakaran, H. H. Slunt, T. Ratovitski, L. J. Martin, A. Kittur, S. Gandy, A. I. Levey, N. Jenkins, N. Copeland, D. L. Price and S. S. Sisodia (1997). "Hyperaccumulation of FAD-linked presenilin 1 variants in vivo." Nat Med **3**(7): 756-60.
- Levine, R. L., J. A. Williams, E. R. Stadtman and E. Shacter (1994). "Carbonyl assays for determination of oxidatively modified proteins." Methods Enzymol **233**: 346-57.
- Li, Y., P. Maher and D. Schubert (1998). "Phosphatidylcholine-specific phospholipase C regulates glutamate-induced nerve cell death." Proc Natl Acad Sci U S A **95**(13): 7748-53.
- Liu, R. and J. Choi (2000). "Age-associated decline in gamma-glutamylcysteine synthetase gene expression in rats." Free Radic Biol Med **28**(4): 566-74.
- Loe, D. W., K. C. Almquist, R. G. Deeley and S. P. Cole (1996). "Multidrug resistance protein (MRP)-mediated transport of leukotriene C4 and chemotherapeutic agents in membrane vesicles. Demonstration of glutathione-dependent vincristine transport." J Biol Chem **271**(16): 9675-82.
- Loe, D. W., R. G. Deeley and S. P. Cole (2000). "Verapamil stimulates glutathione transport by the 190-kDa multidrug resistance protein 1 (MRP1)." J Pharmacol Exp Ther **293**(2): 530-8.
- Loeffen, J. L., J. A. Smeitink, J. M. Trijbels, A. J. Janssen, R. H. Triepels, R. C. Sengers and L. P. van den Heuvel (2000). "Isolated complex I deficiency in children: clinical, biochemical and genetic aspects." Hum Mutat **15**(2): 123-34.

- Lovell, M. A., S. P. Gabbita and W. R. Markesbery (1999). "Increased DNA oxidation and decreased levels of repair products in Alzheimer's disease ventricular CSF." J Neurochem **72**(2): 771-6.
- Lovell, M. A., C. Xie and W. R. Markesbery (1998). "Decreased glutathione transferase activity in brain and ventricular fluid in Alzheimer's disease." Neurology **51**(6): 1562-6.
- Lovell, M. A., C. Xie and W. R. Markesbery (2001). "Acrolein is increased in Alzheimer's disease brain and is toxic to primary hippocampal cultures." Neurobiol Aging **22**(2): 187-94.
- Luberto, C. and Y. A. Hannun (1998). "Sphingomyelin synthase, a potential regulator of intracellular levels of ceramide and diacylglycerol during SV40 transformation. Does sphingomyelin synthase account for the putative phosphatidylcholine-specific phospholipase C?" J Biol Chem **273**(23): 14550-9.
- Luth, H. J., G. Munch and T. Arendt (2002). "Aberrant expression of NOS isoforms in Alzheimer's disease is structurally related to nitrotyrosine formation." Brain Research **953**(1-2): 135-43.
- Machleidt, T., B. Kramer, D. Adam, B. Neumann, S. Schutze, K. Wiegmann and M. Kronke (1996). "Function of the p55 tumor necrosis factor receptor "death domain" mediated by phosphatidylcholine-specific phospholipase C." J Exp Med **184**(2): 725-33.
- Marczin, N., N. El-Habashi, G. S. Hoare, R. E. Bundy and M. Yacoub (2003). "Antioxidants in myocardial ischemia-reperfusion injury: therapeutic potential and basic mechanisms." Arch Biochem Biophys **420**(2): 222-36.

- Mark, R. J., M. A. Lovell, W. R. Markesbery, K. Uchida and M. P. Mattson (1997). "A role for 4-hydroxynonenal, an aldehydic product of lipid peroxidation, in disruption of ion homeostasis and neuronal death induced by amyloid beta-peptide." J. Neurochem **68**(1): 255-64.
- Mark, R. J., Z. Pang, J. W. Geddes, K. Uchida and M. P. Mattson (1997). "Amyloid beta-peptide impairs glucose transport in hippocampal and cortical neurons: involvement of membrane lipid peroxidation." J Neurosci **17**(3): 1046-54.
- Markesbery, W. R. (1997). "Oxidative stress hypothesis in Alzheimer's disease." Free Radic Biol Med **23**(1): 134-47.
- Markesbery, W. R. and M. A. Lovell (1998). "Four-hydroxynonenal, a product of lipid peroxidation, is increased in the brain in Alzheimer's disease." Neurobiol Aging **19**(1): 33-6.
- Mattson, M. P. (1996). "Calcium and Free Radicals: Mediators of neurotrophic factor and excitatory transmitter-regulated developmental plasticity and cell death." Perspect Dev Neurobiol **3**(2): 79-91.
- Mattson, M. P., S. W. Barger, B. Cheng, I. Lieberburg, V. L. Smith-Swintosky and R. E. Rydel (1993). "beta-Amyloid precursor protein metabolites and loss of neuronal Ca<sup>2+</sup> homeostasis in Alzheimer's disease." Trends Neurosci **16**(10): 409-14.
- Mattson, M. P., B. Cheng, A. R. Culwell, F. S. Esch, I. Lieberburg and R. E. Rydel (1993). "Evidence for excitoprotective and intraneuronal calcium-regulating roles for secreted forms of the beta-amyloid precursor protein." Neuron **10**(2): 243-54.

- McClung, J. K., E. R. Jupe, X. T. Liu and R. T. Dell'Orco (1995). "Prohibitin: potential role in senescence, development, and tumor suppression." Exp Gerontol **30**(2): 99-124.
- McIntosh, L. J., M. A. Trush and J. C. Troncoso (1997). "Increased susceptibility of Alzheimer's disease temporal cortex to oxygen free radical-mediated processes." Free Radical Biology and Medicine **23**(2): 183-90.
- Mecocci, P., U. MacGarvey, A. E. Kaufman, D. Koontz, J. M. Shoffner, D. C. Wallace and M. F. Beal (1993). "Oxidative damage to mitochondrial DNA shows marked age-dependent increases in human brain." Ann Neurol **34**(4): 609-16.
- Meier-Ruge, W., P. Iwangoff and K. Reichlmeier (1984). "Neurochemical enzyme changes in Alzheimer's and Pick's disease." Arch Gerontol Geriatr **3**(2): 161-5.
- Meister, A. (1995). "Mitochondrial changes associated with glutathione deficiency." Biochim Biophys Acta **1271**(1): 35-42.
- Meister, A. and M. E. Anderson (1983). "Glutathione." Annu Rev Biochem **52**: 711-60.
- Meng, A., C. Luberto, P. Meier, A. Bai, X. Yang, Y. A. Hannun and D. Zhou (2004). "Sphingomyelin synthase as a potential target for D609-induced apoptosis in U937 human monocytic leukemia cells." Exp Cell Res **292**(2): 385-92.
- Meyers, C. A. (2000). "Neurocognitive dysfunction in cancer patients." Oncology (Williston Park) **14**(1): 75-9; discussion 79, 81-2, 85.
- Michel, P. P., N. Lambeng and M. Ruberg (1999). "Neuropharmacologic aspects of apoptosis: significance for neurodegenerative diseases." Clin Neuropharmacol **22**(3): 137-50.

- Miquel, J., A. C. Economos, J. Fleming and J. E. Johnson, Jr. (1980). "Mitochondrial role in cell aging." Exp Gerontol **15**(6): 575-91.
- Mishra, S., L. C. Murphy and L. J. Murphy (2006). "The Prohibitins: emerging roles in diverse functions." J Cell Mol Med **10**(2): 353-63.
- Mohmmad Abdul, H., R. Sultana, J. N. Keller, D. K. St Clair, W. R. Markesbery and D. A. Butterfield (2006). "Mutations in amyloid precursor protein and presenilin-1 genes increase the basal oxidative stress in murine neuronal cells and lead to increased sensitivity to oxidative stress mediated by amyloid beta-peptide (1-42), HO and kainic acid: implications for Alzheimer's disease." J Neurochem **96**(5): 1322-35.
- Monick, M. M., A. B. Carter, G. Gudmundsson, R. Mallampalli, L. S. Powers and G. W. Hunninghake (1999). "A phosphatidylcholine-specific phospholipase C regulates activation of p42/44 mitogen-activated protein kinases in lipopolysaccharide-stimulated human alveolar macrophages." J Immunol **162**(5): 3005-12.
- Montine, T. J., M. D. Neely, J. F. Quinn, M. F. Beal, W. R. Markesbery, L. J. Roberts and J. D. Morrow (2002). "Lipid peroxidation in aging brain and Alzheimer's disease." Free Radic Biol Med **33**(5): 620-6.
- Morciano, M., J. Burre, C. Corvey, M. Karas, H. Zimmermann and W. Volkandt (2005). "Immunoisolation of two synaptic vesicle pools from synaptosomes: a proteomics analysis." J Neurochem **95**(6): 1732-45.
- Moreira, P. I., M. A. Smith, X. Zhu, A. Nunomura, R. J. Castellani and G. Perry (2005). "Oxidative stress and neurodegeneration." Ann N Y Acad Sci **1043**: 545-52.

- Morris, J. C., M. Storandt, J. P. Miller, D. W. McKeel, J. L. Price, E. H. Rubin and L. Berg (2001). "Mild cognitive impairment represents early-stage Alzheimer disease." Arch Neurol **58**(3): 397-405.
- Nagaraj, R. H. and V. M. Monnier (1995). "Protein modification by the degradation products of ascorbate: formation of a novel pyrrole from the Maillard reaction of L-threose with proteins." Biochim Biophys Acta **1253**(1): 75-84.
- Namba, Y., M. Tomonaga, H. Kawasaki, E. Otomo and K. Ikeda (1991). "Apolipoprotein E immunoreactivity in cerebral amyloid deposits and neurofibrillary tangles in Alzheimer's disease and kuru plaque amyloid in Creutzfeldt-Jakob disease." Brain Res **541**(1): 163-6.
- Nelson, N. and W. R. Harvey (1999). "Vacuolar and plasma membrane proton-adenosinetriphosphatases." Physiol Rev **79**(2): 361-85.
- Neumann, C. A., D. S. Krause, C. V. Carman, S. Das, D. P. Dubey, J. L. Abraham, R. T. Bronson, Y. Fujiwara, S. H. Orkin and R. A. Van Etten (2003). "Essential role for the peroxiredoxin Prdx1 in erythrocyte antioxidant defence and tumour suppression." Nature **424**(6948): 561-5.
- Nies, A. T., G. Jedlitschky, J. Konig, C. Herold-Mende, H. H. Steiner, H. P. Schmitt and D. Keppler (2004). "Expression and immunolocalization of the multidrug resistance proteins, MRP1-MRP6 (ABCC1-ABCC6), in human brain." Neuroscience **129**(2): 349-60.
- Nishi, T. and M. Forgac (2002). "The vacuolar (H<sup>+</sup>)-ATPases--nature's most versatile proton pumps." Nat Rev Mol Cell Biol **3**(2): 94-103.

- Nishibayashi, S., N. Ogawa, M. Asanuma, Y. Kondo and A. Mori (1994). "Tubulin and actin mRNAs in the young-adult and the aged rat brain: effects of repeated administration with bifemelane hydrochloride." Arch Gerontol Geriatr **19**(3): 265-72.
- Nunomura, A., G. Perry, M. A. Pappolla, R. Wade, K. Hirai, S. Chiba and M. A. Smith (1999). "RNA oxidation is a prominent feature of vulnerable neurons in Alzheimer's disease." J Neurosci **19**(6): 1959-64.
- Ogiwara, T., K. Satoh, Y. Kadoma, Y. Murakami, S. Unten, T. Atsumi, H. Sakagami and S. Fujisawa (2002). "Radical scavenging activity and cytotoxicity of ferulic acid." Anticancer Research **22**(5): 2711-7.
- Omar, R. A., Y. J. Chyan, A. C. Andorn, B. Poeggeler, N. K. Robakis and M. A. Pappolla (1999). "Increased Expression but Reduced Activity of Antioxidant Enzymes in Alzheimer's Disease." Journal of Alzheimers Disease **1**(3): 139-145.
- Onyango, I. G., J. P. Bennett, Jr. and J. B. Tuttle (2005). "Endogenous oxidative stress in sporadic Alzheimer's disease neuronal cybrids reduces viability by increasing apoptosis through pro-death signaling pathways and is mimicked by oxidant exposure of control cybrids." Neurobiol Dis **19**(1-2): 312-22.
- Pahan, K., F. G. Sheikh, A. M. Namboodiri and I. Singh (1998). "N-acetyl cysteine inhibits induction of NO production by endotoxin or cytokine stimulated rat peritoneal macrophages, C6 glial cells and astrocytes." Free Radic Biol Med **24**(1): 39-48.
- Pappolla, M. A., Y. J. Chyan, R. A. Omar, K. Hsiao, G. Perry, M. A. Smith and P. Bozner (1998). "Evidence of oxidative stress and in vivo neurotoxicity of beta-



- amyloid in a transgenic mouse model of Alzheimer's disease: a chronic oxidative paradigm for testing antioxidant therapies in vivo." Am J Pathol **152**(4): 871-7.
- Pappolla, M. A., M. Sos, R. A. Omar, R. J. Bick, D. L. Hickson-Bick, R. J. Reiter, S. Efthimiopoulos and N. K. Robakis (1997). "Melatonin prevents death of neuroblastoma cells exposed to the Alzheimer amyloid peptide." J Neurosci **17**(5): 1683-90.
- Park, C. S., G. Krishna, M. S. Ahn, J. H. Kang, W. G. Chung, D. J. Kim, H. K. Hwang, J. N. Lee, S. G. Paik and Y. N. Cha (2000). "Differential and constitutive expression of neuronal, inducible, and endothelial nitric oxide synthase mRNAs and proteins in pathologically normal human tissues." Nitric Oxide **4**(5): 459-71.
- Pennisi, E. (1998). "Structure of key cytoskeletal protein tubulin revealed." Science **279**(5348): 176-7.
- Perluigi, M., H. Fai Poon, K. Hensley, W. M. Pierce, J. B. Klein, V. Calabrese, C. De Marco and D. A. Butterfield (2005). "Proteomic analysis of 4-hydroxy-2-nonenal-modified proteins in G93A-SOD1 transgenic mice--a model of familial amyotrophic lateral sclerosis." Free Radic Biol Med **38**(7): 960-8.
- Perluigi, M., G. Joshi, R. Sultana, V. Calabrese, C. De Marco, R. Coccia and D. A. Butterfield (2006). "In vivo protection by the xanthate tricyclodecan-9-yl-xanthogenate against amyloid beta-peptide (1-42)-induced oxidative stress." Neuroscience **138**(4): 1161-70.
- Perluigi, M., H. F. Poon, W. Maragos, W. M. Pierce, J. B. Klein, V. Calabrese, C. Cini, C. De Marco and D. A. Butterfield (2005). "Proteomic analysis of protein

- expression and oxidative modification in r6/2 transgenic mice: a model of Huntington disease." Mol Cell Proteomics **4**(12): 1849-61.
- Petersen, R. C., R. G. Thomas, M. Grundman, D. Bennett, R. Doody, S. Ferris, D. Galasko, S. Jin, J. Kaye, A. Levey, E. Pfeiffer, M. Sano, C. H. van Dyck and L. J. Thal (2005). "Vitamin E and donepezil for the treatment of mild cognitive impairment." N Engl J Med **352**(23): 2379-88.
- Picklo, M. J., V. Amarnath, J. O. McIntyre, D. G. Graham and T. J. Montine (1999). "4-Hydroxy-2(E)-nonenal inhibits CNS mitochondrial respiration at multiple sites." J Neurochem **72**(4): 1617-24.
- Pocernich, C. B. and D. A. Butterfield (2003). "Acrolein inhibits NADH-linked mitochondrial enzyme activity: implications for Alzheimer's disease." Neurotox Res **5**(7): 515-20.
- Pocernich, C. B., A. L. Cardin, C. L. Racine, C. M. Lauderback and D. A. Butterfield (2001). "Glutathione elevation and its protective role in acrolein-induced protein damage in synaptosomal membranes: relevance to brain lipid peroxidation in neurodegenerative disease." Neurochem Int **39**(2): 141-9.
- Pocernich, C. B., M. La Fontaine and D. A. Butterfield (2000). "In-vivo glutathione elevation protects against hydroxyl free radical-induced protein oxidation in rat brain." Neurochem Int **36**(3): 185-91.
- Pocernich, C. B., R. Sultana, H. Mohammad-Abdul, A. Nath and D. A. Butterfield (2005). "HIV-dementia, Tat-induced oxidative stress, and antioxidant therapeutic considerations." Brain Res Brain Res Rev **50**(1): 14-26.

- Poon, H. F., V. Calabrese, M. Calvani and D. A. Butterfield (2006). "Proteomics analyses of specific protein oxidation and protein expression in aged rat brain and its modulation by L-acetylcarnitine: insights into the mechanisms of action of this proposed therapeutic agent for CNS disorders associated with oxidative stress." Antioxid Redox Signal **8**(3-4): 381-94.
- Poon, H. F., V. Calabrese, G. Scapagnini and D. A. Butterfield (2004). "Free radicals: key to brain aging and heme oxygenase as a cellular response to oxidative stress." The Journals of Gerontology Series A: Biological Sciences and Medical Sciences **59**(5): 478-93.
- Poon, H. F., A. Castegna, S. A. Farr, V. Thongboonkerd, B. C. Lynn, W. A. Banks, J. E. Morley, J. B. Klein and D. A. Butterfield (2004). "Quantitative proteomics analysis of specific protein expression and oxidative modification in aged senescence-accelerated-prone 8 mice brain." Neuroscience **126**(4): 915-26.
- Poon, H. F., M. Frasier, N. Shreve, V. Calabrese, B. Wolozin and D. A. Butterfield (2005). "Mitochondrial associated metabolic proteins are selectively oxidized in A30P alpha-synuclein transgenic mice--a model of familial Parkinson's disease." Neurobiol Dis **18**(3): 492-8.
- Poon, H. F., K. Hensley, V. Thongboonkerd, M. L. Merchant, B. C. Lynn, W. M. Pierce, J. B. Klein, V. Calabrese and D. A. Butterfield (2005). "Redox proteomics analysis of oxidatively modified proteins in G93A-SOD1 transgenic mice--a model of familial amyotrophic lateral sclerosis." Free Radic Biol Med **39**(4): 453-62.

Poon, H. F., R. A. Vaishnav, D. A. Butterfield, M. L. Getchell and T. V. Getchell (2005).

"Proteomic identification of differentially expressed proteins in the aging murine olfactory system and transcriptional analysis of the associated genes." J Neurochem **94**(2): 380-92.

Prasad, K. N., W. C. Cole, A. R. Hovland, K. C. Prasad, P. Nahreini, B. Kumar, J.

Edwards-Prasad and C. P. Andreatta (1999). "Multiple antioxidants in the prevention and treatment of neurodegenerative disease: analysis of biologic rationale." Curr Opin Neurol **12**(6): 761-70.

Prescott, L. F., J. Park, A. Ballantyne, P. Adriaenssens and A. T. Proudfoot (1977).

"Treatment of paracetamol (acetaminophen) poisoning with N-acetylcysteine." Lancet **2**(8035): 432-4.

Price, D. L., S. S. Sisodia and D. R. Borchelt (1998). "Alzheimer disease--when and why?" Nat Genet **19**(4): 314-6.

Priebe, W., M. Krawczyk, M. T. Kuo, Y. Yamane, N. Savaraj and T. Ishikawa (1998).

"Doxorubicin- and daunorubicin-glutathione conjugates, but not unconjugated drugs, competitively inhibit leukotriene C4 transport mediated by MRP/GS-X pump." Biochem Biophys Res Commun **247**(3): 859-63.

Prosperi, M. T., D. Ferbus, D. Rouillard and G. Goubin (1998). "The pag gene product, a physiological inhibitor of c-abl tyrosine kinase, is overexpressed in cells entering S phase and by contact with agents inducing oxidative stress." FEBS Lett **423**(1): 39-44.

Radi, R., J. F. Turrens, L. Y. Chang, K. M. Bush, J. D. Crapo and B. A. Freeman (1991).

"Detection of catalase in rat heart mitochondria." J Biol Chem **266**(32): 22028-34.

- Rao, S. R. (1971). "Xanthates and related compounds (Marcel Dekker, New York)—specific phospholipase C and acidic sphingomyelinase in the propagation of the apoptotic signal." EMBO J **14**: 5859–5868.
- Rao, V. V., J. L. Dahlheimer, M. E. Bardgett, A. Z. Snyder, R. A. Finch, A. C. Sartorelli and D. Piwnica-Worms (1999). "Choroid plexus epithelial expression of MDR1 P glycoprotein and multidrug resistance-associated protein contribute to the blood-cerebrospinal-fluid drug-permeability barrier." Proc Natl Acad Sci U S A **96**(7): 3900-5.
- Reaume, A. G., D. S. Howland, S. P. Trusko, M. J. Savage, D. M. Lang, B. D. Greenberg, R. Siman and R. W. Scott (1996). "Enhanced amyloidogenic processing of the beta-amyloid precursor protein in gene-targeted mice bearing the Swedish familial Alzheimer's disease mutations and a "humanized" Abeta sequence." J Biol Chem **271**(38): 23380-8.
- Rego, A. C. and C. R. Oliveira (2003). "Mitochondrial dysfunction and reactive oxygen species in excitotoxicity and apoptosis: implications for the pathogenesis of neurodegenerative diseases." Neurochem Res **28**(10): 1563-74.
- Renes, J., E. E. de Vries, G. J. Hooiveld, I. Krikken, P. L. Jansen and M. Muller (2000). "Multidrug resistance protein MRP1 protects against the toxicity of the major lipid peroxidation product 4-hydroxynonenal." Biochem J **350 Pt 2**: 555-61.
- Requena, J. R., C. C. Chao, R. L. Levine and E. R. Stadtman (2001). "Glutamic and aminoadipic semialdehydes are the main carbonyl products of metal-catalyzed oxidation of proteins." Proc Natl Acad Sci U S A **98**(1): 69-74.

- Reverter-Branchat, G., E. Cabiscol, J. Tamarit and J. Ros (2004). "Oxidative damage to specific proteins in replicative and chronological-aged *Saccharomyces cerevisiae*: common targets and prevention by calorie restriction." J Biol Chem **279**(30): 31983-9.
- Robinson, B. H., X. P. Luo, S. Pitkanen, S. Bratinova, J. Bourgeois, D. C. Lehotay and S. Raha (1998). "Diagnosis of mitochondrial energy metabolism defects in tissue culture. Induction of MnSOD and bcl-2 in mitochondria from patients with complex I (NADH-CoQ reductase) deficiency." Biofactors **7**(3): 229-30.
- Rogaev, E. I., R. Sherrington, E. A. Rogaeva, G. Levesque, M. Ikeda, Y. Liang, H. Chi, C. Lin, K. Holman, T. Tsuda and et al. (1995). "Familial Alzheimer's disease in kindreds with missense mutations in a gene on chromosome 1 related to the Alzheimer's disease type 3 gene." Nature **376**(6543): 775-8.
- Sano, M., C. Ernesto, R. G. Thomas, M. R. Klauber, K. Schafer, M. Grundman, P. Woodbury, J. Growdon, C. W. Cotman, E. Pfeiffer, L. S. Schneider and L. J. Thal (1997). "A controlled trial of selegiline, alpha-tocopherol, or both as treatment for Alzheimer's disease. The Alzheimer's Disease Cooperative Study." N Engl J Med **336**(17): 1216-22.
- Sarafian, T. A., M. A. Verity, H. V. Vinters, C. C. Shih, L. Shi, X. D. Ji, L. Dong and H. Shau (1999). "Differential expression of peroxiredoxin subtypes in human brain cell types." J Neurosci Res **56**(2): 206-12.
- Sarvazyan, N. (1996). "Visualization of doxorubicin-induced oxidative stress in isolated cardiac myocytes." Am J Physiol **271**(5 Pt 2): H2079-85.

- Sastre, J., F. V. Pallardo and J. Vina (2003). "The role of mitochondrial oxidative stress in aging." Free Radic Biol Med **35**(1): 1-8.
- Sauer, G., E. Amtmann and W. Hofmann (1990). "Systemic treatment of a human epidermoid non-small cell lung carcinoma xenograft with a xanthate compound causes extensive intratumoral necrosis." Cancer Lett **53**(2-3): 97-102.
- Sauer, G., E. Amtmann, K. Melber, A. Knapp, K. Muller, K. Hummel and A. Scherm (1984). "DNA and RNA virus species are inhibited by xanthates, a class of antiviral compounds with unique properties." Proc Natl Acad Sci U S A **81**(11): 3263-7.
- Sayre, L. M., D. A. Zelasko, P. L. Harris, G. Perry, R. G. Salomon and M. A. Smith (1997). "4-Hydroxynonenal-derived advanced lipid peroxidation end products are increased in Alzheimer's disease." J. Neurochem **68**(5): 2092-7.
- Scapagnini, G., D. A. Butterfield, C. Colombrita, R. Sultana, A. Pascale and V. Calabrese (2004). "Ethyl ferulate, a lipophilic polyphenol, induces HO-1 and protects rat neurons against oxidative stress." Antioxidant and Redox Signaling **6**(5): 811-8.
- Schagen, S. B., H. L. Hamburger, M. J. Muller, W. Boogerd and F. S. van Dam (2001). "Neurophysiological evaluation of late effects of adjuvant high-dose chemotherapy on cognitive function." J Neurooncol **51**(2): 159-65.
- Schellenberg, G. D. (1995). "Genetic dissection of Alzheimer disease, a heterogeneous disorder." Proc Natl Acad Sci U S A **92**(19): 8552-9.
- Schipper, H. M. (2000). "Heme oxygenase-1: role in brain aging and neurodegeneration." Exp Gerontol **35**(6-7): 821-30.

- Schnurra, I., H. G. Bernstein, P. Riederer and K. H. Braunewell (2001). "The neuronal calcium sensor protein VILIP-1 is associated with amyloid plaques and extracellular tangles in Alzheimer's disease and promotes cell death and tau phosphorylation in vitro: a link between calcium sensors and Alzheimer's disease?" Neurobiol Dis **8**(5): 900-9.
- Schonberger, S. J., P. F. Edgar, R. Kydd, R. L. Faull and G. J. Cooper (2001). "Proteomic analysis of the brain in Alzheimer's disease: molecular phenotype of a complex disease process." Proteomics **1**(12): 1519-28.
- Schulz, J. B., J. Lindenau, J. Seyfried and J. Dichgans (2000). "Glutathione, oxidative stress and neurodegeneration." Eur J Biochem **267**(16): 4904-11.
- Schutze, S., K. Potthoff, T. Machleidt, D. Berkovic, K. Wiegmann and M. Kronke (1992). "TNF activates NF-kappa B by phosphatidylcholine-specific phospholipase C-induced "acidic" sphingomyelin breakdown." Cell **71**(5): 765-76.
- Selkoe, D. J. (2001). "Alzheimer's disease: genes, proteins, and therapy." Physiol Rev **81**(2): 741-66.
- Sheehan, J. P., R. H. Swerdlow, S. W. Miller, R. E. Davis, J. K. Parks, W. D. Parker and J. B. Tuttle (1997). "Calcium homeostasis and reactive oxygen species production in cells transformed by mitochondria from individuals with sporadic Alzheimer's disease." J Neurosci **17**(12): 4612-22.
- Sheline, C. T. and D. W. Choi (1998). "Neuronal death in cultured murine cortical cells is induced by inhibition of GAPDH and triosephosphate isomerase." Neurobiol Dis **5**(1): 47-54.



- Sherrington, R., E. I. Rogaev, Y. Liang, E. A. Rogaeva, G. Levesque, M. Ikeda, H. Chi, C. Lin, G. Li, K. Holman and et al. (1995). "Cloning of a gene bearing missense mutations in early-onset familial Alzheimer's disease." Nature **375**(6534): 754-60.
- Sies, H. (1999). "Glutathione and its role in cellular functions." Free Radic Biol Med **27**(9-10): 916-21.
- Sies, H., V. S. Sharov, L. O. Klotz and K. Briviba (1997). "Glutathione peroxidase protects against peroxynitrite-mediated oxidations. A new function for selenoproteins as peroxynitrite reductase." J Biol Chem **272**(44): 27812-7.
- Siman, R., A. G. Reaume, M. J. Savage, S. Trusko, Y. G. Lin, R. W. Scott and D. G. Flood (2000). "Presenilin-1 P264L knock-in mutation: differential effects on abeta production, amyloid deposition, and neuronal vulnerability." J Neurosci **20**(23): 8717-26.
- Simpson, E. P., Y. K. Henry, J. S. Henkel, R. G. Smith and S. H. Appel (2004). "Increased lipid peroxidation in sera of ALS patients: a potential biomarker of disease burden." Neurology **62**(10): 1758-65.
- Sims, N. R. (1990). "Rapid isolation of metabolically active mitochondria from rat brain and subregions using Percoll density gradient centrifugation." J Neurochem **55**(2): 698-707.
- Smith, D. H., X. H. Chen, M. Nonaka, J. Q. Trojanowski, V. M. Lee, K. E. Saatman, M. J. Leoni, B. N. Xu, J. A. Wolf and D. F. Meaney (1999). "Accumulation of amyloid beta and tau and the formation of neurofilament inclusions following diffuse brain injury in the pig." J Neuropathol Exp Neurol **58**(9): 982-92.

- Smith, J. V. and Y. Luo (2003). "Elevation of oxidative free radicals in Alzheimer's disease models can be attenuated by Ginkgo biloba extract EGb 761." J Alzheimers Dis. **5**(4): 287-300.
- Sontag, J. M., E. M. Fykse, Y. Ushkaryov, J. P. Liu, P. J. Robinson and T. C. Sudhof (1994). "Differential expression and regulation of multiple dynamins." J Biol Chem **269**(6): 4547-54.
- Sortino, M. A., F. Condorelli, C. Vancheri and P. L. Canonico (1999). "Tumor necrosis factor-alpha induces apoptosis in immortalized hypothalamic neurons: involvement of ceramide-generating pathways." Endocrinology **140**(10): 4841-9.
- Stadtman, E. R. and B. S. Berlett (1997). "Reactive oxygen-mediated protein oxidation in aging and disease." Chem Res Toxicol **10**(5): 485-94.
- Steinherz, L. J., P. G. Steinherz, C. T. Tan, G. Heller and M. L. Murphy (1991). "Cardiac toxicity 4 to 20 years after completing anthracycline therapy." Jama **266**(12): 1672-7.
- Stevens, M. J., I. Obrosova, X. Cao, C. Van Huysen and D. A. Greene (2000). "Effects of DL-alpha-lipoic acid on peripheral nerve conduction, blood flow, energy metabolism, and oxidative stress in experimental diabetic neuropathy." Diabetes **49**(6): 1006-15.
- Stevens, T. H. and M. Forgac (1997). "Structure, function and regulation of the vacuolar (H<sup>+</sup>)-ATPase." Annu Rev Cell Dev Biol **13**: 779-808.
- Subramaniam, R., F. Roediger, B. Jordan, M. P. Mattson, J. N. Keller, G. Waeg and D. A. Butterfield (1997). "The lipid peroxidation product, 4-hydroxy-2-trans-

- nonenal, alters the conformation of cortical synaptosomal membrane proteins." J. Neurochem **69**(3): 1161-9.
- Sultana, R., D. Boyd-Kimball, H. F. Poon, J. Cai, W. M. Pierce, J. B. Klein, W. R. Markesbery, X. Z. Zhou, K. P. Lu and D. A. Butterfield (2006a). "Oxidative modification and down-regulation of Pin1 in Alzheimer's disease hippocampus: A redox proteomics analysis." Neurobiol Aging **27**(7): 918-25.
- Sultana, R., D. Boyd-Kimball, H. F. Poon, J. Cai, W. M. Pierce, J. B. Klein, M. Merchant, W. R. Markesbery and D. A. Butterfield (2006b). "Redox proteomics identification of oxidized proteins in Alzheimer's disease hippocampus and cerebellum: An approach to understand pathological and biochemical alterations in AD." Neurobiol Aging **In press**.
- Sultana, R. and D. A. Butterfield (2004). "Oxidatively modified GST and MRP1 in Alzheimer's disease brain: Implication for accumulation of reactive lipid peroxidation products." Neurochem Res **29**: 2215-2220.
- Sultana, R., S. Newman, H. Mohammad-Abdul, J. N. Keller and D. A. Butterfield (2004). "Protective effect of the xanthate, D609, on Alzheimer's amyloid beta-peptide (1-42)-induced oxidative stress in primary neuronal cells." Free Radic Res **38**(5): 449-58.
- Sultana, R., M. Perluigi and D. A. Butterfield (2006). "Redox proteomics identification of oxidatively modified proteins in Alzheimer's disease brain and in vivo and in vitro models of AD centered around Abeta(1-42)." J Chromatogr B Analyt Technol Biomed Life Sci **833**(1): 3-11.

Sultana, R., H. F. Poon, J. Cai, W. M. Pierce, M. Merchant, J. B. Klein, W. R.

Markesbery and D. A. Butterfield (2006a). "Identification of nitrated proteins in Alzheimer's disease brain using a redox proteomics approach." Neurobiol Dis **22**(1): 76-87.

Sultana, R., H. F. Poon, J. Cai, W. M. Pierce, M. Merchant, J. B. Klein, W. R.

Markesbery and D. A. Butterfield (2006b). "Identification of nitrosatively modified proteins in Alzheimer's disease brain using redox proteomics approach." NeuroBiol Dis. **In press.**

Sultana, R., A. Ravagna, H. Mohmmad-Abdul, V. Calabrese and D. A. Butterfield

(2005). "Ferulic acid ethyl ester protects neurons against amyloid beta- peptide(1-42)-induced oxidative stress and neurotoxicity: relationship to antioxidant activity." J Neurochem **92**(4): 749-58.

Sultana, R., N. Shelley, M. A. Hafiz, J. N. Keller and D. Butterfield (2004). "Protective Effect of the Xanthate, D609, on Alzheimer's Amyloid  $\beta$ -peptide (1-42)-induced Oxidative Stress in Primary Neuronal Cells." Free Radical Research **38**(5): 449-458.

Takahashi, M., S. Dore, C. D. Ferris, T. Tomita, A. Sawa, H. Wolosker, D. R. Borchelt,

T. Iwatsubo, S. H. Kim, G. Thinakaran, S. S. Sisodia and S. H. Snyder (2000). "Amyloid precursor proteins inhibit heme oxygenase activity and augment neurotoxicity in Alzheimer's disease." Neuron **28**(2): 461-73.

Takeda, A., G. Perry, N. G. Abraham, B. E. Dwyer, R. K. Kutty, J. T. Laitinen, R. B.

Petersen and M. A. Smith (2000). "Overexpression of heme oxygenase in neuronal cells, the possible interaction with Tau." J Biol Chem **275**(8): 5395-9.

- Tanaka, S., M. Takehashi, N. Matoh, S. Iida, T. Suzuki, S. Futaki, H. Hamada, E. Masliah, Y. Sugiura and K. Ueda (2002). "Generation of reactive oxygen species and activation of NF-kappaB by non-Abeta component of Alzheimer's disease amyloid." J Neurochem **82**(2): 305-15.
- Tangpong, J., M. P. Cole, R. Sultana, S. Estus, M. Vore, W. St Clair, S. Ratanachaiyavong, D. St Clair and D. A. Butterfield (2006a). "Adriamycin-mediated nitration of manganese superoxide dismutase in the central nervous system: Insight into the mechanism of chemobrain." J Neurochem **In Press**.
- Tangpong, J., M. P. Cole, R. Sultana, G. Joshi, S. Estus, M. Vore, W. St Clair, S. Ratanachaiyavong, D. K. St Clair and D. A. Butterfield (2006b). "Adriamycin-induced, TNF-alpha-mediated central nervous system toxicity." Neurobiol Dis **23**(1): 127-39.
- Tian, G., A. Bhamidipati, N. J. Cowan and S. A. Lewis (1999). "Tubulin folding cofactors as GTPase-activating proteins. GTP hydrolysis and the assembly of the alpha/beta-tubulin heterodimer." J Biol Chem **274**(34): 24054-8.
- Tilleman, K., I. Stevens, K. Spittaels, C. V. Haute, S. Clerens, G. Van Den Bergh, H. Geerts, F. Van Leuven, F. Vandesande and L. Moens (2002). "Differential expression of brain proteins in glycogen synthase kinase-3 transgenic mice: a proteomics point of view." Proteomics **2**(1): 94-104.
- Tschaikowsky, K., J. Schmidt and M. Meisner (1998). "Modulation of mouse endotoxin shock by inhibition of phosphatidylcholine-specific phospholipase C." J Pharmacol Exp Ther **285**(2): 800-4.

- Tyrrell, R. (1999). "Redox regulation and oxidant activation of heme oxygenase-1." Free Radic Res **31**(4): 335-40.
- van der Blik, A. M., T. E. Redelmeier, H. Damke, E. J. Tisdale, E. M. Meyerowitz and S. L. Schmid (1993). "Mutations in human dynamin block an intermediate stage in coated vesicle formation." J Cell Biol **122**(3): 553-63.
- van der Vliet, A., J. P. Eiserich, H. Kaur, C. E. Cross and B. Halliwell (1996). "Nitrotyrosine as biomarker for reactive nitrogen species." Methods. Enzymol **269**: 175-84.
- van Groen, T., A. J. Kiliaan and I. Kadish (2006). "Deposition of mouse amyloid beta in human APP/PS1 double and single AD model transgenic mice." Neurobiol Dis **23**(3): 653-62.
- van Groen, T., L. Liu, S. Ikonen and I. Kadish (2003). "Diffuse amyloid deposition, but not plaque number, is reduced in amyloid precursor protein/presenilin 1 double-transgenic mice by pathway lesions." Neuroscience **119**(4): 1185-97.
- Van Uden, E., Y. Sagara, J. Van Uden, R. Orlando, M. Mallory, E. Rockenstein and E. Masliah (2000). "A protective role of the low density lipoprotein receptor-related protein against amyloid beta-protein toxicity." J Biol Chem **275**(39): 30525-30.
- Varadarajan, S., S. Yatin, M. Aksenova and D. A. Butterfield (2000). "Review: Alzheimer's amyloid beta-peptide-associated free radical oxidative stress and neurotoxicity." J Struct Biol **130**(2-3): 184-208.
- Vasquez-Vivar, J., N. Hogg, P. Martasek, H. Karoui, P. Tordo, K. A. Pritchard, Jr. and B. Kalyanaraman (1999). "Effect of redox-active drugs on superoxide generation

- from nitric oxide synthases: biological and toxicological implications." Free. Radic. Res **31**(6): 607-17.
- Vasquez-Vivar, J., P. Martasek, N. Hogg, B. S. Masters, K. A. Pritchard, Jr. and B. Kalyanaraman (1997). "Endothelial nitric oxide synthase-dependent superoxide generation from adriamycin." Biochemistry **36**(38): 11293-7.
- Ventura, B., M. L. Genova, C. Bovina, G. Formiggini and G. Lenaz (2002). "Control of oxidative phosphorylation by Complex I in rat liver mitochondria: implications for aging." Biochim Biophys Acta **1553**(3): 249-60.
- Verdier, Y., E. Huszar, B. Penke, Z. Penke, G. Woffendin, M. Scigelova, L. Fulop, M. Szucs, K. Medzihradszky and T. Janaky (2005). "Identification of synaptic plasma membrane proteins co-precipitated with fibrillar beta-amyloid peptide." J Neurochem **94**(3): 617-28.
- Villanueva, N., J. Navarro and E. Cubero (1991). "Antiviral effects of xanthate D609 on the human respiratory syncytial virus growth cycle." Virology **181**(1): 101-8.
- Vina, J., A. Lloret, R. Orti and D. Alonso (2004). "Molecular bases of the treatment of Alzheimer's disease with antioxidants: prevention of oxidative stress." Mol Aspects Med **25**(1-2): 117-23.
- Wang, H. and J. A. Joseph (1999). "Quantifying cellular oxidative stress by dichlorofluorescein assay using microplate reader." Free Radic Biol Med **27**(5-6): 612-6.
- Wang, J., S. Xiong, C. Xie, W. R. Markesbery and M. A. Lovell (2005). "Increased oxidative damage in nuclear and mitochondrial DNA in Alzheimer's disease." J Neurochem **93**(4): 953-62.

- Watson, W. H., Y. Chen and D. P. Jones (2003). "Redox state of glutathione and thioredoxin in differentiation and apoptosis." Biofactors **17**(1-4): 307-14.
- Weiss, H., T. Friedrich, G. Hofhaus and D. Preis (1991). "The respiratory-chain NADH dehydrogenase (complex I) of mitochondria." Eur J Biochem **197**(3): 563-76.
- Weiss, R. B., G. Sarosy, K. Clagett-Carr, M. Russo and B. Leyland-Jones (1986). "Anthracycline analogs: the past, present, and future." Cancer Chemother Pharmacol **18**(3): 185-97.
- Welch, W. J. (1992). "Mammalian stress response: cell physiology, structure/function of stress proteins, and implications for medicine and disease." Physiol Rev **72**(4): 1063-81.
- Wheeler, C. R., J. A. Salzman, N. M. Elsayed, S. T. Omaye and D. W. Korte, Jr. (1990). "Automated assays for superoxide dismutase, catalase, glutathione peroxidase, and glutathione reductase activity." Anal Biochem **184**(2): 193-9.
- Whittaker, V. P. (1993). "Thirty years of synaptosome research." J Neurocytol **22**(9): 735-42.
- Wiegmann, K., S. Schutze, T. Machleidt, D. Witte and M. Kronke (1994). "Functional dichotomy of neutral and acidic sphingomyelinases in tumor necrosis factor signaling." Cell **78**(6): 1005-15.
- Wilkens, S., T. Inoue and M. Forgac (2004). "Three-dimensional structure of the vacuolar ATPase. Localization of subunit H by difference imaging and chemical cross-linking." J Biol Chem **279**(40): 41942-9.
- Winblad, B., K. Palmer, M. Kivipelto, V. Jelic, L. Fratiglioni, L. O. Wahlund, A. Nordberg, L. Backman, M. Albert, O. Almkvist, H. Arai, H. Basun, K. Blennow,



- M. de Leon, C. DeCarli, T. Erkinjuntti, E. Giacobini, C. Graff, J. Hardy, C. Jack, A. Jorm, K. Ritchie, C. van Duijn, P. Visser and R. C. Petersen (2004). "Mild cognitive impairment--beyond controversies, towards a consensus: report of the International Working Group on Mild Cognitive Impairment." J Intern Med **256**(3): 240-6.
- Witke, W., A. V. Podtelejnikov, A. Di Nardo, J. D. Sutherland, C. B. Gurniak, C. Dotti and M. Mann (1998). "In mouse brain profilin I and profilin II associate with regulators of the endocytic pathway and actin assembly." Embo J **17**(4): 967-76.
- Wu, G., Y. Z. Fang, S. Yang, J. R. Lupton and N. D. Turner (2004). "Glutathione metabolism and its implications for health." J Nutr **134**(3): 489-92.
- Xie, C., M. A. Lovell and W. R. Markesbery (1998). "Glutathione transferase protects neuronal cultures against four hydroxynonenal toxicity." Free. Radic. Biol. Med **25**(8): 979-88.
- Yan, C. Y. and L. A. Greene (1998). "Prevention of PC12 cell death by N-acetylcysteine requires activation of the Ras pathway." J Neurosci **18**(11): 4042-9.
- Yan, J. J., J. Y. Cho, H. S. Kim, K. L. Kim, J. S. Jung, S. O. Huh, H. W. Suh, Y. H. Kim and D. K. Song (2001). "Protection against beta-amyloid peptide toxicity in vivo with long-term administration of ferulic acid." British Journal of Pharmacology **133**(1): 89-96.
- Yang, J., X. Liu, K. Bhalla, C. N. Kim, A. M. Ibrado, J. Cai, T. I. Peng, D. P. Jones and X. Wang (1997). "Prevention of apoptosis by Bcl-2: release of cytochrome c from mitochondria blocked." Science **275**(5303): 1129-32.

- Yankner, B. A., L. K. Duffy and D. A. Kirschner (1990). "Neurotrophic and neurotoxic effects of amyloid beta protein: reversal by tachykinin neuropeptides." Science **250**(4978): 279-82.
- Yao, P. J., M. Zhu, E. I. Pyun, A. I. Brooks, S. Therianos, V. E. Meyers and P. D. Coleman (2003). "Defects in expression of genes related to synaptic vesicle trafficking in frontal cortex of Alzheimer's disease." Neurobiol Dis **12**(2): 97-109.
- Yatin, S. M., S. Varadarajan, C. D. Link and D. A. Butterfield (1999). "In vitro and in vivo oxidative stress associated with Alzheimer's amyloid beta-peptide (1-42)." Neurobiol Aging **20**(3): 325-30; discussion 339-42.
- Yen, H. C., T. D. Oberley, C. G. Gairola, L. I. Szweda and D. K. St Clair (1999). "Manganese superoxide dismutase protects mitochondrial complex I against adriamycin-induced cardiomyopathy in transgenic mice." Arch Biochem Biophys **362**(1): 59-66.
- Yim, M. B., H. Z. Chae, S. G. Rhee, P. B. Chock and E. R. Stadtman (1994). "On the protective mechanism of the thiol-specific antioxidant enzyme against the oxidative damage of biomacromolecules." J Biol Chem **269**(3): 1621-6.
- Yu, B. P. (1994). "Cellular defenses against damage from reactive oxygen species." Physiol. Rev **74**(1): 139-62.
- Yu, H., J. Hong and D. Wu (1999). "[Effect of sodium ferulate on proliferation of rabbit aortic smooth muscle cells induced by oxidized LDL]." Zhongguo Zhong Yao Za Zhi **24**(6): 365-6, 384.
- Yu, Z. F., M. Nikolova-Karakashian, D. Zhou, G. Cheng, E. H. Schuchman and M. P. Mattson (2000). "Pivotal role for acidic sphingomyelinase in cerebral ischemia-

- induced ceramide and cytokine production, and neuronal apoptosis." J Mol Neurosci **15**(2): 85-97.
- Zamzami, N., P. Marchetti, M. Castedo, D. Decaudin, A. Macho, T. Hirsch, S. A. Susin, P. X. Petit, B. Mignotte and G. Kroemer (1995). "Sequential reduction of mitochondrial transmembrane potential and generation of reactive oxygen species in early programmed cell death." J Exp Med **182**(2): 367-77.
- Zarkovic, K. (2003). "4-hydroxynonenal and neurodegenerative diseases." Mol Aspects Med **24**(4-5): 293-303.
- Zhang, J., V. L. Dawson, T. M. Dawson and S. H. Snyder (1994). "Nitric oxide activation of poly(ADP-ribose) synthetase in neurotoxicity." Science **263**(5147): 687-9.
- Zhang, Q., H. Tian, X. Fu and G. Zhang (2003). "Delayed activation and regulation of MKK7 in hippocampal CA1 region following global cerebral ischemia in rats." Life Sci **74**(1): 37-45.
- Zhou, D., C. M. Lauderback, T. Yu, S. A. Brown, D. A. Butterfield and J. S. Thompson (2001). "D609 inhibits ionizing radiation-induced oxidative damage by acting as a potent antioxidant." J Pharmacol Exp Ther **298**(1): 103-9.

## Vita

Gururaj Vasanth Joshi was born on February 21, 1975 in Secunderabad, Andhra Pradesh, India. He was raised at various places in India and attended Kendriya Vidyalaya, Airforce Station, Begumpet, graduating in 1992. He went to Osmania University, Hyderabad, India and in the Spring of 1996 earned a Bachelor of Science (B.Sc.) in Biology and Chemistry. After joining the Department of Chemistry at Pune University in the Fall of 1996, he joined the research group of Dr. Amitabha Sarkar and Dr. Avinash Kumbhar in the Spring of 1997 as a part of Master of Science (M.Sc.) degree. The author worked in the area of Organometallic Chemistry. After completion of the M.Sc. in Spring 1998, he joined Asian Paints (I) Ltd. as Supervisor Chemist and worked until mid-fall 2001. In the Spring of 2002 he joined the Chemistry Department at University of Kentucky for the PhD program. He joined the research group of Professor Allan Butterfield in the Fall of 2002, working in the area of Bio-analytical/Neurochemistry.

## Publication and Submissions:

1. Poon HF, **Joshi G**, Sultana R, Farr SA, Bank WA, Morley JE, Calabrese V and Butterfield DA: Antisense directed at the Abeta region of APP decreases brain oxidative markers in aged senescence accelerated mice. *Brain Res.* 2004 ;1018:86-96.
2. **Joshi G**, Sultana R, Perluigi M and Butterfield DA: In vivo protection of synaptosomes from oxidative stress mediated by Fe<sup>2+</sup>/H<sub>2</sub>O<sub>2</sub> or 2,2-azobis-(2-amidinopropane) dihydrochloride by the glutathione mimetic tricyclodecan-9-yl-xanthogenate. *Free Radic Biol Med.* 2005 ;38:1023-31.

3. **Joshi G**, Sultana R, Tangpong J, Cole MP, St Clair D, Vore M, Estus S and Butterfield DA: Free radical mediated oxidative stress and toxic side effects in brain induced by the anti-cancer drug adriamycin: Insight into chemobrain. *Free Rad Res.* 2005 ;39:1147-54.
4. **Joshi G**, Perluigi M, Sultana R, Agrippino R, Calabrese V and Butterfield DA: *In Vivo* Protection of Synaptosomes by Ferulic Acid Ethyl Ester (FAEE) from Oxidative Stress Mediated by 2,2-Azobis (2-amidino-propane) Dihydrochloride (AAPH) or  $\text{Fe}^{2+}/\text{H}_2\text{O}_2$ : Insight into Mechanisms of Neuroprotection and Relevance to Oxidative Stress Related Neurodegenerative Disorders. *Neurochem Intl.* 2005 ;48:318-27.
5. Perluigi M, **Joshi G**, Sultana R, Calabrese V, De Marco C, Coccia R and Butterfield DA: *In Vivo* Protection by the Xanthate D609 Against Amyloid  $\beta$ -Peptide (1-42)-Induced Oxidative Stress: Implications for Alzheimer's Disease. *Neuroscience.* 2006; 138:1161-70.
6. Tangpong J, Cole M, Sultana R, **Joshi G**, Estus S, Vore M, St. Clair W, Ratanachaiyawong S, St. Clair D, and Butterfield DA: Adriamycin-induced, TNF- $\alpha$ -mediated Central Nervous System Toxicity. *Neurobiology of Disease.* 2006; 23(1):127-39.
7. Perluigi M, **Joshi G**, Sultana R, Calabrese V, De Marco C, Cini C and Butterfield DA: *In Vivo* Protective Effects of Ferulic Acid Ethyl Ester Against Amyloid  $\beta$ -Peptide (1-42)-Induced Oxidative Stress: Implications for Alzheimer's Disease. *J Neuroscience Res.* 2006; 84(2):418-26.

8. Butterfield DA, Mohammad-Abdul H, Opii W, Newman S, **Joshi G**, Ansari MA and Sultana R: Pin 1 in Alzheimer's disease. *J neurochem.* 2006; 98(6):1697-706.
9. Ansari MA, **Joshi G**, Huang Q, Opii W, Mohammad-Abdul H, Sultana R, Butterfield DA: In vivo protective effects of D609 in brain mitochondria against the free radical-mediated oxidants, 2,2-Azobis (2-amidino-propane) Dihydrochloride (AAPH) or  $\text{Fe}^{2+}/\text{H}_2\text{O}_2$  and Amyloid  $\beta$ - Peptide (1-42): relevance to Alzheimer's disease and other oxidative stress-related neurodegenerative disorders in which mitochondria are involved. *Free Radic Biol Med.* 2006; (In Press)
10. Opii WO, **Joshi G**, Head E, Cottman CW, Butterfield DA: Long-Term Treatment with Antioxidants and a Program of Behavioral Enrichment Decreases Oxidative Damage and Restores Antioxidant Reserves in Brain in the Canine Model of Human Aging: Relevance to Alzheimer's disease.2006; (In press)
11. Ansari MA, Mohammad-Abdul H, **Joshi G**, Opii W and Butterfield DA: *In vitro* protective effect of quercetin in neuronal culture against  $\text{A}\beta(1-42)$ : Relevance to Alzheimer's disease *J Nutritional Biochem.* (submitted)
12. **Joshi G**, Sultana R, Cole MP, St Clair D, Vore M and Butterfield DA: Modulation of glutathione and glutathione related enzyme expression and activity in brain induced by the anti-cancer drug adriamycin: implication for oxidative stress mediated chemobrain. *Brain Res.* (submitted)
13. **Joshi G**, Hardas S, Sultana R, St Clair D, Vore M and Butterfield DA: Glutathione elevation as a potential therapeutic strategy towards oxidative stress

mediated by in vivo administration of adriamycin: Role of the glutathione precursor, GCEE. *J Neuroscience Res.*2006; (In Press)

### **MANUSCRIPTS TO BE SUBMITTED**

1. **Joshi G**, Huang Q, Sultana R and Butterfield DA: N-Acetyl cysteine-mediated protection against oxidative stress in APP/PS-1 mouse models: A pilot study towards therapeutic modulation of Alzheimer's disease.
2. **Joshi G**, Sultana R, St Clair D, Vore M and Butterfield DA: Proteomic identification of NADH ubiquinone oxidoreductase as oxidatively modified and of decreased level in brain of mice treated with adriamycin: Insight into chemobrain.
3. **Joshi G**, Opii W, Sultana R, St Clair D, Vore M and Butterfield DA: Proteomic identification of differentially expressed proteins and redox proteomic identification of oxidized proteins in brain isolated from adriamycin injected mice: Targets for potential therapeutics.